
THE UNIVERSITY
*of* EDINBURGH

# Wastewater Treatment by Filamentous Macro-algae

Michael Eric Ross

Submitted for the degree of Doctor of Philosophy at the University of Edinburgh


Partner institute - Scottish Association for Marine Science, Oban, UK


-2017-

# Wastewater Treatment by filamentous macro-algae

*by*

Michael Eric Ross

*Supervised by*

Dr. Andrea J.C. Semião

Dr. Michele S. Stanley

Prof. John G. Day

*Examined by*

Dr. Raffaella Villa

Dr. Efthalia Chatzisymeon

# Declaration

I hereby declare that this thesis has been completed solely by Michael E. Ross at the University of Edinburgh and at the Scottish Association for Marine Science, under the supervision of Dr. Andrea J.C. Semião, Dr. Michele S. Stanley and Prof. John G. Day. Full reference is given where other sources are used. This work has not been submitted for any other degree or personal qualification.

Michael E. Ross

28/09/2017

# Abstract

An increase in anthropogenic activity has led to the heightened levels of pollution entering aquatic systems. These excessive concentrations of heavy metals, nitrogen (N), and phosphorus (P) in water bodies can lead to several adverse impacts, such as eutrophication and human health risks. Therefore, the removal of pollutants from wastewaters, prior to their discharge into the natural environment, is of paramount importance. However, conventional wastewater treatment (WWT) technologies have their limitations; for instance, large capital/operational costs, and incomplete removal of contaminants. Therefore, innovative and more effective treatment technologies are required.

Macro-algae typically have high growth and solar energy conversion rates, and are able to sequester nutrients, utilise $CO_2$, and adsorb metals from aquatic environments. Therefore, algae may have potential applications in WWT. Furthermore, costs could be negated by the production of renewable algal biomass which may have a variety of commercially exploitable applications. However, issues such as poor selection of species or cultivation systems, and a lack of understanding of the influence of biological, chemical and physical factors, particularly in a highly dynamic wastewater environments, has led to varied results and prevented algal WWT becoming a widespread reality.

In this thesis the algae *Cladophora coelothrix* and *Cladophora parriaudii* were studied as potential organisms for implementation into WWT. In addition to the features mentioned above, *Cladophora* was selected due to its ubiquity, filamentous morphology, which minimises harvesting costs, as well as their natural dominance and bloom forming behaviour in nutrient-rich environments. The influence of dewatering techniques, environmental factors, and nutrient regime upon the growth, nutrient/metal removal, and biochemical composition of the biomass were assessed.

The first aspect of the thesis was an abiotic screening process, in order to investigate the robustness of *Cladophora* and its suitability for WWT applications on a fundamental level. Good rates of growth (4-13.3% $d^{-1}$) and nutrient removal (45.2-99.9%) were observed throughout the screening process, except under the most extreme of conditions, *e.g.* pH 3. This indicated that *Cladophora* are potentially suitable for treating a broad range of wastewaters and merit further research to improve its potential applicability for WWT

applications and commercial realisation. For instance, developing a reliable and accurate method for fresh weight (FW) assessment and hence productivity estimation.

The determination of growth rate via FW measurement is one of the most basic aspects of algal biology, yet no standardised method exists for filamentous macro-algae. A variety of FW methods were systematically assessed in terms of accuracy and physiological impact. Methods involving mechanical pressing to dewater the biomass resulted in >25% reduction in the final biomass yield, compared to control cultures. The best method for FW determination employed a reticulated spinner, which was rapid, reliable, and easily standardised. Furthermore, this approach ensured accurate growth estimation with minimal physiological impact, measured as growth, maintenance of structural integrity and nutrient removal. This indicates that the method developed has the potential for widespread application in macro-algal cultivation, as such the method was employed throughout this thesis.

The influence of nutrient regime on growth, biochemical composition, and bioremediation capacity was studied for both species of *Cladophora*. The nutrient regimes tested, representative of a broad variety of wastewaters, included four different N/P ratios, four N sources (ammonium, nitrate, nitrite and urea), and six different equimolar N source combinations provided at two N/P ratios. There were clear differences in performance between the two species, with higher rates of growth observed in all instances by *C. parriaudii* (4.75-11.2% $d^{-1}$ vs. 3.98-7.37% $d^{-1}$). Furthermore, ammonium was removed preferentially, whereas urea was removed secondarily. However, the presence of urea in the medium enhanced growth and uptake of the other co-existing N-forms, and yielded a carbohydrate-rich biomass (37.6-54% DW). These findings demonstrate that algal strain selection is important for treating wastewaters with specific nutrient profiles. In addition, results from this study suggest that nutrient regimes can be tailored to produce biomass with certain properties or characteristics, which make it suitable for further, potentially commercially viable, applications, such as metal biosorption.

Since the biochemical characteristics of algal biomass were shown to be affected by nutrient regime, the final chapter describes research investigating the influence of nutritional history on metal biosorption. *C. parriaudii* was cultivated under different nutrient regimes to produce biomass of varying biochemical composition. This biomass was then used for metal removal, with maximum removal rates ranging from 1.08-2.35 mmol $g^{-}$

$^{1}$, 0.3-0.62 mmol $g^{-1}$, 0.22-0.48 mmol $g^{-1}$, and 0.43-0.61 mmol $g^{-1}$ for $Al^{2+}$, $Cu^{2+}$, $Mn^{2+}$, and $Pb^{2+}$, respectively. Observations from this work indicate that metal removal is achieved by various mechanisms including adsorption, ion exchange, complexation and micro-precipitation, and that the biosorption efficacy is dependent upon the number and type of functional groups present, which are in turn influenced by the cultures nutrient regime.

Overall, this study demonstrates the inter-relatedness of biological, chemical, and physical factors on algal growth, nutrient removal, biochemical composition, and metal biosorption. Results from this work have highlighted the need for standardisation in protocols, increased understanding of the influence of algal selection and nutrient characteristics in bioremediation, and highlighted the importance of considering biological aspects, specifically nutritional history, in biosorption studies.

# Lay Summary

An increasing human population and growth in agriculture and industry has led to more pollution entering rivers, lakes and seas. These polluted waters need to be treated as high levels of nutrients and metals in both freshwater and the marine environment can have an adverse environmental impact and threaten human health. Current wastewater treatment technologies all have drawbacks, such as a high cost and energy use, and an incomplete removal of pollutants. New and efficient treatment technologies are required. The use of algae, or seaweed, could be a solution, as they can live in nutrient-rich water. The algae will grow and clean the water at the same time, by using the nutrients as a fertiliser. The algal material produced can then be collected and used for a number of different purposes. For instance, algae are already used as a source of food, fertiliser, and fuel. In addition, the surface of algae attracts heavy metals. This means that the algal material could also be used to bind heavy metals, removing them from polluted water. This research investigated an alga called *Cladophora*, which can live and grow in polluted water, for nutrient and metal removal. The influence of different growth conditions on the effectiveness of treatment and the algal material properties was tested. This work could result in greater use of algal treatment technologies and improve our current methods for growing algae for commercial uses.

# Acknowledgments

At this moment in time, I am currently placing the final few pieces of the jigsaw Ph.D. puzzle together. If I squidge up my eyes a bit, this thesis looks a vaguely like it was supposed to, which is a tremendous relief. However, this would not have been possible without the help, guidance, criticism, and encouragement that I have received from many different people throughout the last 3.5 years. These are but a few words which barely scratch the surface of my gratitude.

Firstly, I acknowledge the financial support that I have received from EPSRC and NERC.

I owe a special thank you to Dr. Andrea Semião, to whom I am indebted. Her timely and perceptive feedback were more than could have be asked for. I have benefitted from her attention to detail, good humour and positive outlook. Most of all though, she has made me a better scientist by teaching me to always ask 'why?'.

To my co-supervisors Prof. John Day and Dr. Michele Stanley I thank them for their sage advice, insightful comments, revisions and recommendations. However, most importantly, they have shown complete faith in me for many years. This thesis, and my career, would not exist without them.

To my internal and external examiners Dr. Efthalia Chatzisymeon and Dr. Raffaella Villa, respectively, I thank for their constructive feedback and suggestions during the Viva.

I am also very grateful for the technical assistance that I have received from Alison Mair, Ceci Menendez, Dave Kelly, Kevin Tierney, Lorna Eades, Louise Hogg, Mike Davidson, Naomi Thomas, Phil Kerrison, and Undine Achilles-Day.

I thank Katharine and Rory for being excellent and inquisitive students which forced me shift up a gear. To Craig, Danny, Josh, Maria, Pete, and Steve whom I have learned a lot from, in many different ways. To my building/lab/office mates Sorcha, Laura, Neil and Neil, Kate and Kate, Chris, Eric, Lewis, Gelly, Felix, and Zafiris for providing a welcome distraction in the form of 'would you rathers?', coffees and beers, football, fishing and pub quizzes.

I acknowledge Rolling Stone's '500 Greatest Albums of All Time' for providing the soundtrack to my Ph.D. and Taylor's 'Hot Lava Java' for fuelling it.

I thank my family for their unconditional love and support.

Finally, to Konstantina for being a rock, for listening to me drone on and on and on, for her expressions, for her love, and for a million other things. Σ'αγαπώ.

# Contents

## Table of Contents

# List of Figures

# List of Tables

# Abbreviations

| | |
|---|---|
| ATR | Attenuated Total Reflectance |
| BSA | Bovine Serum Albumin |
| $C_0$ | Initial Metal Concentration in Solution |
| CCAP | Culture Collection of Algae and Protozoa |
| $C_e$ | Residual Metal Concentration in Solution |
| CF | Correction Factor |
| Chl A | Chlorophyll A |
| Chl B | Chlorophyll B |
| DGR | Daily Growth Rate |
| DIN | Dissolved Inorganic Nitrogen |
| DMSO | Dimethylsulfoxide |
| DON | Dissolved Organic Nitrogen |
| DW | Dry Weight |
| EDTA | Ethylenediaminetetraacetic acid |
| FTIR | Fourier Transform Infrared Spectroscopy |
| FW | Fresh Weight |
| GEq | Glucose Equivalent |
| GS | Glutamine Synthase |
| HPLC | High Pressure Liquid Chromatography |
| HRAP | High Rate Algal Pond |
| IC | Ion Chromatography |
| IIE | Institute for Infrastructure and Environment |
| JM | Jaworski's Medium |
| LNSW | Low Nutrient Seawater |
| MCT | Mercury Cadmium Telluride |

| | |
|---|---|
| NADH | Nicotinamide Adenine Dinucleotide |
| NR | Nitrate Reductase |
| $OD_{XYZ}$ | Optical Density $_{\text{wavelength nm}}$ |
| PAR | Photosynthetically Active Radiation |
| psu | Practical Salinity Units |
| PTFE | Polytetrafluoroethylene |
| $Q_e$ | Metal Sorbed at Equilibrium |
| $Q_{max}$ | Maximum Metal Sorption |
| RF | Radio Frequency |
| RT | Room Temperature |
| SAMS | Scottish Association for Marine Science |
| TAN | Total Ammonia Nitrogen |
| TCA | Trichloroacetic Acid |
| US EPA | United States Environmental Protection Agency |
| WHO | World Health Organization |
| WWT | Wastewater Treatment |
| WWTP | Wastewater Treatment Plant |

# Chapter 1
## Introduction

## 1.1 Motivation

Water is invaluable for life on Earth, however, as a resource it is under threat. This is caused by an ever increasing human population and the resultant growth in agriculture, aquaculture, urbanisation, and industrialisation. This has led to greater amounts of nutrient and metal pollution in both terrestrial and aquatic ecosystems [1, 2]. Excessive enrichment of water bodies with nutrients, such as phosphorus (P) and nitrogen (N), as dissolved inorganic nitrogen (DIN) and dissolved organic nitrogen (DON), can lead to eutrophication (Fig. 1.1.). Eutrophication is characterised by the formation of algal blooms, followed by their senescence and death and resultant decay, leading to anoxic conditions [2]. This may result in the serious impairment of local ecosystems and a reduction in biodiversity [1], with secondary issues such as economic losses and human health risks [3]. Eutrophication has become the biggest threat to water quality in both freshwater and marine environments [3]. An extreme example is the increasing prevalence of coastal Dead Zones; for example, those in the Gulf of Mexico or the Baltic Sea, measuring approximately 21,000 and 84,000 $km^2$, respectively (Fig. 1.1B.) [4]. Dead Zones are caused, in part, by anthropogenic nutrient enrichment and are characterised by having dissolved oxygen conditions of less than 2 mL $O_2$ $L^{-1}$; conditions unfavourable to sustain many aquatic organisms [5, 6]. Furthermore, excessive concentrations of DIN, such as ammonia and nitrite, and DON (urea) in water are known to have adverse effects on human health, such as gastric cancer, foetal malformation and death [7]. As such, the Water Framework Directive (WFD) (Directive 2000/60/EC) [8] has issued various directives including the Nitrates Directive 1991 [9]and Dangerous Substances Directive (Directive 2006/11/EC) [10], which highlighted both $NH_3$ and $NO_2^-$ as dangerous substances, in an effort to improve water quality and quantity across Europe, and reduce the occurrence of eutrophic events and risks to human health.

Aquaculture is a comparatively new and globally important industry [11]; with aquaculture derived produce already surpassing that obtained from capture fisheries [12, 13]. However, issues such as disease, alien species invasion, and pollution from uneaten food and excretory products shroud the aquaculture industry [14, 15]. For instance, aquaculture effluents are nutrient rich (DIN = 0.37 – 5047.3 mg L-1) [14, 16] and often in excess of permissible discharge allowances (Table 1.1) [17, 18]. In order to combat these discrepancies and preserve the aquatic environment, in 2016, the WFD issued the Marine Strategies Framework Directive (MSFD) related to aquaculture [19]. This directive listed a

range of good industrial practices and suggestions, including reducing feed inputs and pond fertilisation, limiting stocking density, and developing Integrated Multi-Trophic Aquaculture (IMTA) systems to curtail the discharge of nutrient inputs into the aquatic ecosystem [19]. Furthermore, in 1991, the European commission issued Council Directive 91/271/EEC concerning urban waste-water treatment [20]. This directive specified that in areas subject to eutrophic events, that there should be either a 70-80% reduction in nutrient loading of the influent and/or that effluents should not exceed 10-15 mg $L^{-1}$ N and 1-2 mg $L^{-1}$ of P, depending upon the human population [20].

In addition, there are increasing concentrations of heavy metals in aquatic environments originating from industrial activities such as energy, mining and metallurgy. These toxic and/or heavy metals pose serious health risks, such as skeletal deformities and brain damage [21-24]. Therefore, treating water and wastewater contaminated with excessive concentrations of metals and nutrients is of paramount importance.

Conventional wastewater treatment (WWT) technologies involve biological, physical and chemical methods that are energy intensive, require the use of chemicals, and can produce secondary wastes, by-products, or toxic sludge that requires additional treatment. In addition, they may also result in an incomplete removal of contaminants [25-27], which may lead to some of the issues described above. Waste and wastewater have been highlighted as priority sectors in the Paris Agreement [28] and Horizon 2020 [29]. Emphasis has been placed on resource recovery, reuse, and recycling. In addition, new technologies have been called for which combine WWT with either energy production or reduced greenhouse gas emissions. Additionally, the UN has implemented the 2030 Agenda for Sustainable Development, with clean water and sanitation being one of their goals. More specifically, in an effort to redress environmental issues such as anthropogenic eutrophication, they are aiming to reduce pollution and halve the volume of untreated wastewater, coupled with improvements in wastewater treatment processes, recycling and reuse technologies [30].

**Table 1.1.** Nutrient concentrations reported in finfish (F) and shrimp (S) aquaculture effluents and their water quality standard (WQS) allowances. The discharge allowance requirements from European Urban Waste-Water Treatment (UWWT) plants are also provided. All values are given in mg $L^{-1}$.

| Type | $NH_4$-N | $NO_2$-N | $NO_3$-N | DON | DIN | TN | $PO_4$-P | N/P | Ref |
|---|---|---|---|---|---|---|---|---|---|
| **F** | 0.29 | - | 0.07 | - | 0.37 | 0.37 | - | - | [16] |
| **F** | 0.11 | 0.01 | 0.38 | - | 0.5 | 0.5 | 0.69 | 0.73 | [31] |
| **F** | 0.59 | 0.04 | 0.3 | - | 0.93 | 0.93 | 3.47 | 0.27 | [32] |
| **F** | 0.06 | 0.16 | 2.67 | - | 2.89 | 2.89 | 0.47 | 6.15 | [33] |
| **F** | 0.53 | 0.16 | 1.7 | - | 2.39 | 2.39 | 0.21 | 11.2 | [34] |
| **F** | 1.7 | - | 1.62 | - | 3.32 | 3.32 | 0.59 | 5.67 | [35] |
| **F** | 5.52 | - | - | 0.58 | 5.52 | 6.1 | - | - | [36] |
| **F** | 5.98 | - | 0.43 | - | 6.41 | 6.41 | 0.23 | 28.1 | [37] |
| **F** | 9.1 | 0.1 | 13.1 | - | 22.3 | 22.3 | 9.6 | 2.32 | [38] |
| **F** | 4.1 | - | 45 | 63.4 | 49.1 | 112.5 | 57.2 | 1.97 | [39] |
| **F** | 7 | 5 | 110 | 53 | 122 | 175 | 50.4 | 3.47 | [40] |
| **S** | 0.17 | - | 0.09 | - | 0.25 | 0.25 | 0.01 | 48 | [41] |
| **S** | 1.37 | 0.15 | 3.01 | - | 4.53 | 4.53 | 0.03 | 151 | [42] |
| **S** | 4.24 | 0.13 | 2 | - | 6.37 | 6.37 | 0.42 | 15.2 | [43] |
| **S** | 64.99 | 76.13 | 7.07 | - | 148.19 | 148.19 | - | - | [44] |
| **S** | 78.97 | 79.17 | 7.52 | - | 165.66 | 165.66 | - | - | [45] |
| **S** | 5047.3 | - | - | - | 5047.3 | 5047.3 | - | - | [14] |
| **WQS** | <2-5 | - | - | - | - | | <0.2-0.5 | - | [17, 18] |
| **UWWT*** | | | | | | 15 | 2 | | [20] |
| **UWWT†** | | | | | | 10 | 1 | | [20] |

* = population equivalent of 10,000-100,000. † = population equivalent of > 100,000.

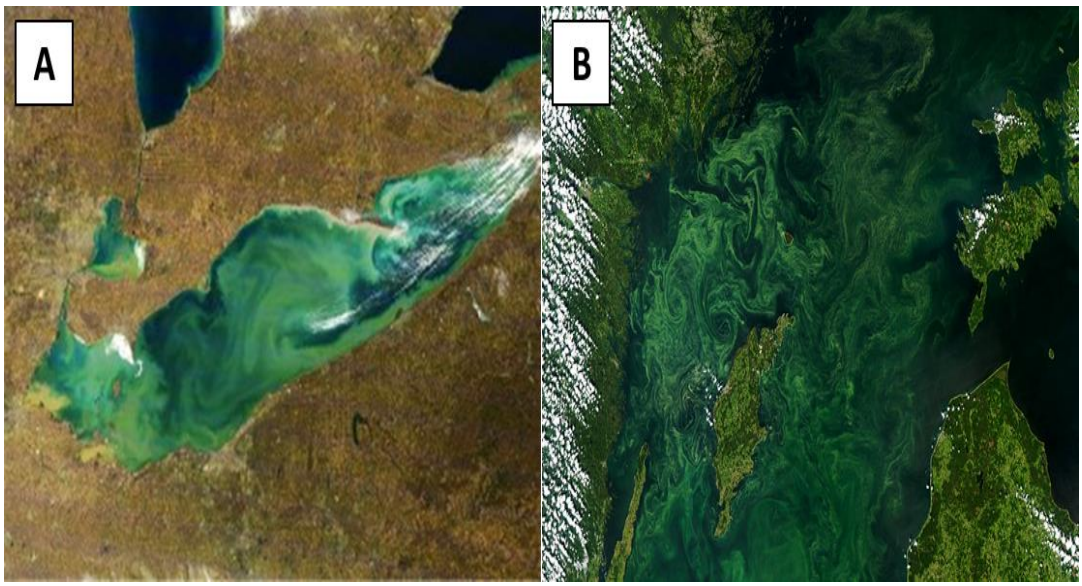


**Figure 1.1.** Satellite images of eutrophication in (A) Lake Erie, USA, and (B) the Dead Zone in the Baltic Sea. Images from [46, 47].

Algae, both micro- and macro-, typically have high rates of growth and a greater capacity for utilising solar energy, in comparison to "higher" or terrestrial plants [48]. In addition, algae are capable of nutrient uptake and the beneficial utilisation of $CO_2$ [14, 49-51], therefore contributing to greenhouse gas reduction. Furthermore, algae can adsorb toxic or heavy metals from aquatic environments [52], with macro-algae known to accumulate metals to several times the concentration of the external environment and are considered as suitable bio-monitors for metal pollution [53, 54]. This means that algal bioremediation could potentially be used in conjunction with conventional treatment technologies for secondary, tertiary, or integrated treatment purposes, acting as a final "polishing" step. For example, algal WWT may be used in small-medium scale rural communities [55], applied in constructed wetlands and sustainable urban drainage systems (SUDS) [56, 57], or integrated with existing industrial effluents (*e.g.* agriculture, aquaculture, anaerobic digestion effluents, and coal-fired power stations) [16, 58-60]. However, algal WWT has a high land requirement and is, therefore, unlikely to be suitable for the treatment of effluents where space is limited, *e.g.* municipal wastewater treatment in a mega-city [55].

In addition, algal WWT is a particularly attractive prospect as it can concomitantly produce algal biomass for potentially remunerative purposes, such as bioenergy, fertilisers, foodstuff, or high-value products [61-63]. This means that algal WWT is potentially circular,

sustainable, and in keeping with the green and blue economy [64]. These features have stimulated interest in exploring the potential of implementing algae for a variety of WWT purposes. For instance, the removal of dissolved inorganic nitrogen (DIN) from real aquaculture effluents by macro-algae ranged from 16.9-96.6% [41, 65, 66]. Whereas, there was a 3-97% removal efficiency of lead by a variety of micro-algae and cyanobacteria [67]. These results indicate that algal bioremediation has potential for implementation into WWT; however, the broad variation in results mentioned above highlights the need for further research in an effort to resolve the challenges facing its widespread application. For instance, selection of suitable algal species and understanding the influence of physical, biological, and chemical factors on algal bioremediation performance.

## 1.2 Algal Taxonomy

Defining what an algae is is challenging. They encompass an incredibly diverse collection of organisms that are not attributed to a single taxon, instead occupying at least 6 different phyla [68-71], having many cross-overs with fungi, bacteria, plants, seagrasses, liverworts and mosses [72, 73].

In the broadest and simplest of terms, algae are aquatic, oxygen-producing autotrophic organisms [74], although terrestrial, heterotrophic, and chemotrophic forms also exist [75]. They are found ubiquitously across the globe ranging from the permafrost of polar regions [76], thermal springs [77] to desert sands [73, 78, 79]. The algal form can be either unicellular (micro-algae) or multicellular (macro-algae), ranging from a few micrometers in diameter to tens of meters in length (Fig. 1.2) [73, 78]. Algae are principally divided into classes based upon their colour, the most common classes being the Cyanophyceae (blue-green) which are prokaryotic, Chlorophyceae (green), Rhodophyceae (red), and Phaeophyceae (brown) (Fig. 1.2). However, several others also exist, including Chrysophyceae (golden) and Xanthophyceae (yellow-green) [72, 80]. The colour of the algae is caused by the type and expression of an array of pigments categorised as chlorophylls, carotenoids, and biliproteins [81]. The key role of these pigments is primarily to harvest light for photosynthesis. However, carotenoids have additional roles within the cell; for example, protection against photo-oxidative damage [76, 82].

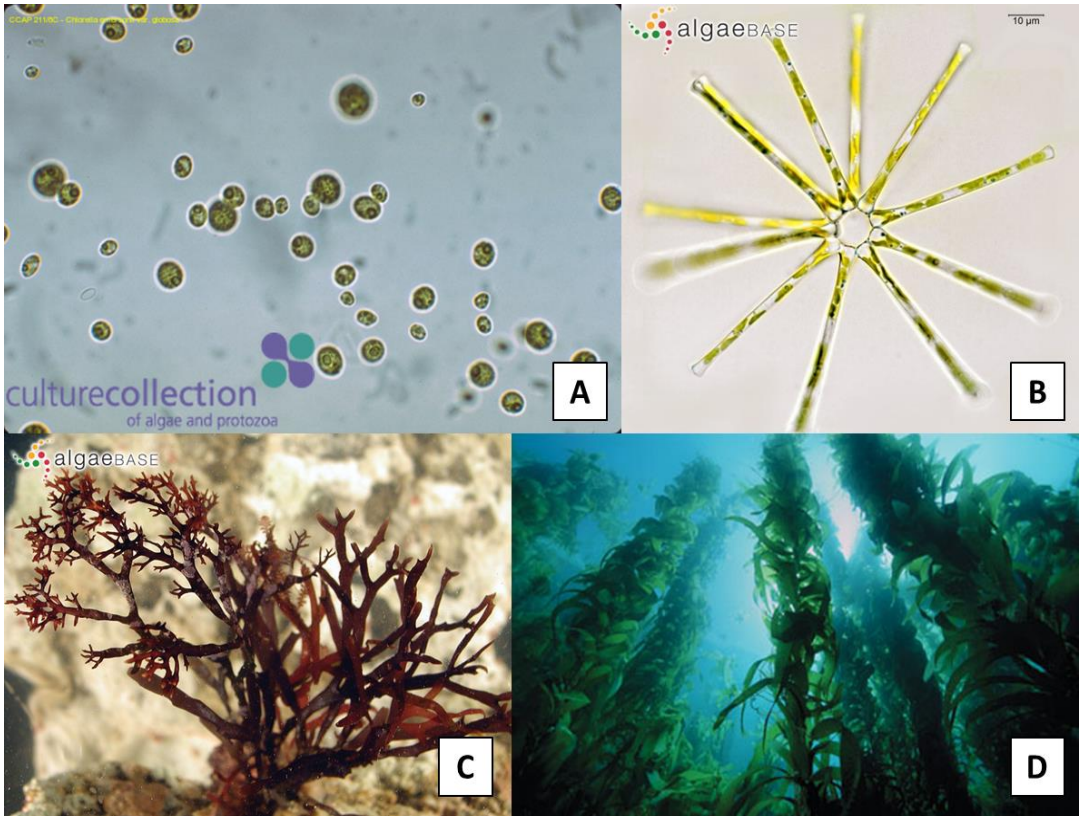


**Figure 1.2.** Plates showing algal diversity; A) a green micro-algae, *Nannochloropsis* sp. (Eustigmatophyceae) B) a colonial diatom, *Asterionella formosa* (Bacillariophyceae) C) a red macro-algae, *Gracilaria corticata* (Florideophyceae) D) the giant kelp, *Macrocystis pyrifera* (Phaeophyceae). Images from [83-85].

Producing a detailed and current account on algal taxonomy is well beyond the scope of this work, therefore the purpose of the above section is to briefly introduce the reader to the vast complexity of algal biology. However, such great diversity offers a rich seam of opportunity! Algae play key environmental and ecological roles and are also a commercially valuable natural resource, with many different applications [74, 86-88].

## 1.3 Algal Uses

**Figure 1.3.** "Seaweed Gatherers, Connemara" by Aloysius O'Kelly in the 1880s [89].

Historically, algae have widespread uses throughout Europe, in the 18$^{th}$ and 19$^{th}$ centuries, as a food, fertiliser/soil enhancer, and were also used for the production of potash, used in glass manufacturing (Fig. 1.3) [63, 90]. Arguably, the genesis of applied/biotechnological algal research was in the 1950's when William J. Oswald cultured algae on a large-scale in high rate algal ponds (HRAPs) (Fig. 1.4) [91-93]. The idea was to cultivate freshwater micro-algal biomass, in a low-impact solar-driven system, for the concomitant treatment of wastewater and production of algal biomass for conversion into methane; essentially coupling together an ecosystem service with a biomass application [94-96]. This forward thinking idea is still pertinent, with current algal research focussing on biofuels and WWT, motivated by the need for fossil fuel replacement and provision of clean water. There has been many publications on algal biofuels and these show some degree of correlation between the cost of oil and the number of scientific publications related to algal bioenergy production, with noticeable spikes linked to the oil crises of 1973, 1979, and the mid-2000s onwards (Fig. 1.5).

**Figure 1.4**. A high rate algal pond (HRAP) at the University of California, Berkeley, 1994, where Oswald worked. Image from [97].

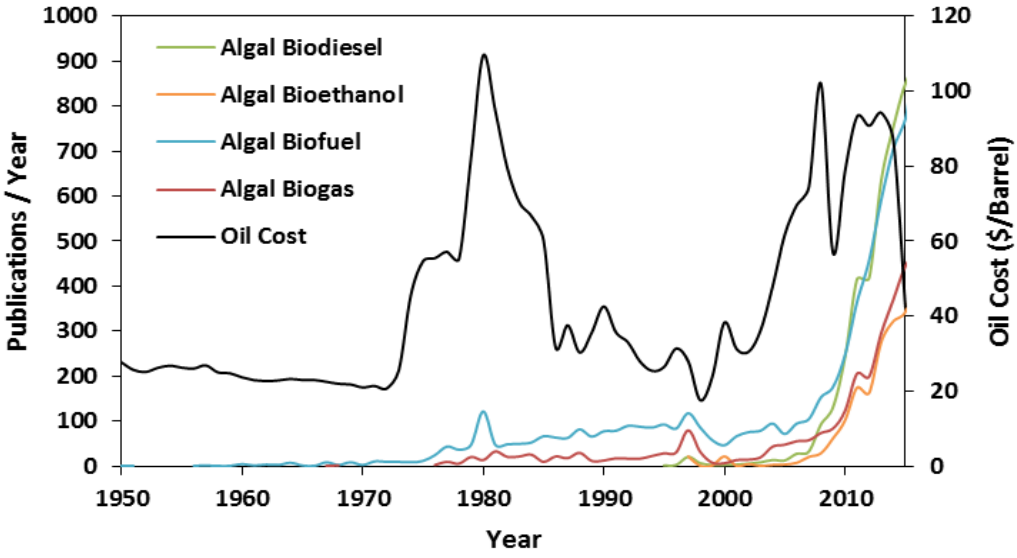


**Figure 1.5.** The number of scientific publications related to algal bioenergy versus the inflation-adjusted cost of oil per barrel. Data obtained from [98, 99].

### 1.3.1 Algal Biofuels

Algae have received considerable scientific interest in recent years as a potential source of renewable bioenergy (Fig. 1.5) due to features such as high rates of growth, nutrient sequestration, and high solar energy conversion ratios [48, 100]. Algae grow and assimilate nutrients, converting them into algal biomass, which depending upon the properties of the biomass can be harvested and used as a feedstock for different forms of bioenergy [91, 100]. For instance, some micro-algal species can accumulate lipids as storage compounds, exceeding 80% per unit dry weight (DW), which can then be converted into biodiesel [101, 102]. In contrast, seaweeds are rich in storage and structural carbohydrates [103, 104], making them better suited for fermentation into bioethanol, or digested anaerobically for conversion into methane or biogas [105-108]. An additional benefit of algal biofuels is that they can be cultivated in areas that are unsuitable for terrestrial crop growth and utilising non-potable water, with potential wastewater and flue gas mitigation. This means that algal biofuel production is not in direct competition for resources required for human consumption [48, 109]. Algal biofuels however, are a low-value product required in a high-volume [88]. In comparison to fossil fuels, the production and processing costs associated with algal biofuels make them currently economically unattractive [91]. However, incorporating new ideas or addressing key issues such as use of low-cost waste streams, developing efficient separation and processing technologies, implementing a biorefinery approach, and governmental incentives, *e.g.* carbon credits, may help increase the commercial realisation of algal biofuel production [110-112]. However, perhaps a more commercially viable option is the production of high-value products [88, 113].

### 1.3.2 Algal Food and Manufacturing

Algae, in general, are chemically complex and produce an array of natural products. Given the current outlook for algal biofuels and the growth in the availability of inexpensive shale oil [114], research has shifted in recent years towards the production of high-value products for use as functional foods, cosmetics, pharmaceuticals and nutraceuticals [63, 88, 115]. For example, *Haematococcus pluvialis* and *Dunaliella* sp. are commercially cultivated for the production of the astaxanthin and β-carotene, respectively, which both have strong anti-oxidant properties (Fig. 1.6A and B.) [116, 117]. Dietary anti-oxidants may help prevent

free-radical associated or degenerative diseases, such as Alzheimer's and Parkinson's, as well as variety of cancers, liver and cardiovascular disease [117, 118]. Meanwhile, the cyanobacterium *Spirulina* is commercially produced as a functional food or health supplement given its high content of vitamins, proteins and pigments (Fig. 1.6C.) [119, 120]. In addition, micro-algal species such as *Chaetoceros*, *Chlorella*, *Isochrysis*, and *Tetraselmis* are rich in proteins and highly unsaturated fatty acids (HUFAs), *e.g.* arachidonic acid (ARA), docosahexaenoic acid (DHA) and eicosapentaenoic acid (EPA) [121]. As such, they are produced as a source of animal feeds, where they play a key role in ornamental fish industry, aquaculture hatcheries for molluscan and crustacean larval nutrition, as well as for live feeds, such as brine shrimp and rotifers [122-125].

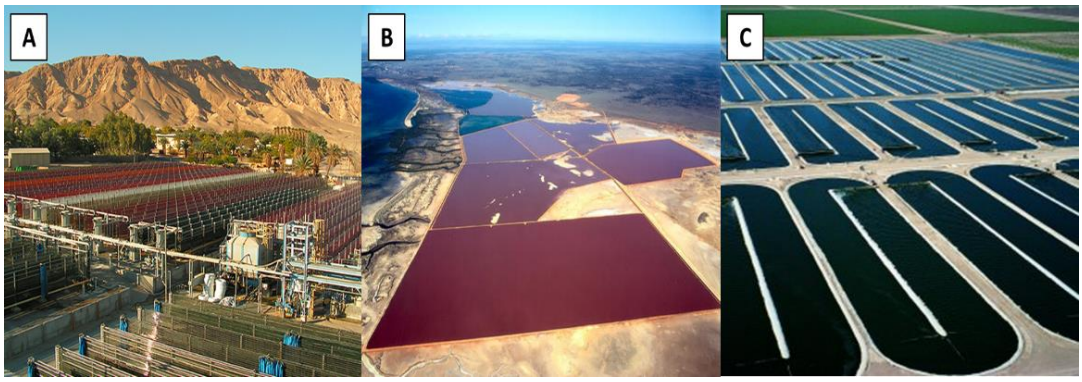


**Figure 1.6.** The commercial production of algae for high-value products; A) *Haematococcus pluvialis* produced in horizontal tubular photobioreactors in Israel, B) *Dunaliella salina* cultivated in a lagoon, Western Australia C) *Spirulina platensis* grown in raceway ponds, California, USA. Images from [126-128].

Seaweed are cultivated on an industrial scale (Fig. 1.7.), with the majority of production occurring in Asia, particularly China and Japan (Fig. 1.8.) [86]. Most of this cultivation is destined for the plate via the production of Kombu, Wakame, or Nori [129]. Red and brown seaweeds are also cultivated on a large-scale for phycocolloids; namely alginate, agar, and carrageenan [86, 103, 129]. Phycocolloids have numerous commercial applications such as stabilisers, thickeners, sizing, emulsifiers, or gelling agents in food, drink, textile and medical industries [129-131]. Seaweeds are also used as a fertiliser/ soil enhancer and animal feedstock [86, 129]. Macro-algae, and their extracts, are also a source of high-value products sold commercially as bio-stimulants, cosmetics, anti-oxidants and health supplements for both humans and animals [132-135]. Environmental applications such as WWT and $CO_2$ mitigation have recently grown in interest and could be coupled with other

aspects of algal production [93, 129]. However, due to health and safety issues and public perception, algal biomass produced on waste streams would not be fit for human consumption, nor would they be employable in pharmaceutical or cosmetic industries [136, 137]; instead, they may be used for bioenergy or additional WWT purposes [138].

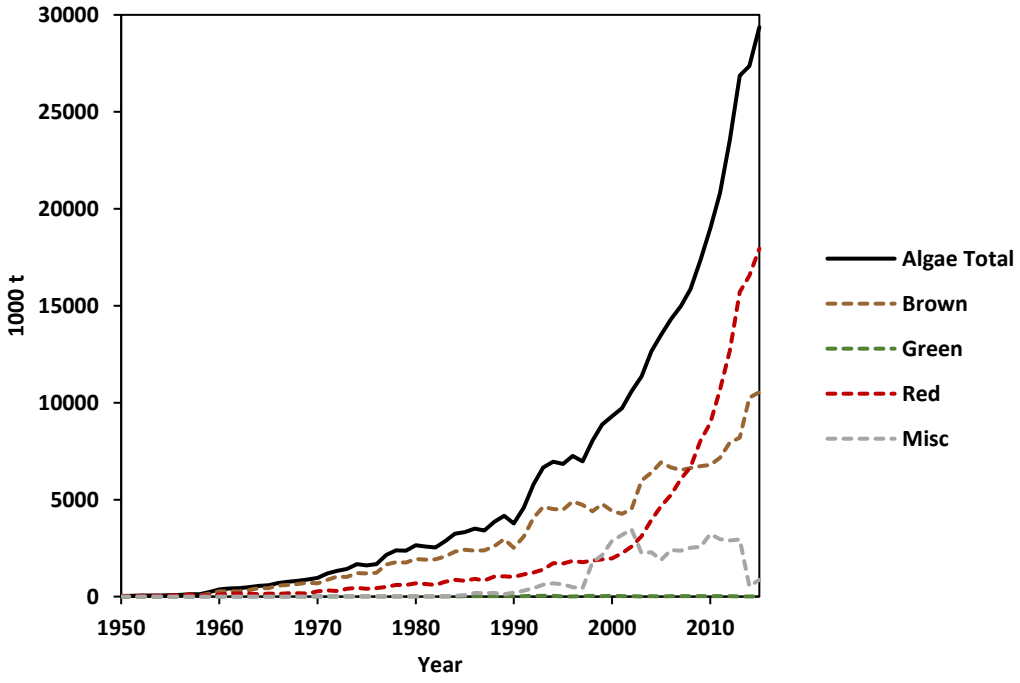


**Figure 1.7.** The production of farmed seaweed over time. Data obtained from [13].

**Figure 1.8.** An image of seaweed production in Jiaozhu Bay, Qiandao, China. Image from [139].

### 1.3.3 Algal Bioremediation

As previously mentioned, algae are capable of removing nutrients and $CO_2$ from water [16, 41, 49, 51]. In addition, they are able to adsorb heavy metals from solution, with some species capable of accumulating high concentrations within their cells [53, 140]. As such, algae have the potential to mitigate the deleterious health, ecological, and environmental effects that excessive levels of nutrients and metals pose, such as eutrophication (Fig. 1.1), caused by population growth and increasing anthropogenic activity on a global scale [1, 3, 23]. Thus, algae are viewed as a promising candidate for implementation into WWT [129, 141].

Both micro- and macro-algae have been shown to be effective at removing nutrients from wastewaters. For instance, after five days cultivation in a 600 L photobioreactor (PBR), a consortium of five freshwater micro-algae removed 99% of total nitrogen and phosphorus from anaerobic digestate (AD) wastewaters, with initial concentrations of 4500 and 690 µM, respectively [52]. Whereas, Ayre *et al.* [58] used a mixed micro-algal culture to treat undiluted anaerobically digested piggery effluent, with a maximum $NH_4^+$-N removal rate of

63.7 mg $L^{-1}$ $d^{-1}$ when the initial concentration was 1600 mg $L^{-1}$. Meanwhile, macro-algae have been employed in a variety of studies to remediate nutrients from aquaculture effluents. For example, the red macro-alga *Gracilaria vermiculophylla* exhibited high productivities (39.9 g DW $m^{-2}$ $day^{-1}$) during summer months when cultivated in finfish effluents, with the resultant biomass having a potential commercial value as a phycocolloid [35]. These aspects will be discussed in greater detail later.

Besides nutrient sequestration, algae have been investigated as a potential low-cost material for toxic metal removal. This is due to their general abundance and interesting cell wall/membrane properties, which naturally bind with metals [142, 143]. For instance, Klimmek *et al.* [67] investigated the ability of thirty different strains of dried micro-algae and cyanobacteria to remove mono-metallic solutions of $Cd^{2+}$, $Ni^{2+}$, $Pb^{2+}$, and $Zn^{2+}$. There was a broad variation in the biosorption capacity by the algae; however, $Cd^{2+}$ and $Pb^{2+}$ were generally removed more efficiently than either $Ni^{2+}$ or $Zn^{2+}$ (Fig 1.9). Whereas, in a recent study Henriques *et al.* [144] used living *Ulva lactuta* and achieved > 95% removal of mono-metallic solutions of 0.1 mg $L^{-1}$ of Cd, Hg, and Pb, after 6 days.

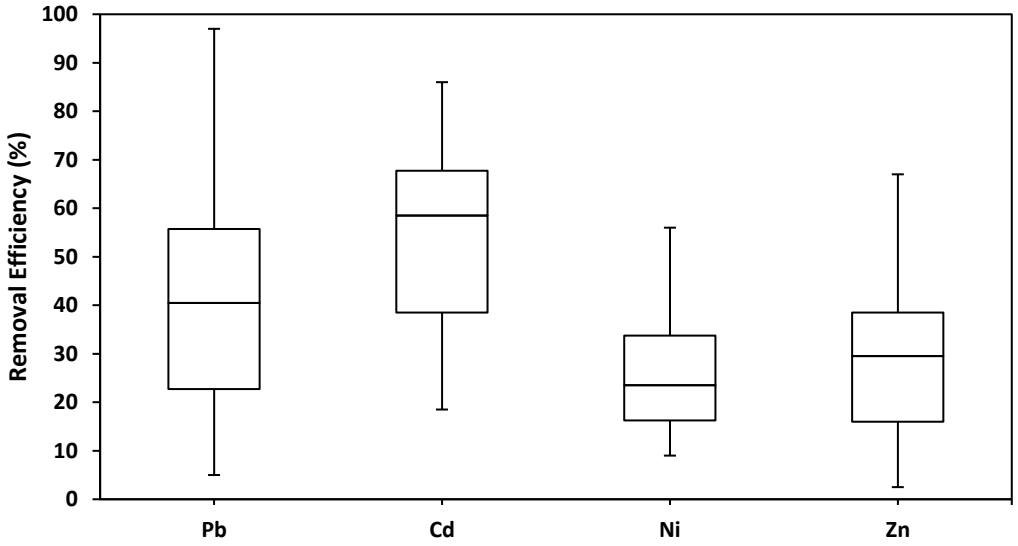


**Figure 1.9.** A box-and-whisker plot of metal removal efficiency (%)of 0.4 g $L^{-1}$ $Pb^{2+}$ and 0.1 g $L^{-1}$ solutions of $Cd^{2+}$, $Ni^{2+}$, and $Zn^{2+}$ by 30 strains of micro-algae and cyanobacteria. Data obtained from Klimmek *et al.* [67].

Algae, therefore, have a considerable potential for treating wastewaters that are rich in either nutrients or metals, excessive concentrations of these may have deleterious effects

on health and the environment. The studies mentioned above show a broad degree of variability and this highlights the need for further research, in order to understand what causes this variability in performance and how to remedy it.

## 1.3.4 Micro- vs. Macro-algae

Although micro-algae are a hugely diverse group of organisms with great potential for a range of applications, commercialisation is limited and only a handful of species which are cultivated primarily for high-value products (Fig. 1.6A and B) [123, 127]. Various biological, economical, management, and physical constraints currently prevent widespread large-scale commercial micro-algal production. These challenges may be overcome through the continued research and development in the following areas: species-selection and genetic engineering, system design and management strategies, development in marketing, infrastructure and the value-added chain, and improvement of separation technologies [48, 111, 123, 127, 145].

### *1.3.4.1 Algal Harvesting*

Harvesting micro-algal biomass is one of the biggest “pinch-points”, contributing to approximately 20-30% of production costs, due to the high moisture content of the micro-algal broths and slurries, in addition to the small size and low specific gravity of micro-algal cells [101, 109, 146]. Harvesting micro-algal biomass is currently achieved in a variety of ways including filtration, centrifugation, chemical or auto-flocculation, sedimentation/settlement, spray-drying, pressing, immobilization/encapsulation, foam-fractionation, or ultra-sonic separation. However, they all have their disadvantages, such as high capital or energy costs, reduction in efficiency with low concentration slurries, or use of non-recoverable or hazardous chemicals [91, 100-102, 147].

Macro-algae, in contrast, are multicellular with collections of cells forming discrete tissues (Fig. 1.2C and D). These tissues can vary drastically in morphology, ranging from relatively simple filamentous arrangements to more complex parenchymal forms [78, 148]. More tangible or solid larger structures facilitate harvesting and greatly reducing dewatering

costs [27]. Macro-algal biomass is generally harvested either manually, or mechanically using boats fitted with dredges, blades, or cutters [149]. In addition, simple, alternative, methods have been suggested for filamentous macro-algal collection and include scraping or screen-filtration and algal turf scrubbers [150-152].

### *1.3.4.2 Algal Dewatering*

Once harvested, the first processing step is to reduce the moisture content of the biomass. This helps reduce transportation costs, increase the shelf-life of the biomass via preservation, and may increase the efficiency of a number of down-stream processing or chemical extraction procedures by eliminating dilution issues [149]. There are a number of techniques that can be used to dewater macro-algal biomass or micro-algal pastes, achieved after harvesting methods outlined above. However, the most appropriate method is selected on the basis of the degree of dehydration required for certain applications (the desired moisture content), intensity/scale of production, and availability of resources and technology.

Some of these methods involve simple drying methods, with no additional energetic input, such as sun- or air-drying [153, 154]. Alternatively, oven- or freeze-drying may be used, albeit at a much greater financial cost [149, 153]. Additional methods include: wet/dry vacuum, screw-press, or belt-driers to reduce the moisture content post-harvest [151, 152]. Whereas, for larger macro-algae domestic washing machines are used to centrifugally reduce the moisture content of *Derbesia tenuissima* and *Ulva ohnoi* in intensive land-based cultivation [155].

As outlined above the methods for harvesting and dewatering algal biomass are expensive and energy-intensive and this pre-processing step contributes significantly to the overall algal production costs. Developments in this area could reduce costs and greatly improve the economic feasibility of algal cultivation [146]. However, in comparison to micro-algae, macro-algae are relatively easy to harvest, so this represents an obstacle of lower importance. For this reason, macro-algae were selected in this study and will be focussed upon for the remainder of this thesis. However, micro-algal examples have been included to emphasise certain points when macro-algal examples are unavailable or insufficient.

## 1.4 Macroalgal WWT – Nitrogen Removal

Nitrogen is present in water and wastewater as either dissolved inorganic nitrogen (DIN) forms such as ammonia ($NH_3$), ammonium ($NH_4^+$), nitrite ($NO_2^-$), and nitrate ($NO_3^-$), or as dissolved organic nitrogen (DON) *i.e.* urea ($CO(NH_2)_2$) or amino acids [156]. Macro-algae are an excellent candidate to treat wastewaters with high loads of these contaminants. However, wastewaters are highly dynamic environments [157] and their characteristics will vary greatly depending upon the catchment area: primary land use (*e.g.* agriculture), population density (human or otherwise), and seasonality [158]. These factors, amongst others, will directly influence the properties of the wastewater: volume and flow rate, total solids and particulate size, organic matter content, biological loading, pH, alkalinity, salinity, and nutrient type and concentration [159]. Furthermore, these biotic and abiotic factors will inevitably have an influence upon various aspects of algal biology, including rates of photosynthesis and respiration, nutrient and $CO_2$ sequestration, growth and metabolism. This will then have a direct impact upon the efficacy of bioremediation by an algal culture: understanding how these factors influence algal performance is of paramount importance for its successful application in WWT.

### 1.4.1 Factors influencing Algal Growth and N Uptake

Nitrogen uptake by macro-algae typically follows Michaelis-Menten type uptake kinetics: with increasing external N concentration, N removal is linear, until a plateau is reached [60, 65, 160-162]. Harrison and Hurd [161] stated that rates and maximum nutrient removal by macro-algae will be influenced by a range of biological, physical, and chemical factors, which will be discussed in more detail below.

#### *1.4.1.1 Physical Factors*

Seasonality, and indeed, a variety of related environmental factors, influence algal productivity and nutrient removal [35, 163-165]. For example, both *Cladophora vagabunda*

and *Gracilaria tikvahiae* grew most during the summer months and least during the winter [165]. Abreu *et al.* [35] noted the influence of various environmental parameters in terms of algal growth and nutrient uptake. A seasonal effect was observed in the growth of *Graciliaria vermiculophylla*; with growth rates of 1.78-6.23% recorded in three distinct patterns based upon seasonality. The authors stated that temperature and number of daylight hours were amongst the most important environmental variables for algal growth [35]. Furthermore, a light intensity of 75 µmol photons $m^{-2}$ $s^{-1}$ resulted in maximum growth rates of 4.3% per day for *Kappaphycus alvarezii*; however, a shift in light intensity, in either direction, resulted in sub-optimal growth. This was thought to be due to either light limitation, or saturation which would result in the algal photoinhibition [164]. Photoinhibition results in a reduction in the photosynthetic rate, caused by damage and subsequent repair to photosystem-II (PS-II) [166, 167]. Fan *et al.* [168] recorded a considerable effect of temperature on both photosynthetic efficiency and N uptake rates by *Ulva prolifera*. For instance, N uptake ranged from 12.7-38.8 µmol $g^{-1}$ DW $h^{-1}$ at temperatures between 5-30°C, with the optimal being 20°C. Although no reason was discussed, both temperature and pH will influence the ion equilibria of nutrients, *e.g.* ammoniacal nitrogen, and the solubility of gases such as $CO_2$ and $O_2$ in water [163, 169], as well as rates of algal metabolism [170, 171].

In addition, salinity can strongly reduce algal growth and nutrient uptake when shifted beyond optimal levels. For instance, the growth and uptake of $NO_3^-$ and $PO_4^{3-}$ by *Ulva pertusa* was significantly reduced when cultivated in 5 practical salinity units (psu), in comparison to maximal performance at 20-25 psu [172]. Similarly, growth rates of approximately 4% per day were achieved by *Graciliaria tenuistipitata* when salinities were between 12-20 psu, but were lowered to <3% when exposed to low (4 psu) or high (> 20 psu) [160]. Salinity may not seem like an immediately obvious concern for algal cultivation or WWT; however, it is an important environmental variable. For instance, salinity may vary on a diurnal or semidiurnal basis due to tidal action or due to seasonal variation, such as periods of drought or heavy rainfall [173]. This will have a profound influence on the salinity in coastal and estuarine ecosystems, where macro-algal cultivation is prevalent. Furthermore, different in-land cultivation systems may experience variable salinity levels, for example shallow race-way ponds such as the types used for WWT (Fig. 1.4) may be prone to evaporative losses, therefore heightened salinity levels [174]. Whereas,

sustainable urban drainage systems (SUDS) ponds may also experience enhanced salinities during winter due to run-off from gritted roads [57].

It is important to study these environmental and seasonal variables in order to better understand their influence on algal biology, and what potential impacts (beneficial or otherwise) that they may have on production. In order to ensure a consistent bioremediation performance, it may be advantageous to select candidate species for WWT based upon their tolerance to these physical factors.

### *1.4.1.2 Biological Factors*

Besides physical factors, biological factors such as stocking density are important for algal performance [35, 65, 164, 175]. The general trend is that the lower the stocking density, the greater the relative growth. Yong *et al.* [164] stated that culture density was closely related to competition for resources, with light and nutrients less available in higher density cultures. For example, the daily growth rates of *Ulva lactuta* ranged from 8.7-9.9% at a stocking density of 2 kg $m^{-2}$, considerably higher than the 0.6-4% achieved at the higher densities [175] (Fig. 1.10). Although, Jimenez del Rio *et al.* [65] observed a similar trend in relative growth, the authors noted that a lower stocking density didn't necessarily equate to the highest absolute algal yield. There is therefore a trade-off between growth and productivity, which raises a potential management decision. In addition, the harvesting regime needs to be considered: how often and how much can be reaped whilst maintaining a consistent level of growth?

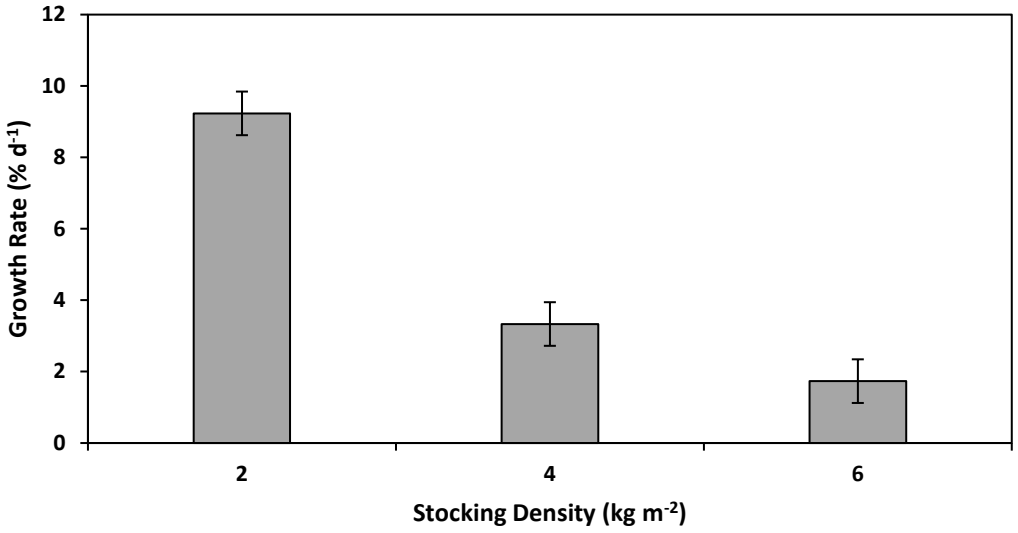


**Figure 1.10.** The mean growth rate of *Ulva lactuta* across a three week period when initially stocked at different densities (2, 4, and 6 kg $m^{-2}$). Data from [175].

The shore-line positioning of inter-tidal macro-algae also influences their performance, as this will determine the duration of immersion/emersion cycles and subsequently the degrees of desiccation, and therefore their access to nutrient pools [176, 177]. Early studies reported that high-intertidal macro-algae have enhanced rates of uptake following mild desiccation [178, 179]. Furthermore, Phillips and Hurd [156] observed species-specific differences in N removal, based upon their intertidal location; high shore-line species exhibited greater uptake rates of $NO_3^-$ and urea, and unsaturated $NH_4^+$ uptake, in comparison with low shore-line species, a strategy designed to maximally exploit pulses of N in a limiting environment. Two similar studies showed that intertidal macro-algae exhibit different rates of N uptake [180, 181]. Pedersen and Borum [181] observed that opportunistic, ephemeral algae had much greater rates of N-uptake in comparison to slower growing species. However, slower-growing, persistent species had a greater capacity for N removal beyond their immediate requirements. This could be considered as an example of the classic r- and K-strategist ecological concept [182]. The preferred habitat and growth strategy of an algal species will doubtless have implications for its suitability and its bioremediation performance, especially in a WWT scenario where conditions may be considered "unnatural": with for example continuous immersion of the algae in nutrient enriched conditions. Furthermore, Pedersen and Borum [181] observed that $NH_4^+$ was removed at greater rates following a period of N limitation. This is due to a process called

"surge uptake", whereby nutrients are removed at transiently enhanced rates due to the replenishment of their internal N pools [181, 183]. This form of uptake may indicate how well suited an individual species is at exploiting pulses of nutrients in an otherwise oligotrophic environment [156, 184], but will be of reduced importance when nutrients are in a continuous or non-limiting supply, such as in the scenario of a wastewater treatment plant. Bracken and Stachowicz [180] cultivated eight different species of macro-algae in monoculture, and fed each with either $NH_4^+$ or $NO_3^-$. Results obtained were similar to those of Pedersen and Borum [181], insofar as species removed $NH_4^+$ at a greater rate than $NO_3^-$, 0.066-0.155 L $h^{-1}$ $g^{-1}$ in comparison to 0.017-0.08 L $h^{-1}$ $g^{-1}$, respectively. The best performers under each nitrogen source were *Ulva taeniata*, or *Porphyra perforata*; however, neither of these were dominant locally as they are preferentially grazed upon by molluscs [180, 185]. This is suggestive of a trade-off strategy between nutrient uptake and growth, versus allocating resources into defence mechanisms. Instead, the dominant local species were *Cladophora columbiana* and *Priontis lanceolata*, which also showed a strong preference towards either $NH_4^+$ or $NO_3^-$, respectively. However, they may have the ability to complementarily utilise multiple N sources [180]. In addition, *Cladophora* have tough, highly crystalline cell walls and the ability to synthesise toxic fatty acids, making them unpalatable to potential grazers [186, 187]. Natural dominance and resistance to herbivory are two very desirable traits for a candidate species for WWT (or any form of algal cultivation), as productivity can be maintained with minimal losses due to disease, grazing, or competitive exclusion by other invasive species.

A final biological consideration is the morphology of the organism. Wallentinus [188] studied macro-algae with different morphologies and found that species with filamentous, delicately branched, or monostromatic phenotypes had the highest rates of nutrient uptake due to a greater surface area/volume (SA/V). This was corroborated by Hein *et al.* [183], who performed a desk study on 76 micro- and macro-algal species and found a strong relationship between nutrient uptake and size. In addition, Luo *et al.* [189] observed differences in growth and N uptake by two co-occurring species of *Ulva,* across a range of irradiances, temperatures, nitrogen types and concentrations. For instance, maximum growth rates of *U. prolifera* were 13.1% $d^{-1}$ and 16.9% $d^{-1}$, in comparison to *U. linza*, which were 9.8% $d^{-1}$ and 11.6% $d^{-1}$ when cultivated under $NO_3^-$ and $NH_4^+$, respectively. The difference in performance between the two was attributed to their thallus structure, with

the faster growing *U. prolifera* being filamentous, whereas *U. linza* is foliaceous. Suggesting that a filamentous morphology may be advantageous for inclusion into WWT applications.

### *1.4.1.3 Chemical Factors*

Macro-algae have a variety of mechanisms to take up nitrogen, depending upon its source. In essence, all mechanisms aim towards the same objective, whereby an N source will enter the cell, either passively or actively, across the membrane, whereupon it is converted into amino acids and assimilated into macromolecules, including proteins, for growth [160]. Both N and P, and their relative molar ratios (N/P), are regarded as important factors that can limit primary productivity [190]. For instance, Fan *et al.* [168] observed that uptake of both $NO_3^-$ and P by *Ulva prolifera* decreased with increasing N/P ratio, with greatest uptake occurring at ratios of 7.5 and 2.2, respectively. Additionally, Mayers *et al.* [191] reported decreasing productivity of the micro-alga *Nannochloropsis* sp. with increasing N/P. This was attributed to P deprivation; while there was little variation in N uptake across treatments, P supply and uptake was strongly correlated, with the lowest P uptake at the highest ratio (80/1). Whereas, Liu and Vyverman [27] found no marked change in the growth of *Cladophora* sp., *Klebsormidium* sp., or the cyanobacterium *Pseudanabaena* sp. when cultivated under eight different N/P ratios ranging from 1-20, with biomass productivities of 52.6-56.7, 29.6-34.1, and 20.2-25.8 mg DW $L^{-1}$ $d^{-1}$, respectively. Wastewaters are highly variable environments, with treatment plants striving for a consistent end-product: clean water. A species that exhibits a parity in growth and nutrient uptake, irrespective of dynamic external substrates would be highly desirable.

Nitrogen source may also play an important role in algal growth and metabolism. A variety of studies have observed elevated macro-algal growth and/or N uptake when cultivated under $NH_4^+$ in comparison to $NO_3^-$ [160, 189, 192, 193]. For example, maximum growth rates of *Ulva lactuta*, cultivated in either $NH_4^+$ or $NO_3^-$, were 16.4% and 9.4% $d^{-1}$, respective to equivalent concentrations of either $NH_4^+$ or $NO_3^-$ [193]. Whereas, after 4 h and an initial concentration of 50 µM, *Graciliaria vermiculophylla* removed ~40 and 100% of $NO_3^-$ and $NH_4^+$, respectively [192]. Differences in efficiency in uptake may be due to the energetic savings that will be made via the utilisation of $NH_4^+$ in comparison to $NO_3^-$, which requires the synthesis of a greater number of enzymes [192]. For example, prior to assimilation, $NO_3^-$

has to undergo a reduction reaction, utilising nitrate reductase (NR) and nicotinamide adenine dinucleotide (NADH), followed by nitrite reductase and ferredoxin. This sequentially reduces $NO_3^-$ to $NO_2^-$ and then to $NH_4^+$. Finally, $NH_4^+$ is converted into amino acids; glutamine synthase (GS) actively condenses $NH_4^+$ and glutamate into glutamine [16, 50]. Whereas, urea is converted into $NH_4^+$ through the activity of either urease or ATP:urea amidolyase (UAL-ase) and also assimilated via the GS pathway [194, 195]. The rate of activity of these reducing enzymes may be partly responsible for limiting N source uptake [161]. Alternatively, algae may preferentially uptake certain forms to make an energetic saving per unit N assimilated.

A similar trend, to those described above, has been found when macro-algae are cultivated in media containing dual nitrogen sources; whereby $NH_4^+$ is removed preferentially ahead of $NO_3^-$ [160, 196]. Indeed, the presence of $NH_4^+$ in the media may suppress $NO_3^-$ uptake [66, 197]. For instance, Smit [198] found a 38% suppression of $NO_3^-$ uptake by *Graciliaria gracilis* in the presence of 5 µM $NH_4^+$. Whereas, Raven *et al.* [199] suggested complete suppression of nitrate uptake by micro-algae in 1000-2000 µM $NH_4^+$. The reason(s) behind this suppression remains uncertain and requires further study.

Nitrogen source preference by macro-algae is complex and may be influenced by: abiotic factors such as light and N form, in addition to species-specific morphology, shore-line position, competition for resources, seasonality, nutritional or life- history, and the physiological capacity and energetic requirement for assimilation of nitrogenous sources [160, 161, 180, 193, 195, 196, 200]. In order to improve potential WWT efforts, further research is required to understand the roles of these factors and to determine which of these takes precedence. Alternatively, species which exhibits excellent bioremediation performance and indiscriminate nutrient removal should be sought.

## 1.4.2 Biochemical Composition

In order to assess the suitability of the biomass produced for certain uses or commercial purposes (section 1.3.), it is necessary to determine its biochemical composition. In an early study Atkinson and Smith [201] analysed the C:N:P ratio of 92 different macro-algal samples, collected from across the globe (Fig. 1.11). The purpose of their study, was to determine if the composition of marine macrophytes is similar to that of the “Redfield

ratio" [202], which is 106/16/1, C/N/P. The Redfield ratio is a biological oceanographic concept in which both planktonic organisms and the marine waters in which they dwell have a closely correlated and characteristic atomic ratio, given the reciprocity of interactions (*i.e.* net nutrient uptake) [203, 204]. However, Atkinson and Smith [201], on studying a wide range of marine algae found large variation in compositional ratios ranging from 183:9:1 to 3550:61:1, with an average of approximately 700:35:1 (Fig. 1.11). This variation is, perhaps, unsurprising given the environmental, seasonal, nutritional, and species-specific variability between the samples (section 1.4.1), which will doubtless have a bearing upon the biochemical composition of the organisms.

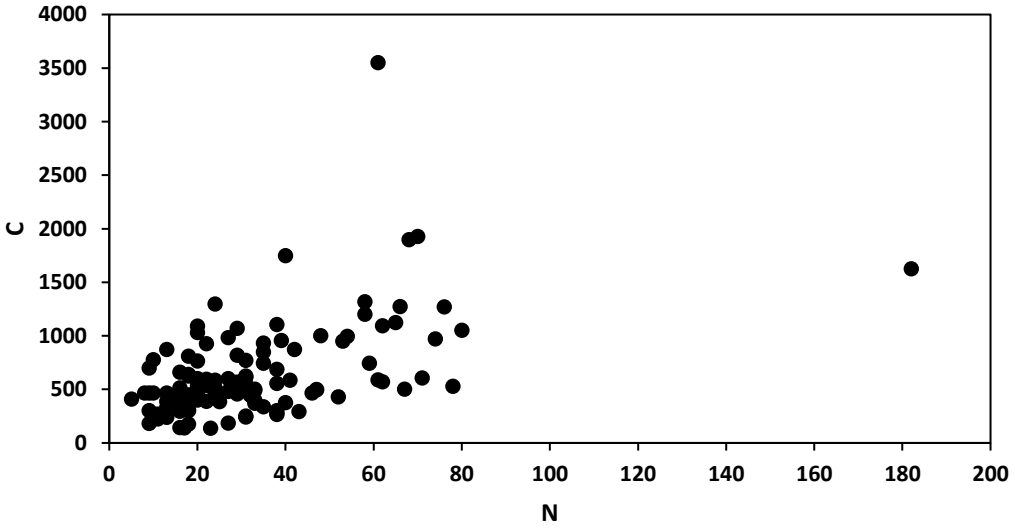


**Figure 1.11**. The atomic C/N values 92 macro-algal species relative to P. Data from Atkinson and Smith [201].

A number of studies have demonstrated seasonal variation in the biochemical composition of macro-algae [103, 105, 173, 205, 206]. For example, Schiener *et al.* [103] observed that across a 14 month time-frame the tissue C and N % of *Saccharina latissima*, *Laminaria digitata*, and *Laminaria hyperborea* ranged from 21.1-30.5% and 0.8-2.2%, 24.5-36.4% and 1.0-2.5%, and 21.8-38.6% & 1.0-2.1%, respectively. This seasonal variability is to be expected, given the inherent change in light (intensity and photoperiod), temperature, salinity, and nutrient concentration (section 1.4.1.).

The N source may also have an influence on the composition of the algal biomass [192, 207]. Although no differences were observed in *Chondrus crispus* biomass, in the same study, Corey *et al.* [196] reported that the composition of *Palmaria palmata* varied

depending upon the N source composition, for example: the tissue N % was either 3.1 ±0.11%, or 4.1 ±0.09% when cultivated under equivalent concentrations of either $NH_4^+$ or $NO_3^-$, respectively. Interestingly, the C content of the biomass was almost identical under the two regimes (36.6% and 36.8%). It is unclear whether or not the N type is directly responsible for this response, or if it is a factor of total N uptake, as $NH_4^+$ was removed at a significantly greater extent in comparison to $NO_3^-$. A similar result was reported by Abreu *et al.* [192], whereby *Gracilaria vermiculophylla* cultivated under $NH_4^+$ had a greater N content, in comparison to cultivation in $NO_3^-$ containing medium; however, this also in coincided with greater levels of $NH_4^+$ removal.

Studies have also indicated that the atomic composition of biomass reflects the concentration of nutrients provided, which validates the underlying theory of the Redfield ratio [27, 65, 208, 209]. The N and P content of biomass mirrored the N/P ratio supplied [27]. Additionally, the N content on *Ulva lactuta* biomass increased in conjunction with greater $NH_4^+$ supplied in the medium [60]. Micro-algae are able to accumulate large amounts of lipid when cultivated under N-deprivation and they have received considerable interest into potential conversion into biofuels (*i.e.* biodiesel) (section 1.3.1.). There is generally a trade-off between micro-algal cell growth and lipid accumulation; so whilst the lipid content of the cells may increase, the overall lipid productivity may remain the same, due to cessation of cell division [210-213]. In contrast, macro-algae synthesise proteins and pigments when N is sufficient and accumulate storage polysaccharides, such as starch, when they are under N-limitation [214, 215]. Macro-algal cultures that have been cultivated under nutrient replete conditions may be suitable for food and fertiliser purposes, whereas those that have been N-starved may be better for conversion into biofuels via digestion or fermentation processes.

Finally, algae may exhibit time-resolved changes in their biochemical composition during a single growth phase [216]. Mayers *et al.* [191] demonstrated this over a 10-day growth period with the micro-alga *Nannochloropsis* sp.; whereby cultures initially increased in protein content at the expense of lipid and carbohydrate. However, this trend was reversed from day 4 onwards as carbohydrate, and especially lipid, were deposited within the cell, with a simultaneous reduction in protein content. These changes are due to initial uptake and depletion of both N and P, coupled with their strategic partitioning within the cell.

Changes in biomass composition are not immediate, they are gradual and continuous across a growth period. The rate and extent of these changes are dependent upon the species, nutrient regime, as well as other physical, chemical and biological factors that have been outlined above. As such these present numerous strategy or management decisions. For example, what sort of cultivation regime do you select, batch, continuous, or semi-continuous? After selection of species, cultivation conditions and supply of nutrients; when do you harvest to ensure maximum growth and product yield, and what do you base this decision upon? Incubation time? Biochemical composition? Concentration of nutrient in the substrate? The apparent health of the culture? A combination of these? The fact is that all of these criteria are variable too, or they make take time to assess, by which time they may be invalid. There is no correct answer. In addition to learning from past and present algal cultivation practices, continued research into the influence of all factors on algal biology can only improve our decision making processes and therefore make algal WWT (any algal cultivation for that matter) a more achievable reality.

## 1.4.3 Macro-algal WWT In Practice - Aquaculture

### *1.4.3.1 Aquaculture*

Aquaculture is the fastest growing animal food production sector worldwide (Fig. 1.12A.) [11]. It already plays a critical role in global food provision and its importance is expected to grow as increasing pressure is placed on food security [15, 217, 218]. This is being further stimulated by growth in the human population combined with an overexploitation of wild fish stocks resulting in a stagnation in captures from fisheries (Fig. 1.12B.) [15, 219, 220]. Although, aquaculture is a potentially viable option to address demands for protein sources in particular, it is not a “silver bullet” for food security. It is a relatively new industry [15], and as such has several significant controversial issues surrounding it. For instance, invasion or inter-breeding of non-native species or escapees, coastal erosion or degradation, and eutrophication (Fig. 1.1.) caused by uneaten food and excretory products [14, 15, 221-225]. In an effort to improve the sustainability of aquaculture industry, there is a lot of ongoing

research, including approaches which maximise the value of products that can be generated, such as integrated multi-trophic aquaculture (IMTA) [218].

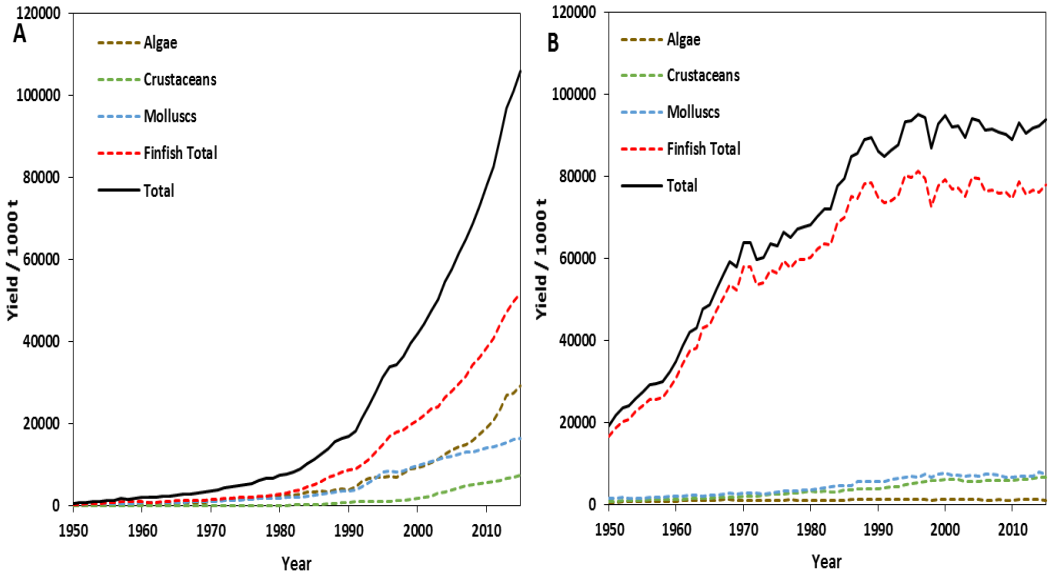


**Figure 1.12.** Global production yields obtained from aquaculture (A) and fisheries (B). Data from [12, 13].

### *1.4.3.2 Integrated Multi-Trophic Aquaculture (IMTA)*

IMTA can be considered as the co-cultivation of aquatic organisms that occupy different trophic levels [218, 226]. The principle is that waste products, or uneaten food from the primary cultivation species (*e.g.* crustaceans and finfish), will be recycled by organisms from a lower trophic level. For instance, molluscs will filter feed particulate matter, whereas macro-algae will assimilate soluble nutrients (Figure 1.13.) [35, 226]. This synergism will have the co-benefit of mitigating waste whilst concomitantly producing an additional potentially commercially viable product (section 1.3.) [227].

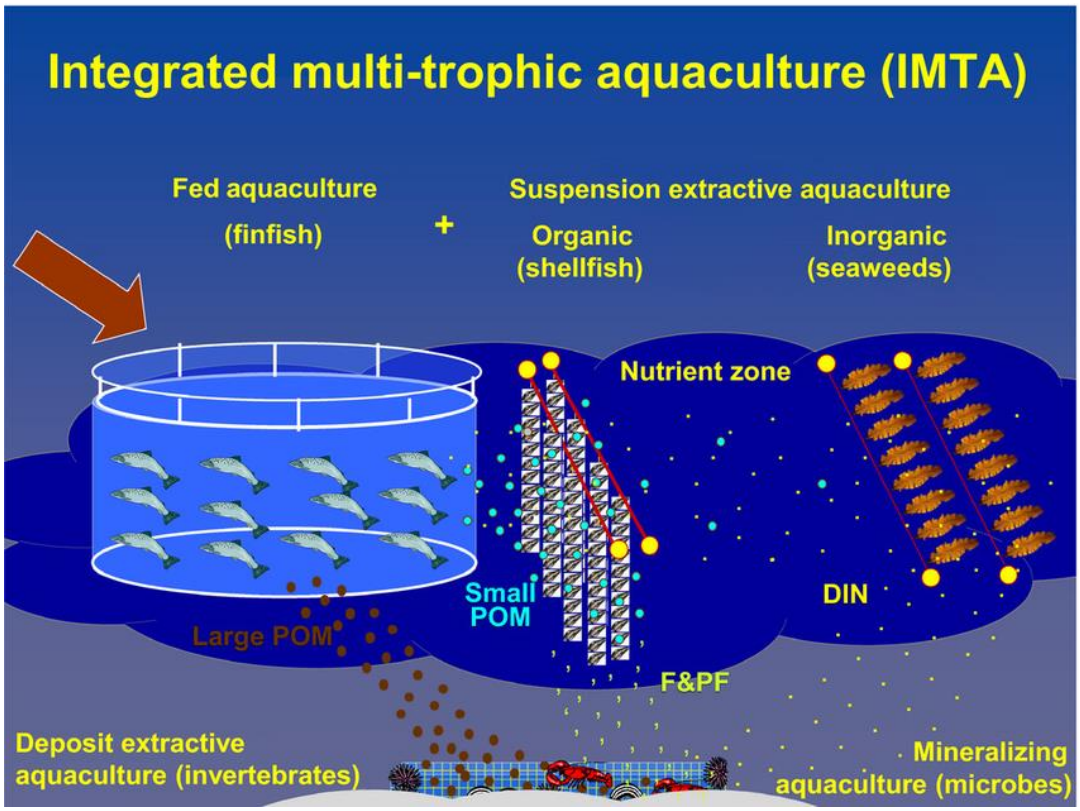


**Figure 1.13.** A hypothetical schematic of integrated multi-trophic aquaculture (IMTA), involving the culture of finfish, particulate removal by molluscs or crustaceans, and solubilised nutrient extraction by seaweed. Image from Chopin [228].

There has been a considerable body of research into IMTA systems over the last 20-30 years, which has coincided with the boom of the aquaculture industry (Fig. 1.12.). These studies typically involve either molluscs or seaweed, or combinations of the two to remediate wastes produced by the primary aquaculture organism, which includes molluscs [229], crustaceans [14, 66], or more commonly finfish [16, 33, 35, 37, 65, 175, 196, 225]. IMTA studies have had mixed success. For example, in an early two-part study the performance of *Ulva lactuta* was tested, under a series of conditions, to grow and remediate fishpond effluents [175, 230]. The authors reported algal growth rates ranging from 2.5 – 17.9% $d^{-1}$, and a weekly $NH_4^+$ removal of 39-96%. This variability was due to the different experimental parameters tested including stocking density, number of daily water exchanges, and influent concentration of $NH_4^+$ (section 1.4.1.). In a subsequent study by Msuya and Neori [37], four different macro-algal species were tested to ameliorate fishpond effluents in Tanzania. However, two of the species failed to grow, possibly caused

by buoyancy issues, or an intolerance to fluctuations in pH, salinity, and nutrient concentration.

There has been a lot of variability in the successes of IMTA applications. For instance, rates of algal growth have ranged from 0.4-17.9% $d^{-1}$ [175, 229], whilst N removal has been in the range of 2.4-99% $d^{-1}$ [16, 37] (Fig. 1.14A and B). The results indicate a high variability in performance, which is unsurprising given the manifold complexity of algal biology (section 1.4). Additionally, there are a multitude of aquaculture system designs and primary and secondary species selection, feeding regimes and hence nitrogenous inputs, and their implementation into the system which introduces another level of complexity.

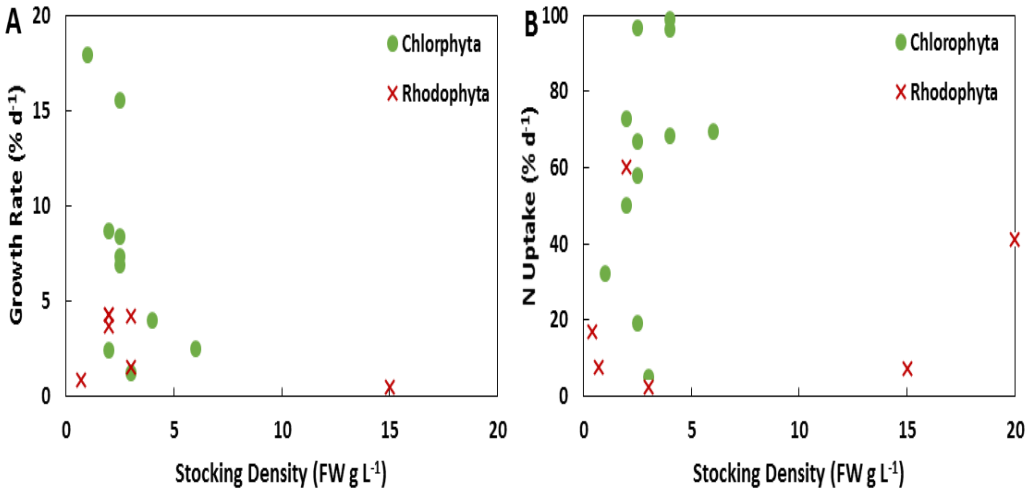


**Figure 1.14**. The variation in reported rates of growth (A) and nitrogen uptake (B) by green and red macro-algae when integrated into aquaculture systems or cultivated in their effluents.

Nevertheless, studies are unanimously positive about the potential for integrating macro-algae into aquaculture systems, due to their capacity for high rates of growth and nutrient sequestration and therefore their ability to improve water quality, as well as being a potentially financially valuable commodity [14, 41, 175, 192, 225, 229, 230]. A number of challenges still need to be resolved prior to any successful implementation of IMTA systems, including appropriate species selection [14, 37, 229], seasonality or capacity for algae to efficiently treat water year-round [35, 65], and cultivation conditions [14, 33, 37, 66].

### 1.4.4 Conclusions

Macro-algal bioremediation has great potential and merits further investigation. However, given the complexity and inter-relatedness of environmental and wastewater conditions and their influence upon algal biology as a whole, an holistic approach to species selection should be employed. Collecting wild cultures found in effluent streams or screening for potential species based on their inherent hardiness and tolerance of fluctuations in environmental conditions should be the first and most fundamental step [52, 58, 231]. Followed by testing their capacity for nutrient removal under a range of nutrient regimes, and therefore how broadly applicable they are for bioremediation, as well as compositional analysis for an insight into their possible applications and financial return.

## 1.5 Macroalgal WWT – Metal Removal

Growth in industries such as energy (petrochemical, atomic, and nuclear), battery, fertiliser, and electrical appliance manufacturing, metallurgy and mining has led to an increase in metal bearing pollution [1, 21]. High concentrations of 18.9-47.7 and 15.8-32.2 mg $L^{-1}$ of copper and lead, respectively, were found in engineering, dye, and chemical manufacture, and paper mill effluents (Table 1.1.) [232]. Furthermore, toxic or heavy metals concentrations in surface waters, across the world, are often in excess of the drinking water quality guidelines prescribed by the World Health Organization (WHO) [233] and the United states Environmental Protection Agency (USEPA) [234] (Table 1.1.). In addition, heavy or toxic metals are highly persistent in nature and can accumulate in the food chain [140].

Whilst a variety of metals, such as copper, iron, and manganese are essential for normal metabolic functioning [235-237], deficiency or over-exposure to these metals, through ingestion, inhalation, and absorption, can be detrimental for human health [24]. For example, acute copper intoxication may have gastrointestinal effects [235]. Whereas, excessive concentrations of manganese can cause a neurodegenerative disorder called Idiopathic Parkinson's Disease [235, 238]. Non-essential metals are also high toxic to human life and chronic or acute lead toxicity is known to damage organs, inhibit haemoglobin synthesis, induce neurological disorders including psychosis and brain damage, in addition to its teratogenic effects and retardation of development of children [24]. It is therefore, of

paramount importance to remove metals from wastewater streams in order to preserve health of both humans and the ecosystem as a whole.

**Table 1.2.** Concentrations of metals found in surface waters and industrial effluents and their permissible limits in drinking water.

| Water Type | Copper ($mg\ L^{-1}$) | Manganese ($mg\ L^{-1}$) | Lead ($mg\ L^{-1}$) | Refs |
|---|---|---|---|---|
| **Surface Waters** | 0.002 - 3.95 | 0.023 – 0.712 | 0.0003 – 0.4 | [239-243] |
| **Industrial Effluents** | 18.9 – 47.7 | | 15.8 – 32.2 | [232] |
| **Drinking Water Quality** | 1 | 0.05 | 0.01 | [233, 234] |

## 1.5.1 Conventional Treatment Technology

Current metal removal/reclamation technologies employ adsorption onto activated carbon, chemical oxidation and reduction, electroplating and electrochemical processes, evaporation, ion exchange, membrane technologies, and precipitation (Table 1.2.) [244, 245]. These technologies are all problematic, for instance, chemical precipitation, electrochemical, and membrane technologies tend to have high capital or operational costs and can generate large volumes of toxic sludge, which requires additional treatment [246] *e.g.* chemical precipitation using lime produced 93-288 ml $L^{-1}$ of sludge [247]. Ion exchange resins have poor removal efficiency when used to treat large volumes of water containing a low concentration of metal ions. In addition, the resins have to undergo chemical regeneration once they are “exhausted”, which also leads to the development of secondary pollution [246]. Adsorption onto activated carbon is a promising method for metal removal, but is prohibited by the high cost of suitable material or pre-treatment processes; this has stimulated interest in research for low-cost adsorbent material [246]. Given the various shortcomings of conventional treatment technologies, there is a need to improve existing methods or to develop novel techniques for the treatment of metal laden water.

## 1.5.2 Biosorption

One option which has received a lot of academic interest, but little industrial application is biosorption [143]. Biosorption can be thought of as the removal of substances from solution by material of a biological origin; living, dead, or biologically derived, *e.g.* alginate

[21, 143, 248]. Practically all biological material has an affinity for metals; so, there is an almost limitless possibility for the choice of biosorbent material [143]. However, there are certain characteristics which are desirable when selecting a biosorbent, such as general abundance, year-round availability, high surface area, high metal removal performance and low cost [143]. Algae fulfil many of the desirable criteria that are sought after in a biosorbent. For instance, they are incredibly diverse, abundant, renewable, and are already cultivated/harvested on a large-scale (section 1.3. and Figs. 1.6., 1.7., and 1.12.); biomass, by-products, or residues from applications could be employed as a low-cost biosorbent material.

Biosorption is a physico-chemical process; its mechanisms for metal removal include; ion exchange, adsorption, absorption, surface complexation and precipitation [143, 249]. Metals typically bind to several different functional groups of the biosorbent surface, including carboxyl, amine, imidazole, phosphate, sulfhydryl, sulfate and hydroxyl groups, which are all typically present on algal cells [21]. In addition, each of these functional groups will have different metal affinities and specificities [250].

Biosorption occurs in a two stage process (Fig. 1.15.); with an initial stage of rapid, passive, bonding is attributed to chemical ion exchange and adsorption onto the cell surface, until an equilibrium is established between the amount of metal ions adsorbed on the sorbent surface and those that remain in solution [142, 245]. The second phase is an active process and is metabolism-dependent, whereby metal ions will be transported across the cell membrane and into the cytoplasm. This second phase is often referred to as "bioaccumulation", which being metabolism-dependent will not apply to dead material [142, 249, 251].

Studies involving algal biosorption have had varied results. For example, the maximum metal sorption capacity (*Qmax*), ranged from 0.004-2.77 mmol $g^{-1}$ for copper and 0.0002-2.9 mmol $g^{-1}$ for lead achieved on using algal biomass (Fig. 1.16) [252-254]. The variation in results obtained is due to differences in experimental design employed in each study, with the rate and extent of biosorption being strongly influenced by physical, chemical, and biological factors [251, 255], many of which will be discussed below.

**Table 1.3.** Metal removal by conventional treatment technologies.

| Method | Metal | Concentration (mg $L^{-1}$) | pH | Variable Parameter | Removal (%) | Ref |
|---|---|---|---|---|---|---|
| **Activated Carbon** | | | | **Biosorbent Dose (g $L^{-1}$)** | | |
| ASAC | $Cu^{2+}$ | 100 | 4.9 | 1 | 97.5 | [256] |
| ASAC | $Pb^{2+}$ | 100 | 4.3-6.5 | 1 | >99.9 | [256] |
| CACSC | $Zn^{2+}$ | 25 | 6 | 30 | 90 | [257] |
| CCSC | $Zn^{2+}$ | 25 | 6 | 30 | 75 | [257] |
| **Chemical Precipitation** | | | | **Precipitant** | | |
| | CuEDTA | 100 | 3 | 1,3,5-hexahydrotriazine dithiocaramate | 99.6 | [258] |
| | $Cu^{2+}$,$Pb^{2+}$,$Zn^{2+}$ | 100 | 7-11 | Fly-ash lime carbonate | 99.37-99.69 | [247] |
| **Electrochemical** | | | | **Current** | | |
| Electro-flotation | $Cu^{2+}$ | 100 | 6 | 300 mA | 98-99 | [259] |
| Electro-coagulation | $Mn^{2+}$ | 100 | 7 | 6.25 mA/$cm^2$ | 78.2 | [260] |
| **Ion Exchange** | | | | **Clinoptilolite (g $L^{-1}$)** | | |
| | $Pb^{2+}$ | 1036 | 4 | 20 | 55 | [261] |
| | $Zn^{2+}$ | 65.4-654 | 5 | 25 | 100 | [262] |
| **Membrane** | | | | **Pressure (bar)** | | |
| RO + NF | $Cu^{2+}$ | 15 | 5 | 3.8 | 95-99* | [263] |
| RO | $Cu^{2+}$ | 100 | 6 | 6 | 85 | [264] |
| RO | $Cu^{2+}$ | 500 | 7.8 | 5 | 98.6 | [265] |

ASAC = Apricot Stone Activated Carbon, CACSC = Acid-treated Chitosan Coated Coconut Shell Carbon, CCSC = Chitosan Coated Coconut Shell Carbon, RO = Reverse Osmosis, NF = Nanofiltration. * = Treatment coupled with filtration and flotation.

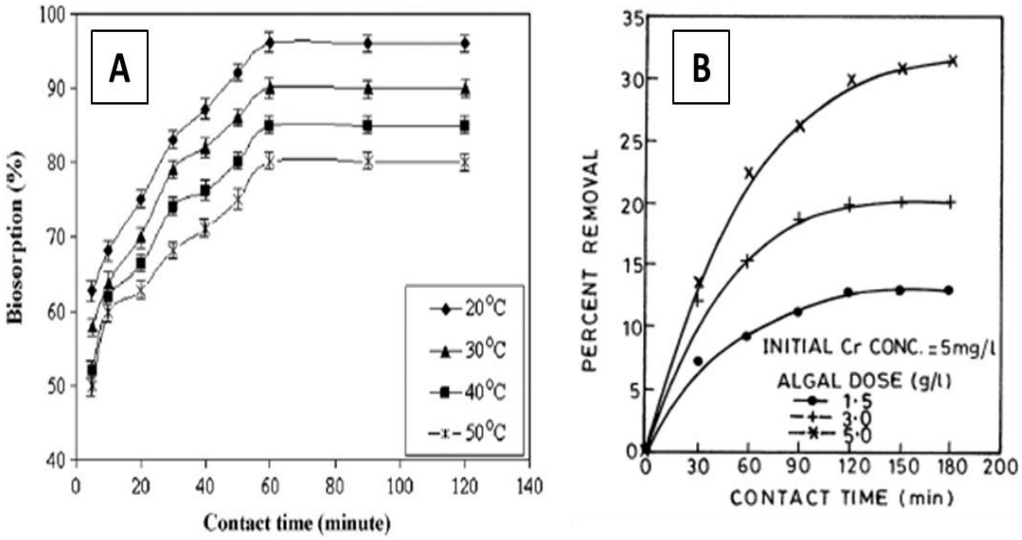


**Figure 1.15.** Examples of the rate of biosorption: A) temporal removal of 10 mg $L^{-1}$ $Se^{4+}$ ions by 8 g $L^{-1}$ of dried *Cladophora hutchinsiae* biomass under different temperature conditions [266], B) temporal removal of 5 mg $L^{-1}$ $Cr^{6+}$ ions from solution by dried *Spirogyra* sp., with a variable biosorbent dose [267].

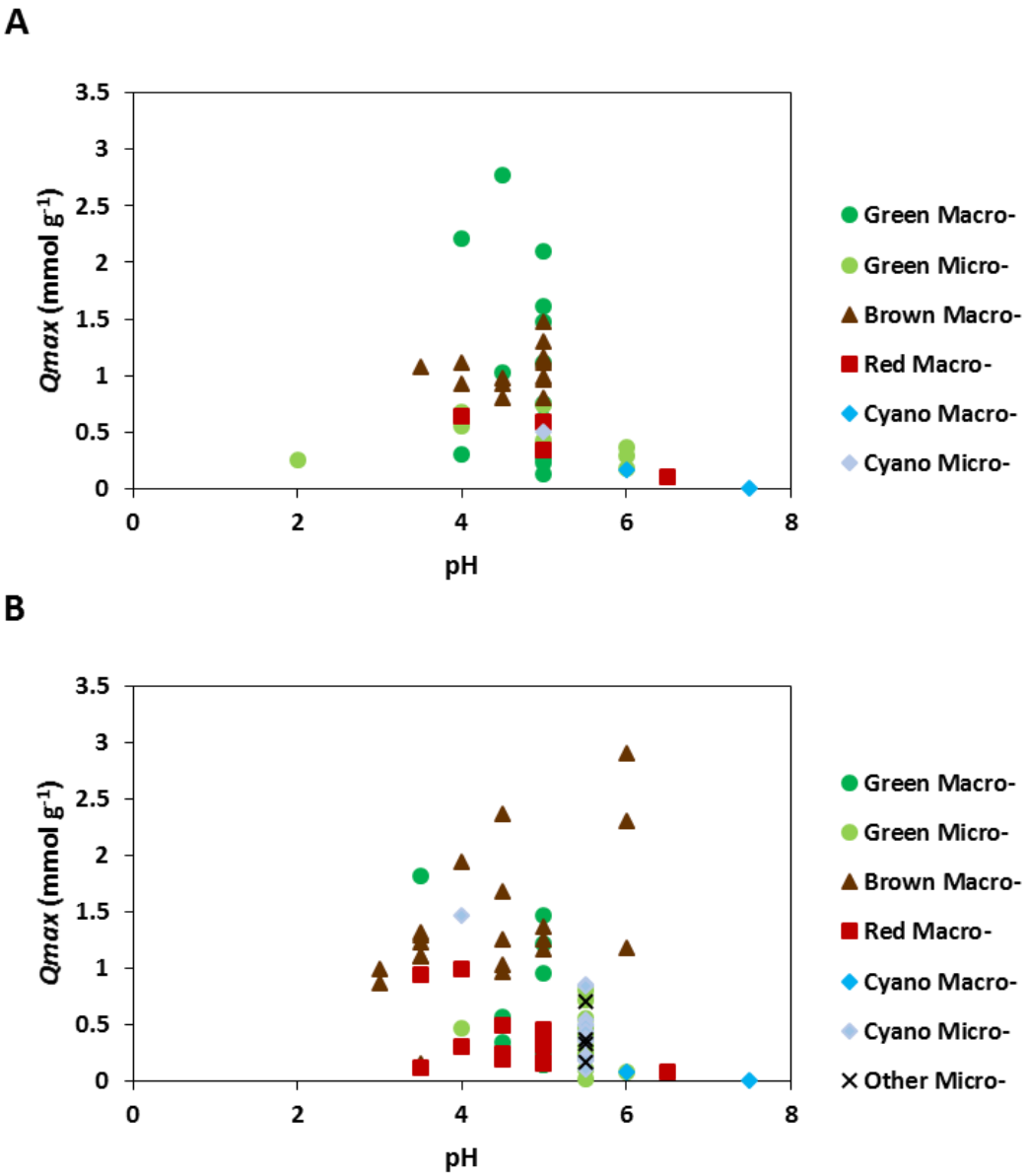


**Figure 1.16.** The maximum sorption capacity of algal biomass for copper (A) and lead (B) across a range of different pH. Data obtained from [67, 244, 251-254, 268-296].

## 1.5.3 Physico-chemical Parameters Affecting Biosorption

### *1.5.3.1 pH*

Biosorption is perhaps most strongly influenced by the pH, as many of the functional groups responsible for metal binding are acidic (*e.g.* carboxyl) and their availability is pH dependent; being negatively charged in acidic conditions. Therefore, interactions occur between the negatively charged surface groups and the positively charged cationic metal species [142]. Secondly, the speciation of metal ions in solution and their bioavailability is determined by pH [297]. In addition, metallic complexes generally become less soluble with increasing pH, leading to precipitation [298]. This makes it difficult to discern between metal removal by biosorption, or via precipitation [298]. Finally, extremes of pH may cause cellular damage to the biosorbent material, amending their structural and functional group properties and hence their capacity for biosorption [298].

### *1.5.3.2 Initial Metal Concentration*

The removal of metals from solution by biosorbents is very dependent upon the initial metal concentration, $C_0$ [299]. Generally, metal biosorption follows a Langmuir-type curve whereby removal increases with increasing metal concentration, until equilibrium concentration (*Ce*) is reached [142, 273]. For example, the amount of $Cu^{2+}$ and $Zn^{2+}$ sorbed at equilibrium (*Qe*) by living *Cladophora fracta* increased from 0.23-2.388 and 0.213-1.623 mg $g^{-1}$, respectively, when the initial concentration, $C_0$, increased from 1 to 10 mg $L^{-1}$ [277]. Whereas, Özer *et al.* [251] noted incremental $Cu^{2+}$ adsorption employing dried *Cladophora crispata* until a $C_0$ of 200 mg $L^{-1}$ where plateau was reached. This plateau is caused by a saturation of possible binding sites for metal sorption [251].

### *1.5.3.3 Biosorbent Dose*

Generally, increasing the amount of biosorbent material results in a greater absolute removal of metal ions (Fig. 1.15B); however, the removal per unit of biosorbent biomass

decreases [142]. For instance, the maximum metal sorption (*Qmax*) achieved by dried *Chlorella vulgaris* for $Ni^{2+}$ and $Cu^{2+}$ ions reduced from 23.47 to 8.91 mg $g^{-1}$ and 89.19 to 6.5 mg $g^{-1}$, respectively, when the amount of biosorbent employed was increased from 5-1000 mg $L^{-1}$ [300]. There are several reasons attributed for this reduction in specific metal sorption including; competition of ions for available binding sites [301], a reduction of the sorption area caused by the formation of aggregates [274], as well as, limited metal availability, increasing electrostatic interactions and a reduction of mixing [142, 299]. Therefore, optimising the amount of algal biomass used to maximise absolute metal removal, as well as per unit biosorbent, is essential and would improve the feasibility of employing algal biosorption in practice.

### *1.5.3.4 Presence of Co-existing Anions and Cations*

The presence of co-existing ions will influence the effectiveness of biosorption. These may have an antagonistic, synergistic, or non-interactive effect on the biosorption of metal ions [142, 143]. Importantly, these interactions cannot be accurately predicted from single-metal studies alone, and can only be understood from multi-element solutions [299]. Klimmek *et al.* [67] noted the following order of metal removal with freeze-dried *Lyngbya taylorii* biomass: Pb >> Cd ≥ Zn > Ni. However, in a three metal system, in the absence of Pb, there was greater uptake of Zn than Cd. Aksu and Dönmez [302] found a similar trend; that dried *C. vulgaris* could bind $Cd^{2+}$ and $Ni^{2+}$ ions simultaneously; however, the uptake capacity for each metal was reduced when compared to their respective individual solutions. In related studies, the influence of co-existing ions on metal removal by dried *Cladophora fascicularis* was assessed [244, 273]. Various concentrations of cations $Na^{+}$, $K^{+}$, and $Mg^{+}$ and anions $Cl^{-}$, $C_2O_4^{2-}$, and $NO_3^{-}$ had negligible impact on metal removal. However, 10 mmol $L^{-1}$ concentration of $Ca^{2+}$ resulted in a 10% and 26% reduction in $Cu^{2+}$ and $Pb^{2+}$ removal, respectively. This was considered to be caused by a competitive exclusion for binding sites and the authors observed a 75-80% reduction in metal sorption with the presence of the chelating agent 10 mmol $L^{-1}$ EDTA, which combines more strongly with metals than the biosorbent does [244, 273].

Wastewaters are highly complex environments, containing a multitude of different nutrients and metals. Understanding the relationships between co-existing ions as well as

interactions between sorbent and sorbate can only stand to improve algal biosorption. Most studies have stated that interaction between co-existing ions and biosorbent material is strictly a chemical process, due for instance to binding site exclusion or chelation. However, there has been little, if any, investigation of any biological influence. Can algal biomass be tailored (genetically, bio-engineered, or cultivated) to produce a greater number or specific type of functional group per cell? This may improve algal biosorption and also opens up avenues such as targeting specific contaminant removal/recovery.

### *1.5.3.5 Temperature*

There have been conflicting results regarding the role of temperature on biosorption [303-306]. In separate biosorption studies conducted by the same authors on dried *Chlorella vulgaris*, it was reported that there was a decrease $Cd^{2+}$ removal, with the *Qmax* reducing from 111.1 to 76.9 mg $g^{-1}$ when the temperature was raised from 20°C to 50°C [304]. Whereas, the opposite effect was observed for $Ni^{2+}$ removal, where the *Qmax* increased from 54.8 to 63.25 mg $g^{-1}$ coinciding with a temperature increase from 15-45°C, it was suggested that bonds were possibly ruptured leading to an increase in availability in binding sites [303]. Temperature interactions on metal biosorption with dried biosorbents remain unclear. However, a biosorbent material which exhibits optimal metal removal at ambient temperature would be desirable, as heating/cooling will incur a cost.

Temperature will likely play a more significant role with viable biomass, in comparison to non-viable or dried material, owing to the influence of metabolism (section 1.4.1.1) and likelihood of cell injury at temperature extremes [142, 307].

### *1.5.3.6 Contact Time*

As outlined in section 1.5.2, biosorption is biphasic. Incubation time will not influence the rate or amount of biosorption *per se*; it is nevertheless an important process factor. For instance, sorption equilibrium will not be attained if the biosorption reaction is stopped prematurely, whereas extended incubation may lead to an inefficiency in metal removal. The time taken to reach equilibrium is dependent on the physico-chemical factors discussed

throughout this section. Typically, steady-state is reached in less than one hour (Fig. 1.15A.) [67, 244, 266, 273, 276, 308, 309]. However, in the cases of Gupta *et al.* [267] (Fig 1.15B) and Jalali *et al.* [293] in their studies on $Cr^{6+}$ removal with *Spirogyra* sp. and $Pb^{2+}$ with *Sargassum hysterix,* equilibrium was attained after 3 hours. The selection of a suitable incubation time will be critical for research and in practice. For instance, extended contact times may reduce the overall process efficiency. Whereas, stopping the reaction prior to a steady-state being attained will result in an underestimation in the metal removal capacity of the biosorbent.

### *1.5.3.7 Others/Biological Factors*

There are additional physical or chemical factors that will influence biosorption and these include: agitation/shaking, the properties of the biosorbent itself such as particle size and if it has undergone any chemical and mechanical modification, or pre-treated in another way such as immobilization [142, 249, 284, 310, 311]. Furthermore, parameters such as light intensity and hours of light, in addition to the provision of nutrients (which may or may not influence the physical act of sorption – Section 1.5.3.4), will be important for living algal biomass. These influence rates of photosynthesis, metabolism and growth (section 1.4.1), therefore the construction of new binding sites and metal removal via bioaccumulation [312]. Additionally, viable algae may exhibit a tolerance or resistance to the toxic effects of metals after chronic exposure, increasing their capacity for metal removal [140, 313].

Very little attention has been paid to the biological influence in macro-algal metal biosorption. Brinza *et al.* [249] mentioned that biological variation may have an important effect on biosorption, stating that algae from various growth stages, or different tissue parts, may have different properties and that seasonality may also influence their characteristics. Whereas, the review by Mehta and Gaur [142] suggested that algal cultivation conditions may influence the cell wall properties and therefore their efficacy as a biosorbent. However, there is a dearth of research in this area. For instance, the vast majority of studies involving macro-algal biosorption obtained biomass from the field, typically material that has washed up on the shore, or collected from irrigation channels [251, 281, 301, 314]. The use of field material offers too many unknowns and is therefore fundamentally flawed. For example, in studies utilising wild biomass, no data is provided on

the duration of time the material has spent washed ashore, the degree of decomposition, or presence of micro-organisms which may influence metal removal performance [281]. Furthermore, it is unknown whether the collected material has been previously exposed to contaminants, including heavy metals. This may result in binding site exclusion of other ions, reducing its performance as a biosorbent material (section 1.5.3.4). However, perhaps most crucially is the lack of data surrounding the life history, nutrient regime or environmental conditions in which the collected biomass was cultivated. As previously discussed, these parameters will have a strong bearing upon the biochemical composition of the biomass and therefore the functional groups present (section 1.4.2), which will then affect its biosorption performance. Unfortunately, employing wild macro-algal biomass is commonplace in macro-algal biosorption studies. As such, there is a lack of clarity in understanding of the mechanisms involved in algal biosorption, in addition comparison between studies is problematic.

## 1.5.4 Conclusions

Biosorption using algal material is viewed as a promising technology that could negate some of the disadvantages present in conventional metal treatment technologies. Algae have interesting cellular properties giving them high metal sorption capacities [144, 315, 316]. In addition, algal biomass is renewable, generally abundant and could serve as a low-cost biosorbent material. For instance, nuisance algal blooms such as those experienced in China prior to the 2008 Olympic Games (Fig. 1.17) could be harvested and used. Additionally, algal biomass, by-products, or residues from industrial-scale algal cultivation and processing (section 1.3) could serve as a low-cost material. Coupling nutrient bioremediation with metal removal, or utilising algal biomass that has been propagated on wastewater streams is an attractive prospect that could prove to be an ecologically and economically sustainable green solution to wastewater treatment which remains under-explored.

**Figure 1.17.** An image of the removal of a nuisance algal bloom of *Ulva prolifera* from the coastal region of Qiandao, China, between May-July 2008, which threatened the preparation of sailing events in the Olympic Games. Approximately 1 million fresh weight (FW) tonnes of seaweed were removed [317]. Image from [318].

## 1.6 Thesis Objectives

The overarching aim of this work was to investigate the effectiveness of filamentous macro-algae for removing nutrients and metals from synthetic wastewaters. In order to achieve this, the following key objectives of this thesis are outlined, as follows:

- To develop and standardise a suite of methods that will facilitate achieving the following objectives.
- To identify a potential candidate species that have desirable physiological characteristics for wastewater treatment. Then to test the feasibility of the species for bioremediation, by measuring its tolerance to a range of abiotic factors that may be encountered in a WWT scenario.
- To assess the capacity for nutrient removal by the candidate species and investigate what influence the nutrient regime has on nitrogen removal, growth, and biochemical composition of the biomass, with a view for future biomass applications.

- To assess the capacity for heavy/toxic metal removal by the candidate species after it has been grown under different cultivation conditions. In order to elucidate how much of an effect life-history has on the cellular properties of the biomass and how much this will influence its efficacy as a biosorbent material.

## 1.7 Thesis Structure

In order to achieve the aforementioned objectives, a "back to basics" experimental approach was employed, and is described in the thesis structure, as follows:

- **Chapter 1 – Introduction:**

  A literature review, which has focussed on four main aspects. Firstly, identification of the driving forces behind this research, namely adverse health and environmental effects that have arisen through increasing levels of nutrient and metal pollution, and the potential for algal mitigation of these contaminants. Secondly, algal diversity and a current perspective on their production and uses. Thirdly, physical, chemical, and biological factors that influence algal nutrient uptake, growth, and metabolism, with an emphasis thereafter on their implementation in integrated treatment systems. Finally, an overview on conventional methods for heavy metal treatment, introducing the concept and factors influencing biosorption.

  This review is not intended as an exhaustive dossier on wastewater treatment, nor was it designed to give a complete account of algal bioremediation. Its main purpose was to introduce the reader to the intricacies of algal biology and the influence of biotic and abiotic factors, the dynamism of wastewaters streams, and how these all intertwine with one another to make algal bioremediation a myriad of complexity.

  Although there is a wealth of literature related to a various aspects covered throughout this thesis, there is however a dearth of applicable or ecologically relevant studies. This shortfall is alluded to throughout the literature review. However, each subsequent chapter will have its own dedicated introduction which refreshes and re-frames the problem.

- **Chapter 2 – Materials and Methods:**

  Gives an account of the methods that were common throughout the experimental chapters. Specific methods or cultivation conditions are given in each subsequent chapter. Method development, calibration curves, and protocols for standardisation are included (Appendices E-H).

- **Chapter 3 – Abiotic Screen:**

  Gives an account on the rationale behind selecting *Cladophora* sp. as a candidate for implementation into WWT applications. The tolerance of *Cladophora coelothrix* and *Cladophora parriaudii* to a range of abiotic conditions was then investigated; therefore, assessing the species suitability.

- **Chapter 4 – Investigating Methodologies for Fresh Weight Determination:**

  Entails the development of a methodology for periodical harvesting and dewatering algae, which has minimal impact upon the functionality of the culture, in terms of growth, nutrient uptake and structural integrity. This allows for higher resolution for growth and nutrient uptake for use in the thesis and future macro-algal study.

- **Chapter 5 – Nutrient Removal:**

  To examine the ability of *Cladophora* to remove nutrients from growth media. Achieved by measuring growth, nutrient removal, and biochemical composition of algal cultures maintained under a range of nutrient regimes. Experimental media was formulated with a range of N/P ratios, N concentrations, and N forms. Mixtures of nitrogen sources were also employed to determine whether *Cladophora* exhibited a preference towards a particular N form, and what were the potential underlying reasons.

- **Chapter 6 – Metal Removal:**

  To test the biosorption capacity of *C. parriaudii*. To highlight the importance of prior nutritional history in metal removal studies. Demonstrating that changes in nutrient regime will elicit a response in the biochemical composition of the algae,

and hence quality/quantity of functional groups present on an algal cell, therefore influencing the efficacy of biosorption.

- **Chapter 7 – Conclusions and Future Work:**
  Finally, the findings of the thesis are discussed sequentially. In addition, future research avenues have been identified to improve the feasibility of algal WWT.

## 1.8 Novelties of this Work

There were several novel research outcomes that were produced from this Ph.D. research, these include:

- The selection of *Cladophora coelothrix* and *Cladophora parriaudii* for potential use in WWT. To the best of the author's knowledge, neither of these species have been previously used to this end;
- A method for fresh weight determination was developed and validated, and can be used to estimate dry weight content and growth rates of filamentous macro-algae. This method is straightforward, portable, inexpensive, and easy to standardise making it a potentially important and widely applicable research tool.
- The use of four different nitrogen sources, including nitrite and urea, to better understand the role of nutrient regime on the rates of growth, nutrient removal, nitrogen preference, and biochemical content of *Cladophora* sp. Results from this work highlighted the importance of appropriate species selection and nutrient regime for bioremediation and algal biotechnology purposes.
- The biological influence on macro-algal biosorption has been vastly understudied. The novelty of the final experimental chapter was in the concerted effort made to propagate biomass with varying biochemical characteristics by cultivating under a range of nutrient regimes. In addition, metals were selected to investigate if there was any discrimination in metal removal based upon levels of toxicity and biological function (if any) within the cell. Furthermore, the depth of biochemical characterisation involved in this study, as well as the use of SEM-BSE imaging to visualise metal bonding on the cell surface, has not been demonstrated before in macro-algal biosorption studies, to the best of my knowledge. The results from this chapter alone could open up several new avenues of biosorption research.

## 1.9 Manuscripts Produced from the Work

- **M.E. Ross,** K. Davis, R. McColl, M.S. Stanley, J.G. Day, A.J.C. Semião, Nitrogen uptake by the macro-algae *Cladophora coelothrix* and *Cladophora parriaudii*: influence on growth, nitrogen preference and biochemical composition, Algal Res. 30 (2018) 1-10.
- **M.E. Ross,** M.S. Stanley, J.G. Day, A.J.C. Semião, A comparison of methods for the non-destructive fresh weight determination of filamentous algae for growth rate analysis and dry weight estimation, J. Appl. Phycol. 29 (2017) 2925-2936.
- **M.E. Ross,** M.S. Stanley, J.G. Day, A.J.C. Semião, Biosorption of heavy metals from aqueous solutions by dried *Cladophora parriaudii* biomass cultivated under different nutrient regimes (In preparation)

# Chapter 2
## Materials and Methods

## 2.1 Introduction

This chapter outlines the procedures used for: macroalgal cultivation; analysis of growth; water chemistry; and biomass composition. More detailed notes and nuances of experimental design are described in each subsequent experimental chapter. Additionally, method development and standardisation of methods are appended (Appendices E-H).

## 2.2 Macro-algal Cultivation

### 2.2.1 Macro-algal strains

The three algal strains used in this work were obtained from the Culture Collection of Algae and Protozoa (CCAP), at the Scottish Association for Marine Science (SAMS, Oban, UK). These include two marine isolates of the genus *Cladophora*: *Cladophora coelothrix* CCAP 505/10; *Cladophora parriaudii* CCAP 505/09; and a freshwater isolate *Spirogyra varians* CCAP 678/3 (Fig. 2.1) [84].

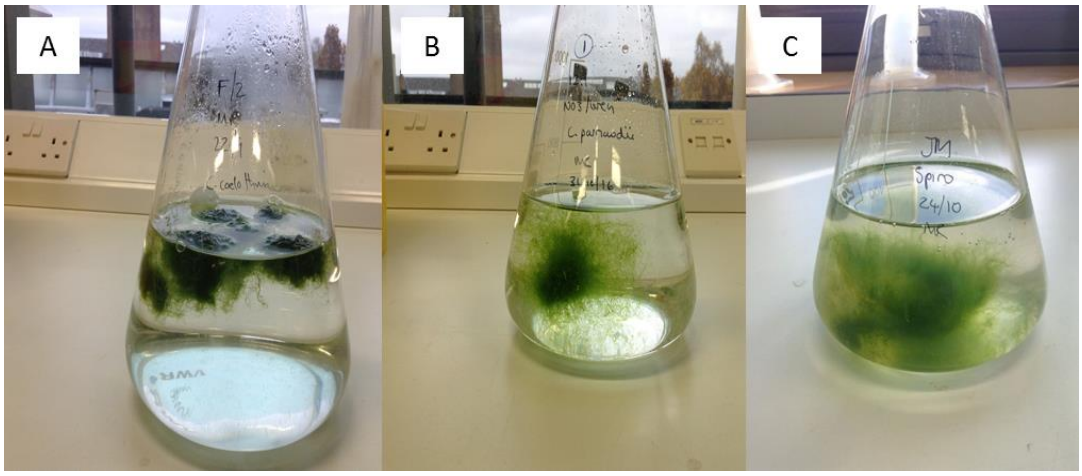


**Figure 2.1.** Erlenmeyer flask cultures of the three macro-algal species used in this work: *Cladophora coelothrix* (A), *Cladophora parriaudii* (B), and *Spirogyra varians* (C) Images from [319].

## 2.2.2 Cultivation and Maintenance

### *2.2.2.1 Media formulation*

Macro-algal cultures were maintained in 50-5,000 mL volumes of either Guillard's f/2 Medium (Appendix A, Table A1.), based on an artificial seawater at 33.5 g $L^{-1}$ (Instant Ocean, UK) [320], or Jaworski's Medium (JM) (Appendix A, Table A2.) [321] for marine and freshwater species, respectively.

In order to ensure a consistent starting inoculum, cultures underwent a series of cultivation steps, outlined below (sections 2.2.2.2-2.2.2.5) (Fig. 2.2) prior to experimentation.

### *2.2.2.2 Master Cultures*

Small volume cultures (<100 mL) were maintained as "master" cultures and were incubated under natural daylight on a north facing windowsill in the laboratory. Growth media was replaced approximately every 8 weeks (Fig. 2.2). At which time, biomass was removed aseptically in a laminar flow cabinet (MSC Advantage, Thermo Scientific), placed on a sterile glass Petri-dish and excessive growth and dead/dying filaments excised with sterile tweezers. Large "clusters" of biomass were divided into smaller clumps to help aid self-propagation. Biomass was then rinsed with deionised water and placed into fresh, sterile, growth medium.

### *2.2.2.3 Propagation Cultures*

Larger volume cultures (> 50 mL) were used to produce adequate biomass for use in experimental trials. The cultures were maintained in an incubator at 24°C (MIR-253, Sanyo, Japan), retrofitted with artificial illumination (Polylux $XL_R$ FT8/18W/830 and FT8/18W/840, GE Lighting, UK), under an 18/6 h L/D (Light/Dark) photoperiod with 30-40 µmol photons $m^{-2}$ $s^{-1}$ of photosynthetically active radiation (PAR: 400-700 nm) (LM-100 Light Meter, Amprobe, Germany), without mixing. The growth media was replaced approximately every 4-8 weeks (Fig. 2.2), using the method described above (section 2.2.2.2.).

### *2.2.2.4 Acclimation cultures*

In order to ensure that the inoculums for each experiment was of a comparable nutritional and biochemical status, to eliminate the likelihood of "surge" nutrient uptake, and to reduce the lag-phase of growth, all cultures underwent an acclimation period prior to experimentation, unless otherwise stated. Biomass harvested from the "propagation cultures" (section 2.2.2.3.) was inoculated at a FW ratio of 0.714/1 (w/v) [319] to the media and acclimated to its corresponding experimental conditions for seven days (Fig. 2.2).

### *2.2.2.5 Experimental Cultures*

To ensure optimal growth, all experimental growth trials were performed in an incubating shaker at 24°C (Certomat® BS-1, Sartorius Stedim Biotech, Germany) at 100 rpm. The incubator was retrofitted with artificial illumination (Polylux $XL_R$ FT8/18W/830 and FT8/18W/840, GE Lighting, UK), and set to an 18/6 h L/D (Light/Dark) photoperiod, with 30-40 µmol photons $m^{-2}$ $s^{-1}$ of photosynthetically active radiation (PAR: 400-700 nm) (LM-100 Light Meter, Amprobe, Germany).

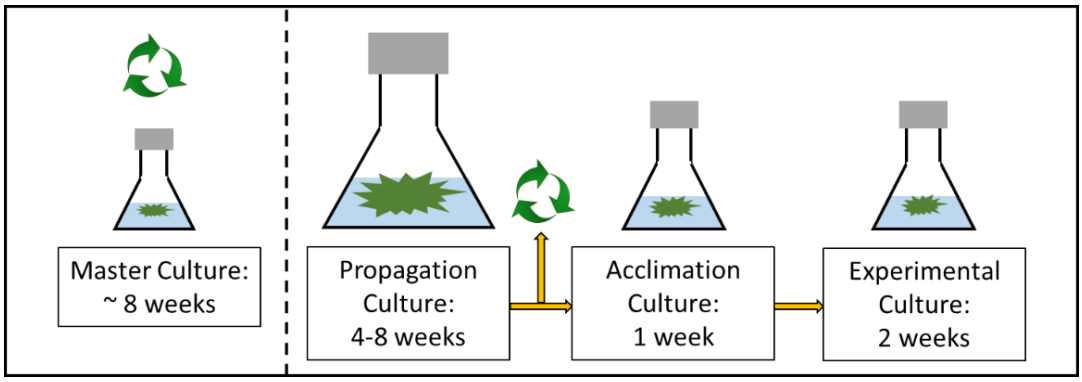


**Figure 2.2.** A schematic outlining the cultivation steps prior to experimentation.

## 2.3 Analysis of Macro-algal Growth

### 2.3.1 Fresh Weight (FW) Determination

*Cladophora* biomass was aseptically removed from culture vessels in a laminar flow cabinet (MSC Advantage, Thermo Scientific) and placed in a small salad spinner (Chef'n, USA). Biomass was rinsed with deionised water to remove extracellular salts and nutrients. To remove excess water, biomass was spun for 90 s (6 * 15 s iterations), followed by gravimetrical weighing on an analytical balance (PS-60, Fisher Brand, UK) for FW determination [319].

FW assessment of *Spirogyra* biomass followed an almost identical protocol, with the exception that a pre-collection step was required. Contents of a flask were poured through a perforated crucible (Coors™ Gooch Crucible) to retain the biomass. This was then rinsed with deionised water and subjected to the drying protocol outlined above [319].

These methods for FW determination were developed in Chapter 4 and were subsequently used throughout the remainder of the thesis.

### 2.3.2 Dry Weight (DW) Determination

Following harvesting and FW determination (section 2.3.2.), algal biomass was frozen, in a domestic freezer, and then freeze-dried overnight (Modulyo 4K Freeze-Dryer), or until a <5% variation in final mass was achieved. The lyophilised material was weighed gravimetrically using an analytical balance (PS-60, Fisher Brand, UK) to determine its dry weight (DW). Biomass was then placed in individual tubes and stored in a vacuum desiccator, in the dark, for future analysis.

Due to its scientific reproducibility and expedience, lyophilisation was the preferred technique for achieving DW material in this thesis. However, this method is energetically expensive and limited by space. In practice, air- or sun-drying would likely be employed.

### 2.3.3 Growth Rate Determination

Growth was expressed as the daily growth rate (DGR) as recommended by Yong *et al.* [322] (Eq. 2.1).

**Equation 2.1: Determination of daily growth rate (DGR).**

$$DGR = \left[\left(\frac{W_t}{W_0}\right)^{1/d} - 1\right] x\ 100$$

Where $W_t$ and $W_0$ are the final and initial FW mass, and *d* is the time in days.

## 2.4 Water Chemistry

Note that Section 2.4. details all methods used in this thesis for water chemistry analysis. Due to locality of work (SAMS, Oban or IIE, University of Edinburgh), instrument availability, and method development, the determination of some ions was performed using multiple methods or techniques. Each subsequent chapter will refer to the specific method employed in each instance.

### 2.4.1 Determination of pH

The pH of the growth media was determined on each sampling day, during medium formulation, as well as at the beginning and end of each trial using a pH meter (HI 9025C, Hanna Instruments, Sigma Aldrich, UK). In addition, the pH of media used for metal removal were also adjusted prior to onset of experimental period. To ensure accurate pH measurements, a 2-point calibration was regularly performed with buffer solutions (Thermo Scientific, UK).

## 2.4.2 Spectroquant® Test-kits

### *2.4.2.1 Total Ammonia Nitrogen (TAN)*

Total ammonia nitrogen (TAN) was determined colourimetrically, using a proprietary test-kit (1.00683.0001, Spectroquant®), and following the manufacturer's instructions (Appendix B, Fig. B1). Briefly, 5 mL of Reagent $NH_4$-1 was added to a clean test tube. To this, 0.2 mL of sample is added and immediately mixed (Vortex 3, IKA®). One level micro-spoon of Reagent $NH_4$-2 was added and vortexed until completely dissolved. The reaction is allowed to stand for 15 min and read in a spectrophotometer (Heλios Gamma UV-vis spectrophotometer, Thermo Scientific) at 680 nm ($OD_{680}$). A blank was composed of 0.2 mL deionised water in the place of the sample. TAN was quantified against a 0-80 mg $L^{-1}$ $NH_4^+$ standard curve (Appendix C, Fig. C1); that could be described by the linear equation (*y = mx + c*), from which the $NH_4^+$ concentration of unknown samples could be determined using Equation 2.2. The f/2 medium (Appendix A, Table A1.) contains some interfering components, most likely from the artificial seawater or the trace metal stock; therefore, f/2 media was tested in conjunction and a correction factor (CF) applied.

TAN can be quantified by following Equations 2.2- 2.5:

**Equation 2.2: $NH_4^+$ (mg $L^{-1}$) quantification in sea-water using Spectroquant® test-kits.**

$$NH_4\ (mg\ L^{-1}) = \frac{(OD_{680} - CF) - c}{m}$$

**Equation 2.3: The proportion of TAN that is in the free $NH_3$ form at 24°C, as a function of pH (Appendix C – Fig. C2).**

$$NH_3\ (\%) = 5.9375x^3 - 129.75x^2 + 946.89x - 2306.3$$

**Equation 2.4: The concentration of TAN (mg $L^{-1}$) in seawater using Spectroquant® test-kits.**

$$TAN\ (mg\ L^{-1}) = NH_4/(\frac{100 - NH_3\%}{100})$$

**Equation 2.5: The concentration of $NH_3$ (mg $L^{-1}$) in seawater using Spectroquant® test-kits.**

$$NH_3\ (mg\ L^{-1}\ ) = TAN - NH_4$$

Where $OD_{680}$ is the optical density at 680 nm, *CF* is the correction factor applied from f/2 media, *c* is the y-axis intercept, *m* is the gradient of the straight line and *x* is the pH of the solution.

### *2.4.2.2 Phosphate*

Soluble phosphate ($PO_4^{3-}$) was determined colourimetrically using a proprietary test-kit (1.14848.0001, Spectroquant®), and following the manufacturer's instructions (Appendix B, Fig. B2.). Briefly, 1 mL of sample was diluted with 4 mL $dH_2O$. To this, five drops of Reagent $PO_4$-1 was added and immediately vortexed (Vortex 3, IKA®), followed by the addition of one level micro-spoon of Reagent $PO_4$-2. This solution was then mixed vigorously until all solids had completely dissolved. Reactions were then left to stand for 5 min and read in a spectrophotometer (Heλios Gamma UV-vis spectrophotometer, Thermo Scientific) at 840 nm ($OD_{840}$). A blank was composed of 5 mL deionised water plus phosphate reagents. Phosphate was quantified against a 0-10 mg $L^{-1}$ $PO_4^{3+}$ standard curve (Appendix C, Fig. C3.); the standard curve produced could be described by the linear equation ($y = mx + c$), from which the phosphate concentration of unknown samples could be determined using Equation 2.6:

**Equation 2.6. $PO_4^{3-}$ (mg $L^{-1}$) quantification in sea-water using Spectroquant® test-kits.**

$$Phosphate\ (mg\ L^{-1}\ ) = \frac{OD_{840} - c}{m}$$

Where $OD_{840}$ is the absorbance at 840 nm, *c* is the y-axis intercept and *m* is the gradient of the line.

## 2.4.3 Ion Chromatography

Anions ($NO_2^-$, $NO_3^-$, and $PO_4^{3-}$) were measured in growth media by Ion Chromatography (883 Basic IC Plus, Metrohm, UK), equipped with a peristaltic pump, an 863 Compact Autosampler, a Metrohm A Supp 250/4.0 mm column, and a 850 Professional IC conductivity detector. The eluent employed was 3.2 mM $L^{-1}$ sodium carbonate and 1 mM $L^{-1}$ sodium bicarbonate in $dH_2O$. A MSM Suppressor, operated at 10 MPa was used to suppress the eluent, using 0.1 M $H_2SO_4$, 0.1 M oxalic acid and 5% (v/v) acetone in $dH_2O$ as the regenerant. Blanks and internal standards were analysed periodically to ensure that the IC was performing to a satisfactory level. Peaks from samples were manually integrated and reprocessed using MagIC Net 3.1 Software and compared against nitrate, nitrite and phosphate calibration curves (Appendix C, Figs. C4-C6) [319].

## 2.4.4 Inorganic Nutrient Auto-analysis

Nutrient analysis was performed spectrophotometrically using a Flow Injection Autoanalyser (FIA) (Lachat 8500, Hach Lange, UK). Nutrients were analysed using Lachat recommended methods 31-115-01-1-I (orthophosphate) and 31-107-04-1-A (nitrate/nitrite) [323]. Peaks were manually integrated using Omnion 3.0 software (Lachat Instruments, Hach Lange, UK). Values obtained were compared against calibration curves formulated with standard solutions diluted with Low Nutrient Seawater (LNSW) (Appendix C, Figs. C7 and C8). Samples were diluted with deionised water in order to fall within the calibration range. Standards and blanks were periodically analysed to ensure satisfactory performance.

## 2.4.5 Urea

A modified version of a method described by Mulvenna and Savidge [324] was used to quantify urea in seawater. Urea reagents were prepared freshly on each day of analysis and were Urea Reagent A and Urea Reagent B (Appendix D). In order to fall within the calibration range, samples were diluted with deionised water, 2 mL of appropriately diluted sample was added to a clean, dry, reaction tube. To this, 143 µL of Urea Reagent A was added and immediately vortexed (Vortex 3, IKA®), followed by 458 µL of Urea Reagent B

and mixed again. Teflon-lined screw caps were loosely placed on the test-tubes and were incubated (Gallenkamp Plus II Incubator, Sanyo, UK) for 30 minutes at 85°C. Samples were then cooled in a water bath for a total of 10 minutes, with the cool water being replaced after 5 minutes. The samples were then read in a spectrophotometer (Heλios Gamma UV-vis spectrophotometer, Thermo Scientific) at 520nm ($OD_{520}$). A blank was composed of 2 mL deionised water, and subjected to the same protocol. Samples were quantified against a urea calibration curve in the range of 0-5 mg $L^{-1}$ (Appendix C, Fig. C9.). The curve from this trend is linear and can be described by the equation: $y = mx + c$. From this calibration curve, the urea concentration of unknown samples could be determined using Equation 2.7:

**Equation 2.7: Urea quantification in seawater (mg $L^{-1}$).**

$$Urea\ (mg\ L^{-1}) = \frac{OD_{520} - c}{m}$$

Where $OD_{520}$ is the absorbance at 520 nm, $c$ is the y-axis intercept and $m$ is the gradient of the line.

## 2.4.6 Multi-elemental Analysis

Heavy metal solutions were analysed by ICP-OES (Optima 5300 DV, Perkin Elmer), utilising a radio frequency (RF) forward power of 1400 W, with Ar gas flows of 15, 0.2, and 0.75 L/$min^{-1}$ for plasma, auxiliary, and nebuliser flows, respectively. A peristaltic pump was employed to draw the sample into a Gem Tip Cross-Flow Nebuliser and Scott's Spray Chamber at 1.5 mL $min^{-1}$. In all instances, the instrument was operated in axial mode. On each sampling occasion, calibration standards were prepared for each metal using single element 1000 mg $L^{-1}$ standards (Fisher Scientific, UK), diluted with 2% $HNO_3$ (v/v) (Aristar® grade, VWR, UK). Several wavelengths were initially selected for each element and were analysed in a fully quantifiable mode (three points per unit wavelength), with three replicates employed per sample. A single wavelength for each element was selected for reporting results; based upon the peak shape, background interference, sensitivity, and the linearity of the calibration curve. The selected wavelengths were 308.213 nm, 324.752 nm, 259.372 nm, and 220.353 nm for Al, Cu, Mn, and Pb, respectively. All calibration curves had a linear regression of $R^2 = 0.99993$, at least.

# 2.5 Analysis of Macro-algal Composition

## 2.5.1 Determination of Ash Content

Ash content was performed on freeze-dried biomass (section 2.3.3.) and followed a standard method [325]. Foil capsules were folded, identified with an indelible marker, and combusted to remove and volatile matter and weighed gravimetrically once they had reached room temperature (RT). Pre-weighed lyophilised algal biomass (5 mg) was enclosed in a foil capsule and the mass recorded. The samples were then combusted at 500°C for a 12 h period in a muffle furnace (GSM 11/8, Carbolite Furnaces). The furnace was pre-programmed to reach 500°C from ambient temperature within 35 minutes. Once the samples had cooled to RT, they were weighed. Ash content was determined as the proportion of residual, non-combusted, material from the original lyophilised macroalgae and was calculated using Equation 2.8:

**Equation 2.8: Determination of Ash Content (% DW).**

$$\%\ Ash = \frac{M2 - M1}{DW}\ \text{x}\ 100$$

Where *M*1 is the mass of the pre-combusted foil capsule, *M*2 is the mass of the foil capsule and ash, *DW* is initial mass of the lyophilised algal sample prior to combustion.

## 2.5.2 Protein Determination

Total soluble protein was extracted from *Cladophora* biomass using a sequential acid and alkaline extraction, followed by the Lowry quantification [326]. This was a modified version of a protocol described by Slocombe *et al.* [327] and is detailed next.

### *2.5.2.1 Protein Extraction Procedure*

Initially, 5 mg lyophilised biomass (section 2.3.3) was placed into 2-mL screw-capped Eppendorf tubes. To this, 200 µL of 24% trichloroacetic acid (TCA) (w/v) was added and

inverted several times, to mix. The caps were replaced and securely fastened and the samples placed into a water bath at 95-100°C for 15 minutes. The tubes were allowed to cool to RT before diluting with 600 µL of deionised water and centrifuging at 15,600 g for 2 minutes (5414 Microcentrifuge, Eppendorf®). The TCA supernatant was discarded and the pellet resuspended with 500 µL of Lowry Reagent D (Appendix D) and incubated overnight in a 55°C water-bath. The tubes were allowed to cool to RT and centrifuged, as above. The supernatant hydrolysate was transferred to a fresh Eppendorf tube.

### *2.5.2.2 Protein Quantification*

Triplicate samples (25 µL) of the protein hydrolysate was added to a new Eppendorf tube. This was reacted with 1000 µL of Lowry Reagent D (Appendix D), by pipette and the solution immediately inverted several times and then incubated for 10 minutes at room temperature (RT). After a 10 minute incubation period at RT, 100 µL of Lowry Reagent E (Appendix D) was added, vortexed immediately (Vortex 3, IKA®) and then transferred to a disposable cuvette. After a further 30 minute incubation, the samples were read at 600 nm ($OD_{600}$) (Heλios Gamma UV-vis spectrophotometer, Thermo Scientific). The concentration of protein present in samples was quantified against a BSA calibration curve described by the linear equation ($y = mx + c$) (Appendix C, Fig. C10.), and expressed as BSA equivalents, using Equation 2.9. The BSA calibration curves were formulated by subjecting stock solutions, in the range of 0-3 mg $mL^{-1}$.

**Equation 2.9: Determination of protein concentrations in hydrolysates, expressed as BSA equivalents (mg $L^{-1}$).**

$$BSA\ equiv.\ (mg\ L^{-1}) = \frac{OD_{600} - c}{m}$$

Where $OD_{600}$ is the optical density at 600 nm, $c$ is the y-axis intercept and $m$ is the gradient.

The BSA equivalents were then used to calculate the protein content per unit DW biomass using Equation 2.10:

**Equation 2.10: Transformation of BSA equivalents to protein content per unit DW.**

$$Protein\ Content\ (\%\ DW) = \left(\frac{BSA\ equiv.\ \mathrm{x}\ V}{M}\right) \mathrm{x}\ 100$$

Where *BSA equiv.* is the outcome from Equation 2.9, *V* is the volume (mL) of the protein hydrolysate and *M* is the DW mass (mg) of the sample from which protein was extracted.

## 2.5.3 Total Soluble Carbohydrate Content

### *2.5.3.1 Carbohydrate Extraction*

The total soluble carbohydrate content of *Cladophora* biomass was determined using a modified phenol-sulphuric acid method derived from that of Fournier [328], originally described by Dubois *et al.* [329]. Initially, 5 mg of lyophilised biomass (section 2.3.3) was placed into a 10 mL test-tube with a teflon-lined screw-cap. To this, 2.5 mL of 1M $H_2SO_4$ was added and the lids loosely replaced. The samples were acid-hydrolysed by placing them in an autoclave at 121°C for 15 min (TCR/40/H, Touchclave-R, LTE Scientific, UK). After cooling to RT, the samples were vortexed (Vortex 3, IKA®) and then the hydrolysate was transferred to an Eppendorf tube. To reduce the likelihood of interference of particulate matter, samples were centrifuged for 2 minutes at 15,600 g (5414 Microcentrifuge, Eppendorf®) and the supernatant transferred to a clean Eppendorf tube.

### *2.5.3.2 Carbohydrate Quantification*

Triplicate samples (30 µL) of the hydrolysate (or glucose stock solutions) were pipetted into a clean reaction tubes and 500 µL of 4% (w/v) phenol solution added, dispensed using a rapid reagent dispenser. The mixture was then gently swirled and 2.5 mL of concentrated (>96%) sulphuric acid added directly to the mixture, using a rapid reagent dispenser. The solution was then lightly vortexed, allowed to cool to RT, and transferred into a quartz cuvette, using a glass Pasteur pipette, and read spectrophotometrically at 490 nm ($OD_{490}$) (Heλios Gamma UV-vis spectrophotometer, Thermo Scientific).

The concentration of soluble carbohydrate present in hydrolysates was compared against a glucose standard curve that had a linear equation (*y = mx + c*) (Appendix C, Fig. C11.), and was expressed as a glucose equivalent (GEq), using Equation 2.11. Calibration curves were generated by performing the carbohydrate quantification method on glucose stock solutions ranging from 0-2 mg $mL^{-1}$. Blanks were composed of 30 µL volumes of $dH_2O$ in the place of samples, or glucose stock solutions.

**Equation 2.11: Determination of total soluble carbohydrates from algal biomass, expressed as glucose equivalents (GEq) (mg $L^{-1}$).**

$$GEq\ (mg\ L^{-1}) = \frac{OD_{490} - c}{m}$$

Where $OD_{490}$ is the optical density at 490 nm, *c* is the y-axis intercept and *m* is the gradient.

The GEq's were then used to calculate the total soluble carbohydrate content per unit DW biomass using Equation 2.12:

**Equation 2.12: Transformation of GEq equivalents to carbohydrate content per unit DW.**

$$Carbohydrate\ Content\ (\%\ DW) = \left(\frac{GEq\ \text{x}\ V}{M}\right) \text{x}\ 100$$

Where *GEq* is the outcome from Equation 2.11, *V* is the volume (mL) of 1M $H_2SO_4$ added and *M* is the DW mass (mg) of the sample from which sugars was extracted.

### *2.5.4.3 Monosaccharide Quantification*

HPLC (Agilent, 1100 Series) was used for the qualification and identification of solubilised monosaccharides present in the carbohydrate hydrolysate (section 2.5.3.1.). The HPLC was equipped with a degasser, autosampler, high pressure pump, refractive index (RI) detector, and a column heater maintained at 40°C (all Agilent, 1100 Series). Monosaccharides were separated using a ROA-Organic Acid H+ (8%) LC Column 150 x 7.8 mm (Rezex™, Phenomenex, UK) operated at 0.2 mL $min^{-1}$ with 5 mM $H_2SO_4$ as the eluent [103].

Hydrolysates were diluted 7.5 times with deionised water and passed through a 0.45 µm PTFE filter into a glass HPLC vials and analysed immediately. The sample injection was 100 µL. Monosaccharide concentration was determined using Agilent ChemStation software (Rev. B.01.01) through comparison against monosaccharide standards (Appendix C, Fig. C12.); concentrations were then expressed as a proportion of the macroalgal dry weight biomass (% DW).

## 2.5.4 Determinations of Pigments

Pigments present in *Cladophora* biomass were quantified spectrophotometrically after an extraction with dimethylsulfoxide (DMSO), based on a method described by Griffiths *et al.* [330]. Briefly, 1.5 ± 0.5 mg of freeze-dried *Cladophora* biomass (section 2.3.3.) was placed into 2 mL screw-capped Eppendorf tubes. Pigments were extracted from the biomass with the addition of 2 mL DMSO and immediately vortexed (Vortex 3, IKA®), followed by incubating overnight in a sealed water bath at 60°C. The samples were allowed to cool to RT in darkness, vortexed again, followed by centrifugation for 2 minutes at 15,600 g (5414 Microcentrifuge, Eppendorf®). DMSO-pigment extracts were carefully transferred to a quartz cuvette, using a glass Pasteur pipette, and the absorbance read at 480 nm ($OD_{480}$), 649 nm ($OD_{649}$) and 665 nm ($OD_{665}$) (Heλios Gamma UV-vis spectrophotometer, Thermo Scientific). The readings obtained from the spectrophotometer were used to calculate the concentration of pigments as mg $L^{-1}$, using Equations 2.13-2.16:

**Equation 2.13: Concentration of chlorophyll *a* (mg $L^{-1}$)**

$$Chl\ a\ (mg\ L^{-1}) = \frac{(12.47 \text{ x } OD_{665}) - (3.62 \text{ x } OD_{649}) \text{ x } V}{M} / 1000$$

**Equation 2.14: Concentration of chlorophyll *b* (mg $L^{-1}$)**

$$Chl\ b\ (mg\ L^{-1}) = \frac{(25.06 \text{ x } OD_{649}) - (6.5 \text{ x } OD_{665}) \text{ x } V}{M} / 1000$$

**Equation 2.15: Concentration of carotenoids (mg $L^{-1}$)**

$$Carotenoid\ (mg\ L^{-1}) = \frac{((1000 \text{ x } OD_{480}) - (1.29 \text{ x } Chl\ a) - (53.78 \text{ x } Chl\ b))/220 \text{ x } V}{M}/1000$$

**Equation 2.16: Total concentration of pigments (mg $L^{-1}$)**

$$Total\ Pigments\ (mg\ L^{-1}) = Chl\ a + Chl\ b + Carotenoids$$

Values above could then be expressed as a proportion of their dry weight (% DW) by multiplying by 100.

## 2.5.5 Fourier-Transform Infrared Spectroscopy (FTIR)

Spectra were collected using FTIR attenuated total reflectance (ATR) using a Perkin Elmer Frontier equipped with a diamond crystal Universal ATR Sampling Accessory, with a mercury cadmium telluride (MCT) detector. Samples were scanned over a wavenumber range of 4000 - 650 $cm^{-1}$ at a resolution of 2 $cm^{-1}$. Approximately 5 mg of lyophilised biomass (section 2.3.3.) was placed onto the crystal surface and pressed onto the crystal head at a force of 60 arbitrary units. Each sample consisted of an average of 25 scans. Sample scans were recorded using Spectrum software (v. 10, Perkin Elmer), with the background automatically corrected for air and atmospheric $CO_2$/$H_2O$.

## 2.5.6 Scanning Electron Microscopy (SEM)

After metal exposure, approximately 2 mg of algal material was placed into individual Eppendorf tubes and dried overnight in an oven at 60°C. Once dried, samples were mounted onto specimen stubs and coated in carbon. Algal samples were visualised using a scanning electron microscope (SEM)(Carl Zeiss SIGMA HD VP field emission SEM); with images recorded using the back-scattered electrons technique (BSE) utilising an accelerating voltage of 20 kV, an aperture size of 30 µm, and a working distance of 7 ± 1 mm.

# Chapter 3

## Testing the rationale for implementing *Cladophora* sp. into wastewater treatment

## 3.1 Introduction

The main objective of all wastewater treatment plants (WWTPs) is the same: to ensure the health of humans and ecosystems through the treatment of wastewaters to a quality that complies with local or regional legislation [331]. Consistent provision of clean, safe, permissible water, however, is a difficult task due to the variability inherent in wastewater streams. Wastewaters are incredibly complex and changeable environments, with characteristics that can change on a daily or even hourly basis [332]. The composition of a wastewater depends upon the catchment area from whence it originates, its uses, and seasonality, amongst others [157, 158]. Many of the physical, chemical, and biological constituents within a wastewater stream are inter-related, for example, temperature will influence biological activity within the wastewater, as well as controlling gas solubility and ion equilibria [331]. These factors, in turn, will influence algal biology and its effectiveness as a tool for bioremediation (section 1.4.1). The selection of a suitable algal species for implementation into wastewater should be the highest priority [231]. The following are examples of criteria that should be considered when identifying or selecting a species for WWT purposes:

- Robustness to abiotic and biotic conditions
- Resistance to grazers/herbivory
- Ease of handling/maintenance
- Ease of cultivation/harvest
- Local species/ubiquity
- Rates of growth
- Rates of nutrient and $CO_2$ removal
- Ease of down-stream processing
- Financial or ecological value

*Cladophora* is a genus of macro-algae that meets many of the aforementioned criteria. They are often associated with eutrophic conditions and are generally regarded as a pest

species [333]. However, instead of viewing them as a nuisance, their potential for nutrient sequestration could be harnessed for bioremediation applications.

*Cladophora* sp. are found across the globe in fresh-water, brackish, and marine ecosystems [186]. Their global distribution is beneficial, as local strains or species could be implemented on a case-by-case basis to prevent the contentious issue of introducing invasive or alien species [334, 335]. *Cladophora* are renowned for their high rates of growth and propensity to form dense "algal mats", particularly in warm, nutrient enriched conditions. Reports of "blooms" include the Great Lakes of North America [336], the Lake District, England [337] Harrington Sound, Bermuda [208], and Waquoit Bay, Massachusetts [165, 338], following an increase in anthropogenic nutrient inputs into these areas.

Liu and Vyverman [27] tested the growth and nutrient removal of filamentous macro-algae and cyanobacteria for potential use in WWT. In their study, *Cladophora* sp., *Klebsormidium* sp., and *Pseudanabaena* sp., were cultivated across a range of nitrogen to phosphorus (N/P) ratios, albeit only under "optimal" growth conditions (*i.e.* temperature and light). Biomass productivities (50-60 mg DW $L^{-1}$ $d^{-1}$) and nutrient removal (90-99% N and 56.3-99% P) by *Cladophora* sp., was generally greater than the other species assessed, irrespective of ratio. In addition, Bracken and Stachowicz [180] observed that *Cladophora* sp. and *Prionitis* sp. were dominant species in the Bodega Marine Reserve, California, despite neither having the greatest N uptake rate of the eight local species tested. Their success was attributed to their ability to complimentarily utilise multiple nitrogen sources, as well as their resistance to herbivory. *Cladophora* have a cell wall composed of highly-crystalline cellulose and hemi-cellulose and are able to synthesise toxic fatty acids, making them unpalatable to potential grazers [186, 187, 339-341].

*Cladophora* are characterised by their filamentous morphology [186]. This gives them a high surface area/ volume ratio and may give them a competitive advantage in comparison to other structural forms [183]. For instance, improved access to potentially growth limiting factors such as light and nutrients [188, 189]. However, *Cladophora* typically grows in clusters or mats which may reduce the availability of these factors to many of the cells located within the mat. For example, Krause-Jensen *et al.* [342] noted distinct gradient of nutrient and light availability within an algal mat. Whereas, Peckol and Rivers [338] described the conditions within an algal mat of *Cladophora vagabunda* as dark, stagnant and hypoxic. These conditions may prove detrimental for WWT applications, acting as a site

for algal decomposition, nutrient release, or as a reservoir for micro-organisms. However, Peckol and Rivers [338] demonstrated the robustness of *Cladophora vagabunda* and by extracting blackened tissue from within the algal mat and reintroduced it to normal, aerated and illuminated conditions, which after two days had made a full physiological recovery. Additionally, Choo *et al.* [343] reported that *Cladophora* was much more tolerant to the action of reactive oxygen species (ROS), in comparison to *Ulva*. Algal cultures were exposed to conditions designed to induce oxidative stress, such as high light exposure and carbon limitation. *Cladophor*a were found to synthesise three separate enzymes (*i.e.* ascorbate peroxidase, catalase, and superoxide dismutase) in order to protect against intracellular ROS, whereas *Ulva* only produced superoxide dimutase. In a WWT scenario, where a consistent bioremediation performance is required, dominance and resistance to grazers will be advantageous, reducing the likelihood of losses in productivity due to grazing or being outcompeted by other species. Furthermore, a tolerance to potentially unfavourable conditions would be an undoubtedly beneficial trait for a species selected for WWT.

The final benefit of algal bioremediation is the production of commercially exploitable biomass that may offset production costs (section 1.1 and 1.3). Biomass of *Cladophora* has been used for a variety of purposes, including as a source of food and fertiliser [344, 345], and has been considered as a potential feedstock for bioenergy [141, 346]. Additionally, the crystallinity of the cell wall of *Cladophora* has stimulated interest in potential applications, such as metal removal [310], electrochemically controlled ion exchange and separation processes [347], paper based batteries [348], and as a matrix for drug delivery [349, 350].

*Cladophora* have a filamentous morphology which will enhance nutrient removal, as well as facilitate harvesting [150]. Their natural dominance, tolerance to sub-optimal conditions and lack of appeal to grazers will ensure that losses in productivity due to biological factors will be minimalised. Finally, the biomass produced may have a variety of commercially exploitable applications. These features make *Cladophora* a potentially suitable genus for WWT and merits further research. However, much remains uncertain about their feasibility for implementation into WWT. For instance, since wastewaters are such a dynamic environment, what influence does this variability have on *Cladophora*? Are *Cladophora* able to continue to grow and remove nutrients irrespective of environmental conditions, or are they only successful when cultivated under favourable conditions?

The aim of this chapter is to investigate the ability of *Cladophora* to grow and remove nutrients across a range of conditions. The objective was to test the suitability of *Cladophora*, on a fundamental level, for use in WWT. A screening process was employed on two members of the Cladophoraceae, exposing them to extremes of salinity, pH, nutrient concentrations, and temperature and daylight hours. Additional objectives of this screening process was to optimise cultivation conditions and to develop methods for use throughout the remainder of the experimental period.

## 3.2 Materials and Methods

### 3.2.1 Macro-algal strains and culture conditions

Two members of the Cladophoraceae family were utilised: *Cladophora coelothrix* and *Cladophora parriaudii* (section 2.2.1). Prior to experimentation, cultures were incubated under the conditions outlined in section 2.2.2.3, at 18°C.

Experiments were performed in 6 multi-well plates (Greiner, UK), containing 7 mL volumes of the experimental growth medium (Table 3.1). Each well was inoculated with 4-10 mg of fresh weight (FW) algae, determined by gently blotting with filter paper. Cultures were maintained in conditions similar to those described in section 2.2.2.5, with exceptions noted in Table 3.1. All experiments lasted for 14 days, with the exception of the salinity (21 days) which was extended due to no visual indication of growth during the initial prescribed period.

### 3.2.2 Experimental variables

Four abiotic variables were tested independently: nutrient concentration, salinity, pH, and temperature and daylight hours (Table 3.1). Growth media used throughout the experimental period was unbuffered Guillard's f/2 medium (Appendix A – Table A1.) [320], with the exception of the Experiment A, where there the concentration of nitrogen and phosphorus were adjusted. Growth media designated f/2, f, 2f, and 4f were formulated by adding increasing doses of N and P stocks. The initial $NO_3$-N and $PO_4^3$-P concentrations

equated to 868 and 21, 1695 and 33, 2990 and 53.2, 4791 and 90 µM for f/2, f, 2f, and 4f, respectively. Whereas, in Experiment B, the initial pH was adjusted to either 3, 5, 7, 9 or 11 using 0.01 M HCl or NaOH. For experiment C, the salinity of the medium was amended by adding either 0, 15, 33.5, 45, or 60 g $L^{-1}$ of the artificial sea-salt mix (Instant Ocean, UK). In Experiment D, temperature and photoperiod (L/D) were set to: 18°C and 18/6 h; 24°C and 18/6 h; and 10°C and 6/18 h to replicate spring, summer, and winter conditions, respectively.

**Table 3.1.** The experimental conditions tested.

| Experiment | Variable | Media | Salinity (g $L^{-1}$) | Initial pH | Season |
|---|---|---|---|---|---|
| **A** | Nutrient Concentration | f/2, f, 2f, 4f | 33.5 | 7 | Spring† |
| **B** | pH | f/2 | 33.5 | 3, 5, 7, 9, 11 | Spring† |
| **C** | Salinity | f/2 | 0, 15, 33.5, 45, 60 | 7 | Spring† |
| **D** | Temperature & Daylight Hours | f/2 | 33.5 | 7 | Spring†, Summer‡, Winter¥ |

† = 18°C & 18/6 h L/D, ‡ = 24°C & 18/6 h L/D, ¥ = 10°C & 6/18 h L/D

## 3.2.3 Determination of algal growth

To remove any extracellular salts or nutrients, algal samples were rinsed with deionised water at the beginning and end of each experiment. Algal biomass was gently blotted with filter paper to remove excess extracellular water. FW was determined by weighing gravimetrically in an analytical balance (PS-60, Fisher Brand, UK), with growth determined and expressed as daily growth rate (DGR) on a FW basis (section 2.3.3).

## 3.2.4 Residual nutrient determination

Soluble $NO_3^-$ and $PO_4^{3-}$ was measured in the media, at the beginning and end of each experiment, by Flow-Injection Auto-analysis (section 2.4.4), except for Experiment B where soluble nutrients were determined by Ion Chromatography (section 2.4.3).

### 3.2.5 Statistical Analysis

All experiments were performed in triplicate ($n$ = 3). The experimental error was determined and expressed as one standard deviation (SD). The significance of difference between the DGR was determined by a one-way ANOVA with Tukey's post-hoc test ($p$ <0.05). Pearson correlation coefficients, $r$, were used to determine the relationship between DGR and nutrient uptake. All statistical analysis was performed using Minitab® Statistical Software version 17.

## 3.3 Results and Discussion

In this study, two species of *Cladophora* were assessed for their suitability, in terms of growth and nutrient uptake, for use in WWT applications. Small algal sample sizes were used to allow for the screening of a range of individual environmental parameters. The broad range selected within each abiotic condition was done so on a 'proof-of-concept' basis, in order to demonstrate the tolerance and potential applicability of *Cladophora* sp., rather than for the targeted treatment of a specific type of wastewater.

### 3.3.1 Nutrient Concentration

The purpose of WWTPs is to remove or reduce the concentration of pollutants from the influent to environmentally and ecologically safe levels that are legislatively compliant [331], regardless of the influent concentrations. The concentration of nutrients, such as nitrogen, can be variable and may reach very high concentrations. For instance, N concentrations in a range of 18 - 124,900 µM have been reported in aquaculture wastes [33, 40, 41]. Therefore, the capacity for growth and nutrient removal across a range of concentrations were tested in this study.

Both species exhibited good levels of growth and nutrient removal (in both relative and absolute terms) in all concentrations (Fig. 3.1A, 3.2A, 3.3A, and 3.4). In all instances, the growth of *C. parriaudii* (7.5-13.3% $d^{-1}$) was greater than that of *C. coelothrix* (7.2-9.4% $d^{-1}$) (Fig. 3.1A), with differences in trend observed. While the growth of *C. coelothrix* was relatively stable, irrespective of external substrate concentration, there was a clear

difference in the rate of growth of *C. parriaudii* with growth increasing from 7.5-7.9 to 12.6-13.3% $d^{-1}$ when cultivated in either the 2f or 4f medium. This pattern of growth was mirrored in the absolute uptake values of both $NO_3$-N and $PO_4^3$-P, with clear 'step' in $NO_3$-N uptake (Fig. 3.1A and 3.4A). For instance, $NO_3$-N uptake by *C. parriaudii* was 392-460 µM in f/2 and f medium, compared to 2298-2429 µM when cultivated in the higher nutrient levels of the 2f and 4f media. A similar trend was observed for *C. coelothrix*, with uptake values of 830-860 µM and 2821-3027 µM $NO_3$-N (Fig. 3.4A), despite little variation in growth rate (Fig. 3.1A). Meanwhile, phosphorus uptake by *C. parriaudii* was incremental with increasing initial concentration, with values of 19.8-86.7 µM P achieved (Fig. 3.4B), corresponding to 89.4-96.7% removal (Fig. 3.3A). Whereas, the trend $PO_4^3$-P uptake by *C. coelothrix* was not as pronounced (20.4-51.1 µM $PO_4^3$-P) (Fig. 3.4B). As such, there was a strong positive correlation between the DGR of *C. parriaudii* and the removal of either $NO_3^-$ or $PO_4^{3-}$, with *r* values of 0.791-0.937 (*p* = <0.001-0.002). A similar relationship was observed for *C. coelothrix*, albeit to a much lesser degree, *r* = 0.562-0.602 (*p* = 0.038-0.057) (Table 3.2). This suggests that the growth of *C. parriaudii* is very strongly influenced by nutrient regime, whereas *C. coelothrix* may be more affected by another abiotic factor.

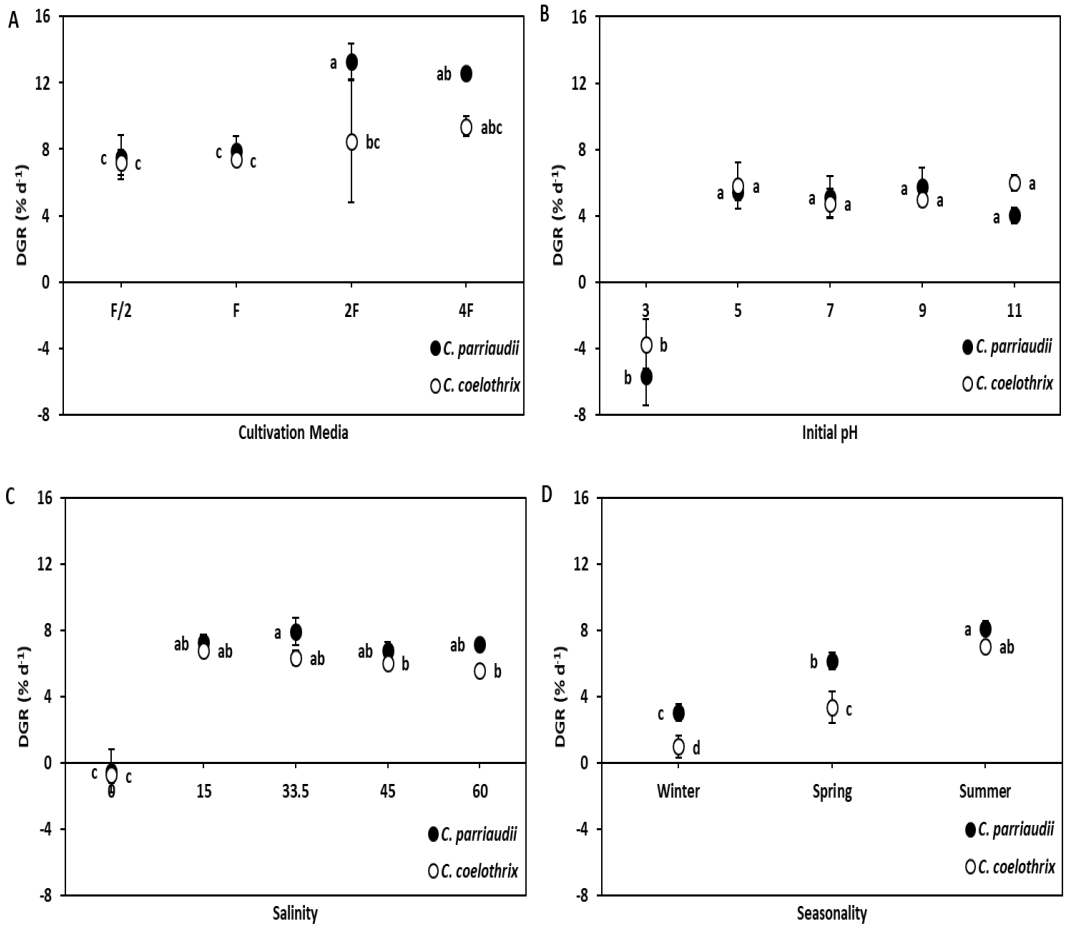


**Figure 3.1**. The daily growth rate (DGR) of *Cladophora parriaudii* (black) and *Cladophora coelothrix* (white) when cultivated in 6 multi-well plates and maintained under a range of different abiotic conditions, described in detail in Table 3.1, including: **A** types of cultivation media, **B** initial pH, **C** salinity, and **D** different seasonality ($n$ = 3, *error bars* = 1 SD). Different letters indicate significant differences in DGR ($p < 0.05$).

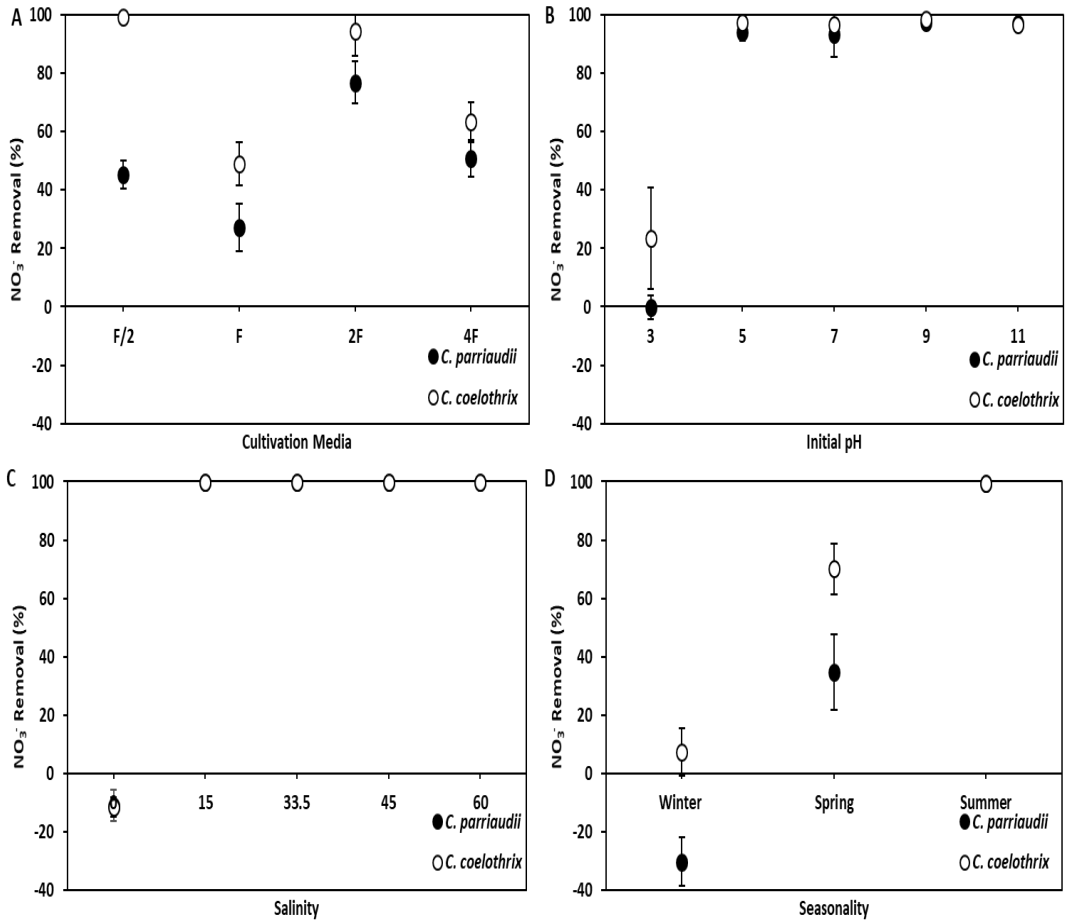


**Figure 3.2.** The relative removal of $NO_3$-N by *Cladophora parriaudii* (black) and *Cladophora coelothrix* (white) when cultivated in 6 multi-well plates and maintained under a range of different abiotic conditions, described in detail in Table 3.1, including: **A** types of cultivation media, **B** initial pH, **C** salinity, and **D** different seasonality (*n* = 3, *error bars* = 1 SD).

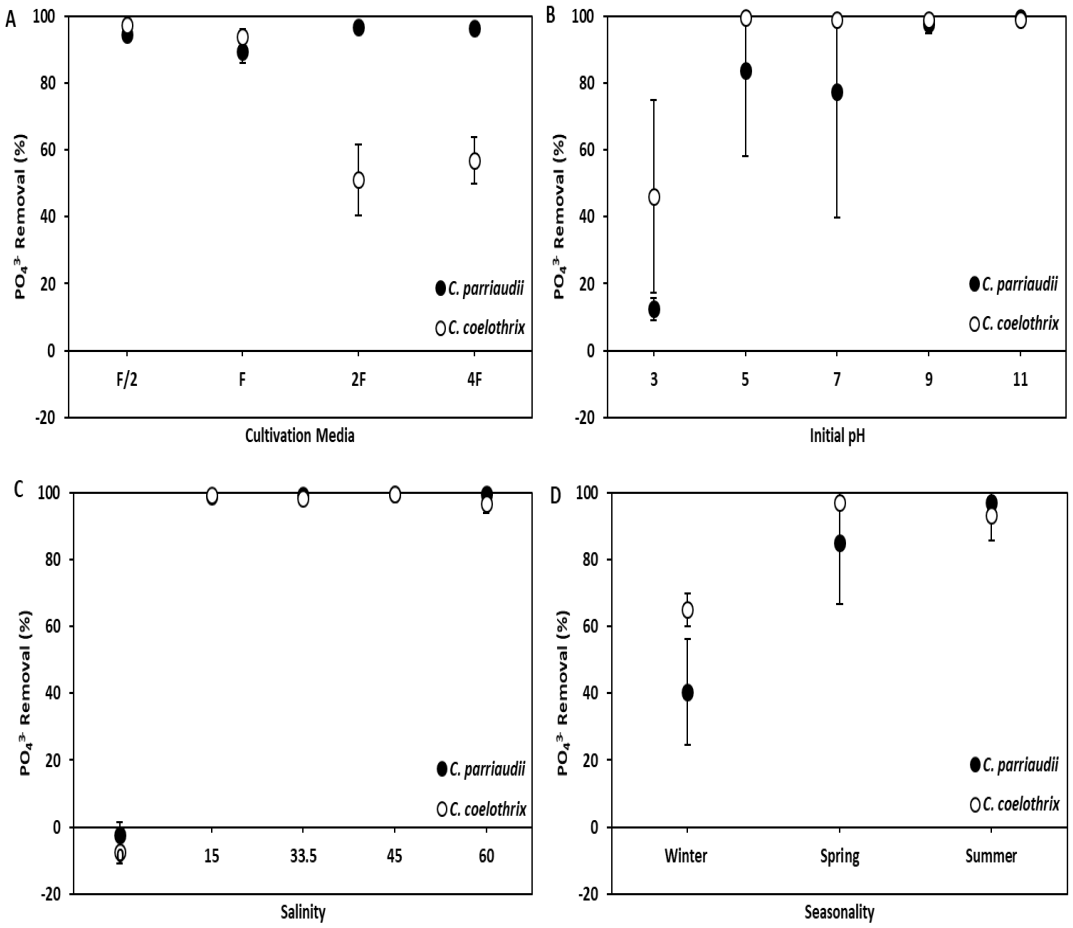


**Figure 3.3**. The relative removal of $PO_4^{3}$-P by *Cladophora parriaudii* (black) and *Cladophora coelothrix* (white) when cultivated in 6 multi-well plates and maintained under a range of different abiotic conditions, described in detail in Table 3.1, including: **A** types of cultivation media, **B** initial pH, **C** salinity, and **D** different seasonality (*n* = 3*, error bars* = 1 SD).

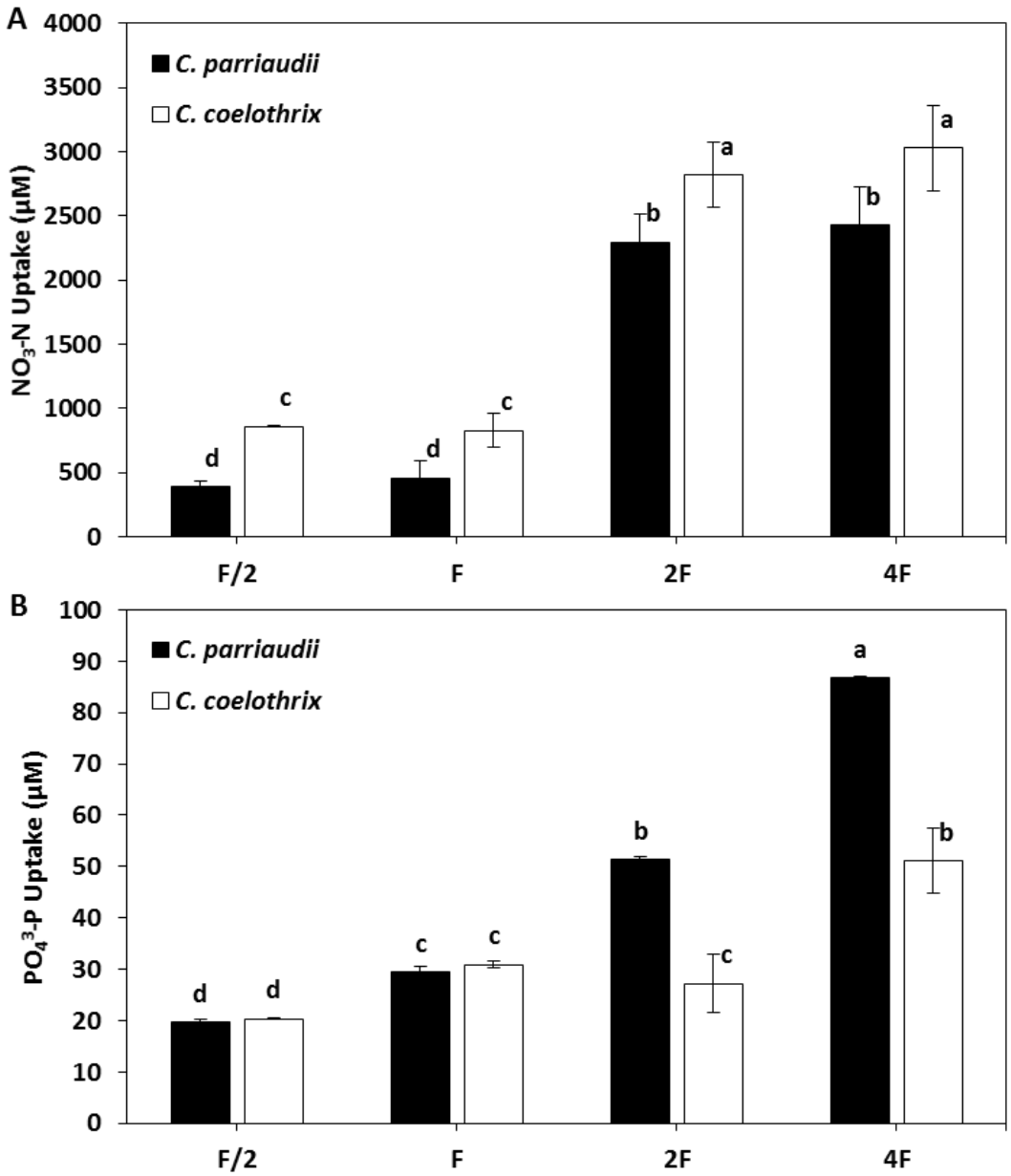


**Figure 3.4**. The absolute uptake of $NO_3$-N (A) and $PO_4^3$-P (B) by *Cladophora parriaudii* (black) and *Cladophora coelothrix* (white) when cultivated in 6 multi-well plates and maintained under a range of different media concentrations, described in detail in Table 3.1 ($n$ = 3, *error bars* = 1 SD). Different letters indicate significant differences in nutrient uptake ($p < 0.05$).

**Table 3.2.** The Pearson correlation coefficients (*r*) of the algal DGR versus nutrient uptake for the Experiment A. Samples were grown in 6 multi-well plates and subjected to different nutrient regimes (Table 3.1) (*n* = 12, degrees of freedom were 2 on 10).

| | DGR | | | |
|---|---|---|---|---|
| | *C. parriaudii* | | *C. coelothrix* | |
| | $NO_3$-N Uptake | $PO_4^3$-P Uptake | $NO_3$-N Uptake | $PO_4^3$-P Uptake |
| *r* | 0.937 | 0.79 | 0.568 | 0.602 |
| *p* | <0.001 | 0.002 | 0.054 | 0.038 |

## 3.3.2 pH

The pH of a wastewater stream is an important variable, as it influences the ion equilibria and solubility of nutrients, metals, and gases [331, 351]. These will, in turn, influence biological interactions of organisms present, for instance nutrient uptake, carbon sequestration, photosynthesis/respiration and metal toxicity [331, 352, 353]. An algal species that is robust and is able to continue to grow and remove nutrients across a fluctuating pH would be advantageous for treating effluent streams in a dynamic environment. Therefore, the performance of both species was tested with initial pH as an experimental variable.

Good growth was observed (Fig. 3.1B), coupled with reasonable to high levels of nutrient removal (Figs. 3.2B and 3.3B) in the majority of regimes tested. The DGR of *C. parriaudii* ranged from 4-5.7% $d^{-1}$ when the initial pH was set to 5-11, whereas, growth of *C. coelothrix* was slightly higher at 4.8-6% $d^{-1}$. However, both species died when the initial pH was 3 (Fig. 3.1B). The proportion of nutrients removed reflected the growth patterns (Figs. 3.2B and 3.3B). For instance, 93.1-97.5% and 96.5-98.6% of $NO_3$-N were removed by *C. parriaudii* and *C. coelothrix*, respectively, when the initial pH was between 5-11. However, only 0-23.4% was removed when the initial pH was 3. Phosphorus removal was similar, with 12.4-46.1% removal at a pH of 3. Whereas, 77.6-99.6% and >99% removal was recorded in all other instances by *C. parriaudii* and *C. coelothrix*, respectively (Fig. 3.3B). In an early study, Brock [354] observed that cyanobacteria prefer alkaline environments and are largely absent in acidic regions, particularly below pH 4. This is thought to be due to the sensitivity of their photosynthetic pigments, which are very labile or unstable in acidic conditions [354]. This seems a potential explanation for the results in this study, *C. parriaudii* was apparently

more sensitive to the lower pH than *C. coelothrix,* which has a thick and recalcitrant cell wall that may offer it greater protection from acid induced injuries [319].

In addition to growth and nutrient removal, the temporal change in pH was also recorded (Fig. 3.5). Again, similar trends occurred between species and treatments. There was an immediate shift in pH towards 8-9 when the initial level was set to between 5-11, with mean external pH from day 2 onwards of 9±0.46 and 9.1±0.56 for *C. parriaudii* and *C. coelothrix*, respectively. Whereas, since growth did not occur in the pH 3 treatment, there was no considerable change in external pH (Fig. 3.5). Shifts in pH are a result of photosynthetic carbon uptake by the algal samples, which makes the external substrate more alkaline [355]. Treated wastewaters that have an excess of alkalinity, or acidity, are required to be neutralised prior to discharge [331], this could be achieved by sparging $CO_2$ or flue gas into algal treatment systems. This would enhance algal growth and photosynthesis, and therefore their bioremediation efficacy of both nutrients and carbon [356]. Introduction of governmental incentives, such as carbon credits, would make this a more likely scenario [110].

Overall, no growth was observed when the initial pH was 3, meaning that *Cladophora* may be unsuitable for the treatment of acidic wastewaters, such as Acid Mine Drainage effluents [357]. However, both species exhibited consistent rates of growth and nutrient uptake, when the media was mildly acidic to alkaline and it may be assumed that *Cladophora* is suitable for treating wastewaters with similar characteristics, for example in IMTA systems [35]. Alternatively, as effluents are required to be neutralised prior to discharge into the environment, *Cladophora* sp. may be used as a tertiary treatment, or "polishing" step [331].

Strict control of pH is critical, given the number of variables it influences [358, 359]. Future experiments, therefore, will employed Tris HCl buffer. In addition, an initial pH of 8 was selected for future experiments. This was selected due to the p*K*a of Tris HCl (8.08), the mean pH value of oceanic surface waters (pH = 8.108) [360], and as it was the median pH tested in this experiment where growth was observed (5-11). Whereas, the use of a more alkaline media would increase the proportion of toxic ammoniacal forms ($NH_3$), and may have adverse effects on growth in future experiments [169].

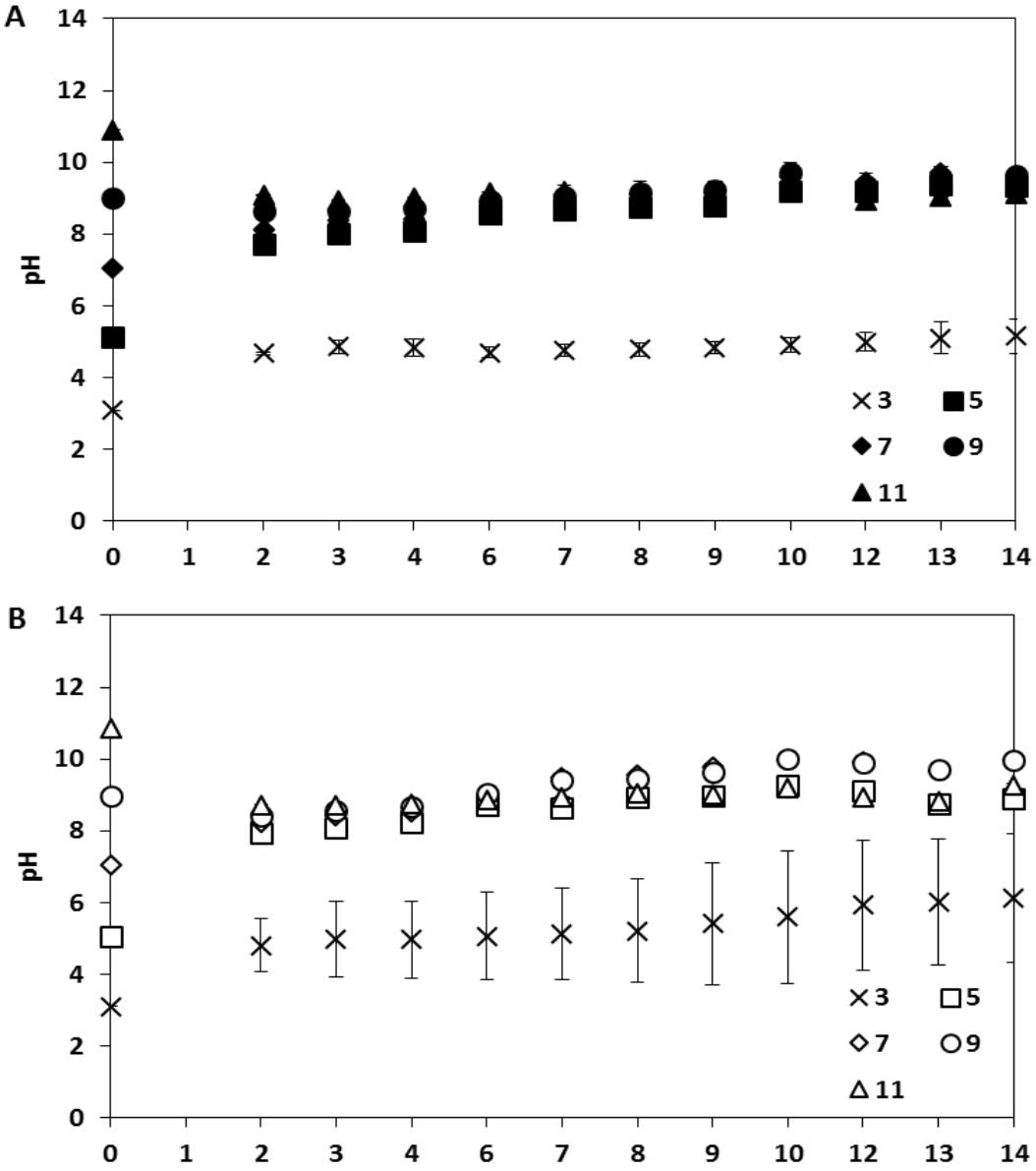


**Figure 3.5.** The temporal change in the pH of the culture media after inoculation with *Cladophora parriaudii* (A) or *Cladophora coelothrix* (B). The unbuffered media was initially adjusted to either 3 (cross), 5 (square), 7 (diamond), 9 (circle), or 11 (triangle) (*n* = 3, *error bars* = 1 SD).

### 3.3.3 Salinity

Salinity is an important variable to consider in a WWT environment. Fluctuations in salinity may occur due to seasonal weather patterns (periods of drought or heavy rainfall), run-off from gritted roads, or due to tidal action which may have implications for coastal treatment

practices, such as shrimp farm IMTA [57, 174, 361]. To ascertain the extent to which *Cladophora* may have potential WWT applications, a broad salinity range was studied.

The trends in growth and nutrient uptake, with varying salinity, were identical for both species (Figs. 3.1C, 3.2C, and 3.3C). High rates of growth and excellent $NO_3$-N and $PO_4^3$-P uptake were achieved in media in which salt was present (15-60 g $L^{-1}$). For example, growth ranged from 5.6-6.8% $d^{-1}$ and 6.8-7.9% $d^{-1}$ for *C. coelothrix* and *C. parriaudii*, respectively (Fig. 3.1C). Nutrient uptake was correspondingly high with >99% and >96.9% removal for $NO_3$-N and $PO_4^3$-P removal, respectively (Figs. 3.2C and 3.3C). However, negative growth rates and a net release of nutrients were observed when samples were cultivated in freshwater medium (0 g $L^{-1}$). For example, -2.4% and -7.5% for $PO_4^3$-P removal and -10.9% and -11.5% for $NO_3$-N removal by *C. parriaudii* and *C. coelothrix*, respectively. This is unsurprising, as both species are of marine origin [84, 319] and would have been under extreme osmotic duress. As a result of the osmotic imbalance, the cells will have swollen and burst, expelling their cellular contents, resulting in the net increase in external nutrient concentration [362].

Both species exhibit a high degree of halotolerance [363], with excellent performance from 15-60 g $L^{-1}$. As such, *Cladophora* may be suitable for a range of WWT applications in brackish, estuarine, marine, or hypersaline environments, including coastal or in-land IMTA systems [35, 361]. However, further study is necessary to determine both the upper and lower levels of osmotic tolerance, to determine the full extent of their applicability.

### 3.3.4 Temperature and Daylight Hours

Wastewater treatment is constant, due to the continuous generation of pollution and its need for treatment. This raises the issue of seasonal effects and their influence on bioremediation capacity. A successful candidate alga should be able to grow and remove nutrients perennially. Seasonality is a broad concept involving different physical factors many of which influence algal biology (section 1.4.1.1). The number of daylight hours and temperature was adjusted to replicate different seasons in a very broad and relatively simple manner.

There was a strong relationship with respect to growth and nutrient uptake with season for both species studied. The DGR of both algae differed significantly, generally with increasing growth coincident with a greater temperature and number of daylight hours. In addition, *C. parriaudii* exhibited higher rates of growth in all seasons than *C. coelothrix* (Fig. 3.1D), for instance, 3.1%, 6.2%, and 8.1% $d^{-1}$ by *C. parriaudii* comparison to 1%, 3.3%, and 7% $d^{-1}$ by *C. coelothrix* in winter, spring, and summer conditions, respectively. The seasonal growth patterns were reflected in the amount of nutrient removal observed (Fig. 3.2D and 3.3D). The uptake of $NO_3$-N by *C. parriaudii* increased from 7.5% in winter conditions to 99.5% in summer (Fig. 3.2D), with $PO_4^3$-P correspondingly increasing from 65% to 97% (Fig. 3.3D).

The results indicate that light and temperature have a strong influence on algal performance, with best growth and nutrient uptake observed during summer conditions. Both Abreu *et al.* [35] and Canale *et al.* [364] reported that temperature and daylight hours are key factors in the seasonal growth of macro-algae. These factors will have a strong influence on the rates of photosynthesis, as well as many aspects other aspects of algal metabolism [171]. In this study, there were statistically significant differences in growth between spring and summer treatments, indicating that temperature had a strong influence on algal performance. More research is required to elucidate the importance of the number of daylight hours, in addition to greater clarity on the effects of seasonality. This could be achieved through continued experimentation, preferably in tightly regulated systems with conditions more representative of seasons; for instance, cultivating *Cladophora* sp. in an environmental modelling photobioreactor, *i.e.* Algem® [365], which has pre-programmed temperature, photoperiod, and light intensity regimes based upon an extensive database of meteorological data.

Another potential reason for the difference in performance between seasons could be due to stress factors. Prior to experimentation, algal samples had been maintained at 18°C with an 18/6 h L/D photoperiod. It is possible that samples transferred to darker, cooler (or hotter) conditions, may have experienced some shock or stress. This may have had an impact upon their performance [366-368]. As such, to negate any potential stress, an acclimation period of a week was implemented prior to future experiments (Chapters 4-6).

### 3.3.5 Long-term Storage

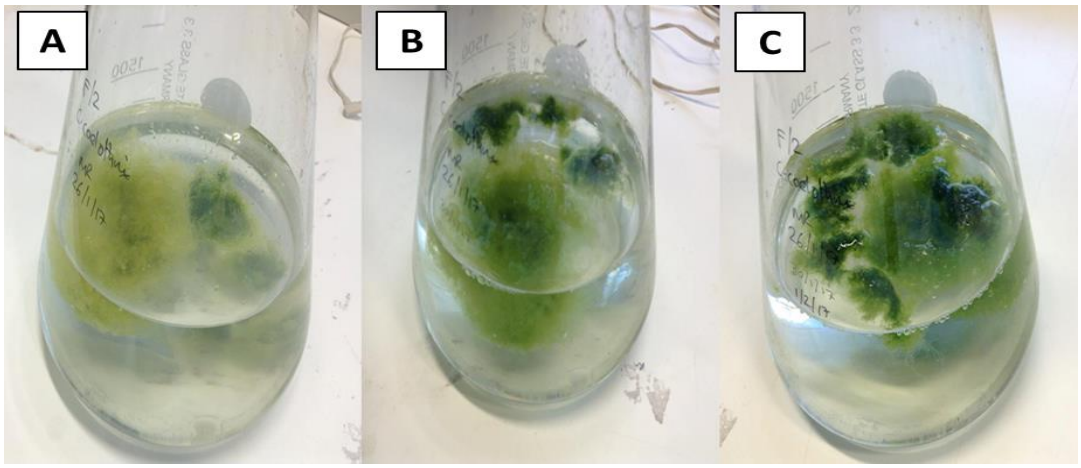


**Figure 3.6.** Recovery of *Cladophora coelothrix* after long-term incubation in a nutrient deplete medium (A), and four (B) and six (C) days after inoculation into fresh media.

*Cladophora* are considered to be extremely durable [338], this robustness was validated during this thesis. After several months of incubation in nutrient deplete medium, *C. coelothrix* which had poor colouration, was re-inoculated into fresh medium and made a full recovery within 6 days, based upon a return to normal pigmentation and the advent of bubbles, indicative of photosynthesis/respiration (Fig 3.6). This hardiness could be of great benefit for use in WWT, or algal cultivation as a whole. For instance, this would allow for the long-term storage of algal cultures; greatly reducing the need for culture maintenance and requirement of frequently purchasing new inoculum.

Both species studied exhibited high rates of growth and nutrient removal during spring and summer seasons, which would make them suitable candidates for treatment during this time of year. Although growth was still observed during winter-like conditions, there was some evidence of net increase in nutrient concentration, which makes them currently unsuitable for WWT in winter. However, WWTPs may have higher discharge limits during winter months due to the unlikelihood of algal bloom formation and dilution effects from increased rainfall. Furthermore, algal performance may be improved through the addition of artificial illumination or heating. However, these cultivation strategies will incur an increased cost with these additional expenses could be alleviated by the revenue obtained from the biomass produced. Alternatively, circular WWT systems could be adopted. For

instance, utilising industrial cooling water or heat generated from anaerobic digestion (AD) plants, where the algal biomass could act as a feedstock [369, 370].

## 3.4 Conclusions

The main objective of the screening study undertaken in this chapter was to test the bioremediation performance of two marine species of *Cladophora* across a range of abiotic conditions. Generally, growth was both high and consistent, with near complete nutrient removal observed in most instances. Poor growth and/or nutrient removal was observed, but only in the most extreme environmental conditions tested. For instance, in freshwater, pH 3, or winter season. These are conditions that may be fundamentally inappropriate for marine species, are infrequently encountered in WWT, or may be coupled with less stringent legislations. Alternatively, provision of light and heat, or acclimation periods may improve algal bioremediation performance. This indicates that *Cladophora* may be suitable for implementation in WWT, subject to further research. Overall, both species of *Cladophora* were considered tolerant to a range of abiotic conditions and robust for long-term storage.

An additional objective of this aspect of the project was to improve macro-algal husbandry through the development and optimisation of cultivation protocols for use throughout the remainder of the thesis. Observations during this research demonstrated a number of weaknesses in experimental design, such as a lack of pH buffering and a small sample size which may lead to cell damage and greater degrees of biological variability. As such, the importance of standardised and controlled experimental conditions was highlighted anda number of precautionary steps subsequently adopted. For instance, the implementation of a standardised cultivation regime with a greater inoculum, including an acclimation period (section 2.2.2.2-2.2.2.5), pH control and buffering. Several other issues were considered or observed during this abiotic screening process that merit further research. These include, examining the influence of different nutrient regimes, which encompasses different nitrogen to phosphorus ratios, nitrogen sources, and concentrations that are more representative of aquaculture effluents. In addition, further optimisation of cultivation practices through the development of a standardised harvesting regime, which is robust,

reliable, and has no adverse physiological impact upon the organism. Some of these are explored and discussed in subsequent chapters.

# Chapter 4

## A comparison of methods for the non-destructive fresh weight determination of filamentous macro-algae

## 4.1 Introduction

The increased realisation of the commercial potential of macro-algae as a direct product, or as a feedstock for further processes (section 1.3) has necessitated the optimisation of current practices and the development of a range of new tools and cultivation approaches [371]. Furthermore, determination of the impact of abiotic and biotic conditions on biomass productivity during an experimental timeline requires the development of a set of standardised methods, which allows comparisons to be made between both treatments and experiments.

Determining algal biomass productivity through its temporal growth rate is one of the most fundamental aspects of algal research in biological, environmental and engineering fields. For example, monitoring algal growth of taxa, including *Cladophora,* in Integrated Multi-Trophic Aquaculture (IMTA), where they perform a key bioremediation role [372], or for potential biomass applications such as bioenergy [141], is critical to assessing both performance and productivity. Yet, there remains no standardised approach for determining growth. The primary parameters to consider when quantifying biomass are reproducibility, reliability and applicability. Other desirable facets of a quantification method include: ease of use/speed, and minimal/no damage to the biomass, where the latter issue is especially relevant for the accurate assessment of growth rates. Errors associated with determining total biomass, or growth rate, can lead to inaccuracies in estimating productivity, economic potential, as well as difficulties with literature comparison. It is therefore important to standardise procedures that are both accurate and reliable. Moreover, the method deployed has to be applicable for the species being studied as macro-algae, and algae in general, have varied phenotypes and growth habits (section 1.2.). These characteristics effectively dictate the approach that may be applicable. In most cases this is straightforward: for instance, many micro-algal taxa are unicellular and their growth can be quantified by counting the cells in a given volume of water, e.g. using either a hemocytometer, or a Coulter counter [373, 374], or alternatively by methods employing absorbance [375], or light scattering [376]. For multicellular algae these approaches are unsatisfactory as optical methods require a uniform suspension of material so that a linear relationship with biomass (weight or cell number) may be determined. In contrast, for large species of seaweed, such as members of the Lamiariales, changes in biomass can be

determined by temporally measuring the length of the fronds, which can reach more than 60 m in length, or using classic hole/needle punch methods [73, 377-380]. However, the morphology of the thalli of some macroalgal species can be quite varied, ranging from simple blades to more structurally complex forms made up of parenchyma and corticated filaments [148]. Therefore, determining the biomass of species with variegated or multifarious thalli can be complex.

A commonly employed method to determine growth rate is based on the dry weight (DW) of the organism, usually achieved by drying in an oven, freeze-drier, or by the sun [153, 154]. Although this approach is reliable, simple and reproducible, the drawback is that it involves sacrificing the whole of the biomass sample, making the determination of growth rates impossible over a time-course. When assessing temporal growth using DW, the problem of sacrificing samples can be overcome by utilizing multiple replicates. However, this approach has its own constraints and pitfalls such as the time taken to ensure the sample has fully dried, a requirement for a large working area and other resources, as well as potential limitations in availability of biological material where sacrificing material would compromise the accuracy of the experiment.

Image analysis is a possible option as a method to determine yields and growth rates. This approach has previously been successfully applied to macro-algae where individual *Cladophora* filaments on agar have been measured temporally using light microscopy [372]. However, from a practicality perspective this approach is better suited for screening projects involving individual filaments. Macleod *et al.* [381] used an alternative imaging software for the analysis of biofouling coverage on buoys as proxies for renewable energy structures in the marine environment. This approach, although simple and time efficient, could only provide data on coverage and not on the biomass of the adhering flora and fauna. Although imaging software is becoming a lot more powerful, making these techniques more readily applicable, there are still constraints including the time and resources required for analysis. Additionally, the three-dimensional and often fractal nature of seaweed makes determination of any correlation between each image and its corresponding DW, or productivity, challenging.

In many environmental and applied studies, both mass and growth rates of macro-algae are expressed as fresh weight (FW) [338, 382, 383]. Despite the fact that FW is widely assessed, no standardized method has been agreed upon and thus comparisons between

different studies are challenging. For instance, the FW of the Chlorophyte *Cladophora* has been determined employing a variety of approaches, the most common of which is drying with a sorbent material, *i.e.* filter paper [295, 337, 384, 385]. However, variations in material used, application time and pressure will inevitably lead to differences in the volume of water removed. In some studies, FW is mentioned but no method of determination is reported [141, 343, 386]. On this basis, it may not be feasible, or valid, to draw conclusive inferences when comparing data from different studies.

Another key consideration is the morphology of algal species. Filamentous algae are multi-cellular, multifarious and often quite fragile [387], which makes accurate growth rate and biomass quantification problematic. If the viability of the algae is impaired during fresh weight quantification, for instance due to excessive pressure or dehydration, this may have major implications on the accuracy of any assessments of subsequent growth. A promising, yet seldom employed method, with seemingly low mechanical impact, involves dewatering filamentous algae using a reticulated spinner (RS). In their respective *in situ* studies on ecology and IMTA, both Peckol *et al*. [165, 338] and de Paula Silva *et al.* [231, 372] employed this approach to remove excess water from *Cladophora*. However, these studies did not detail the number or duration of iterations with the reticulated spinner, thus making a comparison difficult due to the possibility of non-standardisation in approach. Furthermore, FW was only assessed at the beginning and end of each experiment lasting 10-14 days, and the daily growth rate inferred from the two data points. This non-intrusive method could have the potential to be used periodically during an experiment to determine growth rate, with little-to-no physiological detriment to the organism, thus providing a higher degree of resolution to productivity data.

The ability to accurately determine FW and productivity is the cornerstone of any algal research and the development and use of a robust, standardized lab-scale method is an absolute necessity. The aim of this chapter was to investigate the suitability of a variety of methods for the FW determination of filamentous macro-algae employing model strains of *Cladophora* and *Spirogyra*. This is the first study of its kind to make a concerted effort to assess FW methodologies in terms of reliability and reproducibility, as well as their biological impact in terms of viability, growth, and nutrient uptake. Furthermore, the objective was to adopt a dewatering technique that is a good indicator of DW and has no

detrimental impact upon the algae over a time-course, therefore, maintaining their original experimental purpose.

## 4.2 Materials and Methods

### 4.2.1 Macro-algal strains and culture conditions

Three macro-algal strains were used in this chapter: *Cladophora coelothrix* CCAP 505/10, *Cladophora parriaudii* CCAP 505/09, and *Spirogyra varians* CCAP 678/3 (Section 2.2.1) and were cultivated following the steps described throughout section 2.2.2.

After a seven day acclimation period (section 2.2.2.4), 35.7 mg FW sub-samples determined employing the reticulated spinner, B+RS method described in Table 4.1, were inoculated into triplicate 100 ml flasks containing 50 ml of fresh medium, and then incubated as described in section 2.2.2.5 for 14 days. Samples were aseptically removed in a laminar flow five times over the 14-day growth period (MSC Advantage, Thermo Scientific) for FW and nutrient determination.

### 4.2.2 Fresh Weight determination

Seven different techniques for macro-algal FW determination were assessed. The different biomass dewatering methods involved centrifugation with a reticulated spinner (RS), gently blotting with filter paper, agglomeration using a perforated crucible, and pressing between microscope slides or a combination of the above. The methods used are described in detail in Table 4.1. During the 14-day incubation period, the algal biomass was removed a total of five times and the different methods applied, followed by gravimetrical weighing with an analytical balance (PS-60, Fisher Brand, UK) for FW determination. After each assessment the algal samples were transferred back to their original flasks and returned to the standardised cultivation regime.

### 4.2.3 Optimisation of Reticulated Spinner FW determination

Some of the methods tested removed excess water from algal biomass by centrifugation using a small Chef'n Salad Spinner (Fig. 4.1), referred to hereon as "reticulated spinner" (RS). This operates using a lever, which when pressed, rotates an internal basket. The basket has a diameter of 370 mm, with elliptical or circular perforations of minimal and maximal sizes of 3 mm x 3mm to 18.5 mm x 3 mm, respectively. The optimal duration of dehydration using the reticulated spinner was determined for all algal species. Initially samples were measured using the "B" method, as described in Table 4.1, and then sequentially spun in 15 s intervals, for a total of 120 s, with the FW determined after each step by gravimetrical weighing using an analytical balance (PS-60, Fisher Brand, UK).

### 4.2.4 Dry weight determination

After 14 days, algal samples were collected and rinsed with deionised water to remove extracellular salts and nutrients, the biomass was then dewatered using methods B+RS and PC+RS, for *Cladophora* sp. and *S. varians*, respectively (Table 4.1) . Dry weight was determined using the method described in section 2.3.2.

### 4.2.5 Carbohydrate composition

To determine whether the dewatering procedures had any effect on the biochemical composition of the biomass, the total soluble carbohydrate content of the biomass was extracted and quantified, using the methods described in sections 2.5.3.1-2.5.3.2.

**Table 4.1.** A description of methods used for Fresh Weight (FW) determination and their acronyms. Methods marked * were only employed with *Spirogyra varians.*

| Method Employed | Abbreviation | Description of Procedure |
|---|---|---|
| **Beaker** | **B** | Using a spatula, algal biomass was transferred directly from the flask to a weigh-boat, and weighed gravimetrically. |
| **Beaker + Reticulated Spinner** | **B+RS** | **B**, followed by reticulated spinner (**RS**) centrifugation with optimised time (see below) and then weighed gravimetrically. |
| **Beaker + Filter Paper** | **B+FP** | **B**, followed by gently pressing the biomass with GF/F filter paper (**FP**), and then weighed gravimetrically. |
| **Beaker + Reticulated Spinner + Filter Paper** | **B+RS+FP** | **B+RS**, followed by gentle pressing of the biomass with GF/F filter paper, and then weighed gravimetrically. |
| **Beaker + Cavity Microscope Slide*** | **B+MS*** | **B**, followed by placing the biomass between two cavity microscope slides (**MS**) to remove excess water, and then weighed gravimetrically. |
| **Perforated Crucible*** | **PC*** | Cultures were poured through a perforated crucible (**PC**) (Coors™ Gooch crucible), and then weighed gravimetrically. |
| **Perforated Crucible + Reticulated Spinner*** | **PC+RS*** | **PC**, followed by reticulated spinner centrifugation with optimised time (see section below), and then weighed gravimetrically. |
| **Positive Control** | **+ C** | The positive control was only weighed at the end of the experiment. Therefore, it remained unperturbed during the experimental period. |

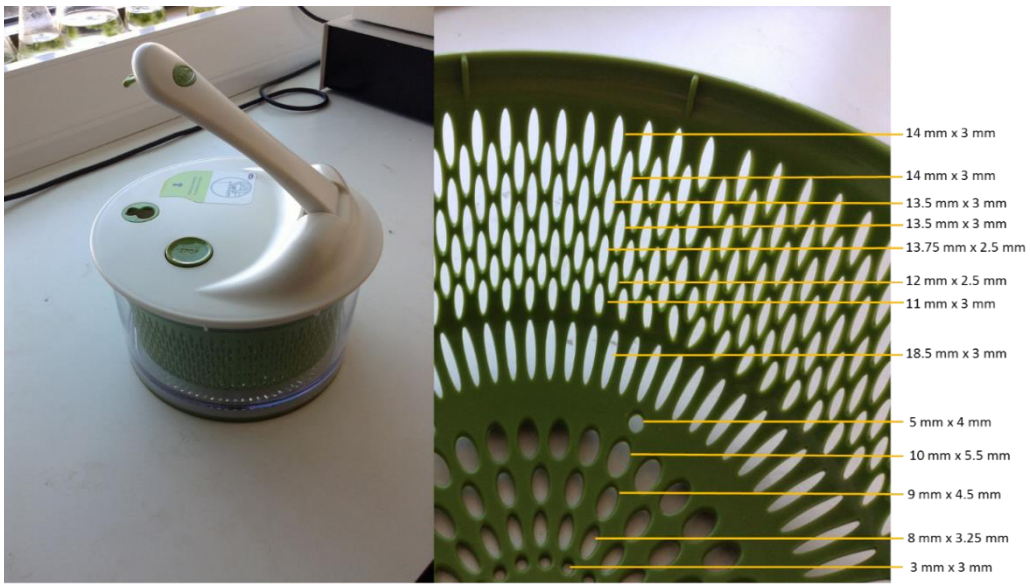


**Figure 4.1**. The reticulated spinner (RS) (Small Salad Spinner, Chef'n) and its characteristics, employed throughout this chapter. Image from [319].

### 4.2.6 Microscopy

The effect of the procedures on gross cellular morphology was examined using an inverted microscope (Eclipse TE2000-U, Nikon, UK). After 14 days, samples were mounted on a microscope slide with a small volume of growth medium, to avoid desiccation. Filaments on the periphery of the culture were selected for ease of visualisation and were with a x100 objective lens. Images were captured using a CoolSNAP HQ2 camera (Photometrics) assisted by MetaMorph® Microscopy Automation and Image Analysis Software (Molecular Devices).

### 4.2.7 Residual nutrient determination

The concentration of nitrate and phosphate in the culture media was measured for each of the five sampling days by Ion Chromatography (section 2.4.3) [319].

### 4.2.8 Optimised method – Validation of the temporal FW/DW relationship

To ensure that FW growth rates determined with the optimal method from Table 4.1 were an accurate measurement of biomass growth, the constancy of the relationship between FW and DW growth rates was determined. A total of 15 flasks of each algal species were inoculated and incubated under the standard regime as outlined above. The algal biomass in these flasks was harvested on days 0, 3, 5, 10 and 14 following the B+RS method for *Cladophora* sp., or PC+RS method for *S. varians* (Table 4.1) and the FW determined gravimetrically using an analytical balance (PS-60, Fisher Brand, UK). Three flasks of each algal species were subsequently sacrificed for the determination of their DW, as outlined above.

Growth rates for FW and DW were determined according to the formula prescribed by Yong *et al.* [388] (section 2.3.3):

$$Growth\ Rate\ (\%) = \left[\left(\frac{W_t}{W_0}\right)^{1/d} - 1\right] x\ 100$$

Where $W_t$ and $W_0$ is the final and initial mass, respectively, and $d$ is time (days).

### 4.2.9 Statistical analysis

All experiments were performed in triplicate and the experimental error was calculated and expressed as one standard deviation (SD). The significance of difference in the DW and carbohydrate yields of macro-algal samples periodically subjected to a variety of dewatering methods was obtained by one-way ANOVA with Tukey's post hoc analysis ($P = < 0.05$) ($n = 3$). Pearson correlation coefficients, $r$, were used to assess the temporal relationship between FW and DW. All Statistical analysis was performed using Minitab® Statistical Software version 17.

## 4.3 Results and Discussion

In this chapter, a variety of methods, described in Table 4.1, were assessed for the determination of the FW of three species of filamentous macro-algae: *C. coelothrix*, *C. parriaudii*, and *S. varians* (Fig. 2.1.). These three species have differing physical appearances and growth characteristics. *C. coelothrix* grows quite slowly in tightly knit "clusters" with thick cell walls, whereas, *C. parriaudii* grows quickly in a loose skein. *Cladophora* has been described as an "ecological engineer": they are a robust, bloom-forming species and have shown high removal rates of nutrients and heavy metals [27, 186, 231, 273, 301]. Furthermore, they are resistant to grazers [186], making them strong candidate species for wastewater bioremediation [231]. *S. varians* has a central core of biomass, from which helical shaped filaments grow towards the water surface, which are very fragile, tending to fragment when disturbed. The three species were selected as model organisms to explore the applicability of dewatering methods across a range of phenotypes. Systematic measurement of FW, final DW, FW/DW ratio, carbohydrate yield, $NO_3^-$ and $PO_4^{3-}$ uptake and microscopic image analysis were used to ascertain the viability, growth and metabolic activity of the algae periodically subjected to the different harvesting methods.

### 4.3.1 Optimisation of the Reticulated Spinner

Some of the harvesting methods tested employ a reticulated spinner, which has the ability to rapidly remove extracellular water from filamentous algae and hence facilitate accurate FW determination. In order to ensure a consistent level of water removal, the operation of the reticulated spinner was standardised. The FW of the three algal species was determined after each 15 s spin, up to a maximum duration of 120 s (Fig. 4.2). There was a reduction in the overall weight corresponding to 77-81% of the original wet weight, irrespective of species studied. This indicated the potential applicability of the method to a wide range of filamentous taxa. The majority of water removal, *i.e.* 61-68%, occurred within the first 15 seconds. This was followed by a reduction in the rate of weight change, with minimal further water removal after 90 s operation, corresponding to a reduction in mass up to 75-80%. Additional spinning, beyond 90 s, resulted in a further reduction in mass of less than 1.5% for all species tested. A spinning time of 90 s was adopted for the reticulated spinner.

It is recommended that a similar approach is employed when implementing and standardising this method for different algal taxa, varying amounts of algal biomass, or when cultivating in very different conditions, such as extremes of salinity [389].

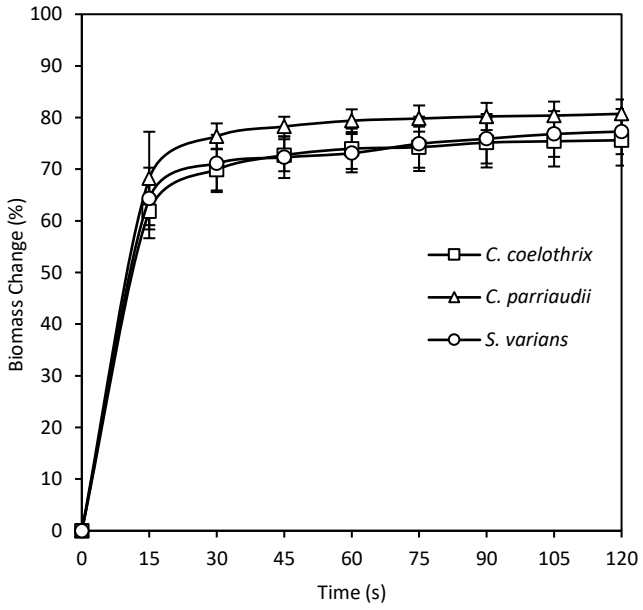


**Figure 4.2.** Optimisation of spinning time required to dewater *Cladophora parriaudii*, *Cladophora coelothrix* and *Spirogyra varians* in the reticulated spinner. Algal FW values were measured after 15 s increments in the reticulated spinner. Biomass Change (%) represents the mass change of FW relative to the initial wet biomass (*n* = 3, *error bars* = 1 SD).

## 4.3.2 Dewatering Efficiency for the Tested Methods

Although DW is an accurate measure of biomass, its determination necessitates the sacrifice of the culture. However, FW determination is non-destructive and can be reiterated across a time-series to give high-resolution productivity data. In this study, cultures were harvested periodically over a 14-day period to obtain FW, and on the final day DW was also determined and an FW/DW ratio obtained (Fig. 4.3). This ratio would be expected to inform how strong an indicator of biomass a particular dewatering method is: the lower the ratio, the more efficient the dewatering method should be. However, the size of the error bars will also indicate how reproducible each method is, therefore providing a more accurate and consistent measure of actual productivity.

Of the methods tested B and PC required the least mechanical effort, but they resulted in high FW/DW ratios for the three species, ranging between 26-44 and >60, respectively for *Cladophora* sp. and *S. varians* (Fig. 4.3). Although one would anticipate that these methods would not result in any physical damage to the alga, and therefore have no deleterious effects on metabolic function or growth, they did have a high degree of error that was associated with the greater volume of unpredictable water carry-over, making these methods unsuitable for implementation. Conversely, B+FP and B+RS+FP have FW/DW ratios of <10 for *S. varians* and <4 for both species of *Cladophora*, with low error throughout. These methods involved lightly pressing the biomass with absorbent filter paper (Table 4.1) and resulted in the highest removal of water from the biomass (Fig. 4.3). The B+RS method, which removes water centrifugally, also has a great degree of highly consistent residual water removal, with ratios of 6.3 (± 0.3) and 8.6 (± 0.2) for *C. coelothrix* and *C. parriaudii*, respectively. Methods B+RS, B+MS, and PC+RS all had a similar degree of water removal when employed with *S. varians*: ratios were 20.3 (± 0.05), 18.6 (± 6.1), and 19.3 (± 4.2), respectively.

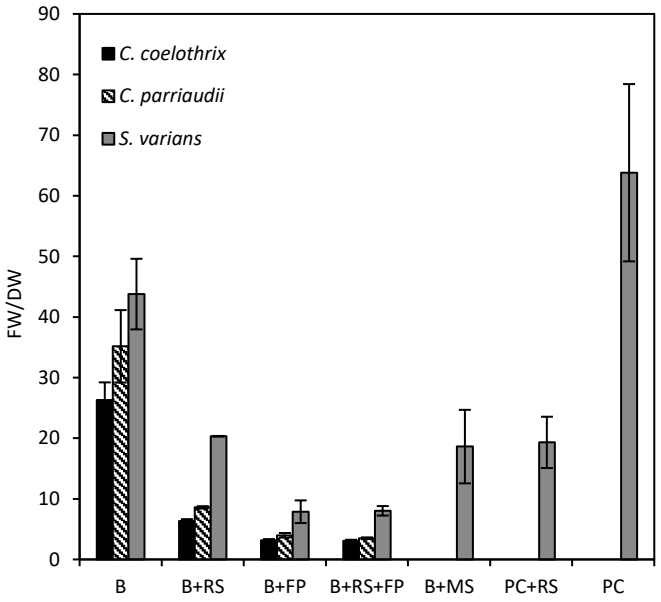


**Figure 4.3.** Final Fresh Weight to Dry Weight ratio of *Cladophora parriaudii*, *Cladophora coelothrix* and *Spirogyra varians*,grown for 14 days (100 rpm, 24°C, light intensity of 30-40 µmol photons $m^{-2}$ $s^{-1}$, 18h/6h L/D photoperiod), periodically harvested and dewatered following the methods: beaker (**B**), beaker + reticulated spinner (**B+RS**), beaker + filter paper (**B+FP**), beaker + reticulated spinner + filter paper (**B+RS+FP**), beaker + cavity microscope slide (**B+MS**), perforated crucible + reticulated spinner (**PC+RS**), perforated crucible (**PC**). More detailed descriptions on each method can be found in Table 4.1 (*n* = 3, *error bars* = 1 SD).

The final DW obtained for the different harvesting methods is shown in Figure 4.4. The + C corresponds to biomass grown and harvested without any additional dewatering procedures being applied and hence acted as a positive control. Variations in the final DW were observed for the different methods adopted, which indicated that there was an impact on the algal growth.

In the case of *S. varians*, the choice of FW method had a significant impact upon DW yield, $p = 0.036$. It was observed that the biomass of *S. varians* was prone to fragmentation when disturbed, and obtaining sufficient biomass to ascertain FW was problematic for several of the methods employed. For instance, disintegrating into a suspension of short filaments meant that the algae would tend to pass through the apertures of the reticulated spinner and were challenging to gently blot with a piece of filter paper. The use of a cavity microscope slide (B+MS) was intended to reduce filament loss and to minimise damage caused by actively blotting or from effects of desiccation. A pre-collection step (PC in Table 4.1), involving pouring the contents of the flask through a perforated crucible (PC), was incorporated into the harvesting protocol for this alga. The apertures were small enough to retain most of the biomass and agglomerate it, allowing it to then be subjected to a further dewatering method with the reticulated spinner. As can be observed (Fig. 4.4) the PC method had no obvious impact on the biomass levels of *S. varians* obtained when compared to the control. However, implementing the PC step prior to utilising the RS method, increased the DW yield from 10.8 mg to 12.4 mg, compared to employing the B+RS technique alone.

The DW obtained for the different treatment on *C. parriaudii* ranged from between 9.6 – 16.03 mg and no statistically significant differences in yield were observed ($p = 0.102$). Likewise, no significant differences ($p = 0.51$) were recorded in the final DW yield of *C. coelothrix* (13.13 – 16.43 mg). This species grows in tightly knit “clusters” and has a basal cell wall thickness of up to 15 μm, which may make it resistant to mechanical damage [390]. It is worth noting that DW measurements, on their own, are insufficient to show any difference between treatments. Dry weight only take into account the total mass of the culture and does not differentiate between viable, damaged, and non-viable cells. As shown in Table 4.1 and Figure 4.3, methods that involve pressing the biomass with absorbent filter paper tend to have a low and reproducible FW/DW ratio, indicating good water removal.

However, high levels of water removal and a low growth suggests that damage may have occurred during the sampling and FW determination procedures. For instance, commonly used large-scale harvesting techniques, such as centrifugation and cross-flow membrane filtration, can exert large amounts of shear stress that can damage and lyse micro-algal cells [391, 392]. In scientific research, however, it is very important to use low-impact methods to avoid the possibility of erroneous or false results.

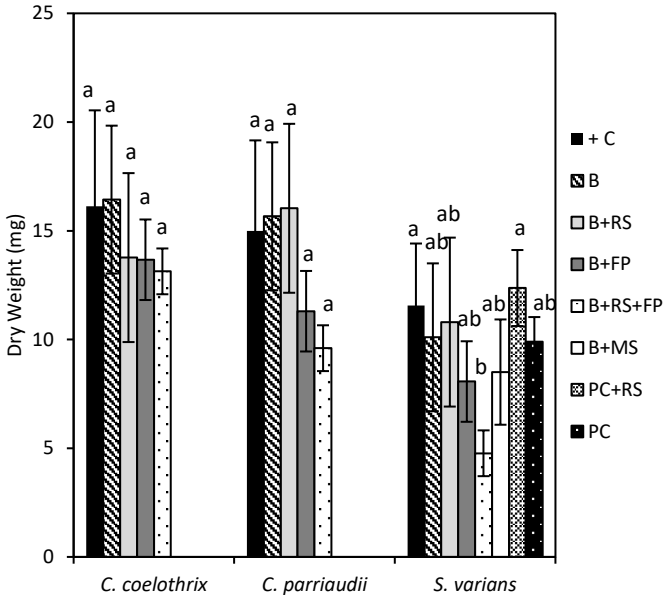


**Figure 4.4.** Final Dry Weight (DW) of *Cladophora parriaudii*, *Cladophora coelothrix* and *Spirogyra varians*, grown for 14 days (100 rpm, 24°C, light intensity of 30-40 µmol photons $m^{-2}$ $s^{-1}$, 18h/6h L/D photoperiod), periodically harvested and dewatered following the methods: beaker (**B**), beaker + reticulated spinner (**B+RS**), beaker + filter paper (**B+FP**), beaker + reticulated spinner + filter paper (**B+RS+FP**), beaker + cavity microscope slide (**B+MS**), perforated crucible + reticulated spinner (**PC+RS**), perforated crucible (**PC**). More detailed descriptions on each method can be found in Table 4.1 [*n* = 3 (except *S. varians* "+ C" *n* = 8), *error bars* = 1 SD]. For each species, means that do not share a letter are significantly different from one another, $p = < 0.05$.

Variation in the FW/DW ratio is dependent upon the growth conditions. For instance, Angell *et al.* [389] reported that the FW/DW of *Ulva ohnoi* was greatest when cultivated in low to optimal salinities, and lowest when exposed to high salinity. This difference in ratio most likely caused by a change in osmotic potential. Care should be taken when determining FW/DW across a range of environmental variables or cultivation conditions. However, this is not the case of the present study as the algae were grown under the same conditions.

The FW/DW ratio was also found to depend upon the dewatering methods applied (Fig. 4.3). Those involving spinning (B+RS, B+RS+FP, and PC+RS) or blotting with filter paper (B+FP, B+RS+FP) will result in a lower FW/DW ratio than those that apply minimal pressure, such as pouring through a perforated crucible (PC). Furthermore, the FW/DW ratio obtained and its degree of error, will also depend upon the species or morphology of the alga that it is applied to. For instance, the FW/DW values varied between species using the same method due to differences in water retention, both intra- and extracellularly. Finally, the DW yield is also species-specific. The choice of dewatering method will have minimal impact upon robust cultures, with thick cell walls or protective growth habits, such as *C. coelothrix*. In contrast, fragile species like *S. varians* are more strongly influenced by the choice of dewatering method, with more stringent methods compromising the viability of the culture. Furthermore, *S. varians* requires a pre-collection step to ensure the minimisation of biomass losses, which would further reduce the DW yield.

### 4.3.3 Physiological Assessment

The reduced DW yields observed for some of the species may be due to the viability of the biomass being compromised as a result of the different protocols employed. Images of the harvested algae subjected to methods + C, B+RS or PC+RS, and B+FP were taken, to ascertain whether the algae showed any physical damage (Fig. 4.5). Healthy, undamaged filaments were observed in the positive control treatment for all three species (Fig. 4.5a, d, and g). The filaments were considered to be phenotypically normal as they exhibited the characteristic large “breeze-block” type cells, with typical green colouration throughout the cells. Furthermore, *C. coelothrix* displayed some branching, indicative of growth (Fig. 4.5a). *Cladophora* cultures that were periodically harvested using the B+RS method (Fig. 4.5b and e), and the amended PC+RS method for *S. varians* (Fig. 4.5h) were similar in appearance to the positive controls, with only some superficial damage visible for *C. coelothrix*. In contrast, algal cultures periodically harvested using the B+FP treatment (Fig. 4.5c, f, and i) displayed obvious damage, with their cellular contents having been expelled, and with chloroplasts observed in large, often discoloured, conglomerates attached to the outside of the cell wall. Although the absorbent filter paper removed superficial water, it was assumed that it caused some shear or mechanical stress upon the organism in the process. The

greater parity between the FW/DW ratio for methods employing filter paper (Fig. 4.3) were potentially not only due to the removal of superficial and interstitial water, but this approach may also have removed intercellular fluid, resulting in cellular injury, as the cells diminished in size and were in some cases devoid of contents. The image analysis evidencing the presence or absence of mechanical or physical damage to the algal cellular morphology is in agreement with the corresponding DW data (Fig. 4.4). The methods employed to determine FW growth might not be appropriate as they adversely impact upon the viability of the cell. Although methods B+FP and B+RS+FP offer a good estimation of DW yield, this comes at a cost. In addition to a reduction in DW yield, visual imaging indicated that the B+FP technique clearly damaged all cultures tested. Given the methodological similarity between B+FP and B+RS+FP, it may be inferred that employing the B+RS+FP method results in comparable levels of cellular damage. On the other hand, B+RS and PC+RS have similar biomass yields compared to the + C for all three species, whilst providing an accurate estimation of DW and with negligible obvious damage to the algae.

Disparities in nutrient uptake were observed, depending on the FW assessment approach employed, further indicated that under some treatment regimes physiological damage had occurred (Figs. 4.6 and 4.7). For all species tested, the positive control cultures demonstrated a high capacity to remove $NO_3^-$ and $PO_4^{3-}$ from the media, with ~ 45% and 19%, 55% and 21%, and 65% and 40% removal for *C. coelothrix*, *C. parriaudii* and *S. varians*, respectively (Fig. 4.6a-d and 4.7a-d). In general, cultures subjected to the mildest dewatering methods (Table 4.1/Fig. 4.3) demonstrated the highest nitrate removal capacity; B with 59% and B+RS with 45-62% removal for both species of *Cladophora*, whereas 76% and 95% $NO_3^-$ removal was observed for *S. varians* with methods PC and PC+RS, respectively. A similar trend was noted for $PO_4^{3-}$ removal whereby the greatest removal in *Cladophora* was with the B treatment (31.6-33.9%) followed by B+RS (25.8-26.7%). In addition, employing methods B+RS, PC+RS, and PC resulted in the greatest $PO_4^{3-}$ removal attained by *S. varians* with values ranging from 47.5-61.5% (Fig. 4.7c-d). Conversely, algae subjected to protocols that featured mechanical pressing (B+FP, B+RS+FP, and B+MS) were amongst those with the lowest rates of nutrient uptake (Fig. 4.6 and 4.7). This indicated that the more harsh methods had a detrimental effect on the algae in terms of algal metabolism. This was further exemplified by the discrepancy in $NO_3^-$ uptake between algae subjected to the FW methods after day 2, which became increasingly

pronounced with each successive harvest. Conversely, in comparison with the + C, algae treated using the B+RS or PC+RS protocols had similar nutrient uptake capabilities for all species tested. This suggests that these harvesting methods have little-to-no impact on the physiological integrity of the organism. This aspect is particularly important for small-scale algal systems where routine sampling is required and sampled algae are returned to the cultivation system.

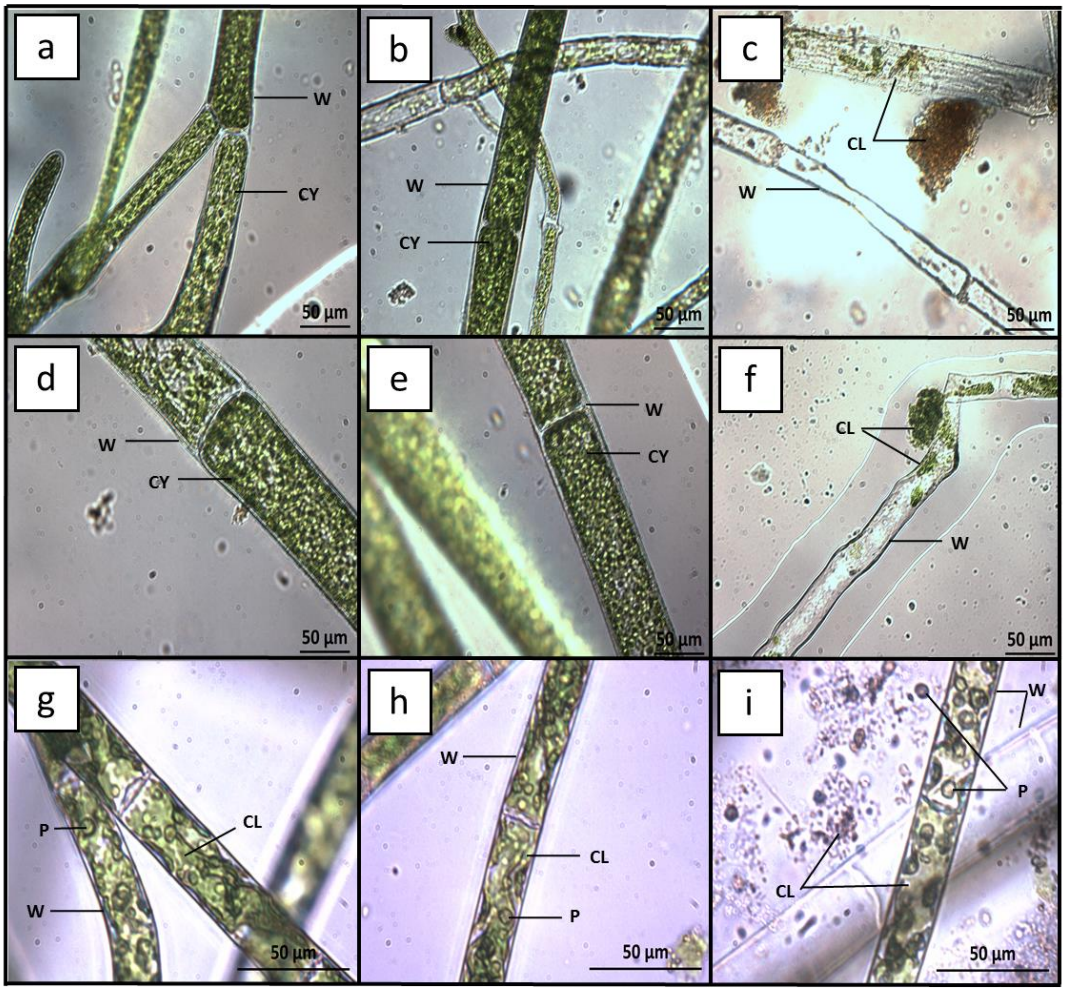


**Figure 4.5.** Plates of *Cladophora coelothrix* (**a-c**), *Cladophora parriaudii* (**d-f**), and *Spirogyra varians* (**g-i**) taken with an inverted microscope after a 14 day growth trial (100 rpm, 24°C, light intensity of 30-40 µmol photons $m^{-2}$ $s^{-1}$, 18/6 h L/D photoperiod) with frequent harvesting using different methods described in Table 1; positive control (**+ C**) (**a, d & g**), beaker + reticulated spinner (**B+RS**) (**b & e**), beaker + filter paper (**B+FP**) (**c, f & i**), perforated crucible + reticulated spinner (**PC+RS**) (**h**). W denotes the cell wall, CL indicates the chloroplasts, P is the pyrenoid and CY highlights the multi-nucleate cytoplasm that contains pyrenoids, chloroplasts and vacuoles.

The different methods for dewatering did not result in any significant alteration in the biochemical content of the biomass ($p$ = 0.155-0.948) (Fig. 4.8), with carbohydrate values ranging from 28-31.4%, 23.9-27.2%, and 60.1-72.9% for *C. coelothrix*, *C. parriaudii* and *S. varians*, respectively.

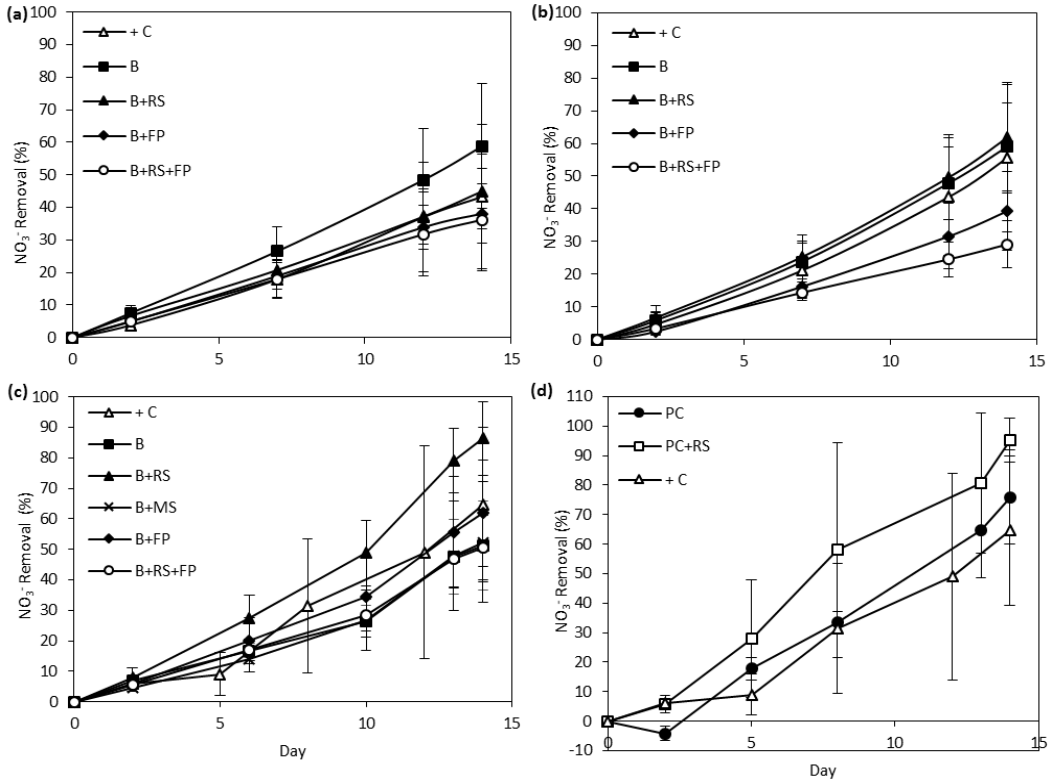


**Figure 4.6**. The temporal removal of nitrate from the media by: *Cladophora coelothrix* (**a**), *Cladophora parriaudii* (**b**), *Spirogyra varians* (**c & d**). Their growth was assessed periodically using different protocols: beaker (**B**), beaker + reticulated spinner (**B+RS**), beaker + filter paper (**B+FP**), beaker + reticulated spinner + filter paper (**B+RS+FP**), beaker + cavity microscope slide (**B+MS**), perforated crucible + reticulated spinner (**PC+RS**), perforated crucible (**PC**) (Table 1). Nitrate was measured in the media using Ion Chromatography ($n$ = 3, [except *S. varians* "+ C" where n = 8] *error bars* = 1 SD).

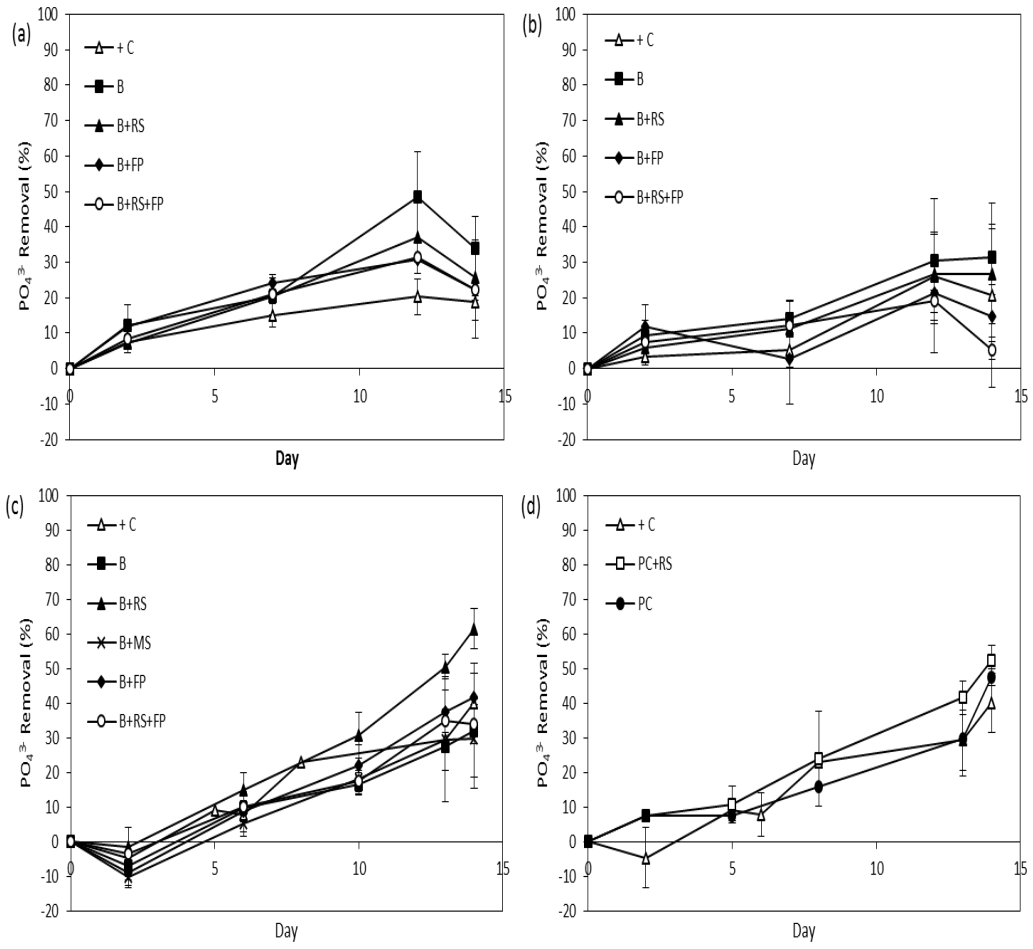


**Figure 4.7.** The temporal removal of phosphate from the media by: *Cladophora coelothrix* (**a**), *Cladophora parriaudii* (**b**), *Spirogyra varians* (**c & d**). Their growth was assessed periodically using different protocols: beaker (**B**), beaker + reticulated spinner (**B+RS**), beaker + filter paper (**B+FP**), beaker + reticulated spinner + filter paper (**B+RS+FP**), beaker + cavity microscope slide (**B+MS**), perforated crucible + reticulated spinner (**PC+RS**), perforated crucible (**PC**) (Table 1). Phosphate was measured in the media using Ion Chromatography (*n* = 3, [except *S. varian*s "+ C" where n = 8] *error bars* = 1 SD.).

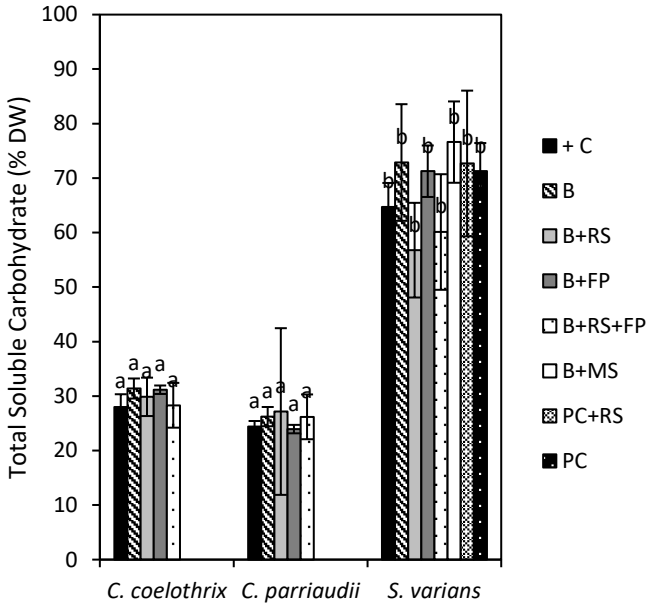


**Figure 4.8**. Total soluble carbohydrate content of the biomass (% DW) of *Cladophora coelothrix*, *Cladophora parriaudii* and *Spirogyra varians*, grown for 14 days (100 rpm, 24°C, light intensity of 30-40 µmol photons $m^{-2}$ $s^{-1}$, 18h/6h L/D photoperiod), periodically harvested and dewatered following the methods: beaker (**B**), beaker + reticulated spinner (**B+RS**), beaker + filter paper (**B+FP**), beaker + reticulated spinner + filter paper (**B+RS+FP**), beaker + cavity microscope slide (**B+MS**), perforated crucible + reticulated spinner (**PC+RS**), perforated crucible (**PC**). More detailed descriptions on each method can be found in Table 4.1 [*n* = 3 (except *S. varians* "+ C" *n* = 8), *error bars* = 1 SD]. For each species, means that do not share a letter are significantly different from one another, $p = < 0.05$.

The results obtained in this study may be partially explained by the differences in morphology and algal growth strategy of the taxa studied. Members of the genus *Cladophora* are characterised by their multi-nucleate cells arranged in either branched or unbranched filaments. Their cell wall is primarily composed of highly crystalline cellulose I [72, 73]. As previously mentioned, *C. coelothrix* typically grows in floating clusters or mats, which are tightly wound (Fig. 2.1A). This characteristic provides mechanical protection to the cells and it was noted in this study that *C. coelothrix* was largely unaffected by the FW determination methods employed. In contrast, *C. parriaudii* tends to grow in a loose skein, with filaments that grow rapidly outwards to any vacant space; this growth strategy will result in the younger, less robust, filaments being more likely to be susceptible to mechanical damage (Fig. 2.1B). This was observed in this study (Fig. 4.4, 4.5f and 4.6b) where DW yield, physical damage, and a reduced metabolic capability/ nutrient sequestration were observed in cultures subjected to the more stringent dewatering

methods. Less mechanically stressful treatments, such as B+RS, were better suited for this species. *Spirogyra* are almost exclusively found in freshwater and are characterised by growing in unbranched filaments with an intracellular helical ribbon of chloroplasts [393]. *S. varians* grows as a benthic mass, with filaments intertwined in a helical arrangement growing toward the water surface (Fig. 2.1C). The filaments are thin, fragile, and readily fragment when agitated, or swirled [72, 80]. This propensity for the colony to disintegrate meant that many of the approaches employed were unsuitable owing to the fragility of its filaments.

### 4.3.4 Investigating the Temporal Relationship between FW/DW under Optimal Harvesting Conditions

In comparison with methods for DW determination, B+RS and PC+RS are rapid, less energetically expensive to perform and are non-destructive to the algal sample. In order to ensure that FW measurements using B+RS and PC+RS were reliable indicators of DW (Fig. 4.9a, c, and e), and consequently of biomass growth (Fig. 4.9b, d, and f), the relationship between FW and DW was determined for a 14 day incubation period. It was noted that there is a strong positive relationship between the FW and DW mass: Pearson correlation coefficients were determined as $r$ = 0.871, 0.948, and 0.954 for *C. coelothrix*, *C. parriaudii*, and *S. varians*, respectively, with P-values of <0.001, and with low error throughout. Interspecies variation in biomass growth rate can be clearly determined using the B+RS and PC+RS methods. The initial "dip" in growth observed for *S. varians* (Fig. 4.9e-f) was assumed to be caused by the fragmentation of the colony and incomplete retention of the biomass on the perforated crucible.

One of the purposes of this study was to be able to assess the feasibility of using non-destructive FW measurements to determine macroalgal growth rates, instead of using sacrificial DW measurements. Employing the FW/DW ratios of 6.3, 8.6, and 19.3 for *C. coelothrix*, *C. parriaudii*, and *S. varians,* respectively, obtained from Figure 4.3 to the temporal FW measurements, which were determined for identical culture conditions, the DW for each species was predicted and compared against actual DW yields. This allows demonstrating the accuracy of the FW method. The results indicated that the B+RS or PC+RS methods can be used to estimate DW yield of filamentous macro-algal species across

time. In addition, the growth rates of FW and DW are comparable. This further demonstrated that the values are closely related and that the prescribed FW methodology can be used as a strong estimation of DW productivity.

The constancy of the FW to DW relationship, irrespective of species, backed up with statistical evidence, demonstrates that a reticulated spinner is a reliable and accurate method for generating samples for FW determination and consequently DW estimation. Moreover, the ability to accurately assess productivity between species mean this approach can be a useful tool for a variety of scientific applications, including experimental growth screening.

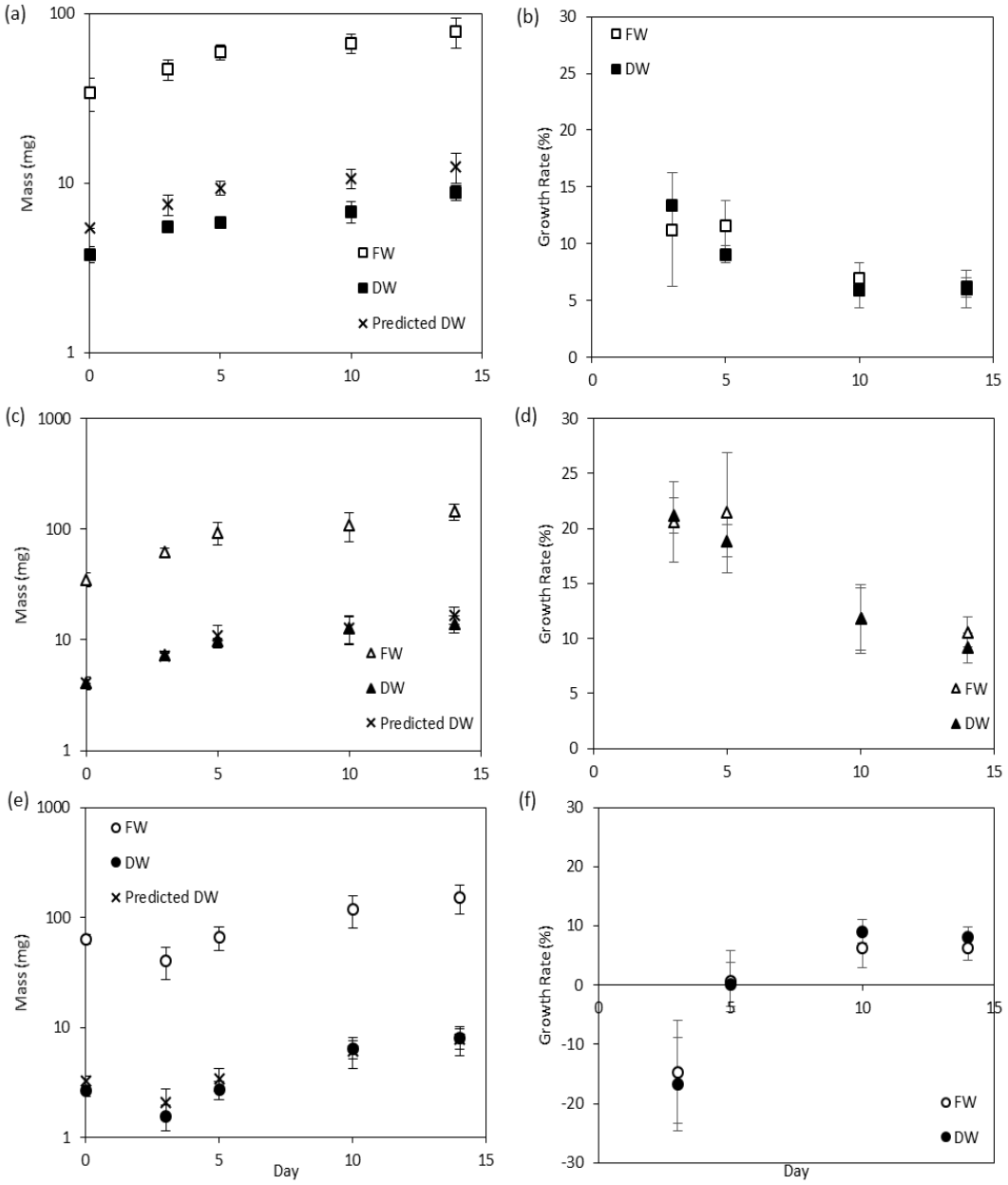


**Figure 4.9.** The FW, DW, predicted DW and rates of FW and DW growth of the three species of algae: *Cladophora coelothrix* (**a & b**), *Cladophora parriaudii* (**c & d**), and *Spirogyra varians* (**e & f**). The temporal relationship between FW and DW (**a, c, & e**) was assessed using Pearson's correlation coefficients, r. On each harvest day, triplicate flasks were harvested and the algal biomass was dewatered using either the optimised beaker + reticulated spinner (**B+RS**) method for *Cladophora* species, or the perforated crucible + reticulated spinner technique (**PC+RS**) for *S. varians* (Table 4.1). The DW for each species was predicted using the FW/DW ratios (6.3, 8.6, and 19.3 for *C. coelothrix*, *C. parriaudii*, and *S. varians*, respectively) obtained from Figure 4.3. The DW was attained by freezing the samples overnight followed by overnight lyophilisation (*n* = 3, *error bars* = 1 SD).

## 4.4 Conclusions

To the best of the author's knowledge, this is the first study to systematically assess a range of dewatering approaches to determine the FW of filamentous macro-algae at lab-scale using effectiveness, reliability, practicality, and biological and physical impact as factors. The results demonstrate differences in the effectiveness of a variety of dewatering methods and the physical and metabolic implications at both species and genus levels.

This study validated a method involving a reticulated spinner that is rapid, robust, inexpensive, and easily implemented or standardised for other algal taxa or amounts of biomass. This method combines high accuracy in biomass assessment due to excellent dewatering capabilities, with negligible impact upon algal performance, assessed as growth, viability, nutrient removal and structural integrity. This method is currently applicable for use with filamentous species on a lab-scale, compartmentalised or modular pilot-scale systems. Furthermore, its portability means that this method is employable in the field or at sea. However, further studies are required for the scaling up of this method for larger cultures at full-scale, which can include assessing and standardising the application of a gentle spinning cycle using a washing machine [155].

# Chapter 5

## Nitrogen uptake by *Cladophora*: influence on growth, nitrogen preference and biochemical composition

## 5.1 Introduction

Wastewater properties, including nutrient characteristics, can be highly variable [157, 331]. For instance, nitrogen and phosphorus concentrations from aquaculture effluents have been reported in the range of 18-360,521 µM [14, 41] and 0.17-1,846 µM [39, 41], respectively, with N/P ratios of 0.3-151 [32, 42]. The variability in nutrient characteristics of aquaculture effluents is due to differences in stocking density, feed quality and regime, fertilisation, species and seasonality [33, 40]. In addition to variable N concentration, nitrogen may be present in aquaculture effluents in different forms including dissolved inorganic nitrogen (DIN) sources, *i.e.* ammonia ($NH_3$), ammonium ($NH_4^+$), nitrite ($NO_2^-$) and nitrate ($NO_3^-$), or as dissolved organic nitrogen (DON), *i.e.* urea ($CO(NH_2)_2$) [156, 394]. However, $NH_4^+$ and $NO_3^-$ are the predominant nitrogenous forms in aquaculture effluents [37, 40].

Some species of macro-algae have high growth rates (7.1-11.7% per day) [395], good nitrogen uptake capacities between 19-96.6% [41, 65] and beneficial utilization of $CO_2$ [49, 51]. In addition, the biomass produced by wild harvest or via cultivation may have a number of potential applications and offer some financial return (section 1.3) [63]. These features have stimulated interest in exploring their potential utilisation for bioremediation in wastewater treatment (WWT), *e.g.* in integrated multi-trophic aquaculture (IMTA) and anaerobic digestion (AD) [41, 60]. However, wastewater characteristics, in particular the chemical factors mentioned above, will influence algal growth rates, biomass production, nutrient uptake and algal composition (section 1.4.2). Therefore, understanding and optimising these parameters, as well as selecting robust species that maintain good performance, despite potential fluctuations in WWT conditions, are prerequisites for their successful implementation [231].

Treatment of nutrient enriched effluents by algae typically occurs in outdoor raceway ponds, or high-rate algal ponds (HRAPs), with treatment lasting several weeks [50, 396]. Many studies involving N-uptake by macro-algae are unsuitable for assessing their potential as a tool for WWT, as their experimental design and environmental conditions are unrepresentative of real conditions: these include the supply of low N concentrations (<35 µM) and/or the use of short incubation times (<24 h), with no data provided on algal growth rates [184, 397]. The determination of algal growth is one of the most fundamental

parameters in phycological research, used for the comparison between treatments, assessment of biomass production and optimisation of culture conditions (Chapter 4) [319]. In addition, studies often employ the use of algal inoculums that have been pre-acclimated in conditions designed to lower their internal nutrient reserves [192]. The subsequent re-introduction to a N replete medium will commonly result in "surge uptake", where N is removed at a transiently enhanced rate due to the replenishment of internal N pools [181]. This form of uptake may indicate how well suited an individual species is at exploiting pulses of nutrients in an otherwise oligotrophic environment [156], but will be of reduced value in a more conventional WWT context [398].

Furthermore, the relationship between algal growth and nutrient uptake is very complex and requires further research. Macro-algal nutrient uptake is dependent upon N concentration and typically follows a Michaelis-Menten-type curve, whereby N removal follows a linear trend with increasing external N concentration until a plateau is reached [65, 160, 161]. The rate and maximum amount of N removal achieved is dependent upon biological, physical, and chemical factors, which includes the form of N present [160, 161]. For instance, Wang *et al.* [160] found uptake rates for $NH_4^+$ and $NO_3^-$ of 130-450 µM $g^{-1}$ DW $h^{-1}$ and 42.1-124.3 130-450 µM $g^{-1}$ DW $h^{-1}$, respectively, achieved by macro-algal Chlorophytes. Furthermore, it has been observed that $NH_4^+$ is generally removed ahead of $NO_3^-$ by algae, when cultivated in media containing multiple nitrogen forms [160, 196], or that $NO_3^-$ uptake was suppressed when $NH_4^+$ was present [198]. The underlying reasons for this nitrogen source preference are complex and not fully understood, they may be influenced by species-specific morphology, shore-line position, nutritional or life-history, the physiological capability and energetic expense for uptake and assimilation of certain nitrogen sources [156, 180, 198].

Fundamentally, mechanisms for N uptake are dependent on the N form present and are geared towards the same objective, namely: an N form enters the cell, passively or actively, across the cell membrane, whereupon it is reduced to $NH_4^+$ and amino acids, before assimilation into macromolecules, like proteins, for growth [160]. Assimilation of $NO_3^-$ occurs by sequentially reducing $NO_3^-$ to $NO_2^-$, followed by $NO_2^-$ to $NH_4^+$, via the action of N reducing enzymes [50]. Urea is converted into $NH_4^+$ by one of either urease or ATP:urea amidolyase (UAL-ase) [194, 195]. However, there is a dearth of studies involving macro-algal removal of other N forms that are also present in wastewaters, such as $NO_2^-$ and urea,

as well as mixtures containing these N forms [397, 399]. These N sources are components of the overall dissolved N pool and may play an important role in the algal N budget [397] and may also affect the efficiency of algal bioremediation.

In addition to growth rate and nutrient uptake capacity, macro-algal biochemical composition is also affected by nutrient regime. Furthermore, the composition of biomass is important to determine in order to assess their suitability for commercial applications [63]. Several studies have demonstrated seasonal changes in macro-algal chemical composition elicited by differences in environmental conditions as well as nutrient supply [103, 105, 173, 205]. It has been shown experimentally that the tissue N content of macro-algal biomass increases with increasing concentrations of N in their growth medium [60], in contrast with an accumulation of polysaccharides under N-limitation [215]. However, there is as yet a lack of publically available data on the influence of nutrient regimes in regards to nutrient type, concentration and N/P ratio on macro-algal growth, N uptake, and biochemical composition.

The primary aim of this study was to examine the ability of two robust marine species of algae from the genus *Cladophora* for N removal when subjected to different nutrient regimes and their influence on growth and biochemical composition, with a view for future use in bioremediation. *Cladophora* sp. was selected as a model because of the high growth rates and propensity to bloom in nutrient rich conditions. They are also renowned for their tolerance to a wide range of abiotic factors and resistance to grazers (Chapter 3) [186, 343]. These features make *Cladophora* a suitable candidate for investigation into WWT [231]. To explore this potential, cultivation media was formulated with four different N/P ratios, in order to simulate those found in wastewater streams [41, 400], with nitrogen supplied in both organic and inorganic forms found in wastewaters, specifically $NH_4^+$, $NO_2^-$, $NO_3^-$ and urea. In addition, N forms were supplied either singly or dually in equimolar concentrations to elucidate if there was preferential N uptake. This is the first study of its kind to cultivate and characterise algae under the conditions described above. Algal performance was assessed on the basis of growth, nitrogen removal and biochemical composition of the biomass produced.

## 5.2 Materials and Methods

### 5.2.1 Macro-algal strains and culture conditions

Two marine macro-algal strains were used for experimental work in this chapter and were: *Cladophora coelothrix* CCAP 505/10 and *Cladophora parriaudii* CCAP 505/09 (section 2.2.1). Prior to experimentation, all cultures underwent the standard cultivation protocol (section 2.2.2). Cultures were grown in Guillard's f/2 medium (Appendix A – Table A1) [320], with modified nitrogen additions. Nitrogen was supplied as either ammonium chloride, sodium nitrite, sodium nitrate, or urea (Fisher Scientific, UK). Molar ratios of N and P 2/1, 12/1, 22/1 or 32/1 relative to the prescribed P content, equating to initial N concentrations of 160, 960, 1760, and 2560 µM, respectively, were incorporated into the media formulations. Equimolar concentrations of N were incorporated in media containing multiple nitrogen sources. Experiments lasted for 14 days and were maintained as described in section 2.2.2.5. Additional flasks containing the experimental media only acted as negative controls, whereas those containing biomass and f/2 medium served as a positive control.

### 5.2.2 Measurement of biomass and its constituents

Cultures were sampled six times during the study period (days 0, 2, 5, 9, 12, and 14) with aliquots (5 mL) of media being aseptically removed in a laminar flow cabinet (MSC Advantage, Thermo Scientific) for FW determination and water chemistry analysis. On each sampling day, FW was determined using a small salad spinner (section 2.3.1) [319]. After which time, biomass was returned to its original flask and incubated under the conditions described above. After the experimental period, the algal cultures were harvested and rinsed with deionised water to remove extracellular salts and nutrients, FW was determined, the samples frozen at -18°C and then freeze-dried overnight or until a <5% variation in mass was achieved (Modulyo 4K Freeze-Dryer).

Biochemical composition analysis was performed on lyophilised material. Protein was extracted and quantified using the method outlined in section 2.5.2 [327]. Total soluble carbohydrate of the biomass was extracted and quantified using a modified phenol-sulphuric acid method detailed in section 2.5.3.1 and 2.5.3.2 [328, 329].

### 5.2.3 Water chemistry analysis

For each sampling day analysis of nutrients present in solution was performed. Soluble $NO_2^-$ and $NO_3^-$ were measured using Ion Chromatography (section 2.4.3) [319]. Total Ammonia Nitrogen (TAN) was determined colourimetrically (section 2.4.2.1). Phosphate was determined colourimetrically (section 2.4.2.2). Urea was determined colourimetrically (section 2.4.5) [324].

### 5.2.4 Data analysis

Algal growth is expressed as daily growth rate (DGR) using FW material (section 2.3.4) [322]. Protein and carbohydrate content of the biomass is portrayed as % DW. Water chemistry data were converted to molar N form and expressed either as total N uptake (μM), or as a proportion of N removed from the growth medium (%), both relative to values obtained from corresponding negative controls. Phosphate was expressed as % removal, relative to the negative control concentration on the day of harvest. All experiments were performed in triplicate and the experimental error was calculated and expressed as one standard deviation (SD). Within a single N/P ratio, comparison of DGR, nutrient uptake, and biochemical composition was performed using a 2-sample *t*-test. A one-way ANOVA with Tukey's post hoc analysis was used to determine differences in DGR of *C. parriaudii* between multiple N sources provided at the same concentration. Relationships between DGR and N removal, and protein to carbohydrate content were described using Pearson's correlation, *r*. Levels of significance were set at $p < 0.05$; all statistical analyses were performed using Minitab® Statistical Software version 17.

## 5.3. Results and discussion

Two species of *Cladophora* were investigated for N and phosphate removal, growth rate, and biochemical composition after 14 days incubation under different nutrient regimes that were designed to simulate a broad range of aquaculture wastewaters (see Table 1.1 and section 5.1). The only experimental variable was nitrogen addition, with growth media

formulated with four different N/P ratios and four different sources of nitrogen: $NH_4^+$, $NO_2^-$, $NO_3^-$, or urea. This study was performed in two main sections. Firstly, N sources were added singly for comparison between species on a fundamental level. Secondly, media was formulated with dual nitrogen sources in equimolar concentrations to elucidate the N source preference of *C. parriaudii*. The removal of N was attributed to the algal strains studied by comparison against negative control flasks, where nutrient removal was not observed. Positive control cultures grew consistently throughout the experimental time-frame, indicating that no unexpected changes in growth occurred (data not shown).

### 5.3.1. Uptake of single nitrogen sources

Experiments were performed in order to determine whether two closely related species of *Cladophora* are able to sequester different N sources indiscriminately, across a range of concentrations, and if this influences growth. Single sources of N were added at four different N/P ratios, with the DGR, N uptake, and $PO_4^{3-}$ removal determined (Figs. 5.1, 5.2 and 5.3).

Both species studied exhibited growth and N uptake irrespective of nutrient regime. *C. parriaudii* outperformed *C. coelothrix* under all nutrient regimes tested, with clear differences in DGR (Fig. 5.1) and N uptake (Fig. 5.2). These differences in DGR were significant at 12/1 $NO_2^-$ ($p = 0.025$) and for all urea concentrations tested ($p = 0.002 – 0.049$) (Fig. 5.1). The disparities in growth between the two species were generally reflected in the amount of N removed (Fig. 5.2). For example, at a 12/1 ratio with $NO_2^-$, DGR for *C. parriaudii* was 8.6% as opposed to 5% for *C. coelothrix*, with corresponding $NO_2$-N uptake of 538 (± 79.9) µM and 193 (± 80.3) µM, respectively (Fig. 5.1b and 5.2b). Overall, differences in DGR and N uptake observed may be accounted for by interspecific variations in physiology, capacity to utilise N forms, growth strategy, as well as morphology [180, 189]. For instance, Luo *et al.* [189] found that *Ulva prolifera* had higher rates of growth and nutrient uptake than *Ulva linza* across a range of temperatures, irradiances, and N concentrations, most likely as a result of them having a different thallus morphology. A similar explanation may be valid in this case: Ross *et al.* [319] noted that *C. parriaudii* grows rapidly outwards in a loose skein, whereas *C. coelothrix* grows slowly in tightly knit clusters (chapter 4). The more dense growth strategy exhibited by *C. coelothrix*, as opposed to *C.*

*parriaudii*, will likely enhance the effects of growth-limiting factors, such as self-shading and low nutrient availability within the tightly knit colony, as observed in other members of Cladophoraceae [188, 342].

Greater differences in performance between the two species occurred when cultivated on urea. Both the highest and lowest DGR was achieved with 11.2% by *C. parriaudii* and 3.98% by *C. coelothrix*, respectively. This indicates that two closely related species of *Cladophora* have different capacities for N source utilisation. Literature on macro-algal urea removal is sparse in comparison to $NO_3^-$ or $NH_4^+$ [156, 401]. However, Phillips and Hurd [156] observed negative values for urea uptake by inter-tidal macro-algal species during winter conditions, but noted uptake saturation during summer months with increasing urea concentrations. It was hypothesized that the energetically expensive enzyme urease, required to convert urea to $NH_4^+$, may be down-regulated during winter months when abiotic conditions are sub-optimal for growth. A similar concept may apply here, where there was a strongly positive correlation between the DGR and N uptake by *C. parriaudii* at each nutrient ratio, with Pearson's *r* values of 0.645-0.848 and $p = <0.001 – 0.024$. However, no such relationship existed with *C. coelothrix*, $p = 0.656 – 0.999$, which indicates that the growth rate of *C. parriaudii* was strongly influenced by the nutrient regime, whereas the growth of *C. coelothrix* is likely to be more strongly influenced by another parameter, such as light intensity. This suggests that *C. coelothrix* may have under-expressed urease production as a consequence of sub-optimal cultivation conditions and the low rate of urea assimilation that occurred may have been for maintenance or housekeeping purposes.

A common trend in N uptake was not shared between *C. coelothrix* and *C. parriaudii* (Fig. 5.2), most likely due to the physical and biological factors mentioned above. In the case of *C. parriaudii*, N uptake followed a Michaelis-Menten-type trend, generally plateauing at a ratio of 12/1 and beyond, which is comparable to observations reported by other studies [65, 160]. The kinetics of nutrient uptake were described in detail by Harrison and Hurd [161], defining this plateau as a period of "internally controlled uptake", with the activity of N reducing enzymes limiting the rate of further N uptake.

A reduction in growth rate for both species with increasing concentrations of $NH_4^+$ was observed (Fig. 5.1a). This was most likely due to the increasing concentration of the toxic un-ionised $NH_3$ form that exists in equilibrium with $NH_4^+$ [402]. Previous studies have reported toxic effects of $NH_3$ with algal cultures at concentrations ranging from 2.34 - 2000

µM [169, 403], whereas $NH_3$ concentrations in this study fell within this range, varying between 0-250 µM.

There was a striking similarity in the trends of N uptake and $PO_4^{3-}$ removal by *C. parriaudii* (Figs. 5.2 and 5.3). For instance, only four of the treatments had phosphate removal of >45%, these were 12/1 $NO_3^-$ (48.7%), 22/1 $NO_3^-$ (53.2%), 12/1 urea (47.7%) and 32/1 urea (52%). These same treatments were coincident with some of the highest rates of growth or N uptake (Figs. 5.1 and 5.2), which further illustrates that *C. parriaudii* is strongly influenced by nutrient regime. On the other hand, *C. coelothrix* was generally poor at removing phosphate (-0.8-19%) and there was no immediately obvious relationship between growth or N uptake with $PO_4^{3-}$ removal. The low and indeed negative values of phosphate removal may be attributed to luxurious phosphorus uptake [404, 405] during the acclimation period (section 2.2.2).

Due to the lower rates of growth and N and phosphate uptake, *C. coelothrix* was not investigated further in this study. Additionally, as N removal by *C. parriaudii* plateaued beyond a 12/1 ratio only ratios of 2/1 and 12/1 were investigated for the remainder of this study.

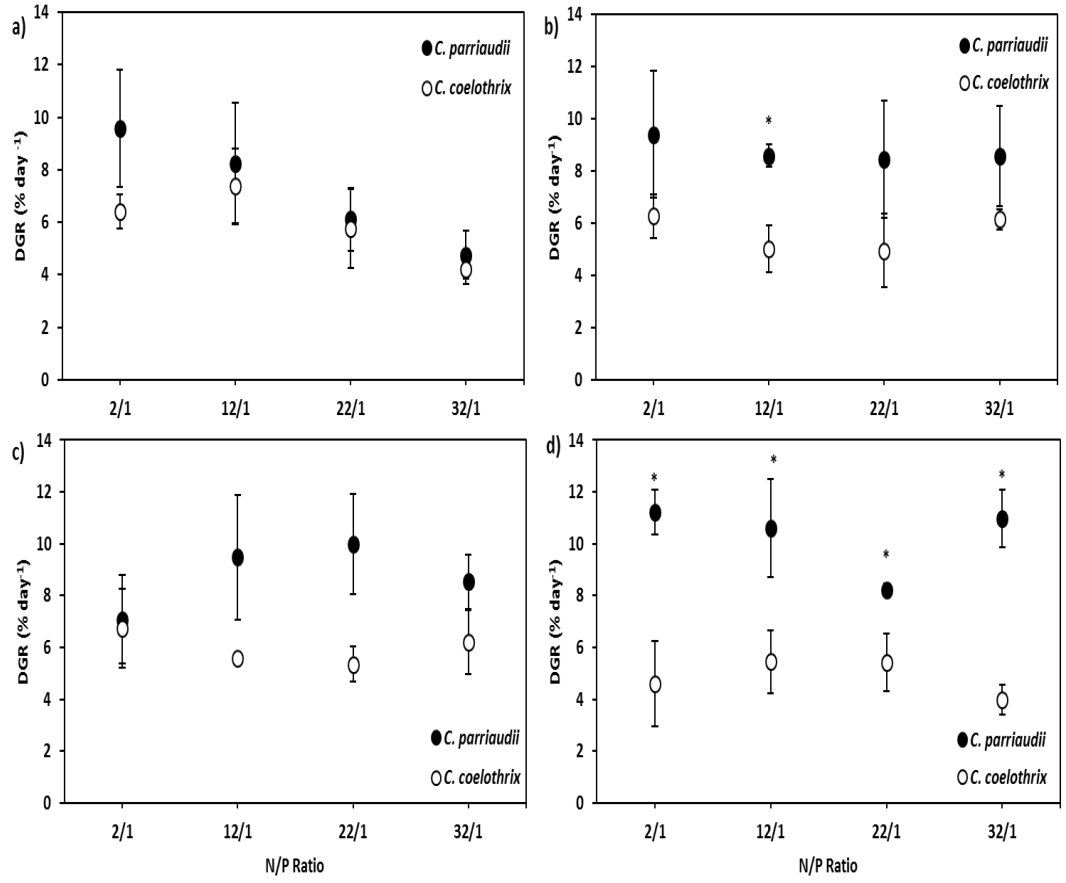


**Figure 5.1.** The daily growth rate (DGR) of *Cladophora parriaudii* (black) and *Cladophora coelothrix* (white) cultivated for 14 days (100 rpm, 24 °C, light intensity of 30-40 µmol photons $m^{-2}$ $s^{-1}$, 18/6 h Light/Dark photoperiod) in different media formulations with N/P ratios of 2/1, 12/1, 22/1, and 32/1, equivalent to initial N concentrations of 160, 960, 1760, and 2560 µM, respectively. N was supplied as $NH_4^+$ (a), $NO_2^-$ (b), $NO_3^-$ (c), or urea (d) (*n* = 3, *error bars* = 1 SD). Statistically different DGR between species are indicated * ($p$ <0.05).

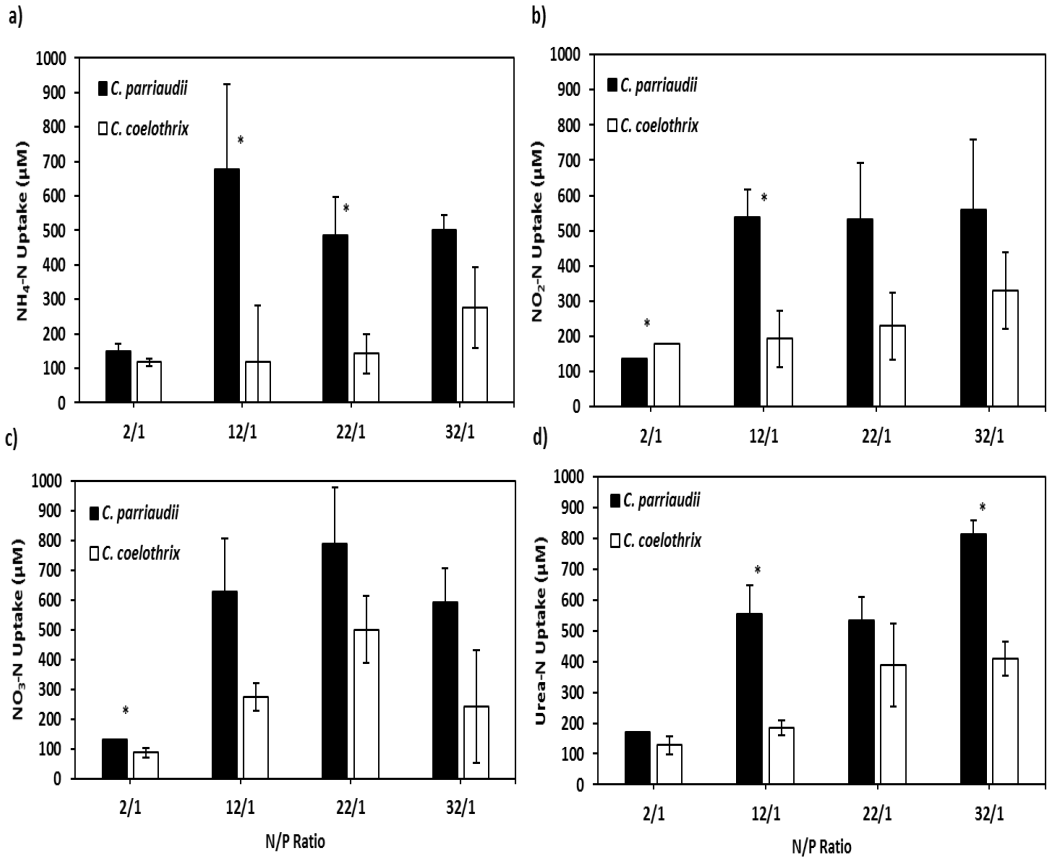


**Figure 5.2.** Total N uptake by *Cladophora parriaudii* (black) and *Cladophora coelothrix* (white) when cultivated for 14 days (100 rpm, 24 °C, light intensity of 30-40 µmol photons $m^{-2}$ $s^{-1}$, 18/6 h Light/Dark photoperiod) in different media formulations with N/P ratios of 2/1, 12/1, 22/1, and 32/1, equivalent to initial N concentrations of 160, 960, 1760, and 2560 µM, respectively. Nitrogen was supplied as $NH_4^+$ (a), $NO_2^-$ (b), $NO_3^-$ (c), or urea (d) (*n* = 3, *error bars* = 1 SD). Statistically different total N uptake between species are indicated * (*p* <0.05).

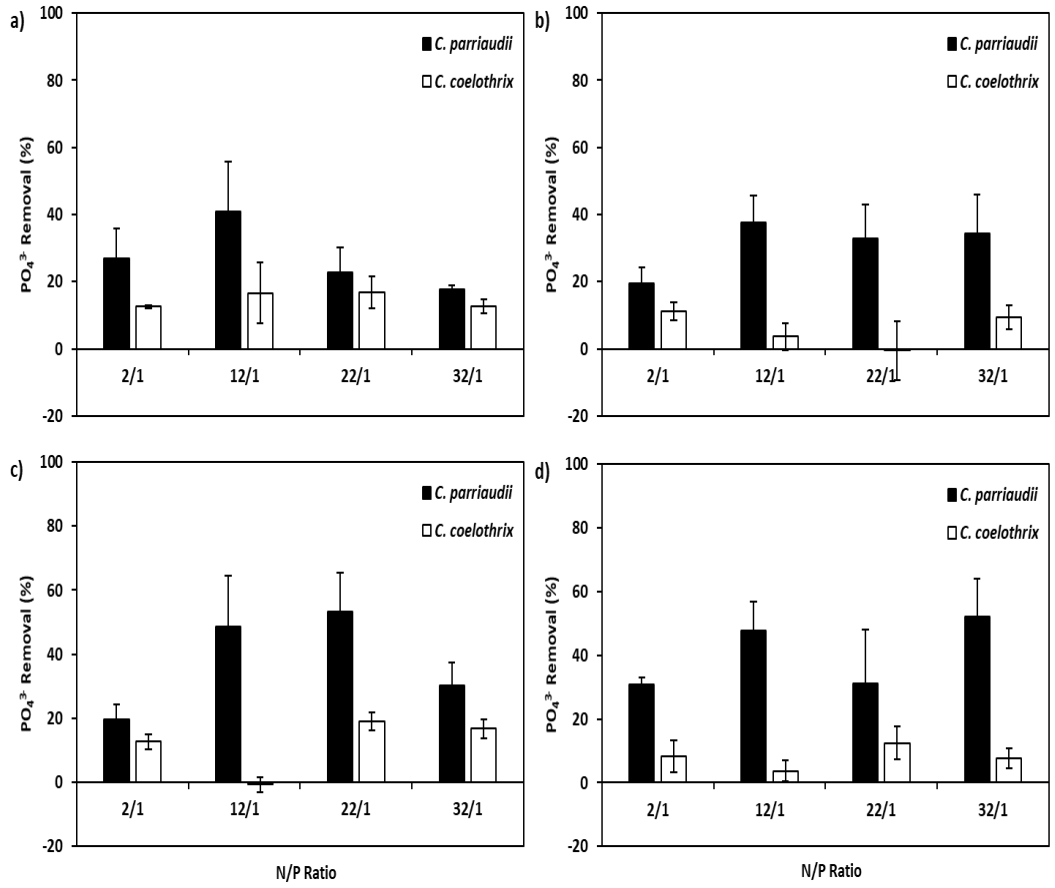


**Figure 5.3.** The relative phosphate removal by *Cladophora parriaudii* (black) and *Cladophora coelothrix* (white) when cultivated for 14 days (100 rpm, 24 °C, light intensity of 30-40 µmol photons $m^{-2}$ $s^{-1}$, 18/6 h Light/Dark photoperiod) in different media formulations with N/P ratios of 2/1, 12/1, 22/1, and 32/1, equivalent to initial N concentrations of 160, 960, 1760, and 2560 µM, respectively. Nitrogen was supplied as $NH_4^+$ (a), $NO_2^-$ (b), $NO_3^-$ (c), or urea (d) (*n* = 3, *error bars* = 1 SD).

## 5.3.2 Uptake of nitrogen combinations

Combinations of different nitrogen sources were added to the growth matrices to determine whether *C. parriaudii* is capable of complimentary N uptake and what effect this has on DGR (Fig. 5.4), total N uptake (Figs. 5.5 and 5.6), and $PO_4^{3-}$ removal (Fig. 5.7).

Similar trends on N uptake occurred between the 2/1 and 12/1 ratios, albeit N removal was generally complete by day 9 (Figs. 5.5 and 5.6). The greater concentration of N in the 12/1 treatment meant that removal rates were reduced, making visualisation of trends easier. In order to avoid repetition, discussion on N uptake mostly focuses on the 12/1 data, although the trends observed apply to both ratios tested.

Generally, cultures that have removed the most N also tend to have a higher DGR. The N source appeared to have a greater effect on the DGR of *C. parriaudii* than N/P ratio (Fig. 5.4): no significant differences in growth were observed between N/P ratios, whilst there was significance in the DGR values within a given N source. For example, the DGR of *C. parriaudii* when cultivated under a 2/1 ratio with urea as the common N source (Fig. 5.4d) ranged from 7.8-11.2% ($p$ = 0.005). The overall lack of statistical significance in the DGR of *C. parriaudii* across treatments suggests that it can grow indiscriminately in different nutrient regimes and could be applied generally for a broad variety of different waste streams.

The inclusion of urea in the media tended to enhance the growth, N uptake, and $PO_4^{3-}$ removal by *C. parriaudii* and may be explained when considering its influence on biochemical composition of the biomass, which will be discussed later. Greater total N removal was achieved by *C. parriaudii* when incubated in $NH_4$-Urea (79.8%), as opposed to $NH_4^+$ alone (67.7%) and mixtures of $NH_4$-$NO_2$ (32.7%) and $NH_4$-$NO_3$ (50.4%) (Fig. 5.6a). The same trend was observed in media combinations with $NO_2^-$ or $NO_3^-$ as the common N source (Figs. 5.6b and c). Interestingly, growth and N uptake was greater in urea mixtures in comparison to a single addition of urea: the DGR of single urea at 12/1 was 9.2%; however, this increased to 10.6%, 10.6%, and 11.2% with combinations of $NH_4$-Urea, $NO_2$-Urea, and $NO_3$-Urea, respectively (Fig. 5.4d). As growth and N removal are strongly related, a corresponding trend was observed for urea uptake. The lowest total N removal was recorded with a single urea addition (61.4%), as opposed to combinations containing urea: $NH_4$-Urea with 79.8%, $NO_2$-Urea with 77.5%, and $NO_3$-Urea with 65.2% (Fig. 5.6d). Overall, these results indicate that *C. parriaudii* is capable of complimentary N uptake and that this can enhance growth. In a previous study, Bracken and Stachowicz [180] reported that of eight local species tested, neither *Cladophora* nor *Prionitis* exhibited the greatest N removal in monoculture. However, *in situ*, they were the most dominant algae in the Bodega Marine Reserve, California, partly attributed to their ability to utilise multiple nitrogen forms when available.

In contrast with urea, incorporating either $NH_4^+$ or $NO_2^-$ into a mixture generally resulted in reduced DGR: for example, a treatment of 12/1 $NO_2$-$NO_3$ resulted in one of the lowest observed rates of growth (6.9%) and total N removal (47.7%). Both $NO_2^-$ and $NH_3$ (which co-

exists in equilibria with $NH_4^+$) are toxic to algae [402, 406], and possibly impaired the functionality of the organism.

Media formulations which resulted in the most growth and N removal also tended to have higher phosphate removal, particularly under a 12/1 N/P ratio (Figs. 5.4, 5.6, and 5.7), emphasising the importance of nutrient regime on algal performance. For instance, phosphate removal was greatest in media formulated with either single N additions (37.6-48.7%), or when urea was a component N source (37.1-47.8%) (Fig. 5.7).

Differences in algal performance may be a result of an inherent preference for a certain nitrogen form, which can be elucidated by measuring temporal N removal of the component N sources.

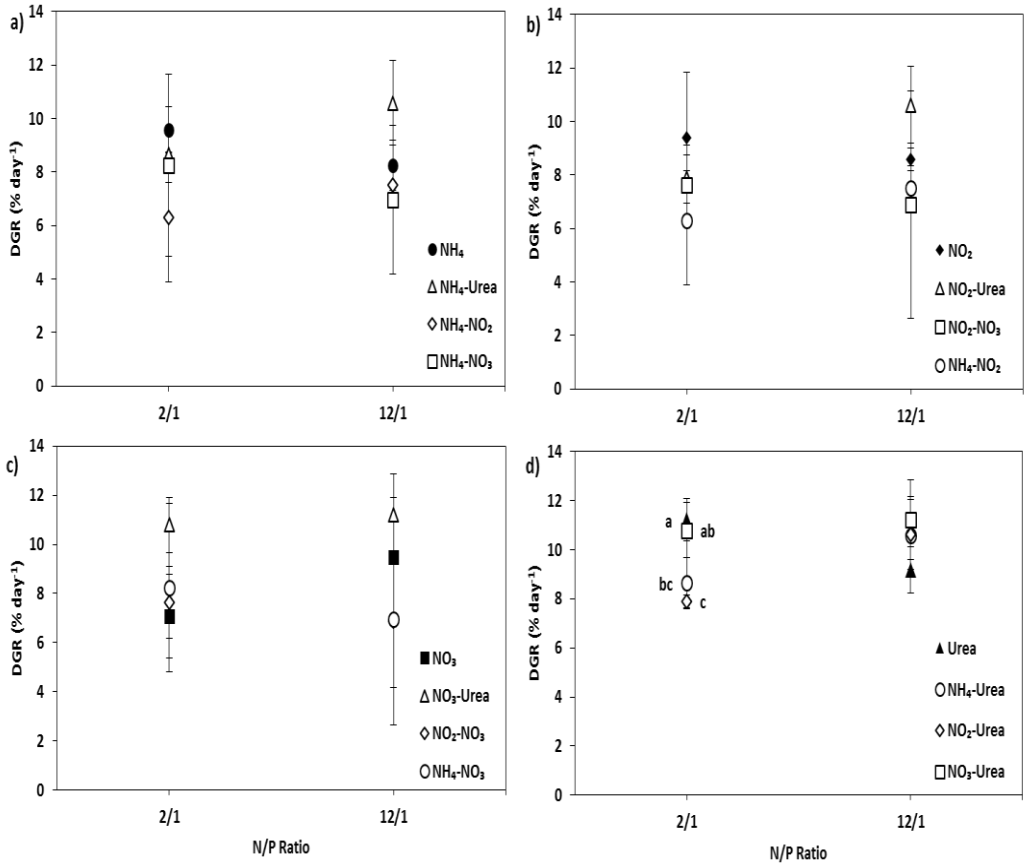


**Figure 5.4.** The daily growth rate (DGR) of *Cladophora parriaudii* cultivated for 14 days (100 rpm, 24 °C, light intensity of 30-40 µmol photons $m^{-2}$ $s^{-1}$, 18/6 h Light/Dark photoperiod) in different media formulations with 2/1 and 12/1 N/P ratios, equivalent to initial N concentrations of 160 and 960 µM, respectively. N was added as $NH_4^+$, $NO_2^-$, $NO_3^-$, or urea, either singularly or dually in equimolar concentrations. The figures have been grouped by common N source as $NH_4^+$ (a), $NO_2^-$ (b), $NO_3^-$, (c), and urea (d), with the darkened shape denoting the common type (*n* = 3, *error bars* = 1 SD). Treatments which do not share a letter are significantly different ($p$ <0.05).

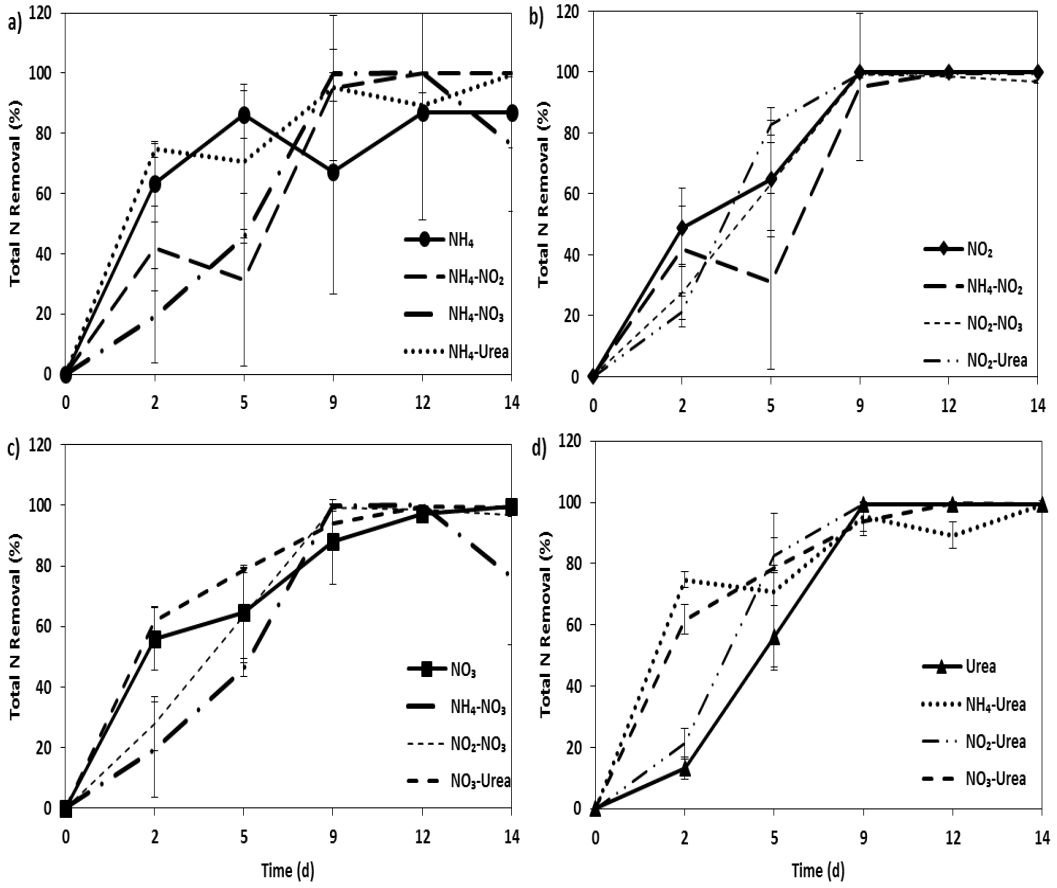


**Figure 5.5.** Temporal total N removal by *Cladophora parriaudii* cultivated for 14 days (100 rpm, 24 °C, light intensity of 30-40 µmol photons $m^{-2}$ $s^{-1}$, 18/6 h Light/Dark photoperiod) in different media formulations with a 2/1 N/P ratio, equivalent to an initial N concentration of 160 µM. Nitrogen was added as $NH_4^+$, $NO_2^-$, $NO_3^-$, or urea, either singularly or dually in equimolar concentrations. The figures have been grouped by common N source as $NH_4^+$ (a), $NO_2^-$ (b), $NO_3^-$, (c), and urea (d) with the darkened shape and solid line denoting the common type for each corresponding graph (*n* = 3, *error bars* = 1 SD).

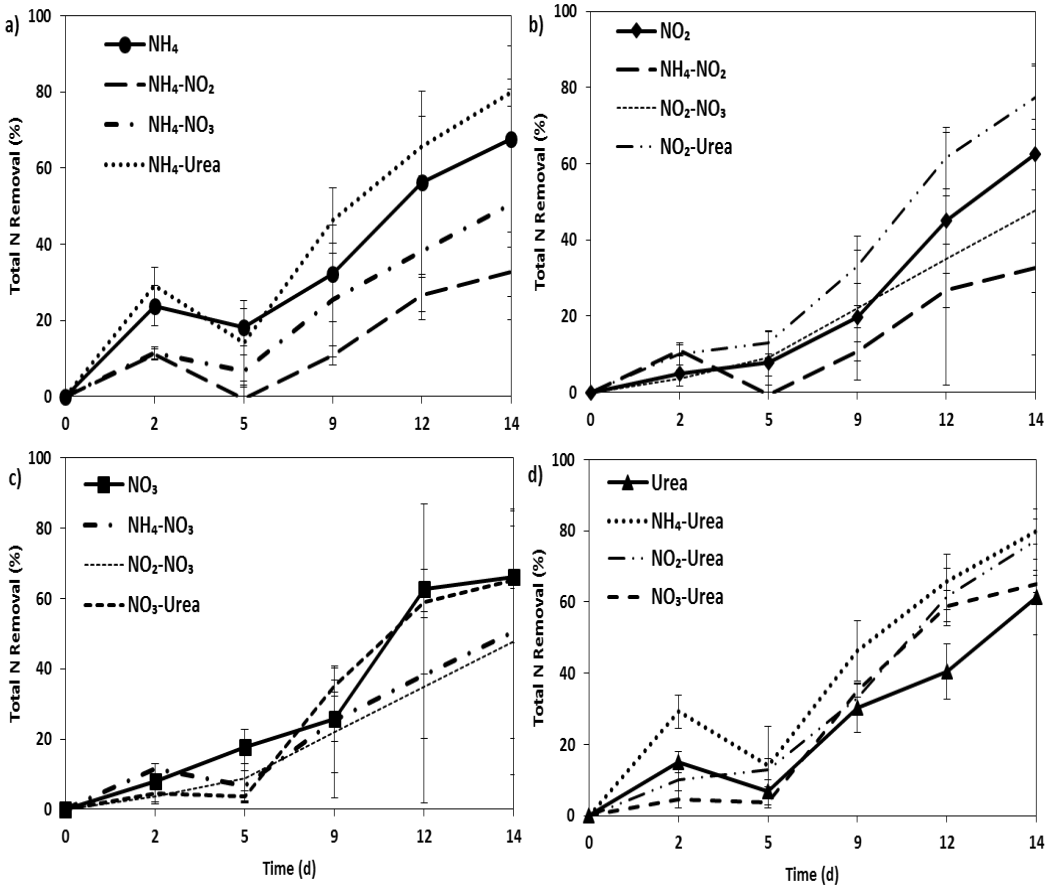


**Figure 5.6.** Temporal total N removal by *Cladophora parriaudii* cultivated for 14 days (100 rpm, 24 °C, light intensity of 30-40 µmol photons $m^{-2}$ $s^{-1}$, 18/6 h Light/Dark photoperiod) in different media formulations with a 12/1 N/P ratio, equivalent to an initial N concentration of 960 µM. Nitrogen was added as $NH_4^+$, $NO_2^-$, $NO_3^-$, or urea, either singularly or dually in equimolar concentrations. The figures have been grouped by common N source as $NH_4^+$ (a), $NO_2^-$ (b), $NO_3^-$, (c), and urea (d) with the darkened shape and solid line denoting the common type for each corresponding graph (*n* = 3*, error bars* = 1 SD).

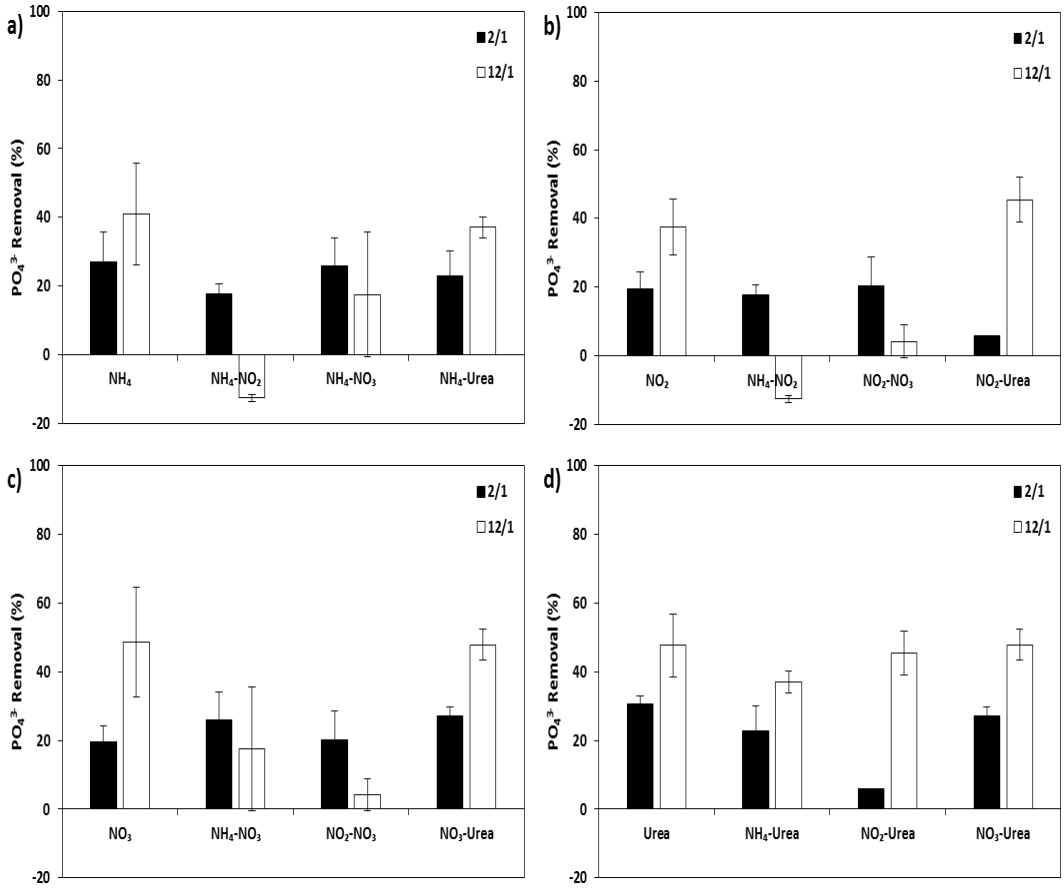


**Figure 5.7.** Relative phosphate removal by *Cladophora parriaudii* cultivated for 14 days (100 rpm, 24 °C, light intensity of 30-40 µmol photons $m^{-2}$ $s^{-1}$, 18/6 h Light/Dark photoperiod) in different media formulations with a 2/1 (black) and 12/1 (white) N/P ratio, equivalent to an initial N concentrations of 160 and 960 µM. Nitrogen was added as $NH_4^+$, $NO_2^-$, $NO_3^-$, or urea, either singularly or dually in equimolar concentrations. The figures have been grouped by common N source as $NH_4^+$ (a), $NO_2^-$ (b), $NO_3^-$, (c), and urea (d) (*n* = 3, *error bars* = 1 SD).

## 5.3.3 Preferential nitrogen uptake

To determine whether *C. parriaudii* exhibited any preference for a particular N source, the removal of the component N sources from the dual N media was investigated (Figs. 5.8 and 5.9). As previously observed, the trends between 2/1 and 12/1 N removal preference were very similar; however, as a lower concentration of N was added in the 2/1 regime, the relationships were achieved more rapidly making them more difficult to discern in the sampling regime employed in this study. For this reason, the discussion focusses upon 12/1, although there is an overlap in trends between rations.

There are clear differences in N uptake preference for *C. parriaudii*: $NH_4^+$ was removed at a faster rate and to a higher degree than any other N source it was mixed with (Figs. 5.8a-c, and 5.9a-c). A preference for $NH_4^+$ over $NO_3^-$ has been reported elsewhere for both eukaryotic algae and cyanobacteria [162, 168, 180, 192, 197]. For instance, Pedersen and Borum [162] observed greater $NH_4^+$ removal following a period of N deprivation, which suggests "surge uptake". Whereas Bracken and Stachowicz [180] found differences in N uptake rate and preference between species most likely due to differences in life strategy; the fastest growing species had the greatest N removal, but were preferentially grazed upon, perhaps due to a lack of resource diversion into defence mechanisms. There are however, very few studies on macro-algal preference in dual N media formulations involving alternative nitrogen sources, such as urea and $NO_2^-$ [397, 399]. This preference for $NH_4^+$ is presumed to be because it is less energetically expensive to assimilate than the other N sources, as $NO_2^-$ or $NO_3^-$ are more oxidised forms of nitrogen that need to be reduced to $NH_4^+$, whereas urea requires different enzymes for its assimilation [192, 195, 199]. Additionally, algal-bacterial interactions may also play a role, such as nutrient mineralization [407, 408].

Similarities between the removal of $NO_2^-$ and $NO_3^-$ by *C. parriaudii* cultivated in $NO_2$-$NO_3$ media were observed, with an overall equal removal of 47% for each, despite a slight initial delay in $NO_3^-$ uptake (Fig. 5.9d). Furthermore, their removal when in conjunction with other forms, in this case with $NH_4^+$ and urea, were similar. There was an initial 5-day lag period for $NO_2^-$ and $NO_3^-$ uptake before 92.2% and 99.8% were removed, respectively, when urea was the additional nitrogen type (Fig. 5.9e and f). However, only 6.8% and 24.3% of $NO_2^-$ and $NO_3^-$, respectively, were removed when $NH_4^+$ was also present in the media (Fig. 5.9a and b). Raven *et al.* [199] suggested that $NO_3^-$ uptake could be completely suppressed when in the presence of 1000-2000 µM $NH_4^+$. The reason(s) underlying this suppression remain unclear, although several hypotheses have been made. For instance, $NH_4^+$ may directly inhibit $NO_2^-$ or $NO_3^-$ uptake, amino acids and/or nucleotides may induce an inhibitory response, or nitrate reductase may be reversibly inactivated in the presence of $NH_4^+$. However, the most plausible reason being that $NH_4^+$ inhibits the biosynthesis of nitrate/nitrite reductase or urease enzymes [195]. In this study, $NO_3^-$ removal only occurred after the concentration of $NH_4^+$ had reduced to 95-207 µM, typically achieved between days 5 and 9. However, in the $NH_4$-$NO_2$ treatment, the concentration of $NH_4^+$ never fell below 154 µM and translated into a low removal of $NO_2^-$ of <7%. This suggests that there is a

threshold $NH_4^+$ concentration above which $NO_2^-$ and $NO_3^-$ removal is suppressed. This was further highlighted at the 2/1 ratio (Fig. 5.8) where the onset of $NO_2^-$ and $NO_3^-$ removal from the $NH_4$-$NO_2$ and $NH_4$-$NO_3$ mixtures occurred once $NH_4^+$ was almost depleted. The presence of $NH_4^+$ in the media was considered to be the causative agent of the poor removal of $NO_2^-$ and $NO_3^-$. These virtually identical trends in removal of $NO_2^-$ and $NO_3^-$ were assumed to be due to their chemical similarity and their common metabolic pathway for nitrogen reduction and assimilation.

A >92% removal of $NH_4^+$, $NO_2^-$, and $NO_3^-$ was observed, when added in an equimolar combination with urea; however, the corresponding removal of urea was comparatively low, amounting to 12.4%, 63.6%, and 38.5%, respectively (Fig. 5.9c, e, and f). This was a somewhat surprising result given the relatively high rate of urea removal when added as a single source (61.4%) (Fig. 5.2), and the correspondingly high DGRs when it was incorporated into dual N media (Fig. 5.4). Tyler *et al.* [397] observed enhanced uptake of urea in the presence of $NH_4^+$ by *Gracilaria vermiculophylla* and *Ulva lactuta*, suggesting that each N form has a distinct uptake mechanism allowing their simultaneous removal. This was in contrast with results observed in this study where urea uptake was suppressed in the presence of other N sources, especially $NH_4^+$. The discrepancy between these findings is likely due to differences in experimental design and cultivation conditions: Tyler *et al.* [397] employed a shorter time-frame and a much greater biomass/nutrient ratio, with an inoculum that was previously maintained in low nutrient seawater, meaning that surge uptake would have played a prominent role in nutrient removal.

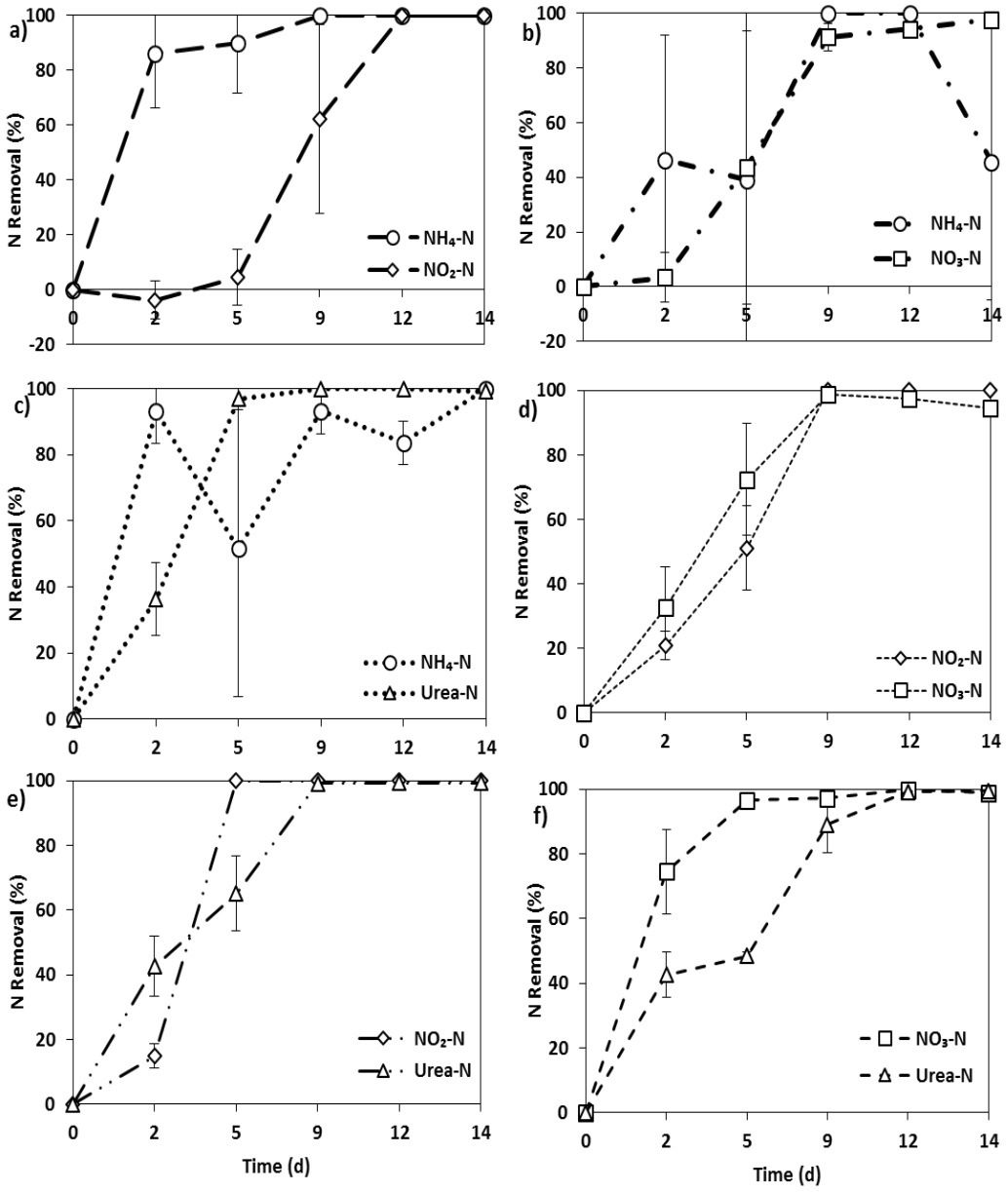


**Figure 5.8**. Preferential removal of component N sources by *Cladophora parriaudii* cultivated for 14 days (100 rpm, 24 °C, light intensity of 30-40 µmol photons $m^{-2}$ $s^{-1}$, 18/6 h Light/Dark photoperiod) in different media formulations with an N/P ratio of 2/1, equivalent to an initial N concentration of 160 µM. Nitrogen was added as $NH_4^+$ (circle), $NO_2^-$ (diamond), $NO_3^-$ (square), or urea (triangle) in equimolar concentrations. The graphs have been grouped by their dual nitrogen additions as $NH_4$-$NO_2$ (a), $NH_4$-$NO_3$ (b), $NH_4$-Urea (c), $NO_2$-$NO_3$ (d), $NO_2$-Urea (e), and $NO_3$-Urea (f) (*n* = 3, *error bars* = 1 SD).

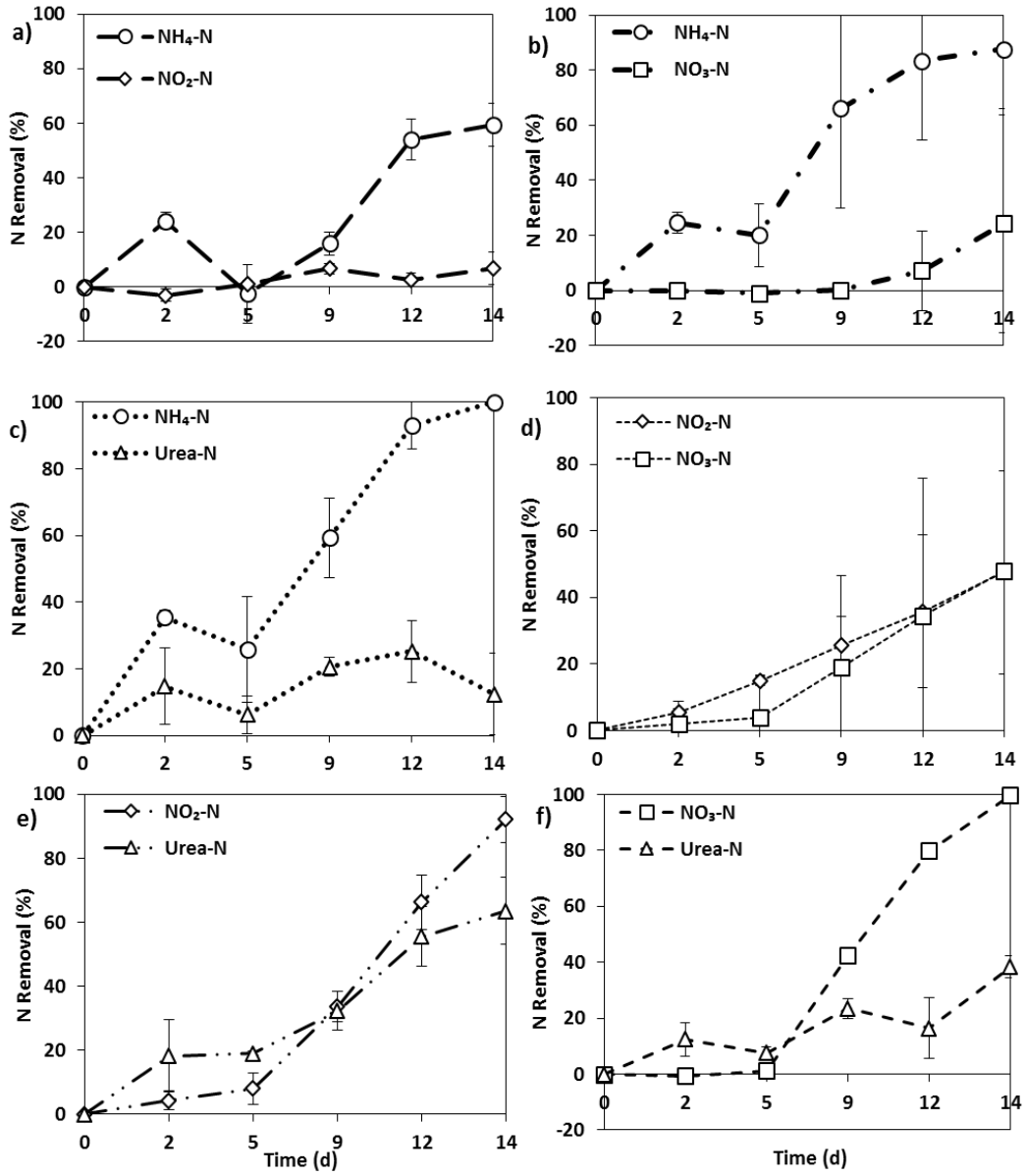


**Figure 5.9. P**referential removal of component N sources by *Cladophora parriaudii* cultivated for 14 days (100 rpm, 24 °C, light intensity of 30-40 µmol photons $m^{-2}$ $s^{-1}$, 18/6 h Light/Dark photoperiod) in different media formulations with an N/P ratio of 12/1, equivalent to an initial N concentration of 960 µM. Nitrogen was added as $NH_4^+$ (circle), $NO_2^-$ (diamond), $NO_3^-$ (square), or urea (triangle) in equimolar concentrations. The graphs have been grouped by their dual nitrogen additions as $NH_4$-$NO_2$ (a), $NH_4$-$NO_3$ (b), $NH_4$-Urea (c), $NO_2$-$NO_3$ (d), $NO_2$-Urea (e), and $NO_3$-Urea (f) (*n* = 3, *error bars* = 1 SD).

### 5.3.4 Biochemical composition

A strong inverse correlation between protein and carbohydrate content ($r$ = -0.585, $p$ < 0.001) was observed: generally, algal cultures maintained in a 2/1 ratio had a low protein and high carbohydrate content, whereas at a 12/1 ratio, they had a high protein and reduced carbohydrate composition (Table 5.1). At a 2/1 ratio, N was completely removed after 9 days (Fig 5.8), which was considered to result in N-limitation and hence a lower protein content levels observed, whereas at the 12/1 ratio, N was never depleted and therefore cultures would not have been N-limited and protein synthesis will have continued (Fig. 5.9). The influence of nutrient supply on biochemical composition has been observed elsewhere, where macro-algae have been observed to accumulate storage polysaccharides under N-deprivation, with a shift towards the synthesis of proteins and pigments when N is sufficient [214, 215]. In this study, the highest protein content at both ratios was observed in *C. parriaudii* maintained under $NH_4$-$NO_2$, with values of 10.8% and 15% at 2/1 and 12/1, respectively, coincident with the lowest DGR and total N uptake (Fig. 5.4 and 5.6). Meanwhile, the highest carbohydrate content (54%) was achieved in flasks where the alga was cultivated under a 2/1 ratio with $NO_2$-Urea, where complete N removal was attained after 9 days (Fig. 5.5).

It appears that N uptake, as observed in different N/P ratios, has a greater influence on biochemical composition than N form (Table 5.1), despite Corey *et al.* [196] reporting that the tissue N content of *Palmaria palmata* significantly changed from 3.1% to 4.1% when cultivated under $NO_3^-$ or $NH_4^+$, respectively. In their study, there was a significantly greater removal of $NH_4^+$ in comparison to $NO_3^-$ [196]. Therefore, it seems more likely that for a specific alga, preference for an N form will influence the uptake rate and absolute N removal, which will in turn affect the biomass composition, in contrast with the N form having a direct influence on biochemical composition.

The inclusion of urea in dual N media combinations resulted in carbohydrate rich biomass. For example, three of the four highest yields at a 2/1 ratio (48.4-54%) and the three highest at a 12/1 ratio (40.6-42.8%) were obtained when urea was part of the growth medium (Table 5.1). Considering that urea is an organic molecule its influence upon the algal biochemical composition may be slightly more complex. Both Choo *et al.* [409] and Raven *et al.* [410] have described multiple mechanisms for inorganic carbon acquisition by *Cladophora* sp., therefore the capacity to utilise carbon from urea is a distinct possibility.

The conversion of urea to $NH_4^+$, via enzymatic activity, results in the formation of 2 $NH_3$ and one $CO_2$ molecule [195]. This $CO_2$ formation may enhance photosynthetic activity and facilitate carbohydrate construction [411]. This theory of complimentary carbon and N sequestration may also explain the enhanced DGR and N uptake by *C. parriaudii* when cultivated in growth medium containing urea (Fig. 3d and 4d). The nutrient regime may have important consequences for cultivation practices, WWT, and algal biotechnology. For instance, this represents a straightforward opportunity to enhance growth, improve remediation performance, or amend the biochemical properties of the algal biomass by tailoring the N/P regime.

**Table 5.1.** Protein and carbohydrate content per unit DW of *Cladophora parriaudii* cultivated for 14 days (100 rpm, 24 °C, light intensity of 30-40 µmol photons $m^{-2}$ $s^{-1}$, 18/6 h Light/Dark photoperiod) in different media formulations with 2/1 and 12/1 N/P ratios, equivalent to initial N concentrations of 160 and 960 µM, respectively. Nitrogen was added as $NH_4^+$, $NO_2^-$, $NO_3^-$, or urea, singly or dually in equimolar concentrations ($n$ = 3, ± 1 SD). Values highlighted * are significantly different from one another within a nitrogen source ($p$ < 0.05).

| Nitrogen Source | Protein (% DW) | | Carbohydrate (% DW) | |
|---|---|---|---|---|
| | 2/1 | 12/1 | 2/1 | 12/1 |
| **$NH_4^+$** | 6.2 (± 1.8)* | 13 (± 0.7)* | 51.1 (± 2)* | 31.1 (± 1.3)* |
| **$NO_2^-$** | 5.4 (± 1.3)* | 10.9 (± 1.2)* | 41.7 (± 6.7) | 38.5 (± 3.1) |
| **$NO_3^-$** | 6.8 (± 1.2) | 9.7 (± 0.5) | 41.1 (± 2)* | 32 (± 1.9)* |
| **Urea** | 6.5 (± 0.6) | 8 (± 0.9) | 43.8 (± 11.9) | 37.6 (± 3.6) |
| **$NH_4$-$NO_2$** | 10.8 (±3.3) | 15 (± 0.4) | 45.6 (± 6.2) | 39.2 (± 1.5) |
| **$NH_4$-$NO_3$** | 8.3 (± 2.9) | 12.1 (± 1.9) | 47.2 (± 5.9) | 36.1 (± 6.5) |
| **$NH_4$-Urea** | 5.1 (± 0.2)* | 11.4 (± 1.8)* | 51.5 (± 0.9) | 40.6 (± 4.5) |
| **$NO_2$-$NO_3$** | 8.4 (± 3) | 11.9 (± 1.1) | 38.8 (± 5.6) | 38.2 (± 2.2) |
| **$NO_2$-Urea** | 6.5 (± 1.1)* | 12 (± 0.9)* | 54 (± 8.1) | 42.7 (± 2.2) |
| **$NO_3$-Urea** | 6.1 (± 0.2)* | 10.7 (± 0.4) | 48.4 (± 1.3) | 42.8 (± 3.1) |

## 5.4 Conclusions

From the present study, three key conclusions were formulated. Firstly, that there were species-specific differences in growth, phosphate removal, N uptake, and ability to utilise certain N forms between two closely related species of *Cladophora*, with *C. parriaudii*

growth strongly influenced by the nutrient regime. Secondly, *C. parriaudii* is capable of complimentary N uptake and its growth is more strongly influenced by N type, rather than concentration. A preference was shown towards $NH_4^+$, assumed to be due to its reduced form and therefore lower energetic requirement for its assimilation, whereas urea was removed secondarily. However the presence of urea in the medium enhanced the uptake of any other nitrogen form present, possibly due to complimentary carbon sequestration. It was noted that the total amount and rate of uptake of both $NO_2^-$ and $NO_3^-$ were almost identical. Thirdly, different nutrient regimes result in a change in the final composition of the biomass *C. parriaudii*, with N concentration having a greater influence than N form. Observations from this study may lead to a paradigm change in our algal cultivation practices in WWT, for instance selecting species for WWT purposes that are able to utilise multiple carbon and nitrogen forms simultaneously, or in utilising alternative, cheaper, and more easily assimilable N sources. In addition, tailoring nutrient regimes may be used to produce biomass with different properties for specific applications and with particular commercially exploitable attributes. For example, algal cultures could be cultivated under different nutrient regimes to elicit a change in their biochemical composition and cell wall properties, therefore improving their metal removal efficiency.

# Chapter 6

## Biosorption of heavy metals from aqueous solutions by dried *Cladophora parriaudii* cultivated under different nutrient regimes

## 6.1 Introduction

A growing population and consequential growth in industries such as metallurgy, mining, appliance manufacture and the production of batteries has led to water bodies becoming increasingly contaminated with toxic, or heavy, metals [21, 412]. For example, concentrations of copper and lead in surface waters reported to be in the range of 0.002-3.95 mg $L^{-1}$ and 0.0003-0.4 mg $L^{-1}$, respectively [239, 240, 243]. These values are in excess of the drinking water quality standards of 1 mg $L^{-1}$ Cu and 0.01 mg $L^{-1}$ Pb as set by the World Health Organization (WHO) [233]. The presence of toxic, or heavy, metals in water is a global problem [316, 413, 414], posing a serious health hazard to both animals and humans alike. Heavy metals are very toxic, non-biodegradable, and highly persistent in nature, and have a propensity to accumulate in the food chain [140, 316]. Exposure to certain toxic metals can adversely affect human health. For example, aluminium exposure is thought to lead to cognitive impairment and neurological disorders such as dementia and Alzheimer's disease [415]. Acute copper intoxication can cause gastrointestinal problems [235]. Overexposure to manganese has toxic effects on the central nervous system, as well as adverse effects on the lungs, liver, cardiovascular and reproductive systems [416]. Lead toxicity may cause organ damage, inhibit the synthesis of haemoglobin, result in neurological disorders, and have teratogenic effects [24]. In addition, the presence of toxic, or heavy, metals can have deleterious effects in the marine environment [23, 417, 418]. For instance, the inclusion of tributyltin (TBT) in antifouling paints is renowned for causing significant sexual disorders, such as imposex, in marine invertebrates [419]. Since the ban of TBT in 2001, there has been an increase in the use of antifouling paints containing other heavy metals, such as copper and zinc [420, 421]. The use of heavy metal based paints is under scrutiny, as copper has been found to be toxic to marine invertebrates at concentrations as low as 5-68.1 µg $L^{-1}$ [421, 422]. The removal of heavy, or toxic, metals from wastewaters, therefore, is of paramount importance to preserve human, aquatic, and environmental health.

Current metal removal technologies from aqueous solutions have centred upon adsorption onto activated carbon, chemical precipitation, electroplating, ion exchange, and membrane technologies [21, 142]. These conventional technologies, however, have their disadvantages. For example, high capital or operational expense, addition of chemicals, loss

of efficiency when treating large volumes of water containing low concentrations of metals, formation of toxic by-products, or the development of secondary and highly toxic sludge, which requires additional treatment [21, 273, 295, 423, 424]. Therefore, novel and more sustainable processes for heavy metal removal from solution are required.

An alternative technology for metal removal from wastewaters is biosorption [425-427], *i.e.* the sorption of metals using material of a biological origin [143]. Biosorption studies have been commonly performed using micro-organisms as a biosorbent material, with the focus mainly centred upon bacteria, yeast, fungi, and to a lesser extent algae [143, 428, 429]. Macro-algae, in particular, are viewed as promising candidates due to their general abundance and availability, as well as high metal sorption capacity [144, 315]. For instance, the removal of copper and lead ions from solution by macro-algal biomass has been reported to be 0.13-2.77 mmol $g^{-1}$ and 0.07-1.31 mmol $g^{-1}$, respectively [253, 254, 271, 285, 316]. The variability in reported results highlights both their potential for metal removal applications, but also the need for further research into this area; understanding the mechanisms influencing biosorption and how to improve them.

Biosorption onto macro-algae is a complex process, which is affected by an array of abiotic factors, including pH, temperature, initial metal concentration and the presence of co-existing ions (see section 1.5.3) [142, 251]. In addition, the properties of the macro-algal biosorbent material will also affect metal sorption, such as the species, age, surface area, initial biosorbent dosage, and pre-treatment of biomass including immobilization or chemical modification [251, 310, 315, 430-432]. Moreover, the type and abundance of functional groups present on a cell will have an impact upon the metal sorption capacity [315]. Metal ions have been found to passively bind on to different functional groups present on a surface or cell which include amine, carboxyl, hydroxyl, imidazole, phosphate, sulfate and sulfhydryl [21, 433]. Differences in culture conditions, for example, will influence the biochemical composition of a biomass (Chapter 5) and result in an alteration in the quality and quantity and types of functional groups present [434, 435]. For instance, Adams *et al.* [205] reported that the tissue C and N % of *Laminaria digitata*, collected from the wild, ranged from 26.4-36.2% and 1.1-3.5%, respectively, across a 12-month period. In addition, Mayers *et al.* [191] demonstrated time and nutrient induced changes, such as amendment of the nitrogen (N) to phosphorus (P) ratio (N/P) in the bulk chemical composition of the micro-alga *Nannochloropsis* sp. Differences in biochemical composition

will result in an alteration in the functional groups present, and therefore impact its usefulness as a biosorbent [433]. However, little attention has been paid to the relationship between macro-algal cellular properties and cultivation conditions, and the resultant influence on biosorption capacity.

Most macro-algal biosorption studies have collected biomass from the field. On return to the laboratory, the material is prepared by rinsing with deionised water, removing any adhering debris and epiphytes, drying and then milling [266, 281, 301, 314, 315, 436-438]. These studies do not provide information about the life or nutritional history of the biomass, environmental conditions, age, time spent washed ashore, prior exposure to contaminants, including heavy metals. Essentially, metal removal in these studies has been performed on a material of unknown biochemical composition and propagated under undefined conditions. This makes comparison with literature difficult and reproducibility problematic. Hence, the main aim of this work was to investigate the extent to which cultivation conditions can alter the biochemical composition and cell surface properties of algal biomass, and how much of an influence this has on its metal removal performance, and whether this will have any impact on the future widespread applicability of algal biosorption.

To the best of the author's knowledge, this is the first study of its kind to make a concerted effort to cultivate macro-algal biomass under different nutrient regimes and assess the influence this has on metal biosorption. More specifically, *Cladophora parriaudii* was cultivated under different nitrogen types ($NH_4^+$, $NO_3^-$, and urea), and different N/P ratios in order to produce biomass with different biochemical characteristics. The tailored biomass was then used for the biosorption of four different metals. Metals were selected based upon their prevalence in nature, varying degrees of toxicity and whether they are essential for algal growth and functionality: aluminium (low toxicity, non-essential), copper (high toxicity, essential), manganese (low-toxicity, essential), and lead (high-toxicity, non-essential) [23, 423, 439].

## 6.2 Materials and Methods

### 6.2.1 Macro-algal strains and culture conditions

The marine macro-alga *Cladophora parriaudii* CCAP 505/09 was used in this experimental chapter (section 2.2.1). Prior to experimentation, *C. parriaudii* underwent the standard cultivation protocol (section 2.2.2). Cultures were grown in Guillard's f/2 medium (Appendix A – Table A1) [320], with modified nitrogen additions. Nitrogen was supplied as either ammonium chloride, sodium nitrate, or urea (Fisher Scientific, UK), with 2/1 or 12/1 N/P molar ratios, equating to an initial N concentration of 160 or 960 µM, respectively. Triplicate 1L flasks containing 650 mL of media were inoculated with 465 mg fresh weight *C. parriaudii*, and maintained in conditions as described in section 2.2.2.5. After 14 days, all cultures were harvested and rinsed with deionised water to remove extracellular salts and nutrients. Residual water was removed from the sample using a reticulated spinner, as described by Ross *et al.* [319] (section 2.3.1). Harvested biomass was frozen and then lyophilised (section 2.3.2).

### 6.2.2 Biochemical analysis

Biochemical composition analysis was performed on lyophilised material. Total soluble protein, total soluble carbohydrate and monosaccharides, ash and pigment content of the biomass was determined using the methods described in section 2.5.1 - 2.5.4. Fourier Transform Infrared Spectroscopy – Attentuated Total Reflection (FTIR-ATR) was used to detect vibrational frequency changes in algal biomass before and after metal sorption (section 2.5.5). After biosorption, algal samples were visualised using scanning electron microscope (SEM) with images recorded using the back-scattered electrons (BSE) technique (section 2.5.6).

### 6.2.3 Stock solutions

Heavy metal stocks solutions (1000 mg $L^{-1}$) were prepared by dissolving analytical grade $Al_2(SO_4)\cdot 16H_2O$, $CuSO_4\cdot 5H_2O$, $MnCl_2\cdot 4H_2O$ and $PbCl_2$ in deionised water, with a few drops of

$HNO_3$ (Aristar® grade, VWR, UK) added to avoid metal precipitation. Working concentrations of 1, 10, 40, 80, and 150 mg $L^{-1}$ were obtained by diluting with deionised water. The pH was adjusted to 4.5, using either 0.1 M HCl or NaOH. This pH was selected based upon an in-depth literature review, where 4.5 was suggested to be the optimal pH for metal biosorption in many studies [251, 254, 272, 292, 293].

## 6.2.4 Metal sorption procedure

Metal sorption experiments were performed in multi-well plates in an incubated shaker, under a light regime of 24/0 L/D h with 30-40 µmol photons $m^{-2}$ $s^{-1}$ photosynthetically active radiation (PAR: 400-700 nm) (Sartorius Stedim Biotech, Germany) at 100 rpm at 24°C with a biosorbent dose of 1 g $L^{-1}$. After 24 hours, the biomass was removed from each well and placed in individual micro-centrifuge tubes and dried overnight in an oven at 60°C. Heavy metal solutions were acidified, with a few drops of $HNO_3$, to prevent precipitation and subsequently analysed for metal concentration. Samples were taken before and after the sorption procedure for metal analysis. Samples were analysed using ICP-OES, as described in section 2.4.6.

## 6.2.5 Mathematical modelling

Adsorption isotherms are the equilibrium relationships between the concentration of sorbed metal and metal in solution, at a given temperature. The amount of metal sorbed by the biosorbent was calculated using Eq. 6.1 [143]:

**Equation 6.1: Mass balance equation for metal removal.**

$$Qe\ (mmol\ g^{-1}) = V(C_0 - Ce)/S$$

Where, *Qe* is the metal sorbed at equilibrium (mmol $g^{-1}$), *V* is the volume of solution (L), $C_0$ and *Ce* are the initial and final (equilibrium) concentration remaining in solution (mmol $L^{-1}$),

and *S* is the biosorbent dose (g). Equilibrium sorption isotherms were generated by plotting *Qe* against *Ce*.

The Langmuir and Freundlich models were used to characterise biosorption. The Langmuir adsorption isotherm is described using Eq. 6.2, and can be linearized as shown in Eq. 6.3 [143, 440]:

**Equation 6.2: The Langmuir isotherm model.**

$$Qe\ (mmol\ g^{-1}) = \frac{Qmax \cdot b \cdot Ce}{1 + b \cdot Ce}$$

**Equation 6.3: The logarithmic form of the Langmuir equation.**

$$\frac{Ce}{Qe} = \frac{1}{b \cdot Qmax} + \frac{Ce}{Qmax}$$

Where *Qmax* is the maximum adsorption capacity by the biosorbent per unit mass, *b* is an affinity parameter related to the energy of adsorption and indicates the strength of attraction of the sorbent for the solute [308].

The Freundlich isotherm is described using Eq. 6.4, and can be linearized as shown in Eq. 6.5 [143, 441]:

**Equation 6.4: The Freundlich isotherm model.**

$$Qe\ (mmol\ g^{-1}) = K_F \cdot Ce^{1/n}$$

**Equation 6.5: The logarithmic form of the Freundlich equation.**

$$Log\ Qe\ = Log\ K_F + \frac{1}{n} \cdot Log\ Ce$$

Where $K_F$ and *n* are Freundlich constants and respectively relate to the adsorption capacity and adsorption intensity of the biosorbent [308].

### 6.2.6 Data analysis

All experiments were performed in triplicate (except where otherwise stated) and the experimental error was calculated and expressed as one standard deviation (SD). Data on the biochemical content of the biomass is portrayed as a proportion of its dry weight (% DW), except for the monosaccharides which are represented as a proportion of the total soluble carbohydrate content. A one-way ANOVA with Tukey's post hoc analysis was used to determine differences in the biochemical content of the biomass. Levels of significance were set at $p < 0.05$; all statistical analyses were performed using Minitab® Statistical Software version 17.

## 6.3 Results and Discussion

The influence of nutritional or life history on macro-algal biosorbent characteristics and the resultant influence on biosorption is poorly understood. In order to greater understand this influence, *Cladophora parriaudii* was grown under six different nutrient regimes designed to produce biomass with differing biochemical composition. Cultivation media was formulated with two different N/P ratios (2/1 and 12/1) and three different N sources ($NH_4^+$, $NO_3^-$, and urea). These media formulations were employed in Chapter 5 and yielded *C. parriaudii* biomass of varying biochemical composition and were hence regarded as suitable for re-testing and use in this study. After cultivation, algal samples were dried, characterised, and used for the biosorption of four different metals. Metals were selected based upon their ecological, toxicological, and biological importance, with initial metal concentrations of 1-150 mg $L^{-1}$ employed in order to generate isothermal data and the theoretical maximum metal removal capacity per unit algal biomass, rather than for testing the applicability in environmentally relevant concentrations.

### 6.3.1 Metal Biosorption

Most studies on biosorption focus upon optimising sorption conditions for a particular biosorbent material and metal. This is achieved by sequentially testing the different operational factors involved in biosorption, including pH, temperature, biosorbent amount,

and initial metal concentration. This approach was not employed in this research, as experimental conditions were selected based upon an in-depth literature review.

Experiments were performed in order to determine how much of an influence biological factors have upon biosorption. Lyophilised biomass of *C. parriaudii*, previously cultivated under six different nutrient regimes was used for the removal of four different types of metal. Metal removal capacity was displayed as an isotherm plotted as the amount of metal sorbed per unit biosorbent (*Qe*) versus the concentration of metal remaining in solution (*Ce*) (Fig. 6.1 and 6.2). The equilibrium isotherms were characterised by mathematical models (Table 6.1, and Appendix I). Langmuir and Freundlich isothermic models were originally used to describe the adsorption of gases onto activated carbon [143, 440, 441]. Both of these models have their drawbacks. For instance, the Langmuir model is based upon the following assumptions: i) that each binding site can accommodate one molecule, and that adsorption forms a monolayer; ii) the adsorption energy of sites is equal, regardless of the presence of adsorbed species on neighbouring sites; iii) molecules only bind with the site and not with one another. These assumptions are unlikely to apply in biological systems [142, 143]. Whereas, the Freundlich model describes multi-layer adsorption onto a heterogenous surface [142, 442]. The Freundlich model is only applicable at a constant pH; however, in an unbuffered system, ion exchange will result in $H^+$ displacement by binding cations [143]. Despite their deficiencies, the Langmuir and Freundlich models are simple and widely used in biosorption studies [143]. Both models have been employed in this study, to ease comparison between treatments and with the literature.

There was a broad variation in the metal sorption capacity between metals and nutrient regime (Figs. 6.1 and 6.2, Table 6.1, and Appendix I). For example, the maximum adsorption capacity (*Qmax*) ranged from 1.08-2.35, 0.3-0.62, 0.22-0.48, and 0.43-0.61 mmol $g^{-1}$ for $Al^{2+}$, $Cu^{2+}$, $Mn^{2+}$, and $Pb^{2+}$, respectively (Table 6.1). Furthermore, there was a tight grouping in the biosorption of $Al^{2+}$ and $Pb^{2+}$, meanwhile there was a much greater spread for the sorption of $Cu^{2+}$ and $Mn^{2+}$ between both nitrogen type and N/P ratio (Figs. 6.1 and 6.2 and Appendix I1). This suggests that non-essential metals can bond onto the algal cell indiscriminately, whereas, there may be specific binding sites or uptake channels for metals that are essential for the normal functioning of the organism [443-445]. In addition, there was not a nutrient regime which produced biomass which consistently resulted in the

greatest or least amount of metal removal (Fig. 6.1 and 6.2). For instance, the nutrient regimes which resulted in the greatest *Qmax* values for each metal were 12/1 Urea for $Al^{2+}$, 12/1 $NO_3^-$ for $Cu^{2+}$, and 2/1 $NH_4^+$ for $Mn^{2+}$ and $Pb^{2+}$. Whereas, the lowest *Qmax* values were observed for 2/1 $NO_3^-$ for $Al^{2+}$ and $Mn^{2+}$, 12/1 Urea for $Cu^{2+}$, and 12/1 $NO_3^-$ for $Pb^{2+}$ (Table 6.1). These results suggest that either different metals have specific affinities for certain functional groups [432] and/or that nutrient regime influences the biochemical composition of the biomass produced, and hence the type and number of function groups present, and therefore biosorption (Chapter 5). In order to greater understand the reasons behind the variation in biosorption performance between treatments, the algal biosorbent material was biochemically characterised. Variation in metal sorption can only be attributed to differences in the biosorbent characteristics as all other experimental factors were constant (*e.g.* time, temperature, biosorbent dose).

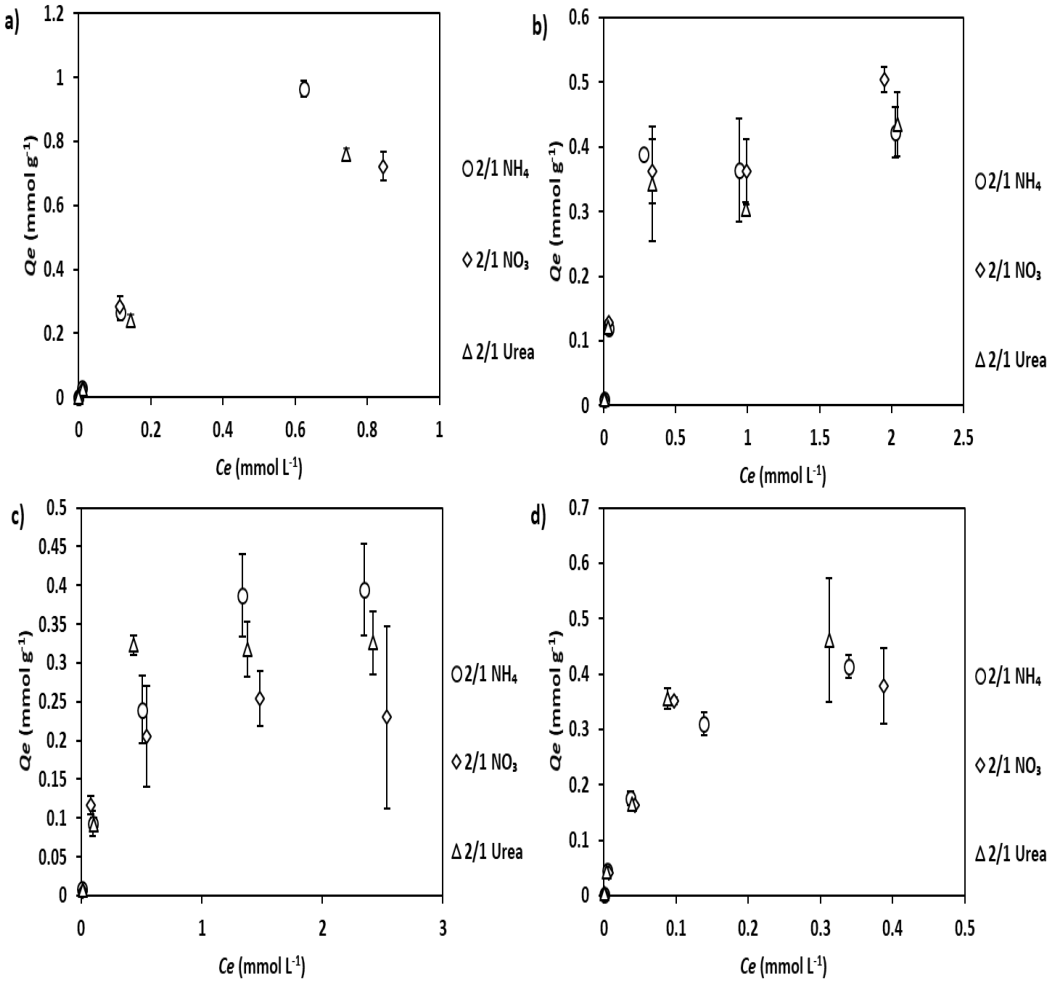


**Figure 6.1.** Sorption isotherms of $Al^{2+}$ (A), $Cu^{2+}$ (B), $Mn^{2+}$ (C), and $Pb^{2+}$ (D) by *Cladophora parriaudii* cultivated under a 2/1 N/P ratio .with different nitrogen sources; $NH_4^+$ (circle), $NO_3^-$ (diamond), Urea (triangle). The adsorption conditions were; pH = 4.5, contact time = 24 h, biosorbent dose = 1 g $L^{-1}$, agitation = 100 rpm, metal concentration = 1-150 mg $L^{-1}$ (except $Al^{2+}$ = 1-40 mg $L^{-1}$), temperature = 24°C, light = 24/0 L/D h with 30-40 µmol photons $m^{-2}$ $s^{-1}$ (*n* = 1-3, *error bars* = 1 SD.).

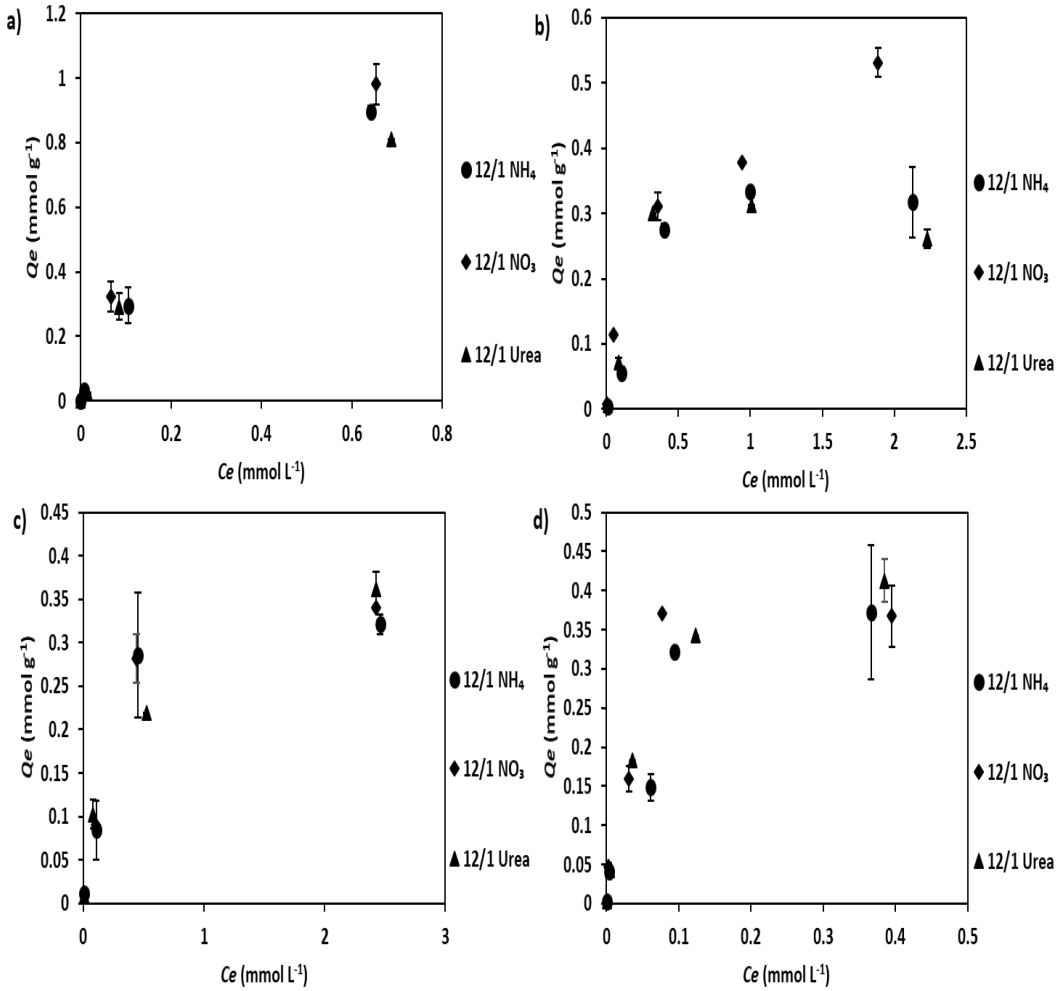


**Figure 6.2.** Sorption isotherms of $Al^{2+}$ (A), $Cu^{2+}$ (B), $Mn^{2+}$ (C), and $Pb^{2+}$ (D) by *Cladophora parriaudii* cultivated under a 12/1 N/P ratio and different nitrogen sources; $NH_4^+$ (circle), $NO_3^-$ (diamond), Urea (triangle). The adsorption conditions were; pH = 4.5, contact time = 24 h, biosorbent dose = 1 g $L^{-1}$, agitation = 100 rpm, metal concentration = 1-150 mg $L^{-1}$ (except $Al^{2+}$ = 1-40 mg $L^{-1}$), temperature = 24°C, light = 24/0 L/D h with 30-40 µmol photons $m^{-2}$ $s^{-1}$ (n = 1-3, error bars = 1 SD.).

**Table 6.1.** Langmuir and Freundlich constants for biosorption of $Al^{2+}$, $Cu^{2+}$, $Mn^{2+}$, and $Pb^{2+}$ with *Cladophora parriaudii* cultivated under different nutrient regimes.

| **Aluminium** | **Langmuir Constants** | | | **Freundlich Constants** | | |
|---|---|---|---|---|---|---|
| | ***Qmax*** **(mmol $g^{-1}$)** | ***b*** | $R^2$ | $K_F$ | ***n*** | $R^2$ |
| **2:1 $NH_4^+$** | 2.01 | 1.45 | 0.955 | 1.49 | 1.21 | 0.999 |
| **12:1 $NH_4^+$** | 1.26 | 3.63 | 0.927 | 1.38 | 1.36 | 0.991 |
| **2:1 $NO_3^-$** | 1.08 | 2.45 | 0.974 | 1.03 | 1.28 | 0.958 |
| **12:1 $NO_3^-$** | 1.45 | 3.22 | 0.967 | 1.71 | 1.28 | 0.948 |
| **2:1 Urea** | 1.37 | 1.65 | 0.976 | 1.03 | 1.25 | 0.997 |
| **12:1 Urea** | 2.35 | 0.81 | 0.3 | 1.54 | 1.09 | 0.89 |
| **Copper** | **Langmuir Constants** | | | **Freundlich Constants** | | |
| | ***Qmax*** **(mmol $g^{-1}$)** | ***b*** | $R^2$ | $K_F$ | ***n*** | $R^2$ |
| **2:1 $NH_4^+$** | 0.45 | 5.87 | 0.984 | 0.45 | 1.62 | 0.827 |
| **12:1 $NH_4^+$** | 0.42 | 1.84 | 0.902 | 0.31 | 1.21 | 0.932 |
| **2:1 $NO_3^-$** | 0.55 | 3.69 | 0.957 | 0.47 | 1.56 | 0.858 |
| **12:1 $NO_3^-$** | 0.62 | 2.55 | 0.967 | 0.47 | 1.41 | 0.92 |
| **2:1 Urea** | 0.46 | 4.31 | 0.961 | 0.4 | 1.67 | 0.828 |
| **12:1 Urea** | 0.3 | 4.68 | 0.946 | 0.3 | 1.37 | 0.864 |
| **Manganese** | **Langmuir Constants** | | | **Freundlich Constants** | | |
| | ***Qmax*** **(mmol $g^{-1}$)** | ***b*** | $R^2$ | $K_F$ | ***n*** | $R^2$ |
| **2:1 $NH_4^+$** | 0.48 | 2.13 | 0.991 | 0.31 | 1.45 | 0.96 |
| **12:1 $NH_4^+$** | 0.36 | 3.73 | 0.987 | 0.28 | 1.69 | 0.942 |
| **2:1 $NO_3^-$** | 0.22 | 5.54 | 0.94 | 0.21 | 1.53 | 0.788 |
| **12:1 $NO_3^-$** | 0.37 | 4.8 | 0.989 | 0.29 | 1.78 | 0.953 |
| **2:1 Urea** | 0.38 | 3.11 | 0.971 | 0.29 | 1.41 | 0.89 |
| **12:1 Urea** | 0.41 | 2.99 | 0.995 | 0.29 | 1.6 | 0.931 |
| **Lead** | **Langmuir Constants** | | | **Freundlich Constants** | | |
| | ***Qmax*** **(mmol $g^{-1}$)** | ***b*** | $R^2$ | $K_F$ | ***n*** | $R^2$ |
| **2:1 $NH_4^+$** | 0.61 | 6.67 | 0.692 | 1.7 | 1.19 | 0.881 |
| **12:1 $NH_4^+$** | 0.45 | 11.1 | 0.895 | 1.35 | 1.28 | 0.893 |
| **2:1 $NO_3^-$** | 0.47 | 9.88 | 0.874 | 1.77 | 1.15 | 0.915 |
| **12:1 $NO_3^-$** | 0.43 | 15.14 | 0.895 | 1.65 | 1.3 | 0.82 |
| **2:1 Urea** | 0.57 | 11.47 | 0.92 | 2.04 | 1.21 | 0.93 |
| **12:1 Urea** | 0.55 | 8.51 | 0.812 | 1.69 | 1.21 | 0.888 |

## 6.3.2 Biochemical Composition

In order to produce biomass with different biochemical properties, *C. parriaudii* was cultivated under six nutrient regimes. The nutrient regimes selected had previously been employed in Chapter 5 and yielded biomass with varying biochemical profiles (Table 5.1). Similar results to those recorded in Chapter 5 were also observed in this study. For example, biomass cultivated under a 2/1 N/P regime had a greater carbohydrate (39.6-

44.2% DW) and lower protein content (8.5-10.5% DW) in comparison to cultures maintained under a 12/1 regime, with values ranging from 32-37.5% DW and 11.5-13.6% DW, respectively (Fig. 6.3 and Table 6.2). Furthermore, differences in protein and carbohydrate content between N/P ratio were greatest and statistically significant ($p$ = 0.005-0.015) when either $NH_4^+$ or urea was the N source. As observed and discussed in Chapter 5, these nitrogen forms were favourably removed under either singular or dual N additions, possibly due to their lesser energetic requirement for assimilation, or as a supplementary carbon source [192, 195, 199, 411]. Therefore, uptake of these N forms would likely be enhanced and would result in a longer period of N-limitation under the 2/1 regime, or greater N removal from the 12/1 regime. This will have an influence on the biochemical composition, as macro-algae have been observed to synthesise proteins under N sufficiency and accumulate carbohydrates under N-deprivation [214, 215]. The monosaccharide composition of the carbohydrates further illustrates this (Fig. 6.3 and Table 6.2). For example, biomass cultivated under a 2/1 regime had a greater proportion of arabinose, glucose, and xylose with values of 24.1-24.9%, 4.2-9.6%, and 22.4-22.6%, respectively. In comparison to the 12/1 N/P regimes with values of 16.3-21.8%, 0-2.9%, and 17.7-21.6%, respective to the previous monosaccharide order. These three monosaccharides are derived from polysaccharides which serve as structural or storage carbohydrates and may have an influence upon metal adsorption on to the cell wall. For instance, glucose is the monomer that makes starch and cellulose [446, 447]. Whereas, hemicelluloses are composed of xylans, mannans, and arabino-xylans of which arabinose and xylose are constituent monosaccharides [448, 449]. On the other hand, the ribose content of *C. parriaudii* cultivated under a 12/1 N/P regime was much greater than biomass propagated under a 2/1 regime, with values of 56.7-63.8% in comparison to 42.9-49.1% of the carbohydrate content, respectively (Fig. 6.3 and Table 6.2). *Cladophora* cells are characterised by being multi-nucleated [72] with D-ribose and 2-deoxy-D-ribose being the sole component sugar of RNA and DNA, respectively [449]. Protein synthesis is one of the primary roles of nucleic acids and ribosomes within the cell [449]. Therefore, cells cultivated under the 12/1 N/P regime will not have been deprived of N, and hence the cultures continued to synthesise proteins and pigments, and as such will have had a greater protein, nucleic acid and ribose content.

Although the differences were not significant, *C. parriaudii* biomass cultivated under the 12/1 N/P nutrient regime tended to have a marginally higher pigment concentration (0.9-

1.2% DW), in comparison to biomass cultivated under a 2/1 N/P regime (0.8-1.0% DW) (Fig. 6.3 and Table 6.2). This trend was expected as chlorophyll *a* and *b* are N containing molecules [450, 451], and algae have been observed to have a decreased pigment content when cultivated under nitrogen deficiency [330].

The ash content of the biomass was comparable across the different nutrient regimes, with no statistically significant difference recorded ($p$ = 0.188) (Fig. 6.3 and Table 6.2). However, the proportion of ash in the *C. parriaudii* biomass cultivated under a 2/1 $NO_3^-$ regime (36.7%) was noticeably higher than all others which were in the range of 29.4-33.5% DW. Metals such as calcium, copper, iron, magnesium, manganese and zinc have many key functions in the cell, such as electron transport in photosynthetic and cytochrome systems, a structural component of chlorophyll, and water oxidation in photosystem II [439, 450-453]. Differences in mineral content may be due to an up- or down-regulation of any of the systems involving trace metals, alternatively, it may have been caused by the incomplete removal of extracellular salts prior to harvesting the biomass. The remaining components of the biomass have been pooled and are defined as “other” (Fig. 6.3 and Table 6.2). The “other” will be most likely be comprised of incomplete extractions of the aforementioned biochemical compounds or insoluble proteins and carbohydrates, uronic acids, water soluble pigments, lipids, metabolites, free amino acids, nucleic acids, and other organic material. The “other” component was lower in biomass cultivated under 2/1 N/P in comparison with the 12/1 N/P regimes, with values ranging from 12.3-17% DW and 18.6-22.1% DW, respectively.

The results observed from this study (Fig. 6.3 and Table 6.2), in addition to those found in Chapter 5 (Table 5.1) indicates that nutrient regime, more specifically the N/P ratio, has a strong influence upon the final biochemical composition of *C. parriaudii*; however, it is uncertain if this translates into a difference in cell surface properties and what effect this has on metal biosorption.

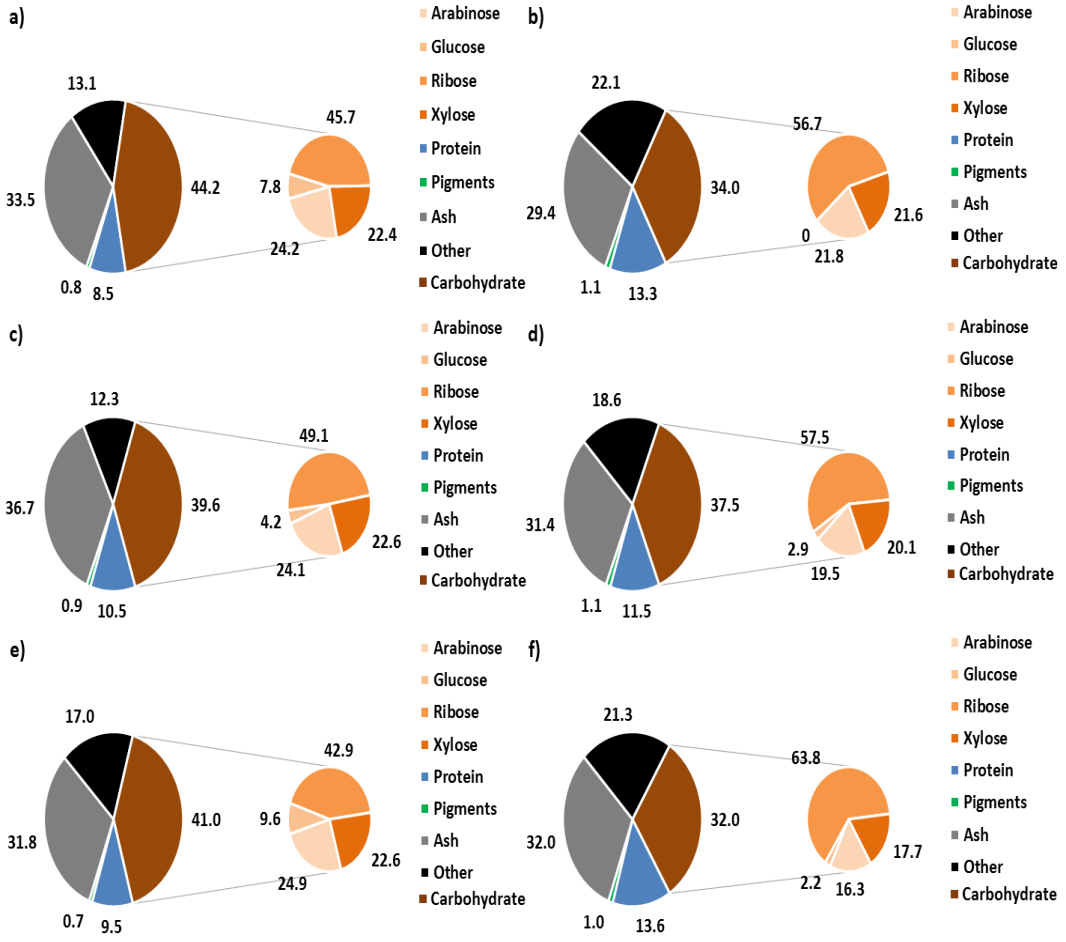


**Figure 6.3.** Biochemical composition of *Cladophora parriaudii* cultivated under different nutrient regimes; a) 2/1 $NH_4^+$, b) 12/1 $NH_4^+$, c) 2/1 $NO_3^-$, d) 12/1 $NO_3^-$, e) 2/1 urea, f) 12/1 urea. The first pie details the bulk chemical composition of the biomass. The second pie details the proportion of monosaccharides in the total soluble carbohydrate extract (*n* = 3).

**Table 6.2**. The biochemical composition of *Cladophora parriaudii* cultivated under different nutrient regimes. Biochemical components that are denoted by different letters are statistically significant ($p < 0.05$).

| Biochemical Component (% DW) | $NH_4^+$ | | $NO_3^-$ | | Urea | |
|---|---|---|---|---|---|---|
| | **2/1** | **12/1** | **2/1** | **12/1** | **2/1** | **12/1** |
| **Ash** | $33.5^{a}$ | $29.4^{a}$ | $36.7^{a}$ | $31.4^{a}$ | $31.8^{a}$ | $32^{a}$ |
| **Carbohydrate** | $44.2^{a}$ | $34^{bc}$ | $39.6^{abc}$ | $37.5^{abc}$ | $41^{ab}$ | $32^{c}$ |
| Arabinose (% Carb) | $24.2^{a}$ | $21.8^{ab}$ | $24.1^{a}$ | $19.5^{ab}$ | $24.9^{a}$ | $16.3^{b}$ |
| Glucose (% Carb) | $7.8^{ab}$ | $0^{c}$ | $4.2^{abc}$ | $2.9^{bc}$ | $9.6^{a}$ | $2.2^{bc}$ |
| Ribose (% Carb) | $45.7^{b}$ | $56.7^{ab}$ | $49.1^{ab}$ | $57.5^{ab}$ | $42.9^{b}$ | $63.8^{a}$ |
| Xylose (% Carb) | $22.4^{a}$ | $21.6^{a}$ | $22.6^{a}$ | $20.1^{a}$ | $22.6^{a}$ | $17.7^{a}$ |
| **Pigments** | $0.9^{a}$ | $1.0^{a}$ | $1.0^{a}$ | $0.9^{a}$ | $0.8^{a}$ | $1.2^{a}$ |
| **Protein** | $8.5^{b}$ | $13.3^{a}$ | $10.5^{ab}$ | $11.5^{ab}$ | $9.5^{ab}$ | $13.6^{a}$ |
| **Other** | $13.1^{bc}$ | $22.1^{a}$ | $12.3^{c}$ | $18.6^{abc}$ | $17^{abc}$ | $21.3^{ab}$ |

## 6.3.3 Cell Surface Characteristics

FTIR-ATR (Fig. 6.4 and Appendix J) and SEM BSE analysis (Figs. 6.7-6.8, and Appendices K and L) were performed on *C. parriaudii* biomass after cultivation under different nutrient regimes and after metal biosorption. This was in order to understand if changes in biochemical composition, induced by different nutrient regime were reflected in the functional groups present on the cell surface and if there is any influence upon the ultra-structure of the cell. In addition, combining this with the biochemical and metal removal data may give greater clarity into the mechanisms underpinning biosorption.

### *6.3.3.1 FTIR Analysis*

FTIR is a vibrational spectroscopic technique used to detect different molecules or functional groups present in a sample [454]. Different molecules, such as protein, lipids, chlorophyll, and carbohydrates absorb infrared (IR) irradiation at different wavelengths [455]. This is due to each bond within a molecule vibrating at a specific frequency, when the vibrational frequency of the bond and the IR coincide, absorption occurs [455, 456]. These vibrations have different motions, *e.g.* symmetric or asymmetric stretching, bending,

rocking or wagging [457]. Taken together, the vibrational spectrum of a molecule is unique, and may be used for identification purposes [456].

The FTIR-ATR method employed in this work should be considered as a qualitative technique only, and not quantitative or semi-quantitative. Quantification using FTIR-ATR is possible as IR absorbance at a given wavenumber is proportional to the concentration of a given bond or molecule, following the Beer-Lambert-Bouguer Law (Beer's Law) [455, 456]. However, sample preparation employed in this work did not meet the implicit requirements for adherence to Beer's Law, particularly that "*the absorbing medium is homogenous and does not scatter the radiation*" [458]; for instance, samples were not ground or homogenised as only functional groups present on the cell surface were desired. In addition, radiation may have been scattered by differences in path length and/or the alignment and crystallinity of the *Cladophora* filaments. As such, comparison between spectra is limited to the presence/absence of bands, changes in wavenumber, the shape of individual peaks, or the relative size of peaks within an individual spectrum.

The IR spectra obtained from pristine *C. parriaudii* after cultivation under different nutrient regimes are displayed in Fig 6.4a-f (green), the main band assignments and functional groups present in *C. parriaudii* samples are provided in Appendix J. The spectra from the pristine biomass are almost identical with a similar distribution of peaks, peak shape, and wavenumber. With strong bands present in the range of 3400-2800 $cm^{-1}$ which are typically associated with a mix of water, protein, carbohydrate, cellulose, and lipids (Fig. 6.4 and Appendix J). Ester bonds of lipids and fatty acids in algal biomass are usually observed in the region of 1780-1708 cm [455, 459, 460]; however, the absence of this peak in *C. parriaudii* biomass suggests that it is a minor component of the overall biochemical content. Strong bands at 1650-1630 $cm^{-1}$ and 1550-1530 $cm^{-1}$ were attributed to Amine Groups I and II, respectively. There are a variety of peaks present in the range of 1460-1310 $cm^{-1}$, and are assigned to cellulose, proteins, lipids, and sulphurous components. The prominent peak at 1250-1210 $cm^{-1}$ is attributed to Amine Group III and phosphodiester bonds from phospholipids. The remaining spectra can mostly be assigned to poly- and monosaccharides, cellulose, aliphatics of the cell wall and aromatic compounds. Coupling together biochemical data (Fig. 6.3 and Table 6.2) with the comparability of the spectra of "pristine" biomass (Fig. 6.4) suggests that cultivation under different nutrient regimes results in biomass with different biochemical properties; however, this does not necessarily

translate into the synthesis of new or different molecules, rather the quantity or proportion of molecules/functional groups may differ. For instance, several studies have measured the IR spectra of micro-organisms across a time-course, and therefore of different biochemical compositions. Generally, the spectra obtained are comparable, with main difference between samples being the relative strength, or proportion, of absorption bands [142, 460-463].

The spectra of the biomass after metal biosorption are also shown in Figure 6.4. Visually, these look very similar to the spectra obtained with corresponding "pristine" biomass; however, there are some subtle and consistent differences between them. This indicates that certain functional groups, or molecules, are involved in metal biosorption. For instance, there is an amine peak in the region of 1409-1403 $cm^{-1}$ in "pristine" biomass; however, after exposure to all metals, this disappears and three distinct pairs of peaks emerge. In addition, the shape of the peak at 1250-1210 $cm^{-1}$ changes after exposure to metal. This region is associated with Amine Group III, as well as the asymmetrical vibrations of phosphodiester bonds from DNA, ATP, and phospholipids which form the cell membrane [461, 462, 464]. There are also changes in peak shape or wavenumber in the regions of: 3400-3200 $cm^{-1}$, attributed to fatty acids, hydroxyl groups, and Amide Group A; 3000-2900 $cm^{-1}$ due to cellulose, carbohydrates, methyl and methylene groups; the relative intensity of the peaks at 1160 $cm^{-1}$ and 1056-990 $cm^{-1}$ which are assigned to cellulose and polysaccharides, respectively.

The FTIR-ATR analysis suggests that there is a consistency between the different functional groups involved in metal biosorption between samples. Cultivating algal biomass in different nutrient regimes may not result in the advent of new or different functional groups; however, it may result in biomass with different proportions of macromolecules, and therefore, relative number of different functional groups. This in turn, may make them more effective as a biosorbent.

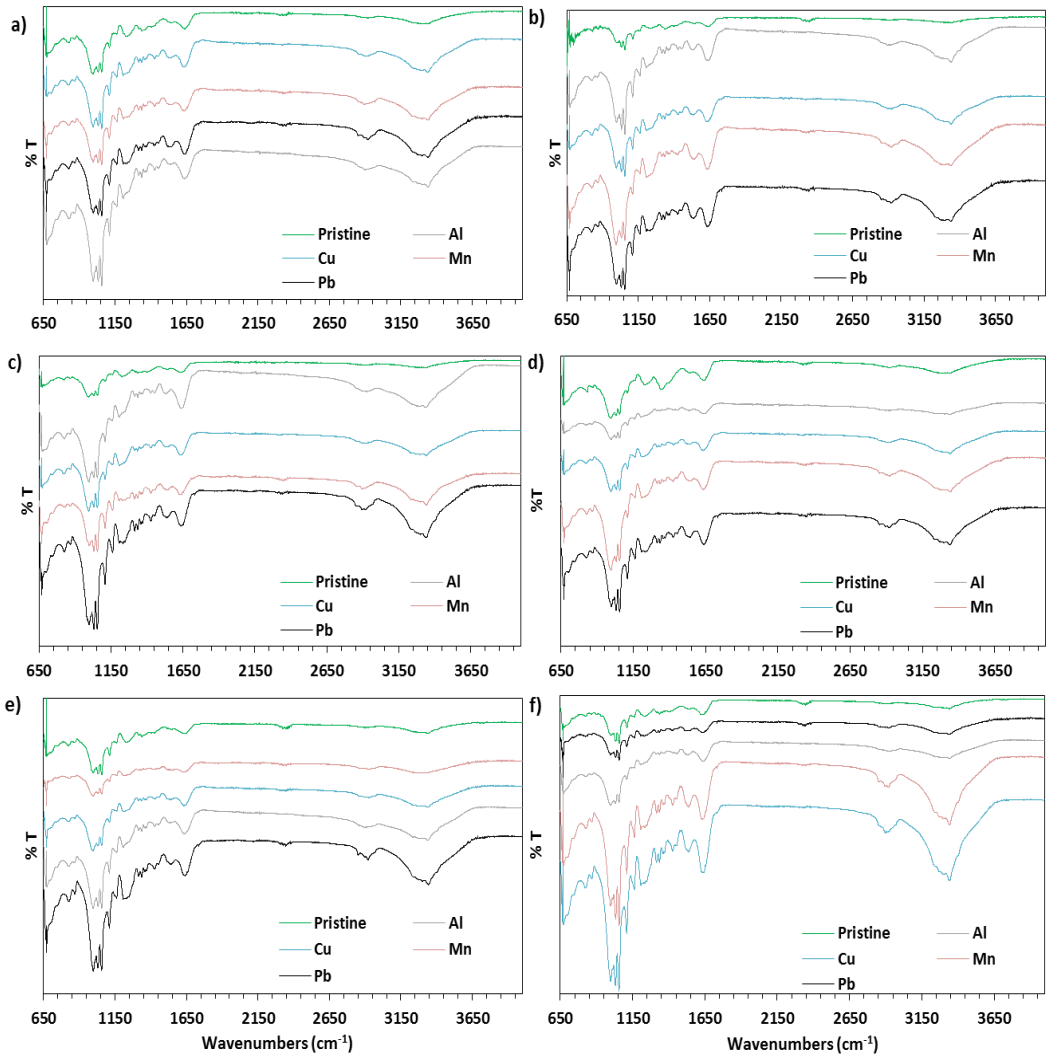


**Figure 6.4.** IR spectra of *Cladophora parriaudii* biomass after cultivation under different nutrient regimes; a) 2/1 $NH_4^+$, b) 12/1 $NH_4^+$, c) 2/1 $NO_3^-$, d) 12/1 $NO_3^-$, e) 2/1 Urea, f) 12/1 Urea. The spectra were then taken before (green) and after metal biosorption with $Al^{2+}$ (grey), $Cu^{2+}$ (blue), $Mn^{2+}$ (pink), and $Pb^{2+}$ (black). Each line is an average of 25 scans, baseline corrected and atmospheric $CO_2$/$H_2O$ removed.

### *6.3.3.2 SEM Analysis*

In order to understand if metal biosorption influenced, or was influenced by, the ultra-structure of the cell, or if metal bonding was localised to specific areas of the cell, SEM-BSE analysis was performed on *C. parriaudii* biomass after exposure to metals.

Preliminary SEM method testing was performed on *C. parriaudii* biomass cultivated under f/2 medium, without exposure to metals, acting as a control. On the same biomass sample,

two SEM imaging techniques were tested; secondary electrons (SE) detection and back-scattered electrons (BSE) (Fig. 6.5). There were clear differences in surface resolution and brightness/contrast between the two methods. This is due to the different ways in which images are attained. The SE are emitted from atoms on the surface of a sample with contrast achieved by surface morphology. As a result, images attained by SE are very detailed with high resolution. On the other hand, BSE images are primary beam electrons that are reflected from atoms on the surface and within the sample. The contrast in the back-scattered micrograph is determined by the atomic number of the elemental sample with heavier elements (*e.g.* lead) appearing brighter as they back-scattering electrons more efficiently than lighter elements (*e.g.* sodium). BSE images do not offer the same degree of surface definition as SE, but they do provide information on the different chemical phases in a sample [465]. Elemental spectra (Fig. 6.6) were taken from two different locations in the sample (Fig. 6.5a; "spectrum 1" and "spectrum 3"). Firstly, from a darker area of the cell (Fig. 6.5a; "spectrum 1"), which was regarded to be "pristine" as the area was relatively flat with no obvious signs of contamination. The elements present from this "pristine" area (Fig. 6.6a) were largely organic, with some light and alkali metals present (Al, Na, Mg). The brighter region that was scanned (Fig. 6.5a; "spectrum 3") also contained these elements, but had a greater signal from Cl and K which are heavier elements (Fig. 6.6b), and therefore appeared brighter in the image. As the purpose of this study was to elucidate bonding of heavy metals to biomass, the BSE technique was employed for future analysis as it offers a greater contrast between elements of different atomic mass.

The SEM-BSE images and elemental spectra were taken from biomass exposed to 40 mg $L^{-1}$ metal solutions, having previously been cultivated under a 2/1 $NO_3^-$ nutrient regime (Figs. 6.7 and 6.8), corresponding data regarding all other nutrient regimes are appended (Appendices K and L). There was no apparent difference in the cellular structure between treatments (Figs. 6.5, 6.7, and Appendix K), the filaments in all samples appeared furrowed, or grooved, which is most likely a result of the drying protocol (sections 6.2.1 and 6.2.4). This indicates that neither the nutrient regime, metal exposure, nor metal type influenced the cellular morphology or surface topography.

Metal bonding occurred in all instances (Fig. 6.7 and Appendix K), with the heavy metals mostly appearing within bright "clusters" in comparison to the darker organic *C. parriaudii* filaments [465]. Elemental spectra obtained from these "clusters" confirmed that they

contained the respective metals used in the biosorption tests (Fig. 6.8b, d, f, and h). This clustering of metals indicates that metal biosorption does not occur as a monolayer, which is one of the main assumptions of the Langmuir model [143, 440], meaning that the usefulness of the Langmuir model is limited when describing biosorption. There was no pattern or trend to the clustering behaviour between biosorbent and the adsorbate. For instance, the clusters were of irregular size and shape. Furthermore, the clustering occurred randomly across the filament surface and was not confined to specific locations, *e.g.* furrows, ridges, or damaged areas of the cell surface (Fig. 676 and Appendix K). This suggests that the cell surface topography has minimal influence on biosorption.

The elemental spectra of different locations on each sample were obtained. Similar locations to those previously described (Figs. 6.5 and 6.6) were targeted. Specifically, "pristine" areas of each cell in order to obtain a background (Fig. 6.8a, c, e, and g) and areas where clustering was evident (Fig. 6.8b, d, f, and h). The "pristine" areas of the samples after exposure to metals were selected over samples without any prior metal exposure to avoid any potential inter-sample variation in biochemical composition. The "pristine" spectra of samples after metal sorption (Fig. 6.8a, c, e, and g) was comparable to that of the f/2 biomass that was not used for biosorption purposes (Fig. 6.6). All samples contained a high proportion of carbon, oxygen and sulphur. In addition, there were also varying amounts of sodium, phosphorus, potassium, magnesium, chlorine, calcium and silicon, elements which are required for the normal functioning of the algal cell [439, 450, 461, 466-470]. The main difference between the "pristine" samples was the presence of trace amounts of the sorbed metal, either Al, Cu, Mn, or Pb (Fig. 6.8b, d, f, and h, and Appendix L). Although these metals were not visualised as "clusters", their occurrence may have been caused by detection from adjacent areas of the cell surface, within the filament, or have been present in trace amounts. The spectra of the "clusters" after biosorption (Fig. 6.8b, d, f, and h, and Appendix L) contained the aforementioned metals. Signals for the toxic or heavy metals were greater in these spectra, indicating that these metals were predominantly present in these clusters.

Interestingly, the "cluster" spectra often contained strong signals for P, Mg, Fe, Ca and Si in comparison to their respective "pristine" samples. These metals all serve different functions within the cell. For instance, P is a constituent element in DNA, ATP, and the phospholipid bi-layer of the cell membrane [461, 462]. Magnesium is the core ion involved in chlorophyll

*a* and *b* [450]; chlorophyll is located in membrane-bound chloroplasts and is, therefore, in close proximity to the cell surface [354]. Iron has numerous functions within an algal cell, mostly related to electron transport in photosynthetic and cytochrome systems, as well as N assimilation via ferredoxin [439]. Calcium has many roles in the algal cell, including: the maintenance of the membrane integrity [468], water oxidation [439], and regulation of photosynthesis and carbon reduction [466]. Furthermore, studies have pre-treated algal biomass with calcium to enhance its ion exchange properties for metal biosorption [433, 471]. Silicon is thought to play several roles in multi-cellular aquatic plants. For example, it is thought to have a growth-enhancing role in *Cladophora glomerata* [472, 473]. Mizuta and Yasui [467] observed protective and healing roles of silicon in sporophytes of *Saccharina japonica*. Whereas, diatoms have siliceous frustules, which have a structural role and protect against predation [474]. In addition, silicon may alleviate stress in plants by complexing, co-precipitating, or compartmentalising (toxic) metals or by stimulating antioxidant systems [475]. These elements, therefore, have important roles in protein synthesis and the structure of the cell wall and cell membrane; all of which were influenced by nutrient regime (Fig. 6.3 and Table 6.2) and involved in biosorption as observed using the FTIR (Fig. 6.4). The "clustering" behaviour observed in the SEM images, together with the elemental spectra and the roles of each element within an algal cell suggests that there are multiple mechanisms involved in biosorption including adsorption, ion exchange, complexation, and micro-precipitation [140, 142, 143, 468, 475]. However, no relationship was observed between the presence or strength of signal for these metals and the type of metal biosorbed or nutrient regime (Fig. 6.8 and appendix L). Further research involving different concentrations and types of toxic/heavy metals, and prior cultivation under a broader range of nutrient regimes would provide a valuable insight into the underlying mechanisms of biosorption.

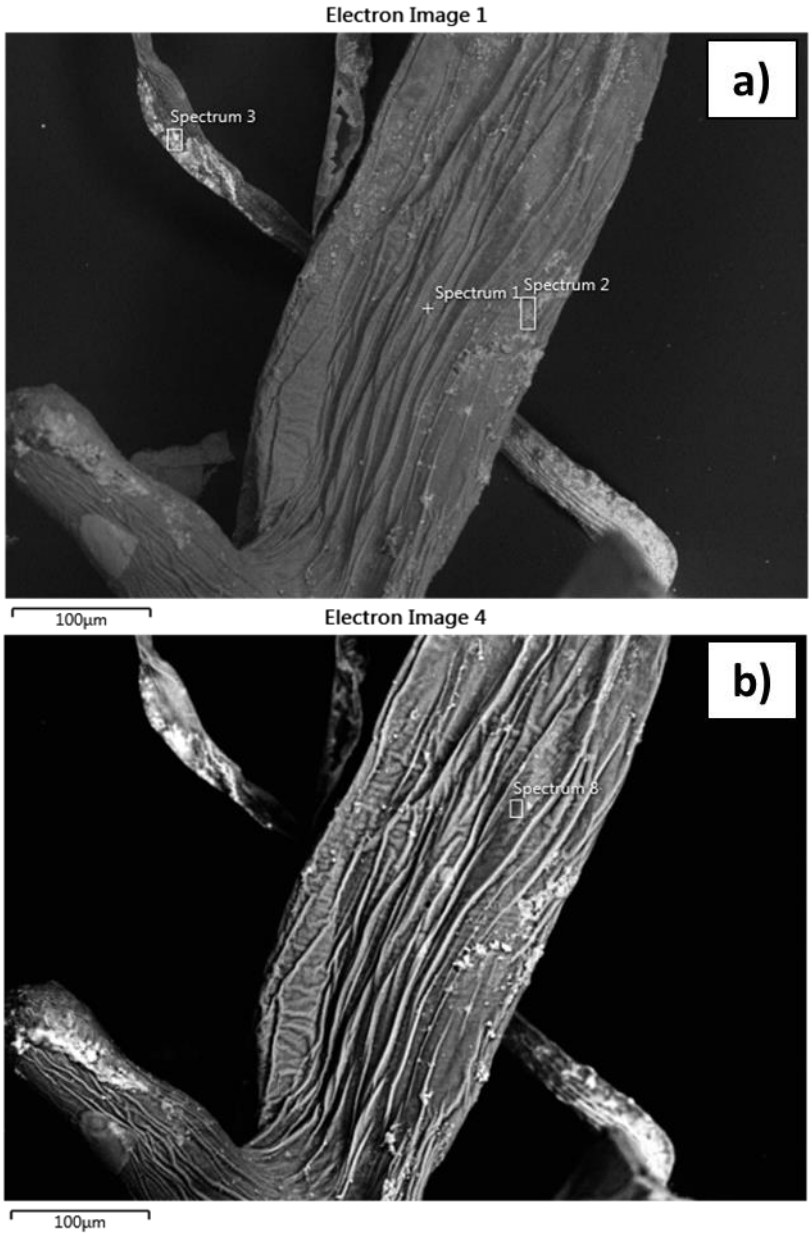


**Figure 6.5.** The cell surface of *Cladophora parriaudii* cultivated in f/2 medium. Images were obtained using two different SEM imaging techniques; a) detection of secondary electrons (SE), b) the back-scattered electrons (BSE), at 10 kV and 562 X magnification.

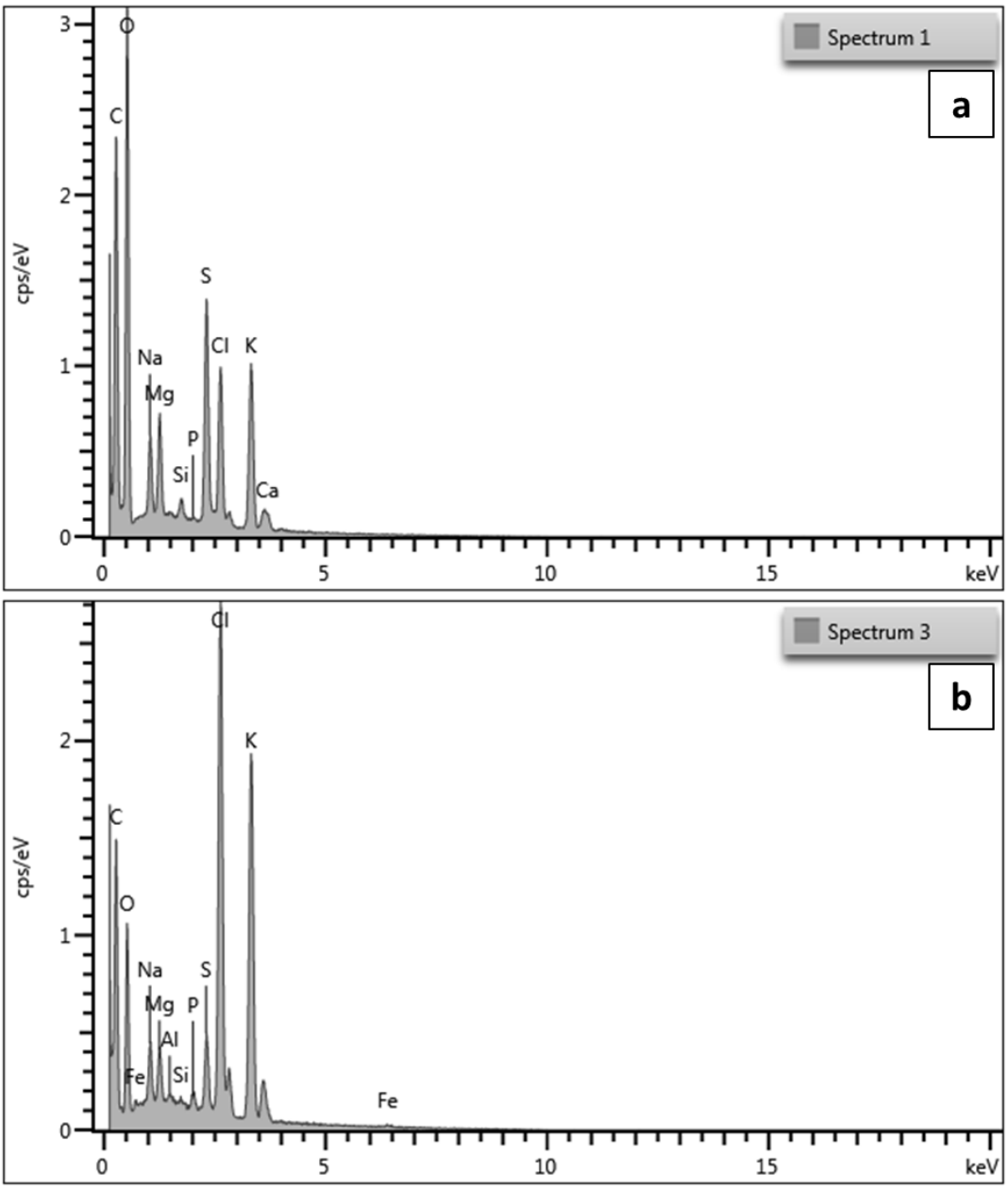


**Figure 6.6.** The SEM elemental spectra of *Cladophora parriaudii* cultivated under f/2 medium. Spectra were obtained from areas of biomass that were a) "pristine", and b) bright cluster. The spectra correspond to locations marked "Spectrum 1" and "Spectrum 3", respectively, from the micrograph above (Fig. 6.4a).

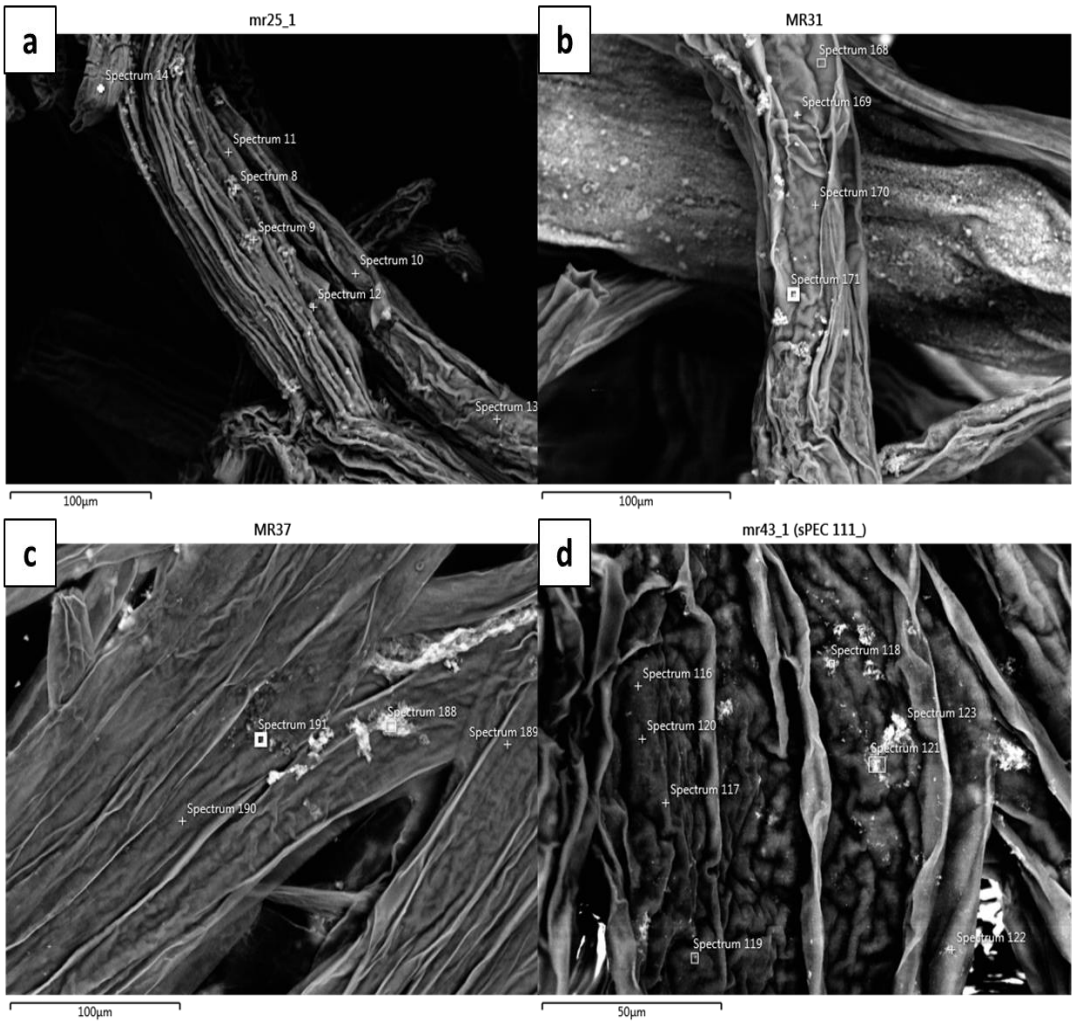


**Figure 6.7.** The cell surface of *Cladophora parriaudii*, previously cultivated under a 2/1 $NO_3^-$ medium, after exposure to a) $Al^{2+}$, b) $Cu^{2+}$, c) $Mn^{2+}$, d) $Pb^{2+}$. Images were attained with an SEM using the back-scattered electrons (BSE) technique (Section 2.5.6), at 20 kV and ~1.2-1.5 K X magnification.

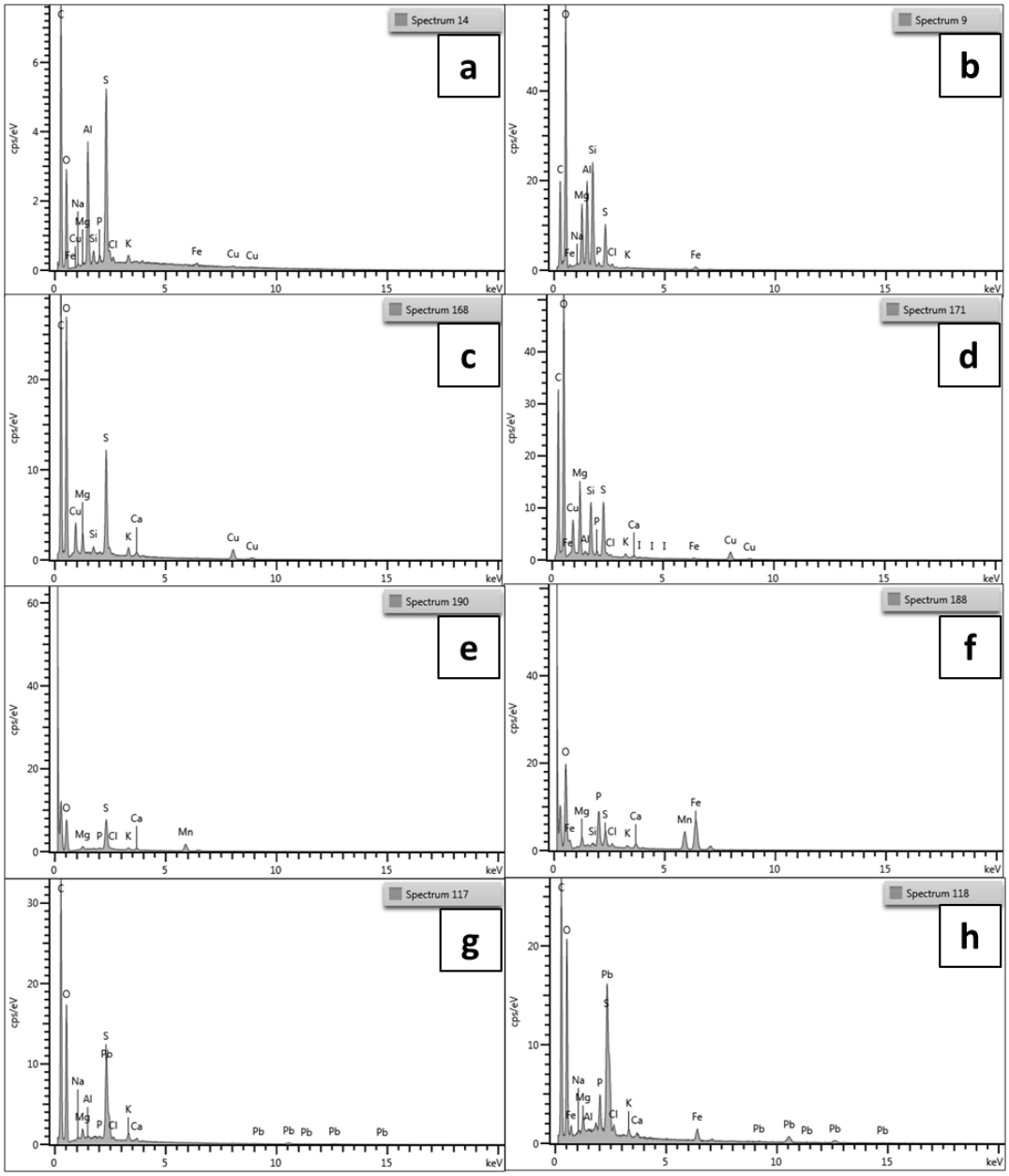


**Figure 6.8.** The SEM elemental spectra of *Cladophora parriaudii*, previously cultivated under a 2/1 $NO_3^-$ nutrient regime and after exposure to metals: $Al^{2+}$ (a and b), $Cu^{2+}$ (c and d), $Mn^{2+}$ (e and f), $Pb^{2+}$ (g and h). The spectra on the left hand side (a, c, e, and g) were obtained from areas on the cell surface which were deemed "pristine", or as having no visual evidence of metal/contaminant bonding. Whereas, spectra on the right hand side (b, d, f, and h) were obtained from areas on the cell surface in which metal was present, typically as a bright "cluster". The specific locations of each spectrum are denoted in the corresponding images in Fig. 6.6. Be aware of differences in the y-axis.

## 6.3.4 Combining Relationships in Metal Biosorption with Cellular Properties

The biochemical and cell surface data obtained (sections 6.3.2-6.3.3) can be used to offer some explanation for the trends observed in metal biosorption (Figs. 6.1 and 6.2 and Table 6.1) and this is discussed below.

### *6.3.4.1 Aluminium*

Aluminium solubility was poor beyond a concentration of 40 mg $L^{-1}$ at pH 4.5. As such isotherms were generated using initial $Al^{2+}$ concentrations of 1, 10, and 40 mg $L^{-1}$ only (Fig. 6.1a and 6.2a). The *Qmax* values, derived from the Langmuir model, ranged from 1.08-2.01 mmol $g^{-1}$; the highest value (2.35 mmol $g^{-1}$) has been discounted due to its very poor fit ($R^2$ = 0.3) (Table 6.1). Nevertheless, these sorption capacities are similar to those recorded with macro-algal and bacterial biosorbents elsewhere (2.05-2.9 mmol $g^{-1}$) [476-478], with sorption thought to be primarily caused by ion exchange [478, 479]. In this study, the highest level of biosorption (2.01 mmol $g^{-1}$) was recorded with *C. parriaudii* cultivated under a 2/1 $NH_4^+$ regime. This treatment was coincident with the highest carbohydrate yield of 44.2% DW (Table 6.2). High metal sorption (1.26-1.45 mmol $g^{-1}$) was also achieved by biomass cultivated under 12/1 N/P regime, which yielded protein rich biomass (11.5-13.3% DW) (Table 6.2), the functional groups of which will have been involved in metal biosorption (Fig. 6.4). The lowest *Qmax* was achieved by biomass previously maintained under a 2/1 $NO_3^-$ nutrient regime (Table 6.1), which had the greatest ash content (Fig. 6.3 and Table 6.2). The inorganic salts and minerals present in, or on, the biomass may have competitively excluded the $Al^{2+}$ ions from bonding with the biomass, or may have bonded more strongly with other cations present [273, 308].

### *6.3.4.2 Copper*

The maximum biosorption of copper by *C. parriaudii* cultivated under different nutrient regimes ranged from 0.3-0.62 mmol $g^{-1}$ (Table 6.1), which is comparable with values

obtained elsewhere with other algal biosorbent material (<0.01-2.77 mmol $g^{-1}$) [252, 254]. The isotherms indicated that there was a broad spread in between treatments, potentially caused by availability and competition for specific binding sites for this essential metal [443-445]. The biosorption trends could be divided into three distinct groups (Fig. 6.1 and 6.2). The best biosorption was achieved by biomass cultivated under $NO_3^-$ (*Qmax* = 0.545-0.616), with the resultant biomass having middle levels of protein and carbohydrates (Table 6.2). The second biosorption group (0.45-0.46 mmol $g^{-1}$) included *C. parriaudii* cultivated under 2/1 N/P ratios, with either $NH_4^+$ or urea as the N source (Fig. 6.1 and 6.2). Biomass cultivated under this regime had the greatest carbohydrate (particularly monosaccharides with a structural function, *i.e.* arabinose, glucose, and xylose) and low protein yields, with values of 41-44.2% DW and 8.5-9.5% DW, respectively. Whereas, biomass with the highest protein (12/1 $NH_4^+$ and 12/1 urea) content had the lowest rate of copper biosorption, 0.3-0.42 mmol $g^{-1}$ (Table 6.1). Overall, this suggests that copper bonds to functional groups that form carbohydrates and proteins, but may be more strongly attracted to hydroxyl and aldehyde groups that are present in mono- and poly-saccharides. Other studies have reported that copper binds to different functional groups on the cell, including: alcohol, amido, amine, amino, ether, carboxyl, sulfonate and sulfonyle [284, 288], functional groups that are all present in the biomass of *C. parriaudii* (Fig. 6.4 and Appendix J).

### *6.3.4.3 Manganese*

The $Mn^{2+}$ isotherm was similar to that achieved with $Al^{2+}$ (Fig. 6.1 and 6.2). For instance, the highest *Qmax* (0.48 mmol $g^{-1}$) was attained using biomass cultivated under the 2/1 $NH_4^+$ treatment, which was carbohydrate rich (44.2%) (Fig. 6.3). *C. parriaudii* cultivated under the 2/1 $NO_3^-$ nutrient regime resulted in the least amount of metal removal (0.22 mmol $g^{-1}$), possibly due to a higher degree of binding site exclusion caused by the mineral rich biomass. Cultivation under a 12/1 N/P regime resulted in similar levels of biosorption (0.36-0.41 mmol $g^{-1}$) (Table 6.1), in conjunction with a comparable protein content (11.5-13.6% DW) (Fig. 6.3). Manganese, like copper, is an essential metal and may have specific binding sites and transporters for its uptake within the cell and hence biosorption, even though the *C. parriaudii* samples were not viable [444, 445]. Manganese may have bonded with the array of functional groups that are associated with proteins, including amine, amido,

alcohol, carboxyl, that were all present in the cells (Fig. 6.4 and Appendix J). There have been few studies involving algal biosorption with manganese; however, results from this study are comparable with the data available. For instance, *Qmax* values of <0.01-0.63 mmol $g^{-1}$ have been reported [480, 481], with bonding typically occurring with functional groups associated with lipids, carbohydrates, and proteins [481].

#### *6.3.4.4 Lead*

In comparison to $Cu^{2+}$ and $Mn^{2+}$ isotherms, much less variation in the lead isotherms was observed (Fig. 6.1), with *Qmax* values of 0.43-0.61 mmol $g^{-1}$ recorded (Fig 6.1 and 6.2 and Table 6.1). Whereas, values of <0.01-1.95 mmol $g^{-1}$ have been recorded elsewhere [252, 294], with alcohol, amide, amine, amino, carboxyl, ether, hydroxyl, sulfate, sulfonate and sulfonyl groups all involved in bonding [142, 284, 288, 292, 293]. As lead serves no known biological function, it may bond indiscriminately with any functional group present on the cell surface, rather than having specific affinities to certain groups or transporters [443]. In this study, the greatest lead removal recorded was by biomass cultivated under 2/1 $NH_4^+$ and 2/1 and 12/1 urea (0.55-0.61 mmol $g^{-1}$). This suggests that biomass with the most "extreme" biochemical properties, such as a high proportion of carbohydrate or protein, would be most suitable for lead biosorption.

### 6.3.5 Macro-algal biosorption – potential applicability

Results from this study suggest that cultivation conditions, specifically nutrient regime, are highly influential in terms of the biochemical composition of the algal biomass produced. This, in turn, has an influence on its effectiveness and mechanisms involved in biosorption for different heavy/toxic metals. Therefore, in biosorption studies, the commonly employed approach of utilising material collected from the field, where the biomass was grown in undefined conditions, should be avoided. In order to better understand the (bio)chemistry underlying biosorption, and to ease inter-study comparability, biomass should be either cultivated under controlled conditions, or fully characterised with the data sufficiently

described. However, from a practicality perspective, the use of wild biomass harvested at the end of a growing season, after an eutrophication event, or beach cast material may represent an abundant, low-cost, renewable, sorbent material that could potentially be broadly used for heavy/toxic metal removal [482]. However, “beach grooming”, or the collection of seaweed cast ashore or harvested from the wild, may result in a loss of biodiversity [483]. Alternatively, algal biomass used for nutrient bioremediation could be collected and re-used for additional metal treatment purposes, creating a more circular and sustainable WWT scenario. This, alongside biofuel conversion, is perhaps the most sensible use of the algal biomass post-WWT [138, 482], due to likely issues surrounding algal material propagated on a waste resource. For instance, potential health hazards and public perception, which would prevent this material from being marketable or fit for human/animal consumption [136, 137]. One further consideration is, that algal material derived from a nitrogen enriched WWT environment [58], will likely have a high protein content [214, 215] and associated functional groups, making it well suited for the removal of metals attracted to these respective groups, in addition to metals that exhibit non-discriminative bonding (*e.g.* lead). However, as has been discussed throughout Chapters 1, 5, and 6; the biochemical composition of the algal material is dependent upon the species selection, cultivation conditions, and wastewater characteristics. Bearing this in mind, biomass with certain biochemical or cellular properties could potentially be “designed” by cultivation under tailored nutrient regimes, targeting specific wastewater types, or employing bioengineering or genetic modification techniques. This would, however, incur an additional expense and may, therefore, only be applicable for the removal, and subsequent recovery, of precious metals (*e.g.* gold and platinum) [427, 484], or highly valuable rare earth elements, such as tellurium, that are mined from deep seamounts [485, 486]. In terms of implementing algal biosorption in practice, perhaps the most feasible scenario would be the use of a reactor, similar to activated carbon towers. These have the benefit of being simple, scalable, and have a low land requirement. They therefore could be broadly applicable for many industries producing metal laden wastewaters (*e.g.* whisky, mining) [413, 487, 488]. Furthermore, these reactors could be intelligently designed to facilitate biosorbent replacement, regeneration, and metal recovery.

## 6.4 Conclusions

From this work, several key conclusions have been generated. Firstly, that cell morphology or surface topography is not influenced by either nutrient regime or metal exposure. Furthermore, the cell surface topography plays a very marginal role (if any) in biosorption of heavy metals. Secondly, that algal biosorption is a very complex process with multiple mechanisms involved in metal removal, including: adsorption, complexation, ion exchange, and micro-precipitation. Further research should focus on the extent that these different processes have on biosorption. Thirdly, that these mechanisms result in biosorption occurring in "clusters" rather than as a single monolayer. This means that widely used mathematical models, which assume monolayer sorption, may be unfit for describing biosorption and should be used with caution. Finally, and arguably most importantly, in additional to operational process factors such as pH, biological factors also strongly influence biosorption. The nutrient regimes employed in this work yielded biomass with different biochemical and molecular properties, which in turn greatly influenced the effectiveness of the material for biosorption applications. The biological aspect of biosorption has previously been largely overlooked, but should be given greater consideration and merits much more detailed research. This work paves the way for future research projects such as cultivating "designer algae" via specifically tailored nutrient regimes, or genetic/bioengineering for specific biosorption purposes.

# Chapter 7
## Conclusions and future work

## 7.1 Conclusions

The main aim of this thesis was to investigate the potential of filamentous macro-algae for the removal of environmentally relevant nutrients and metals from synthetic wastewaters. In order to achieve this, several key objectives were formulated, as outlined below:

- To select suitable candidate species for algal bioremediation and perform an abiotic screen to assess their robustness and hence suitability for WWT purposes;
- To develop and standardise protocols for determining growth, nutrient removal, and biochemical composition of the algal biomass;
- To examine the influence of nutrient regime on algal growth, nutrient uptake, nitrogen preference, and biochemical composition;
- To examine the influence of nutritional history of algal biomass on metal biosorption.

In this work, *Cladophora* were selected for investigation into WWT as they are cosmopolitan and have a propensity to form algal blooms and are naturally dominant in nutrient enriched or eutrophic environments. In addition, *Cladophora* have a filamentous morphology which will reduce harvesting costs. Furthermore, *Cladophora* are regarded as robust, as they are highly persistent in nature and resistant to grazers and herbivory. These properties suggest that *Cladophora* may have potential applications in WWT. In Chapter 3, an abiotic screen was performed on *Cladophora coelothrix* and *Cladophora parriaudii*, in order to assess their tolerance and bioremediation performance under different environmental conditions which may be experienced in a variety of WWT scenarios. Both species of *Cladophora* exhibited good rates of growth (4 – 13.3% $d^{-1}$) and nitrate ($NO_3^-$) and phosphate ($PO_4^{3-}$) removal in the range of 45-99.9%, in the majority of treatments. This indicates that *Cladophora* may be suitable for treatment of a broad range of wastewater types. However, poor or negative rates of growth (-5.7 – 3.1% $d^{-1}$) and, consequently, nutrient removal (-30.2 – 23.4%) were observed under the most extreme treatments, *i.e.* pH 3, freshwater, and winter conditions. The results obtained under these treatments were unsurprising as the cultivation conditions were far-removed from what was considered "optimal": pH 8, 33.5 g $L^{-1}$ seawater, 24°C, and an 18/6 h L/D photoperiod (section 2.2.2). In order to improve the bioremediation capacity under these conditions, cultures could be selectively bred or acclimated to make them more tolerant, or artificial illumination or

heating, from anaerobic digestion or industrial cooling water,could be provided with the additional expense offset by the commercial value of the biomass produced. Alternatively, more appropriate species or strains could be selected, such as those naturally occurring in freshwater environments.

To facilitate literature comparison and ensure reliability, protocols used throughout this thesis were standardised for species specific use, details of which can be found in Chapter 2 and Appendices E-H. In addition, a method for the fresh weight (FW) determination of filamentous algae was developed and validated. The assessment of FW is one of the most basic aspects of phycological research used for the estimation of productivity. Yet, no standardised method exists which makes literature comparison problematic. The use of dry weight (DW) is commonly employed, however, this necessitates the sacrifice of biological samples and does not differentiate between viable and non-viable cultures. In Chapter 4, seven lab-scale FW methods were systematically assessed in terms of ease-of-use, accuracy and physiological impact upon three species of filamentous algae. Although the most stringent protocols tested, involving mechanical pressing, offered a high degree of accuracy, they also impacted upon the growth and viability of the organism with >25% reduction in the final DW yield. Whereas, low impact methods had a large error and were therefore unreliable for estimating productivity. The best method for FW determination employed a reticulated spinner which was operator-friendly, rapid, inexpensive, and easy to standardise. In addition, this approach had negligible impact upon the macro-algae tested, assessed in terms of the maintenance of structural integrity, rates of growth, and nutrient removal, all of which were comparable to control cultures. Furthermore, this method ensured an accurate estimation of DW across a time course, with predicted values a close approximation of the actual DW yields observed. A standardised method employing a reticulated spinner was subsequently used throughout the remaining experimental chapters of this work.

Wastewaters are highly dynamic environments, with a multitude of inter-related, variable parameters, including nutrient type and concentration. In Chapter 5, *C. coelothrix* and *C. parriaudii* were cultivated under different nutrient regimes, representative of different wastewaters, and their growth, nutrient uptake, nitrogen preference, and biochemical composition assessed. Nutrient regimes were formulated with four different nitrogen to phosphorus ratios (N/P), four different sources of N (ammonium, nitrate, nitrite, and urea),

and a total of six equimolar combinations of these N sources. There were clear differences in performance between both species of *Cladophora* tested. In all instances, both the nutrient uptake and daily growth rate (DGR) of *C. parriaudii* (4.75 – 11.2%) was greater than that of *C. coelothrix* (3.98 – 7.37%), with statistically significant differences in growth when either nitrite ($p = 0.025$) or urea ($p = 0.002$) were employed as the N source. In addition, there were differences in growth, within a species, when cultivated in media containing single- or dual-N sources ($p = 0.005$). Ammonium ($NH_4^+$) was preferentially removed by the algae, whereas urea was removed secondarily. However, the inclusion of urea in the medium consistently enhanced growth and uptake of other co-existing nitrogen forms. Furthermore, cultivation under different nutrient regimes influenced the final biochemical composition of the biomass, with the protein and carbohydrate content ranging from 5-15% DW and 36-54% DW, respectively. Overall, results from this chapter could lead to a paradigm shift in current algal cultivation practices towards utilisation of cheap and energetically efficient N sources, selection of bioremediating organism(s) for specific purposes, and indeed tailoring nutrient regimes to produce algae with certain characteristics for additional, commercial applications.

Algal biomass is viewed as a promising candidate for use as a sorbent material to remove and recover heavy metals from wastewaters. Algal biomass is renewable, abundant, inexpensive, has a large surface area with cellular properties that can adsorb metals. The majority of metal biosorption studies employing macro-algal biomass have used material from the field, grown in undefined conditions and of unknown biochemical status. In addition, these studies have centred upon optimising operational parameters, such as pH, temperature, and biosorbent dose, meanwhile biological aspects have been largely overlooked. The results obtained from Chapter 5 demonstrated that the biochemical composition of *C. parriaudii* biomass could be altered through cultivation under different nutrient regimes. The influence of these changes upon metal biosorption was examined in Chapter 6. Four types of metal were used in this study, selected for their varying degrees of toxicity, abundance in nature, and for their role within the cell. Six different nutrient regimes were used to produce *C. parriaudii* biomass with different cellular properties, the biomass was then characterised and used for biosorption purposes. Maximum metal removal rates ranged from 1.08-2.35 mmol $g^{-1}$, 0.3-0.62 mmol $g^{-1}$, 0.22-0.48 mmol $g^{-1}$, and 0.43-0.61 mmol $g^{-1}$ for $Al^{2+}$, $Cu^{2+}$, $Mn^{2+}$, and $Pb^{2+}$, respectively. However, there was no biomass type that consistently resulted in the greatest or least amount of metal removal.

Analysis of the cell surface of *C. parriaudii* using FTIR ATR and SEM BSE techniques demonstrated that functional groups associated with proteins, carbohydrates, and phosphate-containing compounds were involved in biosorption, and that metals bonded to the biomass in "clusters". Overall, the data suggests that there are several mechanisms involved in biosorption, including adsorption, complexation, ion exchange, and micro-precipitation. This means that simple, widely-used, adsorption models, which assume monolayer bonding, may have limited applicability in biosorption studies. The efficacy of specific metal biosorption is likely a function of both the type and quantity of functional groups present, which are in turn influenced by the nutrient regime in which the biomass was cultivated in. Therefore, properties of the biomass and the cultivation conditions should be given much greater attention than they currently receive in biosorption studies. Results from this study suggest that new avenues could be explored in this field, such as cultivating algae under tailored conditions, nutrient regimes, or using genetic/bioengineering tools to produce "designer" biomass for improved metal removal, or to target specific types of metals, *e.g.* precious metals.

## 7.2 Future Work

Observations from this body of work indicate that *Cladophora* has potential WWT applications. However, further research and development is necessary before *Cladophora* could realistically be considered for WWT implementation. Areas which merit further research have been identified on a chapter-by-chapter basis, followed by an overview of how *Cladophora* could be employed in practice.

### 7.2.1 Chapter 3 – Abiotic screen

More experimentation is required in order to understand, with greater confidence, the extent of potential WWT applications that both *C. coelothrix* and *C. parriaudii* may have. High-throughput experiments in multi-well plates, involving a broader range of pH and salinity, with greater resolution between data intervals could be performed. Similar to this, *Cladophora* cultures from this study could be "trained" to treat wastewaters that are out

with their natural habitat (*e.g.* freshwater), through acclimation, selective breeding, or genomic shuffling [489, 490]. However, selection of more suitable species may be a less time-consuming, stable, and viable solution for the treatment of those wastewater streams. Greater clarity on the influence of seasonal conditions (*e.g.* photoperiod, temperature, and light intensity) on algal biology and bioremediation performance could be achieved by cultivation in sophisticated environmental modelling photobioreactors [365]. Data obtained from this could be incorporated into behavioural models, which could be used on a real-time basis to predict algal bioremediation performance, based upon external conditions, and allow steps taken to ensure the continued health and performance of the culture (*e.g.* addition of lights, or cooling). This could help improve the year-round efficiency of algal WWT.

### 7.2.2 Chapter 4 – Fresh weight determination

In order to extend the applicability of the method developed for FW determination in Chapter 4, several approaches could be taken. Firstly, repeating the experiment with a broader range of algal taxa and with different structural forms. Secondly, implementation of this method on a larger scale could help realise the commercial potential of macro-algal cultivation, by improving productivity data and reducing processing costs associated with harvesting and dewatering biomass [146].

### 7.2.3 Chapter 5 – Nutrient regime

Results obtained in Chapter 5 demonstrated the influence of nutrient regime upon growth, nutrient uptake, N type preference and changes in the final biochemical content of the biomass. There are various aspects surrounding the nutrient regime, which if addressed, could add real value to algal cultivation practices.

Phosphorus is a major and essential nutrient for plant and algal growth, and is used extensively in agriculture. However, phosphorus is a finite resource, with mineral deposits expected to be exhausted within the next 50-100 years [491]. As a consequence of continuous demand and an uncertain supply of P, the cost of rock phosphorus continues to increase [492]. The reduction of P-fertiliser inputs into algal cultivation practices can only

improve its economic and commercial feasibility. This has stimulated interest into phosphorus recovery, using algal biomass, from wastewaters [493].

Furthermore, greater investigation into the mechanisms involved in nitrogen preference would be valuable. Experiments investigating the effect of N-type ratio may provide some insight into this area. In this work, equimolar combinations were used, and $NH_4^+$ was the favoured source of nitrogen in all instances. However, would this preference change if other less favoured co-existing N sources, such as urea, were supplied at greater concentrations? In addition, in this work, N combinations were supplied at the beginning of the growth trials; however, what effect would staggered N additions have? For instance, initial addition of $NO_3^-$, followed by $NH_4^+$ after a few days. Would the culture revert to an $NH_4^+$ preference, or would it continue to assimilate $NO_3^-$?

Finally, greater understanding of nutrient assimilation within the cell would be important for commercial applications. This could be achieved by measuring biochemical composition across a time course. Alternatively, isotope analysis could be used to determine resource partitioning within the cell [494, 495].

### 7.2.4 Chapter 6 - Biosorption

Observations from Chapter 6, and from the literature, have suggested that macro-algal biosorption is a complex process, with many mechanisms and factors influencing metal removal efficacy. Further experimentation into these mechanisms could make biosorption, as a whole, a more achievable reality. Repeated experimentation on *C. parriaudii* biomass with more metal types and concentrations, or utilising potentiometric titration coupled with FTIR [496], would improve our knowledge of the attractiveness of different functional groups to specific metals, and to the type of reactions involved (*e.g.* ion exchange, adsorption).

The biological aspect of biosorption has been largely overlooked; however, results from this thesis have indicated that cultivation conditions, specifically nutrient regime, can strongly influence the biochemical properties of biomass, and in turn its effectiveness as a biosorbent material. This could lead to a paradigm shift in approach to biosorption studies,

with focus upon tailoring nutrient regimes to influence biochemical and cell surface qualities. Some potential examples include:

- Cultivation of algal biomass in iron-enriched media. This could enhance rates of photosynthesis and growth [497], and may also improve metal biosorption through ion exchange mechanisms.
- Cultivation under different light regimes and/or additions of Mg and N to induce changes in biochemical composition and the expression or quantity of proteins and pigments [498].
- Measuring biosorption efficiency with algal biomass that has been cultivated in media with varying salinity. This may influence the biochemical content of the algae and hence their quality and quantity of functional groups. Alternatively, the concentration of salt, associated with the cell, will likely change and this may influence metal removal through ion exchange and micro-precipitation.
- Testing metal biosorption, specifically focussing on ion exchange, with diatoms due to the siliceous frustules [474]; with a possible investigation into different silicon additions in media formulations.
- Related to the above point is the possibility of incorporating elements, such as titanium or strontium, into algal biomass or diatomic frustules [499]. These may then have further WWT applications, such as advanced oxidation processes for the degradation of organic contaminants, for instance pharmaceuticals and hormones [500].
- Utilising living *Cladophora* biomass for biosorption. To overcome any potential toxic effects of cultivation in metal enriched environments, an acclimation programme could be implemented. Success in this area could then pave the way for a (semi-) continuous system for the concomitant removal of nutrients and metals from wastewater.

The realisation of algal biosorption may be more attainable through investigation into desorption. Selection of a robust or “designer” species that can maintain performance over multiple sorption/desorption cycles would be advantageous. This could lead to the recovery of precious or valuable metals from wastewaters, to improve their economic feasibility [427]. Additionally, algal biosorbents could be used to potentially treat emergent

contaminants such as hormones, pharmaceuticals, personal care products, dyes, and micro-plastics [501-503].

### 7.2.5 Wastewater treatment with *Cladophora* – the next step?

A holistic overview of this project demonstrates that *Cladophora* is relatively easy to harvest, extremely durable and tolerant to a range of abiotic conditions, has consistently high rates of growth and indiscriminate N removal, with a capacity for metal biosorption. Overall, this suggests that *Cladophora* has potential WWT applications; however, in order to greater understand the feasibility and suitability for incorporating filamentous macro-algae into WWT, the next step in this research would be to scale-up cultivation. Ideally, this would involve a small, pilot-scale system, operating on a continuous or semi-continuous basis, as represented in the schematic below (Fig. 7.1). *C. parriaudii* would be used to concomitantly remove nutrients and metals from real, or synthetically formulated, wastewaters. Real wastewaters may include, for example, effluents from aquaculture. In order to have greater control over waste outputs amid concerns about environmental impact and increasingly stringent discharge allowances, a growing number of aquaculture ventures are now based on land [504]. Initially, the wastewater influent would be directed into primary settling ponds or sedimentation tanks to reduce the total suspended solid (TSS) content [66]. After settling, the solid material could be transferred to, low-cost, but efficient, covered anaerobic ponds for anaerobic digestion (AD); coverting the solid waste into biogas and digestate (solid and liquid fractions), which could be used as a fertiliser [505, 506]. These ponds are deep, which facilitates sedimentation and digestion of solids to methane ($CH_4$) [370]. The ponds are covered which facilitates the collection of a potential source of bioenergy, in addition to preventing the release of odours and/or potentially harmful greenhouse gases [507, 508]. Depending upon the composition of the biogas collected (*e.g.* $CH_4/CO_2$ ratio), it could be used as a direct energy replacement for the WWT plant, with excess redirected to the grid [370]; however, it may need to be scrubbed and purified beforehand. Alternatively, $CO_2$ rich biogas could be sparged into the high-rate algal pond (HRAP) to enhance algal growth and control pH [509]. In addition, the HRAP may have $CO_2$ inputs from canisters or from flue gas [510].

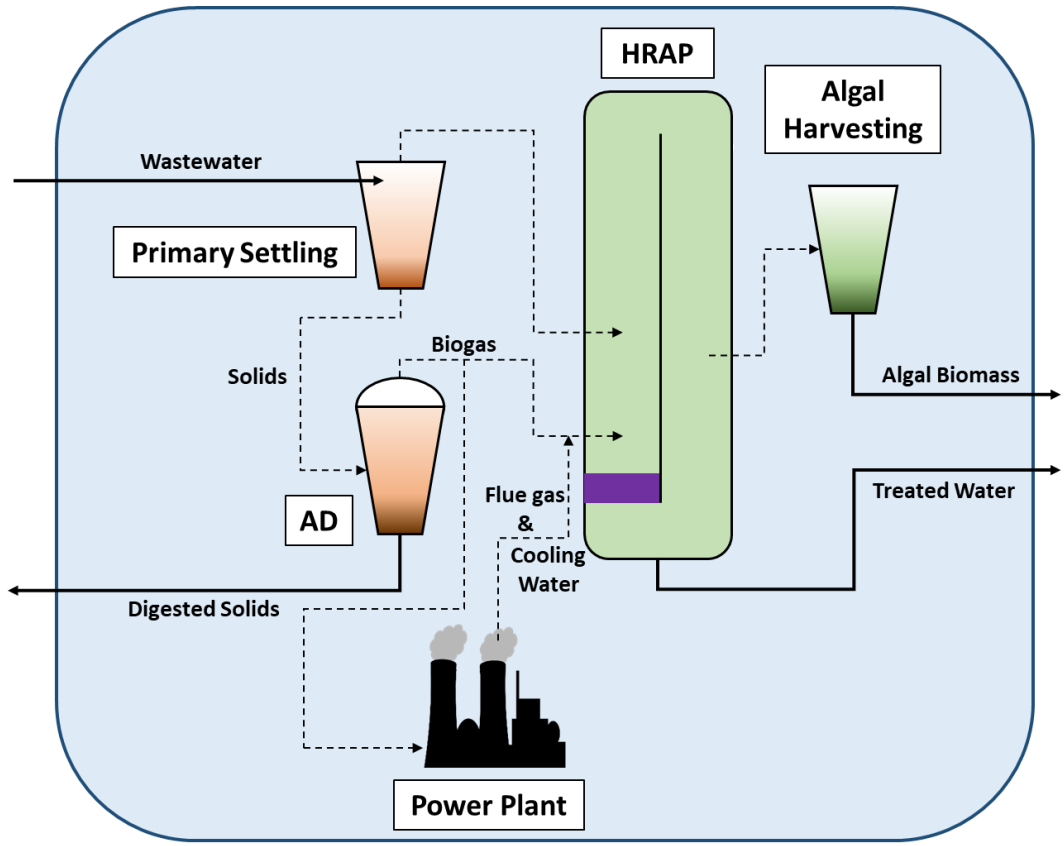


**Figure 7.1.** A schematic diagram of how *Cladophora* biomass could be employed for wastewater treatment in a high-rate algal pond (HRAP) scenario. AD = anaerobic digestion; purple rectangle = paddlewheel; broken lines denote the direction of resource flow within the system; solid lines represent resource inputs and outputs to and from the system.

The remainder of this hypothetical treatment system will focus upon algal treatment of wastewaters within a HRAP. System design and operational conditions are based on a pilot-scale HRAP described by Park and Craggs [398], coupled with algal productivity and nutrient removal values derived from experimental results obtained from this thesis. The HRAP employed by Park and Craggs [398] was a single-loop raceway, similar to that depicted in Fig. 7.1, with the following dimensions: surface area 31.8 $m^2$; depth 0.3 m; volume 8 $m^3$. Wastewater was fed into the system at 1 $m^3$ $d^{-1}$ resulting in a hydraulic retention time (HRT) of 8 days. Wastewater was circulated within the HRAP by the action of a paddlewheel [398]. The stocking density applied throughout this thesis was 714 mg FW $L^{-1}$ (section 2.2.2); however, this value is unfeasible for scaling-up to 8 $m^3$, as an inoculum of only 5.7 kg would be required. Instead, pilot-scale IMTA systems employing filamentous macro-algae have tested stocking densities of 2-7 kg $m^{-2}$, with best relative growth rates observed with 2 or 3

kg $m^{-2}$ [35, 175]. Applying these stocking densities in this system would translate into a total inoculum requirement of 63.6-95.4 kg FW, which is more realistic; however, preliminary trials could be performed to optimise the initial stocking density.

Conventional macro-algal practices involve long-line cultivation. Members of the kelp family and/or *Gracilaria* sp. are typically tied onto, interwoven, or seeded within the rope [511, 512]. Due to its relatively fragile and filamentous morphology, this type of cultivation may be unsuitable for *Cladophora* biomass. Perhaps a more appropriate method would be to utilise lantern nets, such as those used for the aquaculture of bivalve molluscs, including scallops [513]. Lantern nets are long, compartmentalised, cylindrical mesh structures [513], typically measuring 0.4 m in diameter and up to 2 m in length. These could be placed horizontally within the HRAP. Furthermore, the compartmental nature of the lantern nets has several potential benefits. For instance, ease of inoculation, allow algal productivity determination, and facilitate harvesting utilising a reticulated spinner (or a larger version), as discussed throughout Chapter 4 and section 7.2.2.

Hypothetical WWT performance data can be generated utilising results obtained from Chapter 5, where two species of *Cladophora* were independently cultivated under different nutrient regimes. However, the values mentioned below are based upon results obtained from carefully controlled near "optimal" cultivation conditions and are, in all likelihood, unattainable in practice. Furthermore, several broad assumptions have been made, including uniform growth and nutrient removal irrespective of season and stocking density, both of which can influence algal performance (section 1.4.1 and Chapter 3) [35, 164, 175]. Therefore, the values presented are more of an indication of how *C. parriaudii* can be applied in the "bigger picture", rather than a prediction of what could be achieved. The mean removal achieved by *C. parriaudii* across the 14-day study period was 42.9 ±11.2 µM N $d^{-1}$, and can be normalised against FW mass as 1.2 µM N mg FW $d^{-1}$. It should be noted, however, that data from the 2/1 N/P ratio were excluded as the cultures would have been nutrient limited and would underestimate removal rates. Applying this removal rate to a stocking density of 2-3 kg $m^{-2}$ for the HRAP system could hypothetically remove 9540-14310 µM N $d^{-1}$. The calculated removal rates are within range of the N concentration of aquaculture effluents cited in literature (50-124,900 µM N), meaning that *C. parriaudii* is potentially applicable for N removal purposes [14, 16, 33, 35, 40, 44, 45, 65, 66, 229]. Regardless of the rate of nutrient removal, the wastewater after passing through the HRAP

would most likely have to enter a final “polishing” or tertiary treatment step, such as a maturation pond or UV disinfection [370].

In terms of algal productivity, the mean DGR of *C. parriaudii* across all treatments, in Chapter 5, was 8.68 ±2.29 % $d^{-1}$. Therefore, a broad assumption is that 6% of the biomass could be harvested on a daily basis, without resulting in an appreciative net loss of the standing algal stock. This equates to a total daily biomass yield of 3.8-5.7 kg FW, or an annual production yield of 1,387-2,080 kg FW. More informed management based decisions, regarding the degree and frequency of harvesting, could be made based upon a standardised productivity assessment method employing a reticulated spinner (Chapter 4). The harvested material could act as a feedstock for a variety of purposes; however, the biochemical composition of the biomass may effectively determine its eventual fate. One possible option includes being fed back in to the AD system (Fig. 7.1). Alternatively, results obtained from Chapter 6 indicate that *C. parriaudii* is an effective biosorbent material for the removal of heavy/toxic metals. Therefore, the biomass could be dried and employed as a biosorbent material for the treatment of a variety of metal-laden effluents, including the whisky and mining wastewaters [413, 487, 488]. However, in order to determine the biosorbent dose required per unit volume of effluent containing specific metal species and concentrations, feasibility studies would need to be performed beforehand. This will give a better projection on the effective duration, or “shelf-life”, of the *C. parriaudii* biosorbent.

### 7.2.6 Concluding remarks

Wastewaters are incredibly complex environments, with a myriad of inter-related biological, chemical, and physical factors, all of which can influence algal biology, which in itself is a very complicated subject. Results obtained from this study, employing *Cladophora* biomass for treatment purposes were promising, generally exhibiting consistently good rates of growth, nutrient and metal removal and therefore has some potential and certainly merits further investigation. However, WWT is a multi-disciplinary subject and translation of algal-based systems into reality still requires a significant amount of further work. This necessitated input from biologists, chemists, civil and environmental engineers, and collaboration from economists, industrially relevant partners, research councils and funding bodies. Although this represents an enormous challenge, it is a fascinating topic which

holds a lot of promise, and as with all other technologies requires further study and maturation.

# References


[1] C.J. Vörösmarty, P.B. McIntyre, M.O. Gessner, D. Dudgeon, A. Prusevich, P. Green, S. Glidden, S.E. Bunn, C.A. Sullivan, C.R. Liermann, Global threats to human water security and river biodiversity, Nature. 467 (2010) 555-561.

[2] C.M. Crain, B.S. Halpern, M.W. Beck, C.V. Kappel, Understanding and managing human threats to the coastal marine environment, Ann. NY. Acad. Sci. 1162 (2009) 39-62.

[3] V.H. Smith, D.W. Schindler, Eutrophication science: where do we go from here?, Trends Ecol. Evol. 24 (2009) 201-207.

[4] N.N. Rabalais, R.E. Turner, W.J. Wiseman Jr, Gulf of Mexico hypoxia, aka "The dead zone", Annu. Rev. Ecol. Syst. 33 (2002) 235-263.

[5] R.J. Diaz, R. Rosenberg, Spreading dead zones and consequences for marine ecosystems, Science. 321 (2008) 926-929.

[6] D.J. Conley, J. Carstensen, J. Aigars, P. Axe, E. Bonsdorff, T. Eremina, B.-M. Haahti, C. Humborg, P. Jonsson, J. Kotta, Hypoxia is increasing in the coastal zone of the Baltic Sea, Environ. Sci. Technol. 45 (2011) 6777-6783.

[7] C. Bruning-Fann, J. Kaneene, The effects of nitrate, nitrite and N-nitroso compounds on human health: a review, Vet. Hum. Toxicol. 35 (1993) 521-538.

[8] European Commission, The EU water framework directive - integrated river basin management for Europe (2016) Accessed on: 07/07/2017, http://ec.europa.eu/environment/water/water-framework/index_en.html

[9] European Commission, The nitrates directive (2016) Accessed on: 20/06/2017, http://ec.europa.eu/environment/water/water-nitrates/index_en.html

[10] European Commission, Dangerous substances documentation (2016) Accessed on: 26/06/2017, http://ec.europa.eu/environment/water/water-dangersub/lib_dang_substances.htm

[11] M. Ottinger, K. Clauss, C. Kuenzer, Aquaculture: Relevance, distribution, impacts and spatial assessments – A review, Ocean Coast. Manage. 119 (2016) 244-266.

[12] Food and Agriculture Organization of the United Nations, Fishery statistical collections: Global capture production (2017) Accessed on: 06/04/2017, http://www.fao.org/fishery/statistics/global-capture-production/en

[13] Food and Agriculture Organization of the United Nations, Fishery statistical collections: Global aquaculture production (2017) Accessed on: 06/04/2017, http://www.fao.org/fishery/statistics/global-aquaculture-production/en

[14] S. Azman, M.I.M. Said, F. Ahmad, M. Mohamad, Biofiltration potential of macroalgae for ammonium removal in outdoor tank shrimp wastewater recirculation system, Biomass Bioenerg. 66 (2014) 103-109.

[15] J.S. Diana, Aquaculture production and biodiversity conservation, Bioscience. 59 (2009) 27-38.

[16] J. Aníbal, H.T. Madeira, L.F. Carvalho, E. Esteves, C. Veiga-Pires, C. Rocha, Macroalgae mitigation potential for fish aquaculture effluents: an approach coupling nitrogen uptake and metabolic pathways using *Ulva rigida* and *Enteromorpha clathrata*, Environ. Sci. Pollut. R. 21 (2014) 13324-13334.

[17] C.E. Boyd, Guidelines for aquaculture effluent management at the farm-level, Aquaculture. 226 (2003) 101-112.

[18] C.E. Boyd, D. Gautier, Effluent composition & water quality standards: Implementing GAA's responsible aquaculture program, The Advocate. (2000) 61-66.

[19] European Commission, On the application of the Water Framework Directive (WFD) and the Marine Strategy Framework Directive (MSFD) in relation to aquaculture (2016) Accessed on: 03/02/2018, https://ec.europa.eu/fisheries/sites/fisheries/files/docs/body/swd-2016-178_en.pdf
[20] E. Commission, Council Directive 91/271/EEC concerning urban waste-water treatment, (1991).
[21] J. Wang, C. Chen, Biosorbents for heavy metals removal and their future, Biotechnol. Adv. 27 (2009) 195-226.
[22] S.-L. Wang, X.-R. Xu, Y.-X. Sun, J.-L. Liu, H.-B. Li, Heavy metal pollution in coastal areas of South China: A review, Mar. Pollut. Bull. 76 (2013) 7-15.
[23] U. Förstner, G.T. Wittmann, Metal pollution in the aquatic environment, Springer Science & Business Media, 2012
[24] J. Duruibe, M. Ogwuegbu, J. Egwurugwu, Heavy metal pollution and human biotoxic effects, International Journal of Physical Sciences. 2 (2007) 112-118.
[25] J.P. Hoffmann, Wastewater treatment with suspended and nonsuspended algae, J. Phycol. 34 (1998) 757-763.
[26] Q.-X. Kong, L. Li, B. Martinez, P. Chen, R. Ruan, Culture of microalgae *Chlamydomonas reinhardtii* in wastewater for biomass feedstock production, Appl. Biochem. Biotech. 160 (2009) 9-18.
[27] J. Liu, W. Vyverman, Differences in nutrient uptake capacity of the benthic filamentous algae *Cladophora* sp., *Klebsormidium* sp. and *Pseudanabaena* sp. under varying N/P conditions, Bioresource Technol. 179 (2015) 234-242.
[28] United Nations Framework Convention on Climate Change, The Paris Agreement (2014) Accessed on: 11/07/2017, http://unfccc.int/paris_agreement/items/9485.php
[29] European Commission, Horizon 2020: The EU framework programme for research and innovation Accessed on: 11/07/2017, https://ec.europa.eu/programmes/horizon2020/
[30] United Nations Development Programme, Goal 6: Tagets (2017) Accessed on: 21/04/2017, http://www.undp.org/content/undp/en/home/sustainable-development-goals/goal-6-clean-water-and-sanitation/targets/
[31] C. Flora, R. Kröger, Use of vegetated drainage ditches and low-grade weirs for aquaculture effluent mitigation: I. Nutrients, Aquacult. Eng. 60 (2014) 56-62.
[32] Y.-F. Lin, S.-R. Jing, D.-Y. Lee, T.-W. Wang, Nutrient removal from aquaculture wastewater using a constructed wetlands system, Aquaculture. 209 (2002) 169-184.
[33] L. Hayashi, N.S. Yokoya, S. Ostini, R.T. Pereira, E.S. Braga, E.C. Oliveira, Nutrients removed by *Kappaphycus alvarezii* (Rhodophyta, Solieriaceae) in integrated cultivation with fishes in re-circulating water, Aquaculture. 277 (2008) 185-191.
[34] Z. Guo, Y. Liu, H. Guo, S. Yan, J. Mu, Microalgae cultivation using an aquaculture wastewater as growth medium for biomass and biofuel production, J. Environ. Sci. 25 (2013) S85-S88.
[35] M.H. Abreu, R. Pereira, C. Yarish, A.H. Buschmann, I. Sousa-Pinto, IMTA with *Gracilaria vermiculophylla*: Productivity and nutrient removal performance of the seaweed in a land-based pilot scale system, Aquaculture. 312 (2011) 77-87.
[36] M. von Ahnen, L.-F. Pedersen, P.B. Pedersen, J. Dalsgaard, Degradation of urea, ammonia and nitrite in moving bed biofilters operated at different feed loadings, Aquacult. Eng. 69 (2015) 50-59.

[37] F.E. Msuya, A. Neori, *Ulva reticulata* and *Gracilaria crassa*: macroalgae that can biofilter effluent from tidal fishponds in Tanzania, Western Indian Ocean J. Mar. Sci. 1 (2002) 117-126.
[38] J.M. Ebeling, P.L. Sibrell, S.R. Ogden, S.T. Summerfelt, Evaluation of chemical coagulation–flocculation aids for the removal of suspended solids and phosphorus from intensive recirculating aquaculture effluent discharge, Aquacult. Eng. 29 (2003) 23-42.
[39] M.J. Sharrer, Y. Tal, D. Ferrier, J.A. Hankins, S.T. Summerfelt, Membrane biological reactor treatment of a saline backwash flow from a recirculating aquaculture system, Aquacult. Eng. 36 (2007) 159-176.
[40] A.E. Ghaly, M. Kamal, N.S. Mahmoud, Phytoremediation of aquaculture wastewater for water recycling and production of fish feed, Environ. Int. 31 (2005) 1-13.
[41] E. Marinho-Soriano, C.A.A. Azevedo, T.G. Trigueiro, D.C. Pereira, M.A.A. Carneiro, M.R. Camara, Bioremediation of aquaculture wastewater using macroalgae and *Artemia*, Int. Biodeter. Biodegr. 65 (2011) 253-257.
[42] Y. Shi, G. Zhang, J. Liu, Y. Zhu, J. Xu, Performance of a constructed wetland in treating brackish wastewater from commercial recirculating and super-intensive shrimp growout systems, Bioresource Technol. 102 (2011) 9416-9424.
[43] F. Gao, C. Li, Z.-H. Yang, G.-M. Zeng, L.-J. Feng, J.-z. Liu, M. Liu, H.-w. Cai, Continuous microalgae cultivation in aquaculture wastewater by a membrane photobioreactor for biomass production and nutrients removal, Ecol. Eng. 92 (2016) 55-61.
[44] C. Lyles, R. Boopathy, Q. Fontenot, M. Kilgen, Biological treatment of shrimp aquaculture wastewater using a sequencing batch reactor, Appl. Biochem. Biotech. 151 (2008) 474.
[45] R. Boopathy, C. Bonvillain, Q. Fontenot, M. Kilgen, Biological treatment of low-salinity shrimp aquaculture wastewater using sequencing batch reactor, Int. Biodeter. Biodegr. 59 (2007) 16-19.
[46] The National Centres for Coastal Ocean Science, New report addresses re-eutrophication and hypoxia in Lake Erie (2014) Accessed on: 07/07/2017, https://coastalscience.noaa.gov/news/climate/new-report-addresses-re-eutrophication-hypoxia-lake-erie/
[47] J. Owen, National Geographic News: World's largest dead zone suffocating sea (2010) Accessed on: 07/07/2017, http://news.nationalgeographic.com/news/2010/02/100305-baltic-sea-algae-dead-zones-water/
[48] J.G. Day, S.P. Slocombe, M.S. Stanley, Overcoming biological constraints to enable the exploitation of microalgae for biofuels, Bioresource Technol. 109 (2012) 245-251.
[49] J.R. Benemann, Bio-fixation of $CO_2$ and greenhouse gas abatement with microalgae-technology roadmap, Final Report to the US Department of Energy. National Energy Technology Laboratory. (2003).
[50] T. Cai, S.Y. Park, Y. Li, Nutrient recovery from wastewater streams by microalgae: status and prospects, Renew. Sust. Energ. Rev. 19 (2013) 360-369.
[51] A.D. Hughes, K.D. Black, I. Campbell, K. Davidson, M.S. Kelly, M.S. Stanley, Does seaweed offer a solution for bioenergy with biological carbon capture and storage?, Greenhouse Gases: Science and Technology. 2 (2012) 402-407.
[52] A. Silkina, G.D. Nelson, C.E. Bayliss, C.L. Pooley, J.G. Day, Bioremediation efficacy—comparison of nutrient removal from an anaerobic digest waste-based medium by an algal consortium before and after cryopreservation, J. Appl. Phycol. 29 (2017) 1331-1341.

[53] R. Villares, X. Puente, A. Carballeira, *Ulva* and *Enteromorpha* as indicators of heavy metal pollution, Hydrobiologia. 462 (2001) 221-232.
[54] S. Kamala-Kannan, B. Prabhu Dass Batvari, K.J. Lee, N. Kannan, R. Krishnamoorthy, K. Shanthi, M. Jayaprakash, Assessment of heavy metals (Cd, Cr and Pb) in water, sediment and seaweed (*Ulva lactuca*) in the Pulicat Lake, South East India, Chemosphere. 71 (2008) 1233-1240.
[55] R. Muñoz, B. Guieysse, Algal–bacterial processes for the treatment of hazardous contaminants: A review, Water Res. 40 (2006) 2799-2815.
[56] T. Gumbricht, Nutrient removal processes in freshwater submersed macrophyte systems, Ecol. Eng. 2 (1993) 1-30.
[57] C. Johnstone, J. Day, H. Staines, E. Benson, An in vitro oxidative stress test for determining pollutant tolerance in algae, Ecological Indicators. 6 (2006) 770-779.
[58] J.M. Ayre, N.R. Moheimani, M.A. Borowitzka, Growth of microalgae on undiluted anaerobic digestate of piggery effluent with high ammonium concentrations, Algal Res. 24 (2017) 218-226.
[59] D.A. Roberts, N.A. Paul, M.I. Bird, R. de Nys, Bioremediation for coal-fired power stations using macroalgae, J. Environ. Manage. 153 (2015) 25-32.
[60] S. Sode, A. Bruhn, T.J. Balsby, M.M. Larsen, A. Gotfredsen, M.B. Rasmussen, Bioremediation of reject water from anaerobically digested waste water sludge with macroalgae (*Ulva lactuca*, Chlorophyta), Bioresource Technol. 146 (2013) 426-435.
[61] S. Aslan, I.K. Kapdan, Batch kinetics of nitrogen and phosphorus removal from synthetic wastewater by algae, Ecol. Eng. 28 (2006) 64-70.
[62] L. Christenson, R. Sims, Production and harvesting of microalgae for wastewater treatment, biofuels, and bioproducts, Biotechnol. Adv. 29 (2011) 686-702.
[63] J.J. Milledge, B.V. Nielsen, D. Bailey, High-value products from macroalgae: the potential uses of the invasive brown seaweed, *Sargassum muticum*, Reviews in Environmental Science and Bio/Technology. 15 (2016) 67-88.
[64] J.J. Silver, N.J. Gray, L.M. Campbell, L.W. Fairbanks, R.L. Gruby, Blue economy and competing discourses in international oceans governance, The Journal of Environment & Development. 24 (2015) 135-160.
[65] M. Jimenez del Rio, Z. Ramazanov, G. Garcia-Reina, *Ulva rigida* (Ulvales, Chlorophyta) tank culture as biofilters for dissolved inorganic nitrogen from fishpond effluents, Fifteenth International Seaweed Symposium, Springer, 1996, pp. 61-66.
[66] A. Jones, W. Dennison, N. Preston, Integrated treatment of shrimp effluent by sedimentation, oyster filtration and macroalgal absorption: a laboratory scale study, Aquaculture. 193 (2001) 155-178.
[67] S. Klimmek, H.-J. Stan, A. Wilke, G. Bunke, R. Buchholz, Comparative analysis of the biosorption of cadmium, lead, nickel, and zinc by algae, Environ. Sci. Technol. 35 (2001) 4283-4288.
[68] R.A. Andersen, The microalgal cell, in: A. Richmond, Q. Hu (Eds.) Handbook of microalgal culture, John Wiley & Sons, Ltd, 2013, pp. 1-20.
[69] G.R. South, A. Whittick, An Introduction to Phycology, John Wiley & Sons, 2009
[70] S. Malviya, E. Scalco, S. Audic, F. Vincent, A. Veluchamy, J. Poulain, P. Wincker, D. Iudicone, C. de Vargas, L. Bittner, Insights into global diatom distribution and diversity in the world's ocean, Proceedings of the National Academy of Sciences. 113 (2016) E1516-E1525.
[71] C. de Vargas, S. Audic, N. Henry, J. Decelle, F. Mahé, R. Logares, E. Lara, C. Berney, N. Le Bescot, I. Probert, M. Carmichael, J. Poulain, S. Romac, S. Colin, J.-M. Aury, L.

Bittner, S. Chaffron, M. Dunthorn, S. Engelen, O. Flegontova, L. Guidi, A. Horák, O. Jaillon, G. Lima-Mendez, J. Lukeš, S. Malviya, R. Morard, M. Mulot, E. Scalco, R. Siano, F. Vincent, A. Zingone, C. Dimier, M. Picheral, S. Searson, S. Kandels-Lewis, S.G. Acinas, P. Bork, C. Bowler, G. Gorsky, N. Grimsley, P. Hingamp, D. Iudicone, F. Not, H. Ogata, S. Pesant, J. Raes, M.E. Sieracki, S. Speich, L. Stemmann, S. Sunagawa, J. Weissenbach, P. Wincker, E. Karsenti, Eukaryotic plankton diversity in the sunlit ocean, Science. 348 (2015).

[72] C. Hoek, D. Mann, H.M. Jahns, Algae: an introduction to phycology, Cambridge university press, 1995

[73] H. Bold, M. Wynne, Introduction to the Algae. Structure and reproduction. 720 p. Ed, Prentice Hall, Englewood Cliffs, 1985

[74] R.A. Andersen, Diversity of eukaryotic algae, Biodiversity & Conservation. 1 (1992) 267-292.

[75] D. Sahoo, P. Baweja, General Characteristics of Algae, in: D. Sahoo, J. Seckbach (Eds.) The Algae World, Springer, London, 2015.

[76] T. Leya, A. Rahn, C. Lütz, D. Remias, Response of arctic snow and permafrost algae to high light and nitrogen stress by changes in pigment composition and applied aspects for biotechnology, FEMS Microbiol. Ecol. 67 (2009) 432-443.

[77] J. Seckbach, The first eukaryotic cells — Acid hot-spring algae, J. Biol. Phys. 20 (1995) 335-345.

[78] F.E. Round, Biology of the Algae, Biology of the algae, Arnold, 1970.

[79] L.A. Lewis, P.O. Lewis, Unearthing the molecular phylodiversity of desert soil green algae (Chlorophyta), Syst. Biol. 54 (2005) 936-947.

[80] D. Chapman, The algae, Springer, 1973

[81] K.S. Rowan, Photosynthetic pigments of algae, CUP Archive, 1989

[82] A. Salguero, B. de la Morena, J. Vigara, J.M. Vega, C. Vilchez, R. León, Carotenoids as protective response against oxidative damage in *Dunaliella bardawil*, Biomol. Eng. 20 (2003) 249-253.

[83] AlgaeBase, (2017) Accessed on: 05/04/2017, http://www.algaebase.org/

[84] Culture Collection of Algae and Protozoa, Our cultures (2014) Accessed on: 05/04/2017, https://www.ccap.ac.uk/our-cultures.htm

[85] T. Lincoln, Kelp in postglacial time, Nature. 461 (2009) 1066.

[86] W.L. Zemke-White, M. Ohno, World seaweed utilisation: an end-of-century summary, J. Appl. Phycol. 11 (1999) 369-376.

[87] M.A. Borowitzka, Commercial production of microalgae: ponds, tanks, tubes and fermenters, J. Biotechnol. 70 (1999) 313-321.

[88] M.A. Borowitzka, High-value products from microalgae—their development and commercialisation, J. app. Phycol. 25 (2013) 743-756.

[89] P. McEvansoneya, Aloysius O'Kelly: art, nation, empire, Taylor & Francis, 2011.

[90] G. Kenicer, S. Bridgewater, W. Milliken, The ebb and flow of Scottish seaweed use, Botanical Journal of Scotland. 52 (2000) 119-148.

[91] D. Aitken, B. Antizar-Ladislao, Achieving a green solution: limitations and focus points for sustainable algal fuels, Energies 5(2012) 1613-1647.

[92] D.-G. Kim, J. Park, D. Lee, H. Kang, Removal of nitrogen and phosphorus from effluent of a secondary wastewater treatment plant using a pond–marsh wetland system, Water Air Soil Poll. 214 (2011) 37-47.

[93] R. Craggs, S. Heubeck, T. Lundquist, J. Benemann, Algal biofuels from wastewater treatment high rate algal ponds, Water Sci. Technol. 63 (2011) 660-665.

[94] C.G. Golueke, W.J. Oswald, H.B. Gotaas, Anaerobic digestion of algae, Applied Microbiology. 5 (1957) 47-55.

[95] C.G. Golueke, W.J. Oswald, Power from solar energy—Via algae-produced methane, Sol. Energy. 7 (1963) 86-92.
[96] W. Oswald, H. Gotaas, C. Golueke, W. Kellen, E. Gloyna, E. Hermann, Algae in waste treatment Sewage and Industrial Wastes. 29 (1957) 437-457.
[97] T.J. Lundquist, I.C. Woertz, N. Quinn, J.R. Benemann, A realistic technology and engineering assessment of algae biofuel production, Energy Biosciences Institute. (2010) 1-178.
[98] T. McMahon, Historical crude oil prices (Table) (2015) Accessed on: 05/04/2017, https://inflationdata.com/inflation/inflation_rate/Historical_Oil_Prices_Table.asp
[99] Science Direct, (2017) Accessed on: 05/04/2017, http://www.sciencedirect.com/
[100] A. Demirbas, Use of algae as biofuel sources, Energ. Convers. Manage. 51 (2010) 2738-2749.
[101] D.R. Georgianna, S.P. Mayfield, Exploiting diversity and synthetic biology for the production of algal biofuels, Nature. 488 (2012) 329-335.
[102] Y. Chisti, Biodiesel from microalgae, Biotechnol. Adv. 25 (2007) 294-306.
[103] P. Schiener, K.D. Black, M.S. Stanley, D.H. Green, The seasonal variation in the chemical composition of the kelp species *Laminaria digitata*, *Laminaria hyperborea*, *Saccharina latissima* and *Alaria esculenta*, J. App. Phycol. 27 (2015) 363-373.
[104] P. Yazdani, K. Karimi, M.J. Taherzadeh, Improvement of enzymatic hydrolysis of a marine macro-alga by dilute acid hydrolysis pretreatment, World Renewable Energy Congress-Sweden; 8-13 May; 2011; Linköping; Sweden, Linköping University Electronic Press, 2011, pp. 186-191.
[105] J. Adams, T. Toop, I.S. Donnison, J.A. Gallagher, Seasonal variation in *Laminaria digitata* and its impact on biochemical conversion routes to biofuels, Bioresource Technol. 102 (2011) 9976-9984.
[106] S. Horn, I. Aasen, K. Østgaard, Ethanol production from seaweed extract, J. Ind. Microbiol. Biot. 25 (2000) 249-254.
[107] M. Yanagisawa, K. Nakamura, O. Ariga, K. Nakasaki, Production of high concentrations of bioethanol from seaweeds that contain easily hydrolyzable polysaccharides, Process Biochem. 46 (2011) 2111-2116.
[108] J.-S. Jang, Y. Cho, G.-T. Jeong, S.-K. Kim, Optimization of saccharification and ethanol production by simultaneous saccharification and fermentation (SSF) from seaweed, *Saccharina japonica*, Bioprocess and Biosystems Engineering. 35 (2012) 11-18.
[109] T.M. Mata, A.A. Martins, N.S. Caetano, Microalgae for biodiesel production and other applications: A review, Renewable and Sustainable Energy Reviews. 14 (2010) 217-232.
[110] J.A. Mathews, How carbon credits could drive the emergence of renewable energies, Energ. Policy. 36 (2008) 3633-3639.
[111] R.H. Wijffels, M.J. Barbosa, An outlook on microalgal biofuels, Science. 329 (2010) 796-799.
[112] J. Singh, S. Gu, Commercialization potential of microalgae for biofuels production, Renew. Sust. Energ. Rev. 14 (2010) 2596-2610.
[113] L. Gouveia, From tiny microalgae to huge biorefineries, Oceanography. 2 (2014) 2.
[114] L. Kilian, The impact of the shale oil revolution on US oil and gasoline prices, Review of Environmental Economics and Policy. 10 (2016) 185-205.
[115] A.J. Smit, Medicinal and pharmaceutical uses of seaweed natural products: A review, J. Appl. Phycol. 16 (2004) 245-262.
[116] R. Raja, S. Hemaiswarya, R. Rengasamy, Exploitation of *Dunaliella* for β-carotene production, Appl. Microbiol. Biot. 74 (2007) 517-523.

[117] F.A. Reyes, J.A. Mendiola, E. Ibañez, J.M. del Valle, Astaxanthin extraction from *Haematococcus pluvialis* using CO2-expanded ethanol, J. Supercrit. Fluid. 92 (2014) 75-83.
[118] M. Guerin, M.E. Huntley, M. Olaizola, *Haematococcus* astaxanthin: applications for human health and nutrition, Trends Biotechnol. 21 (2003) 210-216.
[119] S. Hoseini, K. Khosravi-Darani, M. Mozafari, Nutritional and Medical Applications of Spirulina Microalgae, Mini-Reviews in Medicinal Chemistry. 13 (2013) 1231-1237.
[120] M.A. Borowitzka, High-value products from microalgae--their development and commercialisation, Journal of applied phycology. 25 (2013) 743.
[121] S. Hemaiswarya, R. Raja, R. Ravi Kumar, V. Ganesan, C. Anbazhagan, Microalgae: a sustainable feed source for aquaculture, World J. Microb. Biot. 27 (2011) 1737-1746.
[122] V. Patil, T. Källqvist, E. Olsen, G. Vogt, H.R. Gislerød, Fatty acid composition of 12 microalgae for possible use in aquaculture feed, Aquacult. Int. 15 (2007) 1-9.
[123] P. Spolaore, C. Joannis-Cassan, E. Duran, A. Isambert, Commercial applications of microalgae, J. Biosci. Bioeng. 101 (2006) 87-96.
[124] L.E.C. Conceição, M. Yúfera, P. Makridis, S. Morais, M.T. Dinis, Live feeds for early stages of fish rearing, Aquac. Res. 41 (2010) 613-640.
[125] I. Priyadarshani, B. Rath, Commercial and industrial applications of micro algae–A review, J. Algal Biomass Utln. 3 (2012) 89-100.
[126] Alga Technologies, Accessed on: 30/06/2017, https://www.algatech.com/
[127] J.J. Milledge, Commercial application of microalgae other than as biofuels: a brief review, Reviews in Environmental Science and Bio/Technology. 10 (2011) 31-41.
[128] SBS Murdoch University, Biotechnological and Environmental Applications of Microalgae: Large-scale algal cultivation systems (2011) Accessed on: 30/06/2017, http://www.bsb.murdoch.edu.au/groups/beam/BEAM-Appl4a.html
[129] D.J. McHugh, A guide to the seaweed industry, Food and Agriculture Organization of the United Nations Rome, 2003
[130] D.J. McHugh, Production, properties and uses of alginates, Production and Utilization of Products from Commercial Seaweeds. FAO. Fish. Tech. Pap. 288 (1987) 58-115.
[131] C.K. Tseng, Algal biotechnology industries and research activities in China, J. Appl. Phycol. 13 (2001) 375-380.
[132] J. Fike, V. Allen, R. Schmidt, X. Zhang, J. Fontenot, C. Bagley, R. Ivy, R. Evans, R. Coelho, D. Wester, Tasco-Forage: I. Influence of a seaweed extract on antioxidant activity in tall fescue and in ruminants, J. Anim. Sci. 79 (2001) 1011-1021.
[133] S. Sharma, C. Fleming, C. Selby, J. Rao, T. Martin, Plant biostimulants: a review on the processing of macroalgae and use of extracts for crop management to reduce abiotic and biotic stresses, J. Appl. Phycol. 26 (2014) 465-490.
[134] S. Mattner, D. Wite, D. Riches, I. Porter, T. Arioli, The effect of kelp extract on seedling establishment of broccoli on contrasting soil types in southern Victoria, Australia, Biol. Agric. Hortic. 29 (2013) 258-270.
[135] J.T. Hafting, A.T. Critchley, M.L. Cornish, S.A. Hubley, A.F. Archibald, On-land cultivation of functional seaweed products for human usage, J. Appl. Phycol. 24 (2012) 385-392.
[136] H.-M.D. Wang, C.-C. Chen, P. Huynh, J.-S. Chang, Exploring the potential of using algae in cosmetics, Bioresource Technol. 184 (2015) 355-362.
[137] M.L. Wells, P. Potin, J.S. Craigie, J.A. Raven, S.S. Merchant, K.E. Helliwell, A.G. Smith, M.E. Camire, S.H. Brawley, Algae as nutritional and functional food sources: revisiting our understanding, J. Appl. Phycol. 29 (2017) 949-982.

[138] T.L. da Silva, L. Gouveia, A. Reis, Integrated microbial processes for biofuels and high value-added products: the way to improve the cost effectiveness of biofuel production, Appl. Microbiol. Biot. 98 (2014) 1043-1053.
[139] M. landscapes, Seaweed farms (2009) Accessed on: 21/04/2017, http://pcgladiator.blogspot.co.uk/2009/03/seaweed-farms.html
[140] A. Malik, Metal bioremediation through growing cells, Environ. Int. 30 (2004) 261-278.
[141] R.J. Lawton, R. de Nys, N.A. Paul, Selecting reliable and robust freshwater macroalgae for biomass applications, PloS one. 8 (2013) e64168.
[142] S.K. Mehta, J.P. Gaur, Use of algae for removing heavy metal ions from wastewater: progress and prospects, Crit. Rev. Biotechnol. 25 (2005) 113-152.
[143] G.M. Gadd, Biosorption: critical review of scientific rationale, environmental importance and significance for pollution treatment, J. Chem. Technol. Biot. 84 (2009) 13-28.
[144] B. Henriques, L.S. Rocha, C.B. Lopes, P. Figueira, A.C. Duarte, C. Vale, M.A. Pardal, E. Pereira, A macroalgae-based biotechnology for water remediation: Simultaneous removal of Cd, Pb and Hg by living *Ulva lactuca*, J. Environ. Manage. 191 (2017) 275-289.
[145] D. Chiaramonti, K. Maniatis, M. Tredici, V. Verdelho, J. Yan, Life cycle assessment of algae biofuels: needs and challenges, Appl. Energ. 154 (2015) 1049-1051.
[146] P.E. Wiley, J.E. Campbell, B. McKuin, Production of biodiesel and biogas from algae: a review of process train options, Water Environ. Res. 83 (2011) 326-338.
[147] J.K. Pittman, A.P. Dean, O. Osundeko, The potential of sustainable algal biofuel production using wastewater resources, Bioresource Technol. 102 (2011) 17-25.
[148] C.L. Hurd, P.J. Harrison, K. Bischof, C.S. Lobban, Seaweed ecology and physiology, Cambridge University Press, 2014
[149] G. Roesijadi, S.B. Jones, L.J. Snowden-Swan, Y. Zhu, Macroalgae as a biomass feedstock: a preliminary analysis, Pacific Northwest National Laboratory (PNNL), Richland, WA (US), 2010.
[150] W. Grayburn, R. Tatara, K.A. Rosentrater, G. Holbrook, Harvesting, oil extraction, and conversion of local filamentous algae growing in wastewater into biodiesel, International Journal of Energy and Environment. 4 (2013) 185.
[151] W. Mulbry, P. Kangas, S. Kondrad, Toward scrubbing the bay: Nutrient removal using small algal turf scrubbers on Chesapeake Bay tributaries, Ecol. Eng. 36 (2010) 536-541.
[152] C. Pizarro, W. Mulbry, D. Blersch, P. Kangas, An economic assessment of algal turf scrubber technology for treatment of dairy manure effluent, Ecol. Eng. 26 (2006) 321-327.
[153] K.K. Sharma, S. Garg, Y. Li, A. Malekizadeh, P.M. Schenk, Critical analysis of current microalgae dewatering techniques, Biofuels. 4 (2013) 397-407.
[154] T.M. Mata, A.A. Martins, N.S. Caetano, Microalgae for biodiesel production and other applications: a review, Renew. Sust. Energ. Rev. 14 (2010) 217-232.
[155] L. Mata, M. Magnusson, N.A. Paul, R. de Nys, The intensive land-based production of the green seaweeds *Derbesia tenuissima* and *Ulva ohnoi*: biomass and bioproducts, J. Appl. Phycol. 28 (2016) 365-375.
[156] J.C. Phillips, C.L. Hurd, Kinetics of nitrate, ammonium, and urea uptake by four intertidal seaweeds from New Zealand, J. Phycol. 40 (2004) 534-545.
[157] D. Dominguez, W. Gujer, Evolution of a wastewater treatment plant challenges traditional design concepts, Water Res. 40 (2006) 1389-1396.
[158] F. Rendell, Water and wastewater project development, Thomas Telford, 1999

[159] M. Von Sperling, Wastewater characteristics, treatment and disposal, IWA publishing, 2007
[160] C. Wang, A. Lei, K. Zhou, Z. Hu, W. Hao, J. Yang, Growth and nitrogen uptake characteristics reveal outbreak mechanism of the opportunistic macroalga *Gracilaria tenuistipitata*, PloS One. 9 (2014) e108980.
[161] P.J. Harrison, C.L. Hurd, Nutrient physiology of seaweeds: application of concepts to aquaculture, Cah. Biol. Mar. 42 (2001) 71-82.
[162] M.F. Pedersen, Transient ammonium uptake in the macroalga *Ulva lactuta* (Chlorophyta): Nature, regulation, and the consequences for choice of measuring technique, J. Phycol. 30 (1994) 980-986.
[163] J. Park, R. Craggs, A. Shilton, Wastewater treatment high rate algal ponds for biofuel production, Bioresource Technol. 102 (2011) 35-42.
[164] W.T.L. Yong, S.H. Ting, Y.S. Yong, V.Y. Thien, S.H. Wong, W.L. Chin, K.F. Rodrigues, A. Anton, Optimization of culture conditions for the direct regeneration of *Kappaphycus alvarezii* (Rhodophyta, Solieriaceae), J. Appl. Phycol. 26 (2014) 1597-1606.
[165] P. Peckol, B. DeMeo-Anderson, J. Rivers, I. Valiela, M. Maldonado, J. Yates, Growth, nutrient uptake capacities and tissue constituents of the macroalgae *Cladophora vagabunda* and *Gracilaria tikvahiae* related to site-specific nitrogen loading rates, Mar. Biol. 121 (1994) 175-185.
[166] B.-P. Han, A mechanistic model of algal photoinhibition induced by photodamage to photosystem-II, J. Theor. Biol. 214 (2002) 519-527.
[167] S. Long, S. Humphries, P.G. Falkowski, Photoinhibition of photosynthesis in nature, Annual Review of Plant Biology. 45 (1994) 633-662.
[168] X. Fan, D. Xu, Y. Wang, X. Zhang, S. Cao, S. Mou, N. Ye, The effect of nutrient concentrations, nutrient ratios and temperature on photosynthesis and nutrient uptake by *Ulva prolifera*: implications for the explosion in green tides, J. App. Phycol. 26 (2014) 537-544.
[169] A. Abeliovich, Y. Azov, Toxicity of ammonia to algae in sewage oxidation ponds, Appl. Environ. Microb. 31 (1976) 801-806.
[170] J.A. Berges, D.E. Varela, P.J. Harrison, Effects of temperature on growth rate, cell composition and nitrogen metabolism in the marine diatom *Thalassiosira pseudonana* (Bacillariophyceae), Mar. Ecol-Prog. Ser. 225 (2002) 139-146.
[171] J.A. Raven, R.J. Geider, Temperature and algal growth, New Phytol. 110 (1988) 441-461.
[172] T.S. Choi, E.J. Kang, J.-h. Kim, K.Y. Kim, Effect of salinity on growth and nutrient uptake of *Ulva pertusa* (Chlorophyta) from an eelgrass bed, Algae. 25 (2010) 17-26.
[173] O. Benjama, P. Masniyom, Nutritional composition and physicochemical properties of two green seaweeds (*Ulva pertusa* and *U. intestinalis*) from the Pattani Bay in Southern Thailand, Sonklanakarin Journal of Science and Technology. 33 (2011) 575.
[174] Z. Wu, W. Dejtisakdi, P. Kermanee, C. Ma, W. Arirob, R. Sathasivam, N. Juntawong, Outdoor cultivation of *Dunaliella salina* KU 11 using brine and saline lake water with race-way ponds in northeastern Thailand, Biotechnol. Appl. Bioc. (2016).
[175] A. Neori, I. Cohen, H. Gordin, *Ulva lactuca* biofilters for marine fishpond effluents. II. Growth rate, yield and C: N ratio, Bot. Mar. 34 (1991) 483-490.
[176] M. Kumar, V. Gupta, N. Trivedi, P. Kumari, A.J. Bijo, C.R.K. Reddy, B. Jha, Desiccation induced oxidative stress and its biochemical responses in intertidal red alga *Gracilaria corticata* (Gracilariales, Rhodophyta), Environ. Exp. Bot. 72 (2011) 194-201.

[177] A. Holzinger, K. Herburger, F. Kaplan, L.A. Lewis, Desiccation tolerance in the chlorophyte green alga *Ulva compressa*: does cell wall architecture contribute to ecological success?, Planta. 242 (2015) 477-492.
[178] T. Thomas, P. Harrison, D. Turpin, Adaptations of *Gracilaria pacifica* (Rhodophyta) to nitrogen procurement at different intertidal locations, Mar. Biol. 93 (1987) 569-580.
[179] T. Thomas, D. Turpin, Desiccation enhanced nutrient uptake rates in the intertidal alga *Fucus distichus*, Bot. Mar. (1980).
[180] M.E. Bracken, J.J. Stachowicz, Seaweed diversity enhances nitrogen uptake via complementary use of nitrate and ammonium, Ecology. 87 (2006) 2397-2403.
[181] M.F. Pedersen, J. Borum, Nutrient control of estuarine macroalgae: growth strategy and the balance between nitrogen requirements and uptake, Mar. Ecol-Prog. Ser. 161 (1997) 155-163.
[182] J.A. Raven, R. Taylor, Macroalgal growth in nutrient-enriched estuaries: a biogeochemical and evolutionary perspective, Water Air Soil Poll. 3 (2003) 7-26.
[183] M. Hein, M.F. Pedersen, K. Sand-Jensen, Size-dependent nitrogen uptake in micro- and macroalgae, Mar. Ecol-Prog. Ser. 118 (1995) 247-253.
[184] D.T. Dy, H.T. Yap, Surge ammonium uptake of the cultured seaweed, *Kappaphycus alvarezii* (Doty) Doty (Rhodophyta: Gigartinales), J. Exp. Mar. Biol. Ecol. 265 (2001) 89-100.
[185] J. Bolton, D. Robertson-Andersson, D. Shuuluka, L. Kandjengo, Growing *Ulva* (Chlorophyta) in integrated systems as a commercial crop for abalone feed in South Africa: a SWOT analysis, J. App. Phycol. 21 (2009) 575-583.
[186] S.B. Zulkifly, J.M. Graham, E.B. Young, R.J. Mayer, M.J. Piotrowski, I. Smith, L.E. Graham, The genus *Cladophora* Kützing (Ulvophyceae) as a globally distributed ecological engineer, J. Phycol. 49 (2013) 1-17.
[187] R. Patrick, C.F. Rhyne, R.W. Richardson, R.A. Larson, T.L. Bott, K. Rogenmuser, The potential for biological controls of *Cladophora glomerata*, US Environmental Protection Agency, Office of Research and Development, Environmental Research Laboratory, 1983
[188] I. Wallentinus, Comparisons of nutrient uptake rates for Baltic macroalgae with different thallus morphologies, Mar. Biol. 80 (1984) 215-225.
[189] M.B. Luo, F. Liu, Z.L. Xu, Growth and nutrient uptake capacity of two co-occurring species, *Ulva prolifera* and *Ulva linza*, Aquat. Bot. 100 (2012) 18-24.
[190] V. Perini, M.E.S. Bracken, Nitrogen availability limits phosphorus uptake in an intertidal macroalga, Oecologia. 175 (2014) 667-676.
[191] J.J. Mayers, K.J. Flynn, R.J. Shields, Influence of the N: P supply ratio on biomass productivity and time-resolved changes in elemental and bulk biochemical composition of *Nannochloropsis* sp, Bioresource Technol. 169 (2014) 588-595.
[192] M.H. Abreu, R. Pereira, A. Buschmann, I. Sousa-Pinto, C. Yarish, Nitrogen uptake responses of *Gracilaria vermiculophylla* (Ohmi) Papenfuss under combined and single addition of nitrate and ammonium, J. Exp. Mar. Biol. Ecol. 407 (2011) 190-199.
[193] M.T. Ale, J.D. Mikkelsen, A.S. Meyer, Differential growth response of *Ulva lactuca* to ammonium and nitrate assimilation, J. App. Phycol. 23 (2011) 345-351.
[194] C.M. Solomon, P.M. Glibert, Urease activity in five phytoplankton species, Aquat. Microb. Ecol. 52 (2008) 149-157.
[195] P. Syrett, J. Leftley, Nitrate and urea assimilation by algae, in: N. Sunderland, E. Simon, J. Heslop-Harrison, P. Brian, D. Boulter (Eds.) Perspectives in experimental biology, Pergamon Press, Oxford, UK, 2016, pp. 221-234.

[196] P. Corey, J.K. Kim, J. Duston, D.J. Garbary, B. Prithiviraj, Bioremediation potential of *Palmaria palmata* and *Chondrus crispus* (Basin Head): effect of nitrate and ammonium ratio as nitrogen source on nutrient removal, J. Appl. Phycol. 25 (2013) 1349-1358.
[197] M. Ohmori, K. Ohmori, H. Strotmann, Inhibition of nitrate uptake by ammonia in a blue-green alga, *Anabaena cylindrica*, Arch. Microbiol. 114 (1977) 225-229.
[198] A. Smit, Nitrogen uptake by *Gracilaria gracilis* (Rhodophyta): adaptations to a temporally variable nitrogen environment, Bot. Mar. 45 (2002) 196-209.
[199] J.A. Raven, B. Wollenweber, L.L. Handley, A comparison of ammonium and nitrate as nitrogen sources for photolithotrophs, New Phytol. 121 (1992) 19-32.
[200] B. Song, B.B. Ward, Molecular characterization of the assimilatory nitrate reductase gene and its expression in the marine green alga *Dunaliella tertiolecta* (Chlorophyceae), J. Phycol. 40 (2004) 721-731.
[201] M. Atkinson, S. Smith, C: N: P ratios of benthic marine plants, Limnol. Oceanogr. 28 (1983) 568-574.
[202] A.C. Redfield, The biological control of chemical factors in the environment, Am. Sci. 46 (1958) 205-221.
[203] P. Tett, M. Droop, S. Heaney, The Redfield ratio and phytoplankton growth rate, J. Mar. Biol. Assoc. UK. 65 (1985) 487-504.
[204] C.C. Cleveland, D. Liptzin, C:N:P stoichiometry in soil: is there a “Redfield ratio” for the microbial biomass?, Biogeochemistry. 85 (2007) 235-252.
[205] J. Adams, A.á. Ross, K. Anastasakis, E. Hodgson, J. Gallagher, J. Jones, I. Donnison, Seasonal variation in the chemical composition of the bioenergy feedstock *Laminaria digitata* for thermochemical conversion, Bioresource Technol. 102 (2011) 226-234.
[206] H.R. Fletcher, P. Biller, A.B. Ross, J.M.M. Adams, The seasonal variation of fucoidan within three species of brown macroalgae, Algal Res. 22 (2017) 79-86.
[207] M. Piorreck, K.-H. Baasch, P. Pohl, Biomass production, total protein, chlorophylls, lipids and fatty acids of freshwater green and blue-green algae under different nitrogen regimes, Phytochemistry. 23 (1984) 207-216.
[208] B.E. Lapointe, J. O'Connell, Nutrient-enhanced growth of *Cladophora prolifera* in Harrington Sound, Bermuda: eutrophication of a confined, phosphorus-limited marine ecosystem, Estuar. Coast. Shelf S. 28 (1989) 347-360.
[209] S. Myklestad, A. Haug, Production of carbohydrates by the marine diatom *Chaetoceros affinis* var. willei (Gran) Hustedt. I. Effect of the concentration of nutrients in the culture medium, J. Exp. Mar. Biol. Ecol. 9 (1972) 125-136.
[210] L. Xin, H. Hong-ying, G. Ke, S. Ying-xue, Effects of different nitrogen and phosphorus concentrations on the growth, nutrient uptake, and lipid accumulation of a freshwater microalga *Scenedesmus* sp, Bioresource Technol. 101 (2010) 5494-5500.
[211] C. Adams, B. Bugbee, Nitrogen retention and partitioning at the initiation of lipid accumulation in nitrogen-deficient algae, J. Phycol. 50 (2014) 356-365.
[212] C. Adams, V. Godfrey, B. Wahlen, L. Seefeldt, B. Bugbee, Understanding precision nitrogen stress to optimize the growth and lipid content tradeoff in oleaginous green microalgae, Bioresource Technol. 131 (2013) 188-194.
[213] S.P. Slocombe, Q. Zhang, M. Ross, A. Anderson, N.J. Thomas, Á. Lapresa, C. Rad-Menéndez, C.N. Campbell, K.D. Black, M.S. Stanley, Unlocking nature’s treasure-chest: screening for oleaginous algae, Scientific Reports. 5 (2015).
[214] T. Chopin, T. Gallant, I. Davison, Phosphorus and nitrogen nutrition in *Chondrus crispus* (Rhodophyta): effects on total phosphorus and nitrogen content,

carrageenan production, and photosynthetic pigments and metabolism, J. Phycol. 31 (1995) 283-293.
[215] A.J. Smit, B.L. Robertson, D.R. du Preez, Influence of ammonium-N pulse concentrations and frequency, tank condition and nitrogen starvation on growth rate and biochemical composition of *Gracilaria gracilis*, J. App. Phycol. 8 (1997) 473-481.
[216] M. Piorreck, P. Pohl, Formation of biomass, total protein, chlorophylls, lipids and fatty acids in green and blue-green algae during one growth phase, Phytochemistry. 23 (1984) 217-223.
[217] S.M. Garcia, A.A. Rosenberg, Food security and marine capture fisheries: characteristics, trends, drivers and future perspectives, Philos. T. Roy. Soc. B. 365 (2010) 2869-2880.
[218] J. Bostock, B. McAndrew, R. Richards, K. Jauncey, T. Telfer, K. Lorenzen, D. Little, L. Ross, N. Handisyde, I. Gatward, Aquaculture: global status and trends, Philos. T. Roy. Soc. B. 365 (2010) 2897-2912.
[219] H.C.J. Godfray, J.R. Beddington, I.R. Crute, L. Haddad, D. Lawrence, J.F. Muir, J. Pretty, S. Robinson, S.M. Thomas, C. Toulmin, Food Security: The Challenge of Feeding 9 Billion People, Science. 327 (2010) 812-818.
[220] R. Hannesson, Aquaculture and fisheries, Mar. Policy. 27 (2003) 169-178.
[221] D.H. Bubb, T.J. Thom, M.C. Lucas, Movement and dispersal of the invasive signal crayfish *Pacifastacus leniusculus* in upland rivers, Freshwater Biol. 49 (2004) 357-368.
[222] U. Thampanya, J. Vermaat, S. Sinsakul, N. Panapitukkul, Coastal erosion and mangrove progradation of Southern Thailand, Estuar. Coast. Shelf S. 68 (2006) 75-85.
[223] I.A. Fleming, K. Hindar, I.B. MjÖlnerÖd, B. Jonsson, T. Balstad, A. Lamberg, Lifetime success and interactions of farm salmon invading a native population, P. Roy. Soc. Lond. B Bio. 267 (2000) 1517-1523.
[224] B. Qin, P. Xu, Q. Wu, L. Luo, Y. Zhang, Environmental issues of lake Taihu, China, Hydrobiologia. 581 (2007) 3-14.
[225] X. Wang, O.J. Broch, S. Forbord, A. Handå, J. Skjermo, K.I. Reitan, O. Vadstein, Y. Olsen, Assimilation of inorganic nutrients from salmon (*Salmo salar*) farming by the macroalgae (*Saccharina latissima*) in an exposed coastal environment: implications for integrated multi-trophic aquaculture, J. Appl. Phycol. 26 (2014) 1869-1878.
[226] M. Troell, A. Joyce, T. Chopin, A. Neori, A.H. Buschmann, J.-G. Fang, Ecological engineering in aquaculture — Potential for integrated multi-trophic aquaculture (IMTA) in marine offshore systems, Aquaculture. 297 (2009) 1-9.
[227] N. Ridler, M. Wowchuk, B. Robinson, K. Barrington, T. Chopin, S. Robinson, F. Page, G. Reid, M. Szemerda, J. Sewuster, S. Boyne-Travis, Integrated multi-trophic aquaculture (IMTA): A potential strategic choice for farmers, Aquaculture Economics & Management. 11 (2007) 99-110.
[228] T. Chopin, Aquaculture, Integrated multi-trophic (IMTA), in: R.A. Meyers (Ed.) Encyclopedia of Sustainability Science and Technology, Springer New York, New York, NY, 2012, pp. 542-564.
[229] A. Neori, M. Shpigel, D. Ben-Ezra, A sustainable integrated system for culture of fish, seaweed and abalone, Aquaculture. 186 (2000) 279-291.
[230] I. Cohen, A. Neori, *Ulva lactuca* biofilters for marine fishpond effluents. I. Ammonia uptake kinetics and nitrogen content, Bot. Mar. 34 (1991) 475-482.

[231] P.H. de Paula Silva, R. De Nys, N.A. Paul, Seasonal growth dynamics and resilience of the green tide alga *Cladophora coelothrix* in high-nutrient tropical aquaculture, Aquaculture Environment Interactions. 2 (2012) 253-266.
[232] R.S. Lokhande, P.U. Singare, D.S. Pimple, Toxicity study of heavy metals pollutants in waste water effluent samples collected from Taloja Industrial Estate of Mumbai, India, Resources and Environment. 1 (2011) 13-19.
[233] World Health Organization, Guidelines for drinking-water quality, Fourth Edition ed., 2011
[234] United States Environmental Protection Agency, Drinking water health advisory for manganese, 2004.
[235] C.G. Fraga, Relevance, essentiality and toxicity of trace elements in human health, Mol. Aspects Med. 26 (2005) 235-244.
[236] O. Rabin, L. Hegedus, J.M. Bourre, Q.R. Smith, Rapid brain uptake of manganese (II) across the blood-brain barrier, J. Neurochem. 61 (1993) 509-517.
[237] S. Kanumakala, A. Boneh, M. Zacharin, Pamidronate treatment improves bone mineral density in children with Menkes disease, J. Inherit. Metab. Dis. 25 (2002) 391-398.
[238] M. Aschner, Manganese: brain transport and emerging research needs, Environ. Health Persp. 108 (2000) 429.
[239] D. Kar, P. Sur, S. Mandal, T. Saha, R. Kole, Assessment of heavy metal pollution in surface water, International Journal of Environmental Science and Technology. 5 (2008) 119.
[240] R. Reza, G. Singh, Heavy metal contamination and its indexing approach for river water, International Journal of Environmental Science and Technology. 7 (2010) 785.
[241] S.M. Saeed, I.M. Shaker, Assessment of heavy metals pollution in water and sediments and their effect on *Oreochromis niloticus* in the northern delta lakes, Egypt, 8th International Symposium on Tilapia in Aquaculture, 2008, pp. 475-490.
[242] V. Simeonov, J.A. Stratis, C. Samara, G. Zachariadis, D. Voutsa, A. Anthemidis, M. Sofoniou, T. Kouimtzis, Assessment of the surface water quality in Northern Greece, Water Res. 37 (2003) 4119-4124.
[243] M. Varol, B. Şen, Assessment of nutrient and heavy metal contamination in surface water and sediments of the upper Tigris River, Turkey, Catena. 92 (2012) 1-10.
[244] L. Deng, X. Zhu, X. Wang, Y. Su, H. Su, Biosorption of copper(II) from aqueous solutions by green alga *Cladophora fascicularis*, Biodegradation. 18 (2007) 393-402.
[245] Z. Aksu, D. Özer, H.I. Ekiz, T. Kutsal, A. Çaglar, Investigation of biosorption of chromium(VI) on *Cladophora crispata* in two-staged batch reactor, Environ. Technol. 17 (1996) 215-220.
[246] F. Fu, Q. Wang, Removal of heavy metal ions from wastewaters: a review, J. Environ. Manage. 92 (2011) 407-418.
[247] Q. Chen, Z. Luo, C. Hills, G. Xue, M. Tyrer, Precipitation of heavy metals from wastewater using simulated flue gas: Sequent additions of fly ash, lime and carbon dioxide, Water Res. 43 (2009) 2605-2614.
[248] H.G. Park, M.Y. Chae, Novel type of alginate gel-based adsorbents for heavy metal removal, J. Chem. Technol. Biot. 79 (2004) 1080-1083.
[249] L. Brinza, M.J. Dring, M. Gavrilescu, Marine micro-and macro-algal species as biosorbents for heavy metals, Environmental Engineering and Management Journal. 6 (2007) 237-251.
[250] C.J. Tien, Biosorption of metal ions by freshwater algae with different surface characteristics, Process Biochem. 38 (2002) 605-613.

[251] A. Özer, D. Özer, H. İbrahim Ekİz, The equilibrium and kinetic modelling of the biosorption of copper(II) ions on *Cladophora crispata*, Adsorption. 10 (2005) 317-326.
[252] K. Chojnacka, A. Chojnacki, H. Górecka, Trace element removal by *Spirulina* sp. from copper smelter and refinery effluents, Hydrometallurgy. 73 (2004) 147-153.
[253] Z.R. Holan, B. Volesky, Biosorption of lead and nickel by biomass of marine algae, Biotechnol. Bioeng. 43 (1994) 1001-1009.
[254] Y. Nuhoglu, E. Malkoc, A. Gürses, N. Canpolat, The removal of Cu(II) from aqueous solutions by *Ulothrix zonata*, Bioresource Technol. 85 (2002) 331-333.
[255] F. Pagnanelli, A. Esposito, L. Toro, F. Veglio, Metal speciation and pH effect on Pb, Cu, Zn and Cd biosorption onto *Sphaerotilus natans*: Langmuir-type empirical model, Water Res. 37 (2003) 627-633.
[256] M. Kobya, E. Demirbas, E. Senturk, M. Ince, Adsorption of heavy metal ions from aqueous solutions by activated carbon prepared from apricot stone, Bioresource Technol. 96 (2005) 1518-1521.
[257] O.S. Amuda, A.A. Giwa, I.A. Bello, Removal of heavy metal from industrial wastewater using modified activated coconut shell carbon, Biochem. Eng. J. 36 (2007) 174-181.
[258] F. Fu, H. Zeng, Q. Cai, R. Qiu, J. Yu, Y. Xiong, Effective removal of coordinated copper from wastewater using a new dithiocarbamate-type supramolecular heavy metal precipitant, Chemosphere. 69 (2007) 1783-1789.
[259] A. Khelifa, S. Moulay, A. Naceur, Treatment of metal finishing effluents by the electroflotation technique, Desalination. 181 (2005) 27-33.
[260] A. Shafaei, M. Rezayee, M. Arami, M. Nikazar, Removal of Mn 2+ ions from synthetic wastewater by electrocoagulation process, Desalination. 260 (2010) 23-28.
[261] V.J. Inglezakis, M.A. Stylianou, D. Gkantzou, M.D. Loizidou, Removal of Pb(II) from aqueous solutions by using clinoptilolite and bentonite as adsorbents, Desalination. 210 (2007) 248-256.
[262] K. Athanasiadis, B. Helmreich, Influence of chemical conditioning on the ion exchange capacity and on kinetic of zinc uptake by clinoptilolite, Water Res. 39 (2005) 1527-1532.
[263] P.S. Sudilovskiy, G.G. Kagramanov, V.A. Kolesnikov, Use of RO and NF for treatment of copper containing wastewaters in combination with flotation, Desalination. 221 (2008) 192-201.
[264] L. Zhang, Y. Wu, X. Qu, Z. Li, J. Ni, Mechanism of combination membrane and electro-winning process on treatment and remediation of Cu2+ polluted water body, J. Environ. Sci. 21 (2009) 764-769.
[265] M. Mohsen-Nia, P. Montazeri, H. Modarress, Removal of Cu2+ and Ni2+ from wastewater with a chelating agent and reverse osmosis processes, Desalination. 217 (2007) 276-281.
[266] M. Tuzen, A. Sarı, Biosorption of selenium from aqueous solution by green algae (*Cladophora hutchinsiae*) biomass: Equilibrium, thermodynamic and kinetic studies, Chem. Eng. J. 158 (2010) 200-206.
[267] V. Gupta, A. Shrivastava, N. Jain, Biosorption of chromium (VI) from aqueous solutions by green algae *Spirogyra* species, Water Res. 35 (2001) 4079-4085.
[268] Z. Aksu, Ü. AÇIkel, T. Kutsal, Investigation of simultaneous biosorption of copper(II) and chromium(VI) on dried *Chlorella vulgaris* from binary metal mixtures: application of multicomponent adsorption isotherms, Separ. Sci. and Technol. 34 (1999) 501-524.

[269] Z. Aksu, Y. Sag, T. Kutsal, The biosorpnon of copperod by *C. vulgaris* and *Z. ramigera*, Environ. Technol. 13 (1992) 579-586.
[270] W.M. Antunes, A.S. Luna, C.A. Henriques, A.C.A. da Costa, An evaluation of copper biosorption by a brown seaweed under optimized conditions, Electronic Journal of Biotechnology. 6 (2003) 174-184.
[271] R. Apiratikul, P. Pavasant, Sorption isotherm model for binary component sorption of copper, cadmium, and lead ions using dried green macroalga, *Caulerpa lentillifera*, Chem. Eng J. 119 (2006) 135-145.
[272] T.A. Davis, B. Volesky, R.H.S.F. Vieira, *Sargassum* seaweed as biosorbent for heavy metals, Water Res. 34 (2000) 4270-4278.
[273] L. Deng, Y. Su, H. Su, X. Wang, X. Zhu, Biosorption of copper (II) and lead (II) from aqueous solutions by nonliving green algae *Cladophora fascicularis*: Equilibrium, kinetics and environmental effects, Adsorption. 12 (2006) 267-277.
[274] G.Ç. Dönmez, Z. Aksu, A. Öztürk, T. Kutsal, A comparative study on heavy metal biosorption characteristics of some algae, Process Biochem. 34 (1999) 885-892.
[275] A. Fraile, S. Penche, F. González, M.L. Blázquez, J.A. Muñoz, A. Ballester, Biosorption of copper, zinc, cadmium and nickel by *Chlorella vulgaris*, Chemistry and Ecology. 21 (2005) 61-75.
[276] V. Gupta, A. Rastogi, V. Saini, N. Jain, Biosorption of copper (II) from aqueous solutions by *Spirogyra* species, J. Colloid Interf. Sci. 296 (2006) 59-63.
[277] L. Ji, S. Xie, J. Feng, Y. Li, L. Chen, Heavy metal uptake capacities by the common freshwater green alga *Cladophora fracta*, J. Appl. Phycol. 24 (2012) 979-983.
[278] P. Kaewsarn, Biosorption of copper(II) from aqueous solutions by pre-treated biomass of marine algae *Padina* sp, Chemosphere. 47 (2002) 1081-1085.
[279] D. Kratochvil, E. Fourest, B. Volesky, Biosorption of copper by *Sargassum fluitans* biomass in fixed-bed column, Biotechnol. Lett. 17 (1995) 777-782.
[280] P.S. Lau, H.Y. Lee, C.C.K. Tsang, N.F.Y. Tam, Y.S. Wong, Effect of metal interference, pH and temperature on Cu and Ni biosorption by *Chlorella vulgaris* and *Chlorella miniata*, Environ. Technol. 20 (1999) 953-961.
[281] Y.-C. Lee, S.-P. Chang, The biosorption of heavy metals from aqueous solution by *Spirogyra* and *Cladophora* filamentous macroalgae, Bioresource Technol. 102 (2011) 5297-5304.
[282] J.T. Matheickal, Q. Yu, Biosorption of lead from aqueous solutions by marine algae *Ecklonia radiata*, Water Sci. Technol. 34 (1996) 1-7.
[283] J.T. Matheickal, Q. Yu, Biosorption of lead(II) and copper(II) from aqueous solutions by pre-treated biomass of Australian marine algae, Bioresource Technol. 69 (1999) 223-229.
[284] P. Pavasant, R. Apiratikul, V. Sungkhum, P. Suthiparinyanont, S. Wattanachira, T.F. Marhaba, Biosorption of Cu 2+, Cd 2+, Pb 2+, and Zn 2+ using dried marine green macroalga *Caulerpa lentillifera*, Bioresource Technol. 97 (2006) 2321-2329.
[285] S. Prasher, M. Beaugeard, J. Hawari, P. Bera, R. Patel, S. Kim, Biosorption of heavy metals by red algae (*Palmaria palmata*), Environ. Technol. 25 (2004) 1097-1106.
[286] E. Romera, F. González, A. Ballester, M.L. Blázquez, J.A. Muñoz, Comparative study of biosorption of heavy metals using different types of algae, Bioresource Technol. 98 (2007) 3344-3353.
[287] E. Sandau, P. Sandau, O. Pulz, Heavy metal sorption by microalgae, Acta Biotechnol. 16 (1996) 227-235.
[288] P.X. Sheng, Y.-P. Ting, J.P. Chen, L. Hong, Sorption of lead, copper, cadmium, zinc, and nickel by marine algal biomass: characterization of biosorptive capacity and investigation of mechanisms, J. Colloid Interf. Sci. 275 (2004) 131-141.

[289] E.A. Silva, E.S. Cossich, C.G. Tavares, L. Cardozo Filho, R. Guirardello, Biosorption of binary mixtures of Cr(III) and Cu(II) ions by *Sargassum* sp, Braz. J. Chem. Eng. 20 (2003) 213-227.
[290] D. Feng, C. Aldrich, Adsorption of heavy metals by biomaterials derived from the marine alga *Ecklonia maxima*, Hydrometallurgy. 73 (2004) 1-10.
[291] W.M. Ibrahim, Biosorption of heavy metal ions from aqueous solution by red macroalgae, J. Hazard. Mater. 192 (2011) 1827-1835.
[292] N. Jafari, Z. Senobari, Removal of Pb (II) ions from aqueous solutions by *Cladophora rivularis* (Linnaeus) Hoek, The Scientific World Journal. 2012 (2012) 6.
[293] R. Jalali, H. Ghafourian, Y. Asef, S.J. Davarpanah, S. Sepehr, Removal and recovery of lead using nonliving biomass of marine algae, J. Hazard. Mater. 92 (2002) 253-262.
[294] Y.H. Kim, J. Yeon Park, Y.J. Yoo, J.W. Kwak, Removal of lead using xanthated marine brown alga, *Undaria pinnatifida*, Process Biochem. 34 (1999) 647-652.
[295] C. Lamai, M. Kruatrachuea, P. Pokethitiyooka, E.S. Upathamb, V. Soonthornsarathoola, Toxicity and accumulation of lead and cadmium in the filamentous green alga *Cladophora fracta* (OF Muller ex Vahl) Kutzing: A laboratory study, Science Asia. 31 (2005) 121-127.
[296] P. Srinivasa Rao, S. Kalyani, K. Suresh Reddy, A. Krishnaiah, Comparison of biosorption of nickel (II) and copper (II) ions from aqueous solution by *Sphaeroplea* algae and acid treated *Sphaeroplea* algae, Separ. Sci. Technol. 40 (2005) 3149-3165.
[297] I. Riba, E. Garcia-Luque, J. Blasco, T. DelValls, Bioavailability of heavy metals bound to estuarine sediments as a function of pH and salinity values, Chem. Spec. Bioavailab. 15 (2003) 101-114.
[298] S. Schiewer, B. Volesky, Modeling of the proton-metal ion exchange in biosorption, Environ. Sci. Technol. 29 (1995) 3049-3058.
[299] M. Beaugeard, Biosorption of heavy metals by red algae (*Palmaria palmata*), 2001.
[300] S.K. Mehta, J.P. Gaur, Characterization and optimization of Ni and Cu sorption from aqueous solution by *Chlorella vulgaris*, Ecol. Eng. 18 (2001) 1-13.
[301] L. Deng, Y. Zhang, J. Qin, X. Wang, X. Zhu, Biosorption of Cr(VI) from aqueous solutions by nonliving green algae *Cladophora albida*, Miner. Eng. 22 (2009) 372-377.
[302] Z. Aksu, G. Dönmez, Binary biosorption of cadmium (II) and nickel (II) onto dried *Chlorella vulgaris*: co-ion effect on mono-component isotherm parameters, Process Biochem. 41 (2006) 860-868.
[303] Z. Aksu, Determination of the equilibrium, kinetic and thermodynamic parameters of the batch biosorption of nickel(II) ions onto *Chlorella vulgaris*, Process Biochem. 38 (2002) 89-99.
[304] Z. Aksu, Equilibrium and kinetic modelling of cadmium(II) biosorption by *C. vulgaris* in a batch system: effect of temperature, Sep. Purif. Technol. 21 (2001) 285-294.
[305] V.J.P. Vilar, C.M.S. Botelho, R.A.R. Boaventura, Influence of pH, ionic strength and temperature on lead biosorption by *Gelidium* and agar extraction algal waste, Process Biochem. 40 (2005) 3267-3275.
[306] D. Özer, Z. Aksu, T. Kutsal, A. Çaglar, Adsorption isotherms of lead(II) and chromium(VI) on *Cladophora crispata*, Environ. Technol. 15 (1994) 439-448.
[307] S. Mehta, A. Singh, J. Gaur, Kinetics of adsorption and uptake of Cu2+ by *Chlorella vulgaris*: influence of pH, temperature, culture age, and cations, J. Environ. Sci. Heal. A. 37 (2002) 399-414.

[308] L. Deng, Y. Su, H. Su, X. Wang, X. Zhu, Sorption and desorption of lead (II) from wastewater by green algae *Cladophora fascicularis*, J. Hazard. Mater. 143 (2007) 220-225.
[309] M. Hashim, K. Chu, Biosorption of cadmium by brown, green, and red seaweeds, Chem. Eng. J. 97 (2004) 249-255.
[310] D.H. Camacho, S.R.C. Gerongay, J.P.C. Macalinao, *Cladophora* cellulose-polyaniline composite for remediation of toxic chromium (VI), Cell. Chem. Technol. 47 (2013) 125-132.
[311] J.L. Gardea-Torresdey, M.K. Becker-Hapak, J.M. Hosea, D.W. Darnall, Effect of chemical modification of algal carboxyl groups on metal ion binding, Environ. Sci. Technol. 24 (1990) 1372-1378.
[312] R. Rakhshaee, M. Khosravi, M.T. Ganji, Kinetic modeling and thermodynamic study to remove Pb(II), Cd(II), Ni(II) and Zn(II) from aqueous solution using dead and living *Azolla filiculoides*, J. Hazard. Mater. 134 (2006) 120-129.
[313] B.M. McHardy, J.J. George, Bioaccumulation and toxicity of zinc in the green alga, *Cladophora glomerata*, Environ. Pollut. 66 (1990) 55-66.
[314] K. Vijayaraghavan, S. Rangabhashiyam, T. Ashokkumar, J. Arockiaraj, Assessment of samarium biosorption from aqueous solution by brown macroalga *Turbinaria conoides*, Journal of the Taiwan Institute of Chemical Engineers. 74 (2017) 113-120.
[315] P. Figueira, B. Henriques, A. Teixeira, C.B. Lopes, A.T. Reis, R.J.R. Monteiro, A.C. Duarte, M.A. Pardal, E. Pereira, Comparative study on metal biosorption by two macroalgae in saline waters: single and ternary systems, Environ. Sci. Pollut. Res. 23 (2016) 11985-11997.
[316] J. He, J.P. Chen, A comprehensive review on biosorption of heavy metals by algal biomass: Materials, performances, chemistry, and modeling simulation tools, Bioresource Technol. 160 (2014) 67-78.
[317] S. Sun, F. Wang, C. Li, S. Qin, M. Zhou, L. Ding, S. Pang, D. Duan, G. Wang, B. Yin, Emerging challenges: Massive green algae blooms in the Yellow Sea, Nature Proceedings. (2008).
[318] Shanghai Daily, Algae cleaning in full swing (2008) Accessed on: 06/07/2017, http://www.china.org.cn/government/focus_news/2008-07/04/content_15953482.htm
[319] M.E. Ross, M.S. Stanley, J.G. Day, A.J.C. Semião, A comparison of methods for the non-destructive fresh weight determination of filamentous algae for growth rate analysis and dry weight estimation, J. App. Phycol. (2017) 1-12.
[320] R.R. Guillard, J.H. Ryther, Studies of marine planktonic diatoms: I. *Cyclotella nana* Hustedt, and *Detonula confervacea* (Cleve) Gran, Can. J. Microbiol. 8 (1962) 229-239.
[321] Culture Collection of Algae and Protozoa, Recipes: List of media used to maintain strains at CCAP (2014) Accessed on: 07/12/2016, https://www.ccap.ac.uk/pdfrecipes.htm
[322] Y.S. Yong, W.T.L. Yong, A. Anton, Analysis of formulae for determination of seaweed growth rate, J. App. Phycol. 25 (2013) 1831-1834.
[323] C. Woulds, M.C. Schwartz, T. Brand, G.L. Cowie, G. Law, S.R. Mowbray, Porewater nutrient concentrations and benthic nutrient fluxes across the Pakistan margin OMZ, Deep-Sea Res. Pt II. 56 (2009) 333-346.
[324] P.F. Mulvenna, G. Savidge, A modified manual method for the determination of urea in seawater using diacetylmonoxime reagent, Estuar. Coast. Shelf S. 34 (1992) 429-438.

[325] A. Sluiter, B. Hames, R. Ruiz, C. Scarlata, J. Sluiter, D. Templeton, Determination of ash in biomass, National Renewable Energy Laboratory (NREL) Technical Report, 2008, pp. NREL/TP-510-42622.
[326] O.H. Lowry, N.J. Rosebrough, A.L. Farr, R.J. Randall, Protein measurement with the Folin phenol reagent, J. Biol. Chem. 193 (1951) 265-275.
[327] S.P. Slocombe, M. Ross, N. Thomas, S. McNeill, M.S. Stanley, A rapid and general method for measurement of protein in micro-algal biomass, Bioresource Technol. 129 (2013) 51-57.
[328] E. Fournier, Colorimetric quantification of carbohydrates, in: R.E. Wrolstad (Ed.) Current Protocols in Food Analytical Chemistry, John Wiley and Sons, Hoboken, NJ, USA, 2001, pp. E1.1.1–E1.1.8.
[329] M. Dubois, K.A. Gilles, J.K. Hamilton, P. Rebers, F. Smith, Colorimetric method for determination of sugars and related substances, Anal. Chem. 28 (1956) 350-356.
[330] M.J. Griffiths, C. Garcin, R.P. van Hille, S.T. Harrison, Interference by pigment in the estimation of microalgal biomass concentration by optical density, J. Microbiol. Meth. 85 (2011) 119-123.
[331] E. Metcalf, M. Eddy, Wastewater engineering: treatment and resource recovery, 2014
[332] M. Henze, Wastewater, volumes and composition, Wastewater Treatment, Springer, 1997, pp. 11-36.
[333] M. Verhougstraete, M.N. Byappanahalli, J. Rose, R.L. Whitman, *Cladophora* in the Great Lakes: impacts on beach water quality and human health, Water Sci. Technol. 62 (2010) 68-76.
[334] F. Williams, R. Eschen, A. Harris, D. Djeddour, C. Pratt, R. Shaw, S. Varia, J. Lamontagne-Godwin, S. Thomas, S. Murphy, The economic cost of invasive non-native species on Great Britain, CABIWallingford, 2010.
[335] D.M. Wotton, C. O'Brien, M.D. Stuart, D.J. Fergus, Eradication success down under: heat treatment of a sunken trawler to kill the invasive seaweed *Undaria pinnatifida*, Mar. Pollut. Bull. 49 (2004) 844-849.
[336] M.T. Auer, L.M. Tomlinson, S.N. Higgins, S.Y. Malkin, E.T. Howell, H.A. Bootsma, Great Lakes *Cladophora* in the 21st century: same algae-different ecosystem, J. Great Lakes Res. 36 (2010) 248-255.
[337] D. Planas, S. Maberly, J. Parker, Phosphorus and nitrogen relationships of *Cladophora glomerata* in two lake basins of different trophic status, Freshwater Biol. 35 (1996) 609-622.
[338] P. Peckol, J. Rivers, Physiological responses of the opportunistic macroalgae *Cladophora vagabunda* (L.) van den Hoek and *Gracilaria tikvahiae* (McLachlan) to environmental disturbances associated with eutrophication, J. Exp. Mar. Biol. Ecol. 190 (1995) 1-16.
[339] H. Håkansson, P. Ahlgren, Acid hydrolysis of some industrial pulps: effect of hydrolysis conditions and raw material, Cellulose. 12 (2005) 177-183.
[340] Y. Sun, J. Cheng, Hydrolysis of lignocellulosic materials for ethanol production: a review, Bioresource Technol. 83 (2002) 1-11.
[341] M. Yoshida, Y. Liu, S. Uchida, K. Kawarada, Y. Ukagami, H. Ichinose, S. Kaneko, K. Fukuda, Effects of cellulose crystallinity, hemicellulose, and lignin on the enzymatic hydrolysis of *Miscanthus sinensis* to monosaccharides, Biosci. Biotech. Bioch. 72 (2008) 805-810.
[342] D. Krause-Jensen, K. McGlathery, S. Rysgaard, P.B. Christensen, Production within dense mats of the filamentous macroalga *Chaetomorpha linum* in relation to light and nutrient availability, Mar. Ecol-Prog. Ser. 134 (1996) 207-216.

[343] K.-s. Choo, P. Snoeijs, M. Pedersén, Oxidative stress tolerance in the filamentous green algae *Cladophora glomerata* and *Enteromorpha ahlneriana*, J. Exp. Mar. Biol. Ecol. 298 (2004) 111-123.
[344] V. Chapman, Seaweeds and their uses, Springer Science & Business Media, 2012
[345] A. Giangrande, A. Cavallo, C. Pierri, Ammonium uptake of *Cladophora prolifera* (Chlorophyta, Cladophorales) a candidate species for bioremediation of aquaculture wastes, Thalassia Salentina. 30 (2007) 107-116.
[346] G. Khola, B. Ghazala, Biodiesel production from algae, Pak. J. Bot. 44 (2012) 379-381.
[347] A. Mihranyan, L. Nyholm, A.E.G. Bennett, M. Strømme, A novel high specific surface area conducting paper material composed of polypyrrole and *Cladophora* cellulose, J. Phys. Chem. B. 112 (2008) 12249-12255.
[348] G. Nyström, A. Razaq, M. Strømme, L. Nyholm, A. Mihranyan, Ultrafast all-polymer paper-based batteries, Nano Letters 9(2009) 3635-3639.
[349] P. Hedenus, M. Strømme Mattsson, G.A. Niklasson, O. Camber, R. Ek, Characterisation of instantaneous water absorption properties of pharmaceutical excipients, Int. J. Pharm. 202 (2000) 141-149.
[350] C. Gustafsson, H. Lennholm, T. Iversen, C. Nyström, Evaluation of surface and bulk characteristics of cellulose I powders in relation to compaction behavior and tablet properties, Drug Dev. Ind. Pharm. 29 (2003) 1095-1107.
[351] C.Y. Chen, Effect of pH on the growth and carbon uptake of marine phytoplankton, Mar. Ecol-Prog. Ser. 109 (1994) 83-94.
[352] J.A. Raven, J. Beardall, Carbon dioxide as the exogenous inorganic carbon source for *Batrachospermum* and *Lemanea*, Brit. Phycol. J. 16 (1981) 165-175.
[353] H.G. Peterson, F.P. Healey, R. Wagemann, Metal toxicity to algae: a highly pH dependent phenomenon, Can. J. Fish. Aquat. Sci. 41 (1984) 974-979.
[354] T.D. Brock, Lower pH limit for the existence of blue-green algae: Evolutionary and ecological implications, Science. 179 (1973) 480-483.
[355] L. Axelsson, Changes in pH as a measure of photosynthesis by marine macroalgae, Mar. Biol. 97 (1988) 287-294.
[356] I. Douskova, J. Doucha, K. Livansky, J. Machat, P. Novak, D. Umysova, V. Zachleder, M. Vitova, Simultaneous flue gas bioremediation and reduction of microalgal biomass production costs, Appl. Microbiol. Biot. 82 (2009) 179-185.
[357] A. Akcil, S. Koldas, Acid mine drainage (AMD): causes, treatment and case studies, Journal of Cleaner Production. 14 (2006) 1139-1145.
[358] R. Smith, R. Foy, Improved hydrogen ion buffering of media for the culture of freshwater algae, Brit. Phycol. J. 9 (1974) 239-245.
[359] M. Droop, Water-soluble factors in the nutrition of *Oxyrrhis marina*, J. Mar. Biol. Assoc. UK. 38 (1959) 605-620.
[360] R.A. Feely, S.C. Doney, S.R. Cooley, Ocean acidification: Present conditions and future changes in a high-$CO_2$ world, Oceanography. 22 (2009) 36-47.
[361] K. Barrington, T. Chopin, S. Robinson, Integrated multi-trophic aquaculture (IMTA) in marine temperate waters, Integrated mariculture: a global review. FAO Fisheries and Aquaculture Technical Paper, 2009, pp. 7-46.
[362] A. Holzinger, U. Karsten, Desiccation stress and tolerance in green algae: consequences for ultrastructure, physiological and molecular mechanisms, Frontiers in Plant Science. 4 (2013) 327.
[363] A. Ben-Amotz, M. Avron, Accumulation of metabolites by halotolerant algae and its industrial potential, Annual Reviews in Microbiology. 37 (1983) 95-119.

[364] R.P. Canale, M.T. Auer, J.M. Graham, Ecological studies and mathematical modeling of *Cladophora* in Lake Huron: 6. Seasonal and spatial variation in growth kinetics, J. Great Lakes Res. 8 (1982) 126-133.
[365] Algenuity, Algem® - environment modelling labscale photobioreactor (2017) Accessed on: 01/08/2017, https://www.algenuity.com/algem-photobioreactor
[366] N. Fujimoto, Y. Inamori, N. Sugiura, R. Sudo, Effects of temperature change on algal growth, Environ. Technol. 15 (1994) 497-500.
[367] P.G. Falkowski, J. LaRoche, Acclimation to spectral irradiance in algae, J. Phycol. 27 (1991) 8-14.
[368] A. Eggert, U. Nitschke, J.A. West, D. Michalik, U. Karsten, Acclimation of the intertidal red alga *Bangiopsis subsimplex* (Stylonematophyceae) to salinity changes, J. Exp. Mar. Biol. Ecol. 343 (2007) 176-186.
[369] A. Schuenhoff, M. Shpigel, I. Lupatsch, A. Ashkenazi, F.E. Msuya, A. Neori, A semi-recirculating, integrated system for the culture of fish and seaweed, Aquaculture. 221 (2003) 167-181.
[370] R. Craggs, J. Park, S. Heubeck, D. Sutherland, High rate algal pond systems for low-energy wastewater treatment, nutrient recovery and energy production, New Zeal. J. Bot. 52 (2014) 60-73.
[371] M. Griffiths, S.T. Harrison, M. Smit, D. Maharajh, Major Commercial Products from Micro-and Macroalgae, Algae Biotechnology, Springer, 2016, pp. 269-300.
[372] P.H. de Paula Silva, S. McBride, R. de Nys, N.A. Paul, Integrating filamentous 'green tide'algae into tropical pond-based aquaculture, Aquaculture. 284 (2008) 74-80.
[373] R.R. Guillard, M.S. Sieracki, Counting cells in cultures with the light microscope, in: R.A. Andersen (Ed.) Algal culturing techniques, Elsevier Academic Press, London, 2005, pp. 239-252.
[374] D. Marie, N. Simon, D. Vaulot, Phytoplankton cell counting by flow cytometry, in: R.A. Andersen (Ed.) Algal culturing techniques, Elsevier Academic Press, London, 2005, pp. 253-267.
[375] P. Das, W. Lei, S.S. Aziz, J.P. Obbard, Enhanced algae growth in both phototrophic and mixotrophic culture under blue light, Bioresource Technol. 102 (2011) 3883-3887.
[376] T. Yamaoka, K. Satoh, S. Katoh, Photosynthetic activities of a thermophilic blue-green alga, Plant Cell Physiol. 19 (1978) 943-954.
[377] T. Dean, F. Jacobsen, Nutrient-limited growth of juvenile kelp, *Macrocystis pyrifera*, during the 1982–1984 "El Niño" in southern California, Mar. Biol. 90 (1986) 597-601.
[378] C.D. Hepburn, C.L. Hurd, Conditional mutualism between the giant kelp *Macrocystis pyrifera* and colonial epifauna, Mar. Ecol-Prog. Ser. 302 (2005) 37-48.
[379] J. Kain, Morphology and growth of the giant kelp *Macrocystis pyrifera* in New Zealand and California, Mar. Biol. 67 (1982) 143-157.
[380] M.B. Westera, P.S. Lavery, A comparison of hole punch and needle punch methods for the measurement of seagrass productivity, Aquat. Bot. 85 (2006) 267-269.
[381] A.K. Macleod, M.S. Stanley, J.G. Day, E.J. Cook, Biofouling community composition across a range of environmental conditions and geographical locations suitable for floating marine renewable energy generation, Biofouling. 32 (2016) 261-276.
[382] D. Gordon, A. McComb, Growth and production of the green alga *Cladophora montagneana* in a eutrophic Australian estuary and its interpretation using a computer program, Water Res. 23 (1989) 633-645.

[383] J. Rivers, P. Peckol, Interactive effects of nitrogen and dissolved inorganic carbon on photosynthesis, growth, and ammonium uptake of the macroalgae *Cladophora vagabunda* and *Gracilaria tikvahiae*, Mar. Biol. 121 (1995) 747-753.
[384] A. Pinowska, Effects of snail grazing and nutrient release on growth of the macrophytes *Ceratophyllum demersum* and *Elodea canadensis* and the filamentous green alga *Cladophora* sp, Hydrobiologia. 479 (2002) 83-94.
[385] P. Robinson, H. Hawkes, Studies on the growth of *Cladophora glomerata* in laboratory continuous-flow culture, Brit. Phycol. J. 21 (1986) 437-444.
[386] T. Ozimek, E. Pieczyńska, A. Hankiewicz, Effects of filamentous algae on submerged macrophyte growth: a laboratory experiment, Aquat. Bot. 41 (1991) 309-315.
[387] P.K. Robinson, Factors affecting the growth of *Cladophora* in relation to river pollution, Aston University, 1983.
[388] Y.S. Yong, W.T.L. Yong, A. Anton, Analysis of formulae for determination of seaweed growth rate, J. Appl. Phycol. 25 (2013) 1831-1834.
[389] A.R. Angell, L. Mata, R. Nys, N.A. Paul, Indirect and direct effects of salinity on the quantity and quality of total amino acids in Ulva ohnoi (Chlorophyta), Journal of phycology. 51 (2015) 536-545.
[390] F. Leliaert, E. Coppejans, The marine species of *Cladophora* (Chlorophyta) from the South African east coast, Nova Hedwigia. 76 (2003) 45-82.
[391] M.R. Bilad, V. Discart, D. Vandamme, I. Foubert, K. Muylaert, I.F.J. Vankelecom, Harvesting microalgal biomass using a magnetically induced membrane vibration (MMV) system: Filtration performance and energy consumption, Bioresour. Technol. 138 (2013) 329-338.
[392] C.-Y. Chen, K.-L. Yeh, R. Aisyah, D.-J. Lee, J.-S. Chang, Cultivation, photobioreactor design and harvesting of microalgae for biodiesel production: A critical review, Bioresour. Technol. 102 (2011) 71-81.
[393] B.A. Whitton, Phycology, edited by Robert Edward Lee, J. Appl. Phycol. 11 (1999) 598-598.
[394] T.E.I. Wik, B.T. Lindén, P.I. Wramner, Integrated dynamic aquaculture and wastewater treatment modelling for recirculating aquaculture systems, Aquaculture. 287 (2009) 361-370.
[395] Y.-F. Yang, X.-G. Fei, J.-M. Song, H.-Y. Hu, G.-C. Wang, I.K. Chung, Growth of *Gracilaria lemaneiformis* under different cultivation conditions and its effects on nutrient removal in Chinese coastal waters, Aquaculture. 254 (2006) 248-255.
[396] A. Mehrabadi, R. Craggs, M.M. Farid, Wastewater treatment high rate algal ponds (WWT HRAP) for low-cost biofuel production, Bioresource Technol. 184 (2015) 202-214.
[397] A.C. Tyler, K.J. McGlathery, S.A. Macko, Uptake of urea and amino acids by the macroalgae *Ulva lactuca* (Chlorophyta) and *Gracilaria vermiculophylla* (Rhodophyta), Mar. Ecol-Prog. Ser. 294 (2005) 161-172.
[398] J. Park, R. Craggs, Wastewater treatment and algal production in high rate algal ponds with carbon dioxide addition, Water Sci. Technol. 61 (2010) 633-639.
[399] N.A. Waser, K. Yin, Z. Yu, K. Tada, P.J. Harrison, D.H. Turpin, S.E. Calvert, Nitrogen isotope fractionation during nitrate, ammonium and urea uptake by marine diatoms and coccolithophores under various conditions of N availability, Mar. Ecol-Prog. Ser. 169 (1998) 29-41.
[400] M.S. Islam, Nitrogen and phosphorus budget in coastal and marine cage aquaculture and impacts of effluent loading on ecosystem: review and analysis towards model development, Mar. Pollut. Bull. 50 (2005) 48-61.

[401] A. Converti, S. Scapazzoni, A. Lodi, J. Carvalho, Ammonium and urea removal by *Spirulina platensis*, J. Ind. Microbiol. Biot. 33 (2006) 8-16.
[402] A. Konig, H.W. Pearson, S.A. Silva, Ammonia toxicity to algal growth in waste stabilization ponds, Water Sci. Technol. 19 (1987) 115-122.
[403] T. Källqvist, A. Svenson, Assessment of ammonia toxicity in tests with the microalga, *Nephroselmis pyriformis*, Chlorophyta, Water Res. 37 (2003) 477-484.
[404] N. Powell, A.N. Shilton, S. Pratt, Y. Chisti, Factors influencing luxury uptake of phosphorus by microalgae in waste stabilization ponds, Environ. Sci. Technol. 42 (2008) 5958-5962.
[405] V. Perini, M.E. Bracken, Nitrogen availability limits phosphorus uptake in an intertidal macroalga, Oecologia. 175 (2014) 667-676.
[406] S. Philips, H.J. Laanbroek, W. Verstraete, Origin, causes and effects of increased nitrite concentrations in aquatic environments, Reviews in Environmental Science and Biotechnology. 1 (2002) 115-141.
[407] J.J. Cole, Interactions between bacteria and algae in aquatic ecosystems, Annu. Rev. Ecol. Syst. 13 (1982) 291-314.
[408] L.E. Gonzalez-Bashan, V.K. Lebsky, J.P. Hernandez, J.J. Bustillos, Y. Bashan, Changes in the metabolism of the microalga *Chlorella vulgaris* when coimmobilized in alginate with the nitrogen-fixing *Phyllobacterium myrsinacearum*, Can. J. Microbiol. 46 (2000) 653-659.
[409] K.-S. Choo, P. Snoeijs, M. Pedersén, Uptake of inorganic carbon by *Cladophora glomerata* (Chlorophyta) from the Baltic Sea, J. Phycol. 38 (2002) 493-502.
[410] J. Raven, J. Beardall, H. Griffiths, Inorganic C-sources for *Lemanea*, *Cladophora* and *Ranunculus* in a fast-flowing stream: measurements of gas exchange and of carbon isotope ratio and their ecological implications, Oecologia. 53 (1982) 68-78.
[411] T. Berman, S. Chava, Algal growth on organic compounds as nitrogen sources, J. Plankton Res. 21 (1999) 1423-1437.
[412] P. Kotrba, Microbial biosorption of metals—General Introduction, Microbial biosorption of metals, Springer, 2011, pp. 1-6.
[413] H. Ali, E. Khan, M.A. Sajad, Phytoremediation of heavy metals—concepts and applications, Chemosphere. 91 (2013) 869-881.
[414] M.S. Islam, M.K. Ahmed, M. Raknuzzaman, M. Habibullah-Al-Mamun, M.K. Islam, Heavy metal pollution in surface water and sediment: a preliminary assessment of an urban river in a developing country, Ecological Indicators. 48 (2015) 282-291.
[415] D. Krewski, R.A. Yokel, E. Nieboer, D. Borchelt, J. Cohen, J. Harry, S. Kacew, J. Lindsay, A.M. Mahfouz, V. Rondeau, Human health risk assessment for aluminium, aluminium oxide, and aluminium hydroxide, J. Toxicol. Env. Heal. B. 10 (2007) 1-269.
[416] J. Crossgrove, W. Zheng, Manganese toxicity upon overexposure, NMR Biomed. 17 (2004) 544-553.
[417] A. Buccolieri, G. Buccolieri, N. Cardellicchio, A. Dell'Atti, A. Di Leo, A. Maci, Heavy metals in marine sediments of Taranto Gulf (Ionian Sea, Southern Italy), Mar. Chem. 99 (2006) 227-235.
[418] K. Schiff, D. Diehl, A. Valkirs, Copper emissions from antifouling paint on recreational vessels, Mar. Pollut. Bull. 48 (2004) 371-377.
[419] C. Alzieu, Environmental problems caused by TBT in France: assessment, regulations, prospects, Mar. Environ. Res. 32 (1991) 7-17.
[420] K.V. Thomas, S. Brooks, The environmental fate and effects of antifouling paint biocides, Biofouling. 26 (2010) 73-88.

[421] L.D. Chambers, K.R. Stokes, F.C. Walsh, R.J.K. Wood, Modern approaches to marine antifouling coatings, Surface and Coatings Technology. 201 (2006) 3642-3652.
[422] R. Brown, T. Galloway, D. Lowe, M. Browne, A. Dissanayake, M. Jones, M. Depledge, Differential sensitivity of three marine invertebrates to copper assessed using multiple biomarkers, Aquat. Toxicol. 66 (2004) 267-278.
[423] B. Volesky, Detoxification of metal-bearing effluents: biosorption for the next century, Hydrometallurgy. 59 (2001) 203-216.
[424] P.-S. Li, H.-C. Tao, Cell surface engineering of microorganisms towards adsorption of heavy metals, Crit. Rev. Microbiol. 41 (2015) 140-149.
[425] B. Volesky, Z. Holan, Biosorption of heavy metals, Biotechnol. Progr. 11 (1995) 235-250.
[426] H.D. Utomo, K.X.D. Tan, Z.Y.D. Choong, J.J. Yu, J.J. Ong, Z.B. Lim, Biosorption of heavy metal by algae biomass in surface water, Journal of Environmental Protection. 7 (2016) 1547-1560.
[427] C. Mack, B. Wilhelmi, J.R. Duncan, J.E. Burgess, Biosorption of precious metals, Biotechnol. Adv. 25 (2007) 264-271.
[428] F. Veglio, F. Beolchini, Removal of metals by biosorption: a review, Hydrometallurgy. 44 (1997) 301-316.
[429] D. Park, Y.-S. Yun, J.M. Park, The past, present, and future trends of biosorption, Biotechnology and Bioprocess Engineering. 15 (2010) 86-102.
[430] K. Chojnacka, Biosorption and bioaccumulation – the prospects for practical applications, Environ. Int. 36 (2010) 299-307.
[431] G.M. Gadd, Bioremedial potential of microbial mechanisms of metal mobilization and immobilization, Curr. Opin. Biotech. 11 (2000) 271-279.
[432] C.-J. Tien, Biosorption of metal ions by freshwater algae with different surface characteristics, Process Biochem. 38 (2002) 605-613.
[433] T.A. Davis, B. Volesky, A. Mucci, A review of the biochemistry of heavy metal biosorption by brown algae, Water Res. 37 (2003) 4311-4330.
[434] M.C. Meinert, D.P. Delmer, Changes in biochemical composition of the cell wall of the cotton fiber during development, Plant Physiol. 59 (1977) 1088-1097.
[435] Z.A. Popper, M.-C. Ralet, D.S. Domozych, Plant and algal cell walls: diversity and functionality, Ann. Bot. 114 (2014) 1043-1048.
[436] S. Jasrotia, A. Kansal, V.V.N. Kishore, Arsenic phyco-remediation by *Cladophora* algae and measurement of arsenic speciation and location of active absorption site using electron microscopy, Microchem. J. 114 (2014) 197-202.
[437] I. Michalak, K. Chojnacka, K. Marycz, Using ICP-OES and SEM-EDX in biosorption studies, Microchimica Acta. 172 (2011) 65-74.
[438] S. Rangabhashiyam, E. Suganya, A.V. Lity, N. Selvaraju, Equilibrium and kinetics studies of hexavalent chromium biosorption on a novel green macroalgae *Enteromorpha* sp, Res. Chem. Intermediat. 42 (2016) 1275-1294.
[439] J.A. Raven, M.C.W. Evans, R.E. Korb, The role of trace metals in photosynthetic electron transport in O2-evolving organisms, Photosynth. Res. 60 (1999) 111-150.
[440] I. Langmuir, The adsorption of gases on plane surfaces of glass, mica and platinum, J. Am. Chem. Soc. 40 (1918) 1361-1403.
[441] H. Freundlich, Über die adsorption in lösungen, Zeitschrift für physikalische Chemie. 57 (1907) 385-470.
[442] C. Ng, J.N. Losso, W.E. Marshall, R.M. Rao, Freundlich adsorption isotherms of agricultural by-product-based powdered activated carbons in a geosmin–water system, Bioresource Technol. 85 (2002) 131-135.

[443] P. Sánchez-Marín, C. Fortin, P.G.C. Campbell, Lead (Pb) and copper (Cu) share a common uptake transporter in the unicellular alga *Chlamydomonas reinhardtii*, Biometals. 27 (2014) 173-181.
[444] M.J. Hall, M.T. Brown, Copper and manganese influence the uptake of cadmium in marine macroalgae, B. Environ. Contam. Tox. 68 (2002) 49-55.
[445] I.A.M. Worms, K.J. Wilkinson, Ni uptake by a green alga. 2. Validation of equilibrium models for competition effects, Environ. Sci. Technol. 41 (2007) 4264-4270.
[446] J. Kennedy, Carbohydrate chemistry, Clarendon Press, Oxford, 1988
[447] E.T. Reese, Advances in enzymatic hydrolysis of cellulose and related materials, Pergamon Press, Oxford, 1962
[448] J.A. Gascoigne, M. Gascoigne, Biological degradation of cellulose, in: J. Cook, M. Stacey (Eds.), Butterworths, London, 1960.
[449] J.F. Kennedy, C.A. White, Bioactive carbohydrates: in chemistry, biochemistry and biology, Ellis Horwood Ltd., Chichester, 1983
[450] K. Ballschmiter, J.J. Katz, Infrared study of chlorophyll-chlorophyll and chlorophyll-water interactions, J. Am. Chem. Soc. 91 (1969) 2661-2677.
[451] B.t. Schoefs, Chlorophyll and carotenoid analysis in food products. Properties of the pigments and methods of analysis, Trends Food Sci. Tech. 13 (2002) 361-371.
[452] R.K. Hocking, R. Brimblecombe, L.-Y. Chang, A. Singh, M.H. Cheah, C. Glover, W.H. Casey, L. Spiccia, Water-oxidation catalysis by manganese in a geochemical-like cycle, Nature Chemistry. 3 (2011) 461-466.
[453] G.W. Garnham, G.A. Codd, G.M. Gadd, Kinetics of uptake and intracellular location of cobalt, manganese and zinc in the estuarine green alga *Chlorella salina*, Appl. Microbiol. Biot. 37 (1992) 270-276.
[454] Z. Movasaghi, S. Rehman, D.I. ur Rehman, Fourier Transform Infrared (FTIR) spectroscopy of biological tissues, Appl. Spectrosc. Rev. 43 (2008) 134-179.
[455] J.J. Mayers, K.J. Flynn, R.J. Shields, Rapid determination of bulk microalgal biochemical composition by Fourier-Transform Infrared spectroscopy, Bioresource Technol. 148 (2013) 215-220.
[456] P. Griffiths, Introduction to vibrational spectroscopy, in: J. Chalmers, P. Griffiths (Eds.) Handbook of vibrational spectroscopy, John Wiley and Sons, Chichester, 2002, pp. 33-44.
[457] D.H. Williams, I. Fleming, Spectroscopic methods in organic chemistry, McGraw-Hill, 1980
[458] P. Griffiths, Beer's Law, in: J. Chalmers, P. Griffiths (Eds.) Handbook of Vibrational Spectroscopy, John Wiley and Sons, Chichester, 2002, pp. 2225-2235.
[459] K. Stehfest, J. Toepel, C. Wilhelm, The application of micro-FTIR spectroscopy to analyze nutrient stress-related changes in biomass composition of phytoplankton algae, Plant Physiol. Bioch. 43 (2005) 717-726.
[460] A.P. Dean, D.C. Sigee, B. Estrada, J.K. Pittman, Using FTIR spectroscopy for rapid determination of lipid accumulation in response to nitrogen limitation in freshwater microalgae, Bioresource Technol. 101 (2010) 4499-4507.
[461] D. Ami, R. Posteri, P. Mereghetti, D. Porro, S.M. Doglia, P. Branduardi, Fourier transform infrared spectroscopy as a method to study lipid accumulation in oleaginous yeasts, Biotechnology for Biofuels. 7 (2014) 12.
[462] D.Y. Duygu, A.U. Udoh, T.B. Ozer, A. Akbulut, I.A. Erkaya, K. Yildiz, D. Guler, Fourier transform infrared (FTIR) spectroscopy for identification of *Chlorella vulgaris* Beijerinck 1890 and *Scenedesmus obliquus* (Turpin) Kützing 1833, African Journal of Biotechnology. 11 (2012) 3817-3824.

[463] J. Mayers, Investigating the physiological response and biochemical composition of the microalga *Nannochloropsis* sp. to varied nutrient supply and production strategies, Swansea University, 2014.
[464] Z. Filip, S. Herrmann, J. Kubat, FT-IR spectroscopic characteristics of differently cultivated *Bacillus subtilis*, Microbiol. Res. 159 (2004) 257-262.
[465] M.A. Saghiri, K. Asgar, M. Lotfi, K. Karamifar, A.M. Saghiri, P. Neelakantan, J.L. Gutmann, A. Sheibaninia, Back-scattered and secondary electron images of scanning electron microscopy in dentistry: a new method for surface analysis, Acta Odontol. Scand. 70 (2012) 603-609.
[466] J.J. Brand, D.W. Becker, Evidence for direct roles of calcium in photosynthesis, J. Bioenerg. Biomembr. 16 (1984) 239-249.
[467] H. Mizuta, H. Yasui, Protective function of silicon deposition in *Saccharina japonica* sporophytes (Phaeophyceae), J. Appl. Phycol. 24 (2012) 1177-1182.
[468] C.S. Sikes, Calcium and cation sorption by *Cladophora* from the Great Lakes, J. Great Lakes Res. 3 (1977) 100-105.
[469] C. Critchley, The role of chloride in Photosystem II, BBA-Bioenergetics. 811 (1985) 33-46.
[470] J. Talling, Potassium—a non-limiting nutrient in fresh waters?, Freshwater Reviews. 3 (2010) 97-104.
[471] B. Southichak, K. Nakano, M. Nomura, N. Chiba, O. Nishimura, Marine macroalga *Sargassum horneri* as biosorbent for heavy metal removal: roles of calcium in ion exchange mechanism, Water Sci. Technol. 58 (2008) 697-704.
[472] J.A. Raven, The transport and fucntion of silicon in plants, Biol. Rev. 58 (1983) 179-207.
[473] L.F. Moore, J.A. Traquair, Silicon, a required nutrient for *Cladophora glomerata* (L) Kütz. (Chlorophyta), Planta. 128 (1976) 179-182.
[474] C.E. Hamm, R. Merkel, O. Springer, P. Jurkojc, Architecture and material properties of diatom shells provide effective mechanical protection, Nature. 421 (2003) 841-843.
[475] Y. Liang, W. Sun, Y.-G. Zhu, P. Christie, Mechanisms of silicon-mediated alleviation of abiotic stresses in higher plants: a review, Environ. Pollut. 147 (2007) 422-428.
[476] H.S. Lee, Biosorption of Cr, Cu and Al by *Sargassum* biomass, Biotechnology and Bioprocess Engineering. 2 (1997) 126-131.
[477] G. Ozdemir, S.H. Baysal, Chromium and aluminum biosorption on *Chryseomonas luteola* TEM05, Appl. Microbiol. Biot. 64 (2004) 599-603.
[478] A. Sarı, M. Tuzen, Equilibrium, thermodynamic and kinetic studies on aluminum biosorption from aqueous solution by brown algae (*Padina pavonica*) biomass, J. Hazard. Mater. 171 (2009) 973-979.
[479] R.H. Crist, K. Oberholser, J. McGarrity, D.R. Crist, J.K. Johnson, J.M. Brittsan, Interaction of metals and protons with algae. 3. Marine algae, with emphasis on lead and aluminum, Environ. Sci. Technol. 26 (1992) 496-502.
[480] M. Rajfur, A. Kłos, M. Wacławek, Sorption properties of algae *Spirogyra* sp. and their use for determination of heavy metal ions concentrations in surface water, Bioelectrochemistry. 80 (2010) 81-86.
[481] J. Yang, J. Cao, G. Xing, H. Yuan, Lipid production combined with biosorption and bioaccumulation of cadmium, copper, manganese and zinc by oleaginous microalgae *Chlorella minutissima* UTEX2341, Bioresource Technol. 175 (2015) 537-544.

[482] K. Wang, Y. Liu, D. Li, Biosorption of copper by cyanobacterial bloom-derived biomass harvested from the eutrophic Lake Dianchi in China, Curr. Microbiol. 61 (2010) 340-345.
[483] A.S. Gilburn, Mechanical grooming and beach award status are associated with low strandline biodiversity in Scotland, Estuar. Coast. Shelf S. 107 (2012) 81-88.
[484] S.W. Won, J. Mao, I.-S. Kwak, M. Sathishkumar, Y.-S. Yun, Platinum recovery from ICP wastewater by a combined method of biosorption and incineration, Bioresource Technol. 101 (2010) 1135-1140.
[485] D. Aleynik, M.E. Inall, A. Dale, A. Vink, Impact of remotely generated eddies on plume dispersion at abyssal mining sites in the Pacific, Scientific Reports. 7 (2017) 16959.
[486] J.R. Hein, K. Mizell, A. Koschinsky, T.A. Conrad, Deep-ocean mineral deposits as a source of critical metals for high- and green-technology applications: Comparison with land-based resources, Ore Geol. Rev. 51 (2013) 1-14.
[487] V.K. Mishra, A.R. Upadhyaya, S.K. Pandey, B.D. Tripathi, Heavy metal pollution induced due to coal mining effluent on surrounding aquatic ecosystem and its management through naturally occurring aquatic macrophytes, Bioresource Technol. 99 (2008) 930-936.
[488] G.I. Paton, G. Palmer, A. Kindness, C. Campbell, L.A. Glover, K. Killham, Use of luminescence-marked bacteria to assess copper bioavailability in malt whisky distillery effluent, Chemosphere. 31 (1995) 3217-3224.
[489] S.J. Takouridis, D.E. Tribe, S.L. Gras, G.J.O. Martin, The selective breeding of the freshwater microalga *Chlamydomonas reinhardtii* for growth in salinity, Bioresource Technol. 184 (2015) 18-22.
[490] K. Yamada, H. Suzuki, T. Takeuchi, Y. Kazama, S. Mitra, T. Abe, K. Goda, K. Suzuki, O. Iwata, Efficient selective breeding of live oil-rich *Euglena gracilis* with fluorescence-activated cell sorting, Scientific Reports. 6 (2016) 26327.
[491] D. Cordell, J.-O. Drangert, S. White, The story of phosphorus: Global food security and food for thought, Glob. Environ. Chang. 19 (2009) 292-305.
[492] E.D. Roy, P.D. Richards, L.A. Martinelli, L. Della Coletta, S.R.M. Lins, F.F. Vazquez, E. Willig, S.A. Spera, L.K. VanWey, S. Porder, The phosphorus cost of agricultural intensification in the tropics, Nature Plants. 2 (2016) 16043.
[493] A. Solovchenko, A.M. Verschoor, N.D. Jablonowski, L. Nedbal, Phosphorus from wastewater to crops: An alternative path involving microalgae, Biotechnol. Adv. 34 (2016) 550-564.
[494] L.A. Cifuentes, J.H. Sharp, M.L. Fogel, Stable carbon and nitrogen isotope biogeochemistry in the Delaware estuary, Limnol. Oceanogr. 33 (1988) 1102-1115.
[495] G.D. Farquhar, J.R. Ehleringer, K.T. Hubick, Carbon isotope discrimination and photosynthesis, Annual Review of Plant Biology. 40 (1989) 503-537.
[496] A. Andrade, M. Rollemberg, J. Nobrega, Proton and metal binding capacity of the green freshwater alga *Chaetophora elegans*, Process Biochem. 40 (2005) 1931-1936.
[497] W.G. Sunda, S.A. Huntsman, Interrelated influence of iron, light and cell size on marine phytoplankton growth, Nature. 390 (1997) 389.
[498] A. Nicklisch, P. Woitke, Pigment content of selected planktonic algae in response to simulated natural light fluctuations and a short photoperiod, Int. Rev. Hydrobiol. 84 (1999) 479-495.
[499] M.S. Chauton, L.M. Skolem, L.M. Olsen, P.E. Vullum, J. Walmsley, O. Vadstein, Titanium uptake and incorporation into silica nanostructures by the diatom *Pinnularia* sp. (Bacillariophyceae), J. Appl. Phycol. 27 (2015) 777-786.

[500] E. Van Eynde, Z.-Y. Hu, T. Tytgat, S. Verbruggen, J. Watté, G. Van Tendeloo, I. Van Driessche, R. Blust, S. Lenaerts, Diatom silica–titania photocatalysts for air purification by bio-accumulation of different titanium sources, Environmental Science: Nano. 3 (2016) 1052-1061.
[501] M. Petrović, S. Gonzalez, D. Barceló, Analysis and removal of emerging contaminants in wastewater and drinking water, TRAC-Trend. Anal. Chem. 22 (2003) 685-696.
[502] T.V.N. Padmesh, K. Vijayaraghavan, G. Sekaran, M. Velan, Batch and column studies on biosorption of acid dyes on fresh water macro alga *Azolla filiculoides*, J. Hazard. Mater. 125 (2005) 121-129.
[503] P. Bhattacharya, S. Lin, J.P. Turner, P.C. Ke, Physical adsorption of charged plastic nanoparticles affects algal photosynthesis, J. Phys. Chem. C. 114 (2010) 16556-16561.
[504] U. Yogev, K.R. Sowers, N. Mozes, A. Gross, Nitrogen and carbon balance in a novel near-zero water exchange saline recirculating aquaculture system, Aquaculture. 467 (2017) 118-126.
[505] J. Park, R. Craggs, Biogas production from anaerobic waste stabilisation ponds treating dairy and piggery wastewater in New Zealand, Water Sci. Ttechnol. 55 (2007) 257-264.
[506] J.J. Walsh, D.L. Jones, G. Edwards-Jones, A.P. Williams, Replacing inorganic fertilizer with anaerobic digestate may maintain agricultural productivity at less environmental cost, J. Plant Nutr. Soil Sc. 175 (2012) 840-845.
[507] J. Park, R. Craggs, Biogas production from anaerobic waste stabilisation ponds treating dairy and piggery wastewater in New Zealand, Water Sci. Technol. 55 (2007) 257-264.
[508] R.J. McGrath, I.G. Mason, An observational method for the assessment of biogas production from an anaerobic waste stabilisation pond treating farm dairy wastewater, Biosystems Engineering. 87 (2004) 471-478.
[509] G. Lastella, C. Testa, G. Cornacchia, M. Notornicola, F. Voltasio, V.K. Sharma, Anaerobic digestion of semi-solid organic waste: biogas production and its purification, Energ. Convers. Manage. 43 (2002) 63-75.
[510] J. Doucha, F. Straka, K. Lívanský, Utilization of flue gas for cultivation of microalgae (*Chlorella* sp.) in an outdoor open thin-layer photobioreactor, J. Appl. Phycol. 17 (2005) 403-412.
[511] D. Aitken, C. Bulboa, A. Godoy-Faundez, J.L. Turrion-Gomez, B. Antizar-Ladislao, Life cycle assessment of macroalgae cultivation and processing for biofuel production, Journal of Cleaner Production. 75 (2014) 45-56.
[512] A.D. Hughes, M.S. Kelly, K.D. Black, M.S. Stanley, Biogas from Macroalgae: is it time to revisit the idea?, Biotechnology for Biofuels. 5 (2012) 86.
[513] Y. Zhou, H. Yang, S. Liu, X. Yuan, Y. Mao, Y. Liu, X. Xu, F. Zhang, Feeding and growth on bivalve biodeposits by the deposit feeder *Stichopus japonicus* Selenka (Echinodermata: Holothuroidea) co-cultured in lantern nets, Aquaculture. 256 (2006) 510-520.
[514] P.F. Mulvenna, G. Savidge, A modified manual method for the determination of urea in seawater using diacetylmonoxime reagent, Estuar. Coast. Shelf Sci. 34 (1992) 429-438.
[515] M. Duncan, P. Harrison, Comparison of solvents for extracting chlorophylls from marine macrophytes, Bot. Mar. 25 (1982) 445-448.

[516] T. Vimala, T. Poonghuzhali, Estimation of Pigments from Seaweeds by Using Acetone and DMSO, International Journal of Science and Research. 4 (2014) 1850-1854.
[517] J. Schmitt, H.-C. Flemming, FTIR-spectroscopy in microbial and material analysis, Int. Biodeter. Biodegr. 41 (1998) 1-11.
[518] M. Poletto, V. Pistor, A.J. Zattera, Structural characteristics and thermal properties of native cellulose, Cellulose-fundamental Aspects. (2013) 45-68.
[519] M. Poletto, A.J. Zattera, R. Santana, Structural differences between wood species: evidence from chemical composition, FTIR spectroscopy, and thermogravimetric analysis, J. Appl. Polym. Sci. 126 (2012).
[520] C.M. Simonescu, Application of FTIR spectroscopy in environmental studies, Advanced Aspects of Spectroscopy, InTech, 2012.
[521] M. Fan, D. Dai, B. Huang, Fourier transform infrared spectroscopy for natural fibres, Fourier Transform–Materials Analysis. (2012).
[522] Ochem Online, Infrared spectrooscopy absorption table (2011) Accessed on: 31/07/2017, http://www.ochemonline.com/Infrared_spectroscopy_absorption_table
[523] H. Schulz, M. Baranska, Identification and quantification of valuable plant substances by IR and Raman spectroscopy, Vib. Spectrosc. 43 (2007) 13-25.
[524] K. Kato, M. Nitta, T. Mizuno, Infrared spectroscopy of some mannans, Agr. Biol. Chem. Tokyo. 37 (1973) 433-435.
[525] S. Gunasekaran, E. Sailatha, S. Seshadri, S. Kumaresan, FTIR, FT Raman spectra and molecular structural confirmation of isoniazid, Indian J. Pure Ap. Phy. 47 (2009) 12-18.
[526] K. Dokken, L.E. Erickson, S. Castro, Fourier-transform infrared spectroscopy as a tool to monitor changes in plant structure in response to soil contaminants, Proceedings- Waste Res. Technol. 7 (2002).

# Appendices

## Appendix A – Media Recipes

**Table A1.** Recipe for Guillard's f/2 Medium.

| **Stock A - Nitrogen** | **(g $L^{-1}$)** |
|---|---|
| $NaNO_3$ | 75 |
| **Stock B - Phosphorus** | **(g $L^{-1}$)** |
| $NaH_2PO_4 \cdot 2H_2O$ | 5.65 |
| **Stock C – Trace Metals** | **(mg $L^{-1}$)** |
| $Na_2EDTA$ | 4160 |
| $FeCl_3 \cdot 6H_2O$ | 3150 |
| $CuSO_4 \cdot 5H_2O$ | 10 |
| $ZnSO_4 \cdot 7H_2O$ | 22 |
| $CoCl_2 \cdot 6H_2O$ | 10 |
| $MnCl_2 \cdot 4H_2O$ | 180 |
| $Na_2MoO_4 \cdot 2H_2O$ | 6 |
| **Stock D - Buffer** | **(g $L^{-1}$)** |
| Tric-HCl | 63.04 |
| **Stock E - Vitamins** | **(mg 100 $mL^{-1}$)** |
| Thiamine HCl (Vit $B_1$) | 10 |
| Cyanocobalamin (Vit $B_{12}$) | 0.05 |
| Biotin | 0.05 |
| **Media Formulation** | **(mL $L^{-1}$)** |
| Stock A | 1 |
| Stock B | 1 |
| Stock C | 1 |
| Stock D | 5 |
| Stock E | 1 |

**Notes**

- Stock D pH = 5.65
- To ~ 900 mL of artifical seawater (33.5 g $L^{-1}$), add stocks A-D. Bring volume to 1L and sterilise (*i.e.* 121°C for 15 minutes, in an autoclave). Once cooled to room temperature, add Stock E and adjust pH to 8.0 using 0.1 M HCl or NaOH.
- Keep stock solutions refrigerated

**Table A2.** Recipe for Jaworski's Medium.

| **Stock A** | **(g $L^{-1}$)** |
|---|---|
| $Ca(NO_3)_2 \cdot 4H_2O$ | 20 |
| **Stock B** | **(g $L^{-1}$)** |
| $KH_2PO_4$ | 12.4 |
| **Stock C** | **(g $L^{-1}$)** |
| $MgSO_4 \cdot 7H_2O$ | 50 |
| **Stock D** | **(g $L^{-1}$)** |
| $NaHCO_3$ | 15.9 |
| **Stock E** | **(g $L^{-1}$)** |
| EDTA-FeNa | 2.25 |
| $Na_2EDTA$ | 2.25 |
| **Stock F** | **(g $L^{-1}$)** |
| $H_3BO_3$ | 2.48 |
| $MnCl_2 \cdot 4H_2O$ | 1.39 |
| $(NH_4)6Mo_7O_{24} \cdot 4H_2O$ | 1 |
| **Stock G** | **(g $L^{-1}$)** |
| $NaNO_3$ | 80 |
| **Stock H** | **(g $L^{-1}$)** |
| $Na_2HPO_4 \cdot 12H_2O$ | 36 |
| **Stock I** | **(g $L^{-1}$)** |
| Tris-HCl | 63.04 |
| **Stock J** | **(mg 100 $mL^{-1}$)** |
| Thiamine HCl (Vit $B_1$) | 4 |
| Cyanocobalamin (Vit $B_{12}$) | 4 |
| Biotin | 4 |
| **Media Formulation** | **(mL $L^{-1}$)** |
| Stocks A-J | 1 |

**Notes**

- Stock D pH = 5.65
- To ~ 900 mL of deionised seawater , add stocks A-I. Bring volume to 1L and sterilise (i.e. 121°C for 15 minutes, in an autoclave). Once cooled to room temperature, add Stock J and adjust pH to 8.0 using 0.1 M HCl or NaOH.
- Keep stock solutions refrigerated

# Appendix B – Test-Kit Instructions

7.75731.0004-xxxxxxxxxx msp.

December 2013

1.00683.0001

Spectroquant®

## Ammonium Test

$NH_4^+$

### 1. Method

Ammonium nitrogen ($NH_4$-**N**) occurs partly in the form of ammonium ions and partly as ammonia. A pH-dependent equilibrium exists between the two forms. In strongly alkaline solution ammonium nitrogen is present almost entirely as ammonia, which reacts with hypochlorite ions to form monochloramine. This in turn reacts with a substituted phenol to form a blue indophenol derivative that is determined photometrically. Due to the intrinsic yellow coloration of the reagent blank, the measurement solution is yellow-green to green in color.
**The method is analogous to EPA 350.1, APHA 4500-$NH_3$ F, ISO 7150-1, and DIN 38406-5.**

### 2. Measuring range and number of determinations

| Cell | Measuring range | | Number of determinations |
|---|---|---|---|
| mm | mg/l $NH_4$-N | mg/l $NH_4^+$ | |
| 10 | 2.0 - 75.0 | 2.6 - 96.6 | 100 |
| | 5 - 150 | 6 - 193 | |

For programming data for selected photometers / spectrophotometers see www.service-test-kits.com.

### 3. Applications

This test measures both ammonium ions and dissolved ammonia.

**Sample material:**
Groundwater and surface water, seawater
Drinking water
Wastewater
Nutrient solutions for fertilization
Soils and food after appropriate sample pretreatment

### 4. Influence of foreign substances

This was checked in solutions containing 40 and 0 mg/l $NH_4$-N. The determination is not yet interfered with up to the concentrations of foreign substances given in the table.

| Concentrations of foreign substances in mg/l or % | | | | | |
|---|---|---|---|---|---|
| $Al^{3+}$ | 1000 | $Mn^{2+}$ | 100 | EDTA | 1000 |
| $Ca^{2+}$ | 1000 | $Ni^{2+}$ | 250 | **Primary amines**[1] | **0** |
| $Cd^{2+}$ | 1000 | $NO_3^-$ | 1000 | Secondary amines[2] | 250 |
| $CN^-$ | 100 | $Pb^{2+}$ | 1000 | **Aminophenols** | **10** |
| $Cr^{3+}$ | 100 | $PO_4^{3-}$ | 1000 | Aniline | 50 |
| $Cr_2O_7^{2-}$ | 1000 | $S^{2-}$ | 50 | Triethanolamine | 1000 |
| $Cu^{2+}$ | 1000 | $SiO_3^{2-}$ | 1000 | Surfactants[3] | 1000 |
| $F^-$ | 1000 | $Zn^{2+}$ | 500 | Na-acetate | 10 % |
| $Fe^{3+}$ | 25 | | | NaCl | 20 % |
| $Hg^{2+}$ | 500 | | | $NaNO_3$ | 20 % |
| $Mg^{2+}$ | 500 | | | $Na_2SO_4$ | 20 % |

Reducing agents interfere with the determination.
[1] tested with methylamine
[2] tested with dimethylamine
[3] tested with nonionic, cationic, and anionic surfactants

### 5. Reagents and auxiliaries

**Please note the warnings on the packaging materials!**

The test reagents stable up to the date stated on the pack when stored closed at +15 to +25 °C.

**Package contents:**
1 bottle of reagent $NH_4$-1
1 bottle of reagent $NH_4$-2 (contains granulate + desiccant capsule)
2 AutoSelectors

**Other reagents and accessories:**
MQuant™ Ammonium Test, Cat. No. 110024,
measuring range 10 - 400 mg/l $NH_4^+$ (8 - 310 mg/l $NH_4$-N)
MColorpHast™ Universal indicator strips pH 0 - 14, Cat. No. 109535
Sodium hydroxide solution 1 mol/l TitriPUR®, Cat. No. 109137
Sulfuric acid 0.5 mol/l TitriPUR®, Cat. No. 109072
Spectroquant® CombiCheck 70, Cat. No. 114689
Ammonium standard solution CRM, 6.00 mg/l $NH_4$-N, Cat. No. 125025
Ammonium standard solution CRM, 12.0 mg/l $NH_4$-N, Cat. No. 125026
Ammonium standard solution CRM, 50.0 mg/l $NH_4$-N, Cat. No. 125027

Pipettes for pipetting volumes of 0.10, 0.20, and 5.0 ml
Rectangular cells 10 mm (2 pcs), Cat. No. 114946

### 6. Preparation

- Rinse glassware ammonium-free with distilled water. **Do not use detergent!**
- Analyze immediately after sampling.
- Check the ammonium content with the MQuant™ Ammonium Test. Samples containing more than 150 mg/l $NH_4$-N must be diluted with distilled water.
- **The pH must be within the range 4 - 13.** Adjust, if necessary, with sodium hydroxide solution or sulfuric acid.
- Filter turbid samples.

### 7. Procedure

**Measuring range 2.0 - 75.0 mg/l $NH_4$-N (2.6 - 96.6 mg/l $NH_4^+$):**

| | | |
|---|---|---|
| Reagent $NH_4$-1 (20 - 30 °C) | 5,0 ml | Pipette into a test tube. |
| Pretreated sample (20 - 30 °C) | **0,20 ml** | Add with pipette and mix. |
| Reagent $NH_4$-2 | 1 level blue microspoon (in the cap of the $NH_4$-2 bottle) | Add and shake **vigorously until the reagent is completely dissolved.** |
| **Leave to stand for 15 min (reaction time)**, then fill the sample into a 10-mm cell, and measure in the photometer. | | |

**Measuring range 5 - 150 mg/l $NH_4$-N (6 - 193 mg/l $NH_4^+$):**

| | | |
|---|---|---|
| Reagent $NH_4$-1 (20 - 30 °C) | 5,0 ml | Pipette into a test tube. |
| Pretreated sample (20 - 30 °C) | **0,10 ml** | Add with pipette and mix. |
| Reagent $NH_4$-2 | 1 level blue microspoon (in the cap of the $NH_4$-2 bottle) | Add and shake **vigorously until the reagent is completely dissolved.** |
| **Leave to stand for 15 min (reaction time)**, then fill the sample into a 10-mm cell, and measure in the photometer. | | |

**Notes on the measurement:**

- Due to the strong temperature dependence of the color reaction, the temperature of the reagents should be between 20 and 30 °C.
- **Certain photometers may require a blank** (preparation as per measurement sample, but with distilled water instead of sample).
- For photometric measurement the cells must be clean. Wipe, if necessary, with a clean dry cloth.
- Measurement of turbid solutions yields false-high readings.
- Ammonium-free samples turn yellow on addition of reagent $NH_4$-2.
- The pH of the measurement solution must be within the range 11.5 - 11.8.
- The color of the measurement solution remains stable for at least 60 min after the end of the reaction time stated above.
- In the event of ammonium concentrations exceeding 2500 mg/l, other reaction products are formed and false-low readings are yielded. In such cases it is advisable to conduct a plausibility check of the measurement results by diluting the sample (1:10, 1:100).

### 8. Analytical quality assurance

recommended before each measurement series
To check the photometric measurement system (test reagent, measurement device, handling) and the mode of working, the ammonium standard solutions CRM, 6.00 mg/l $NH_4$-N (Cat. No. 125025), 12.0 mg/l $NH_4$-N (Cat. No. 125026), and 50.0 mg/l $NH_4$-N (Cat. No. 125027) or Spectroquant® CombiCheck 70 can be used. Besides a **standard solution** with 50.0 mg/l $NH_4$-N, CombiCheck 70 also contains an **addition solution** for determining sample-dependent interferences (matrix effects).
Additional notes see under **www.qa-test-kits.com**.

**Characteristic quality data:**
In the production control, the following data were determined in accordance with ISO 8466-1 and DIN 38402 A51:

| | Measuring range mg/l $NH_4$-N | |
|---|---|---|
| | 2.0 - 75.0 | 5 - 150 |
| Standard deviation of the method (mg/l $NH_4$-N) | ± 0.48 | ± 1.0 |
| Coefficient of variation of the method (%) | ± 1.2 | ± 1.2 |
| Confidence interval (mg/l $NH_4$-N) | ± 1.2 | ± 2 |
| Number of lots | 23 | 23 |

**Characteristic data of the procedure:**

| | Measuring range mg/l $NH_4$-N | |
|---|---|---|
| | 2.0 - 75.0 | 5 - 150 |
| Sensitivity: Absorbance 0.010 A corresponds to (mg/l $NH_4$-N) | 0.3 | 1 |
| Accuracy of a measurement value (mg/l $NH_4$-N) | max. ± 1.7 | max. ± 3 |

For quality and batch certificates for Spectroquant® test kits see the website.

### 9. Notes

- Reclose the reagent bottles immediately after use.
- **Information on disposal can be obtained at www.disposal-test-kits.com.**

Merck KGaA, 64271 Darmstadt, Germany,
Tel. +49(0)6151 72-2440
www.analytical-test-kits.com

EMD Millipore Corporation, 290 Concord Road,
Billerica, MA 01821, USA, Tel. +1-978-715-4321

**Figure B1.** Spectroquant® manufacturer's instructions for the $NH_4^+$ test-kit.

7.75041.0004-8001527826 msp.

July 2013

**1.14848.0001**
**1.14848.0002**

Spectroquant®

# Phosphate Test

**P**

**for the determination of orthophosphate**

## 1. Method

In sulfuric solution orthophosphate ions react with molybdate ions to form molybdophosphoric acid. Ascorbic acid reduces this to phosphomolybdenum blue (PMB) that is determined photometrically.
**The method is analogous to EPA 365.2+3, APHA 4500-P E, and DIN EN ISO 6878.**

## 2. Measuring range and number of determinations

| Cell | Measuring range | | | Number of determinations |
|---|---|---|---|---|
| mm | mg/l $PO_4$-P | mg/l $PO_4^{3-}$ | mg/l $P_2O_5$ | |
| 50 | 0.010 - 1.000 | 0.03 - 3.07 | 0.02 - 2.29 | 220 (Cat. No. 1.14848.0002) or 420 (Cat. No. 1.14848.0001) |
| 20 | 0.03 - 2.50 | 0.09 - 7.67 | 0.07 - 5.73 | |
| 10 | 0.05 - 5.00 | 0.2 - 15.3 | 0.11 - 11.46 | |

For programming data for selected photometers / spectrophotometers see www.service-test-kits.com.

## 3. Applications

This test measures only orthophosphate. Samples must be decomposed by digestion before total phosphorus can be measured (see section 6).

**Sample material:**
Groundwater and surface water, seawater
Drinking water
Wastewater
Nutrient solutions for fertilization
Soils after appropriate sample pretreatment
Food after appropriate sample pretreatment

## 4. Influence of foreign substances

This was checked in solutions containing 2 and 0 mg/l $PO_4$-P. The determination is not yet interfered with up to the concentrations of foreign substances given in the table.

| Concentrations of foreign substances in mg/l or % | | | | | | | |
|---|---|---|---|---|---|---|---|
| $Ag^+$ | 1000 | $F^-$ | 50 | $Pb^{2+}$ | 25 | EDTA | 1000 |
| $AsO_4^{3-}$ | 0.2 | $Fe^{3+}$ | 1000 | $S^{2-}$ | 2.5 | Surfactants[1] | 100 |
| $Ca^{2+}$ | 1000 | $Hg^{2+}$ | 10 | $SiO_3^{2-}$ | 1000 | COD (K-hydrogen phthalate) | 150 |
| $Cd^{2+}$ | 1000 | $Mg^{2+}$ | 1000 | $SO_4^{2-}$ | 1000 | Na-acetate | 1 % |
| $CN^-$ | 1000 | $Mn^{2+}$ | 1000 | $Zn^{2+}$ | 1000 | NaCl | 5 % |
| $Cr^{3+}$ | 1000 | $NH_4^+$ | 1000 | | | $NaNO_3$ | 10 % |
| $Cr_2O_7^{2-}$ | 5 | $Ni^{2+}$ | 500 | | | $Na_2SO_4$ | 10 % |
| $Cu^{2+}$ | 250 | $NO_3^-$ | 1000 | | | | |

Reducing agents interfere with the determination.
[1] tested with nonionic, cationic, and anionic surfactants

## 5. Reagents and auxiliaries

**Please note the warnings on the packaging materials!**

The test reagents are stable up to the date stated on the pack when stored closed at +15 to +25 °C.

**Package contents:**
Reagent $PO_4$-1: 1 bottle (Cat. No. 1.14848.0002) or 2 bottles (Cat. No. 1.14848.0001)
Reagent $PO_4$-2: 1 bottle (Cat. No. 1.14848.0002) or 2 bottles (Cat. No. 1.14848.0001)
1 AutoSelector

**Other reagents and accessories:**
Spectroquant® Crack Set 10C, Cat. No. 114688
+ thermoreactor
or
Spectroquant® Crack Set 10, Cat. No. 114687
+ empty cells 16 mm with screw caps (25 pcs), Cat. No. 114724
+ thermoreactor
MQuant™ Phosphate Test, Cat. No. 110428,
measuring range 10 - 500 mg/l $PO_4^{3-}$ (3.3 - 163 mg/l $PO_4$-P)
MColorpHast™ Universal indicator strips pH 0 - 14, Cat. No. 109535
Sulfuric acid 0.5 mol/l TitriPUR®, Cat. No. 109072
Spectroquant® CombiCheck 10, Cat. No. 114676
Hydrochloric acid 25 % for analysis EMSURE®, Cat. No. 100316
Sodium hydroxide solution 1 mol/l (approx. 4 %) TitriPUR®, Cat. No. 109137

Pipette for a pipetting volume of 5.0 ml
Rectangular cells 10, 20, and 50 mm (2 of each), Cat. Nos. 114946, 114947, and 114944
Semi-microcells 50 mm (2 pcs), Cat. No. 173502

## 6. Preparation

- Use only phosphate-free detergents to rinse glassware. Otherwise fill with hydrochloric acid (approx. 10 %) and leave to stand for several hours.
- Analyze immediately after sampling.
- Total phosphorus can be determined after pretreatment of the sample using one of the Spectroquant® Crack Sets.
- Check the phosphate content with the MQuant™ Phosphate Test. Samples containing more than 5.00 mg/l $PO_4$-P must be diluted with distilled water prior to digestion.
- **The pH must be within the range 0 - 10.** Adjust, if necessary, with sulfuric acid.
- Filter turbid samples.

## 7. Procedure

| | | |
|---|---|---|
| Pretreated sample (10 - 35 °C) | 5.0 ml | Pipette into a test tube. |
| Reagent $PO_4$-1 | 5 drops[1] | Add and mix. |
| Reagent $PO_4$-2 | 1 level blue microspoon (in the cap of the $PO_4$-2 bottle) | Add and shake vigorously until the reagent is completely dissolved. |
| **Leave to stand for 5 min (reaction time)**, then fill the sample into the cell, and measure in the photometer. | | |

[1] **Hold the bottle vertically while adding the reagent!**

For measurement in the **50-mm cell** both the sample volume as well as the quantities of reagents $PO_4$-1 and $PO_4$-2 must be doubled. Alternatively, the semi-microcell Cat. No. 173502 can be used.

**Notes on the measurement:**

- **Certain photometers may require a blank** (preparation as per measurement sample, but with distilled water instead of sample). The blank is slightly yellow.
- For photometric measurement the cells must be clean. Wipe, if necessary, with a clean dry cloth.
- Measurement of turbid solutions yields false-high readings.
- The pH of the measurement solution must be within the range 0.80 - 0.95.
- The color of the measurement solution remains stable for at least 60 min after the end of the reaction time stated above.

## 8. Analytical quality assurance

recommended before each measurement series
To check the photometric measurement system (test reagents, measurement device, handling) and the mode of working, Spectroquant® CombiCheck 10 can be used. Besides a **standard solution** with 0.80 mg/l $PO_4$-P, this article also contains an **addition solution** for determining sample-dependent interferences (matrix effects).
Additional notes see under **www.qa-test-kits.com.**

**Characteristic quality data:**
In the production control, the following data were determined in accordance with ISO 8466-1 and DIN 38402 A51 (10-mm cell):

| | |
|---|---|
| Standard deviation of the method (mg/l $PO_4$-P) | ±0.029 |
| Coefficient of variation of the method (%) | ±1.2 |
| Confidence interval (mg/l $PO_4$-P) | ±0.06 |
| Number of lots | 41 |

**Characteristic data of the procedure:**

| | Measuring range mg/l $PO_4$-P | |
|---|---|---|
| | 0.010 - 1.000 | 0.05 - 5.00 |
| Sensitivity: Absorbance 0.010 A corresponds to (mg/l $PO_4$-P) | 0.004 | 0.02 |
| Accuracy of a measurement value (mg/l $PO_4$-P) | max. ± 0.016 | max. ± 0.08 |

For quality and batch certificates for Spectroquant® test kits see the website.

## 9. Notes

- Reclose the reagent bottles immediately after use.
- All glass surfaces coming into contact with the blue complex must be cleansed from time to time as follows: Fill the test tubes and the cells with sodium hydroxide solution (approx. 0.4 %) and leave to stand for max. 1 hour.
- **Information on disposal can be obtained at www.disposal-test-kits.com.**

Merck KGaA, 64271 Darmstadt, Germany,
Tel. +49(0)6151 72-3440
www.analytical-test-kits.com

EMD Millipore Corporation, 290 Concord Road,
Billerica, MA 01821, USA, Tel. +1-978-715-4321

**Figure B2.** Spectroquant® manufacturer's instructions for the $PO_4^{3-}$ test-kit.

# Appendix C – Calibration Curves

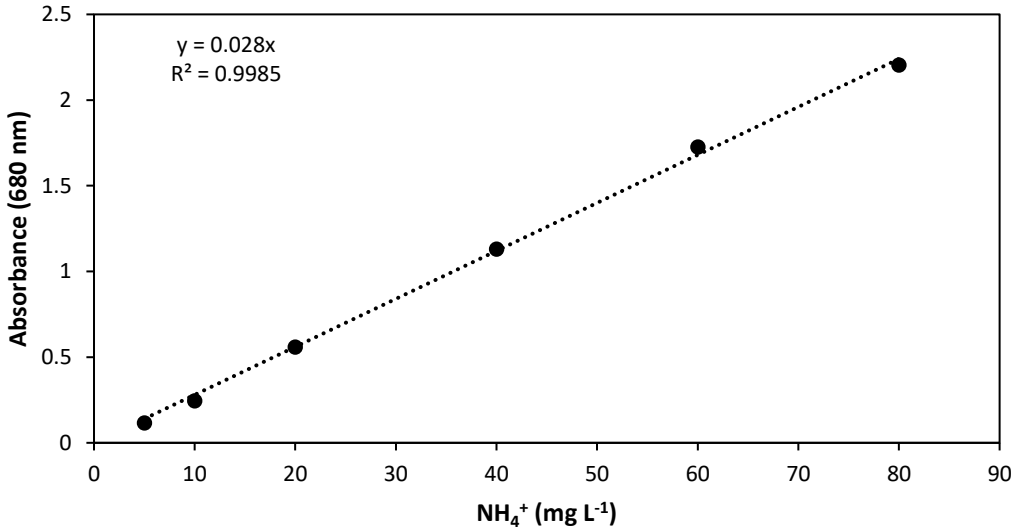


**Figure C1.** $NH_4^+$ calibration curve using a test-kit (1.00683.0001, Spectroquant®) and following the manufacturer's instructions (*n* = 3, *error bars* = 1 SD).

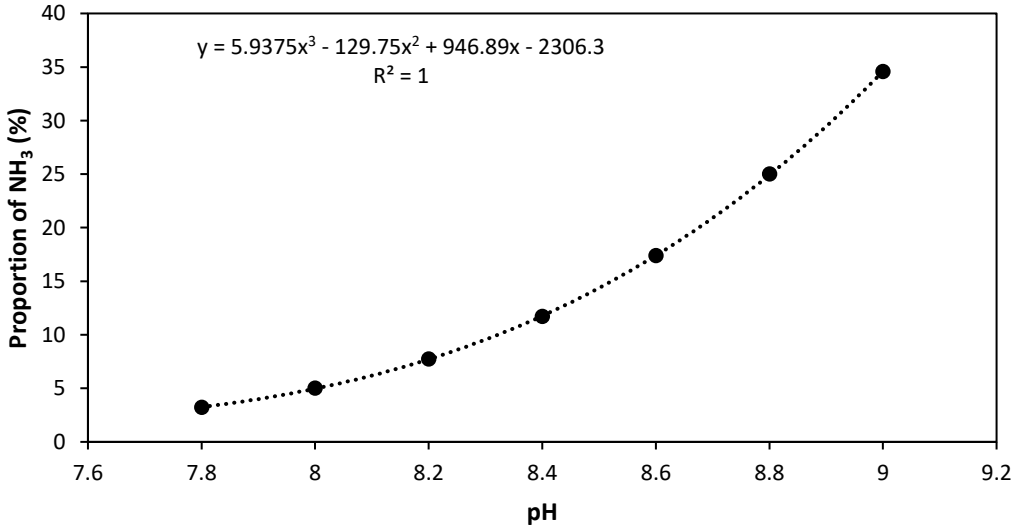


**Figure C2.** The proportion of free ammonia ($NH_3$) in the Total Ammonia Nitrogen (TAN) as a function of pH at a water temperature of 24°C. The equation of the curve follows a 3rd order polynomial trend.

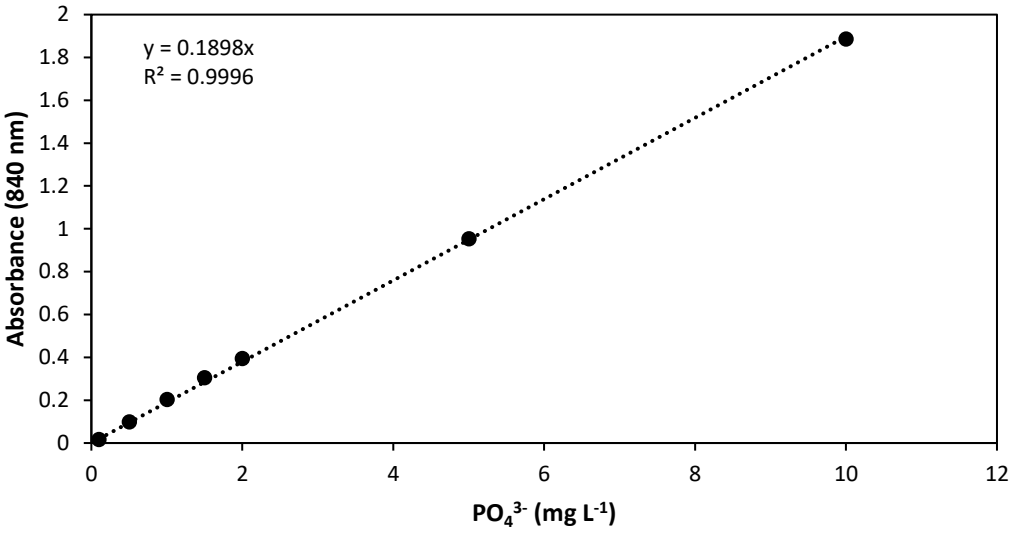


**Figure C3.** Phosphate calibration curve using a test-kit (1.14848.0001, Spectroquant®) and following the manufacturer's instructions (*n* = 3, *error bars* = 1 SD).

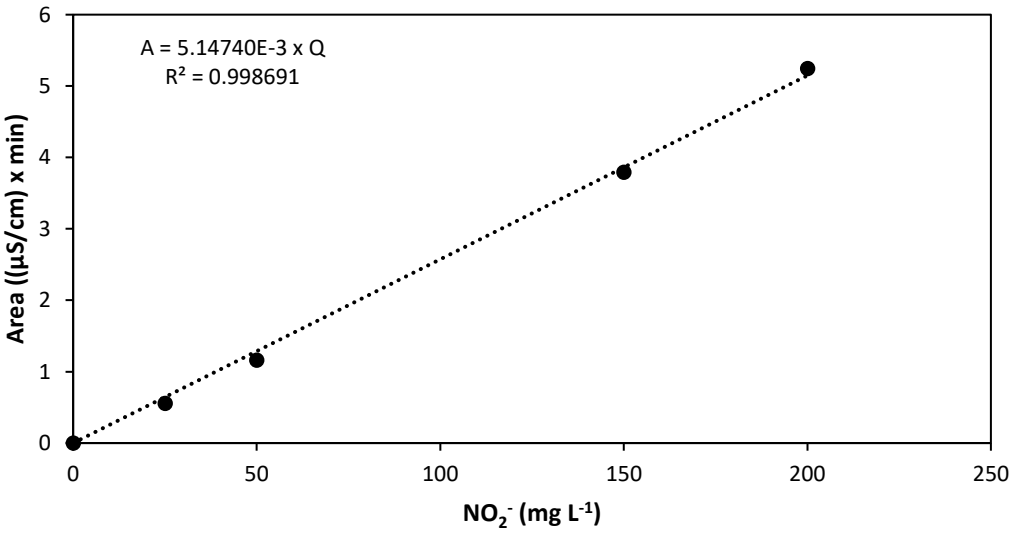


**Figure C4.** Nitrite calibration curve using ion chromatography, determined by manually integrating peak area across a concentration range.

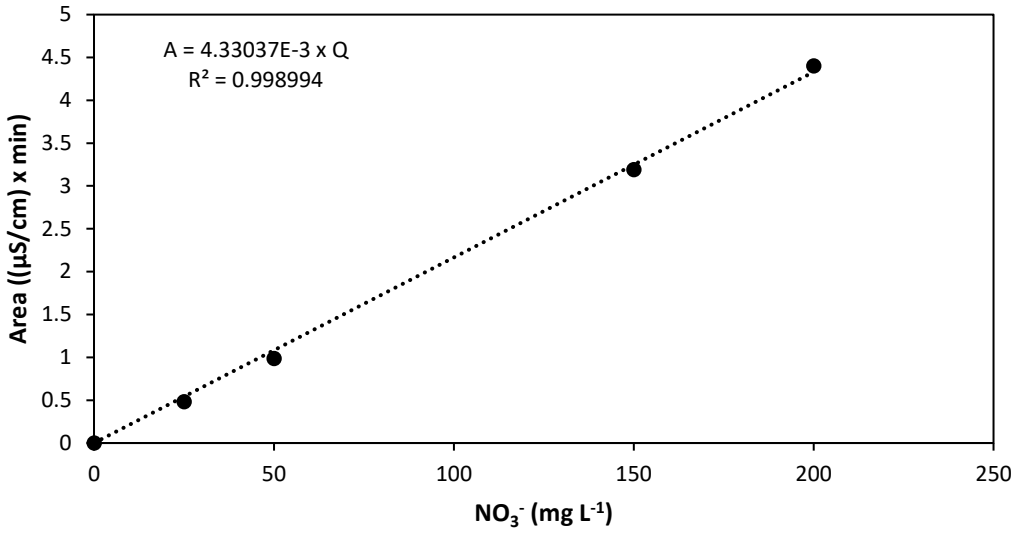


**Figure C5.** Nitrate calibration curve using ion chromatography, determined by manually integrating peak area across a concentration range.

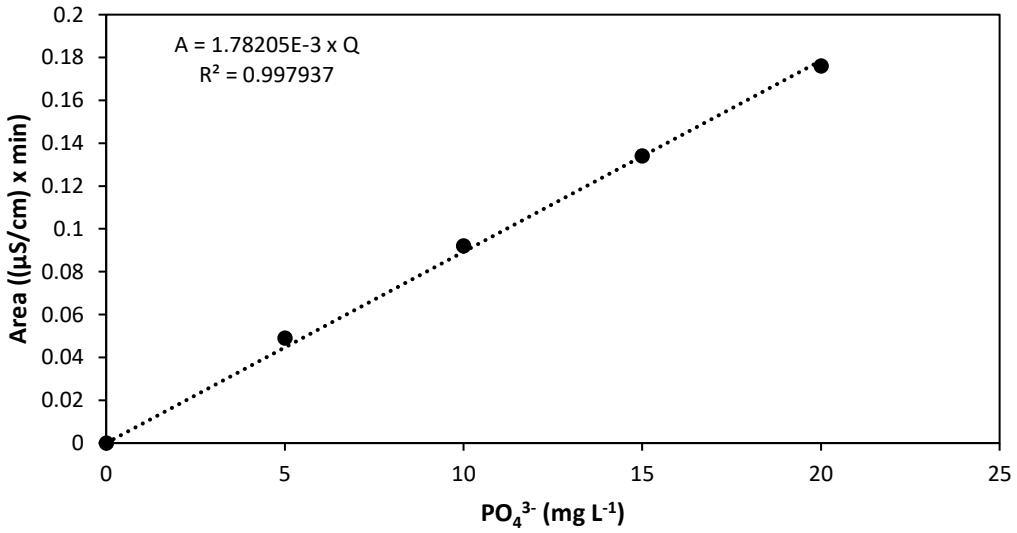


**Figure C6.** Phosphate calibration curve using ion chromatography, determined by manually integrating peak area across a concentration range.

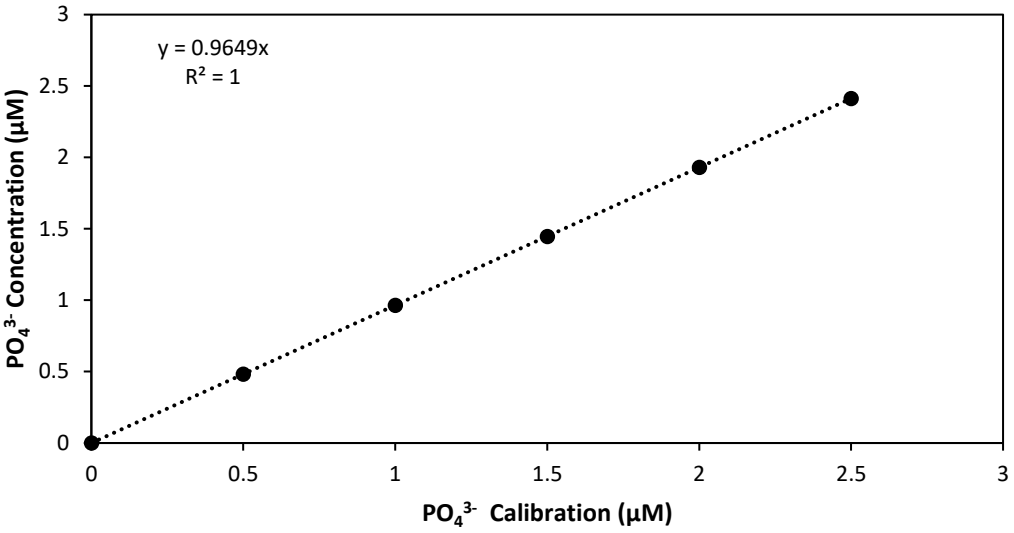


**Figure C7.** Orthophosphate calibration curve using Flow Injection Autoanalysis (Lachat 8500, Hach Lange, UK) and manually integrated as concentration (µM) using Omnion 3.0 software (Lachat Instruments, Hach Lange, UK).

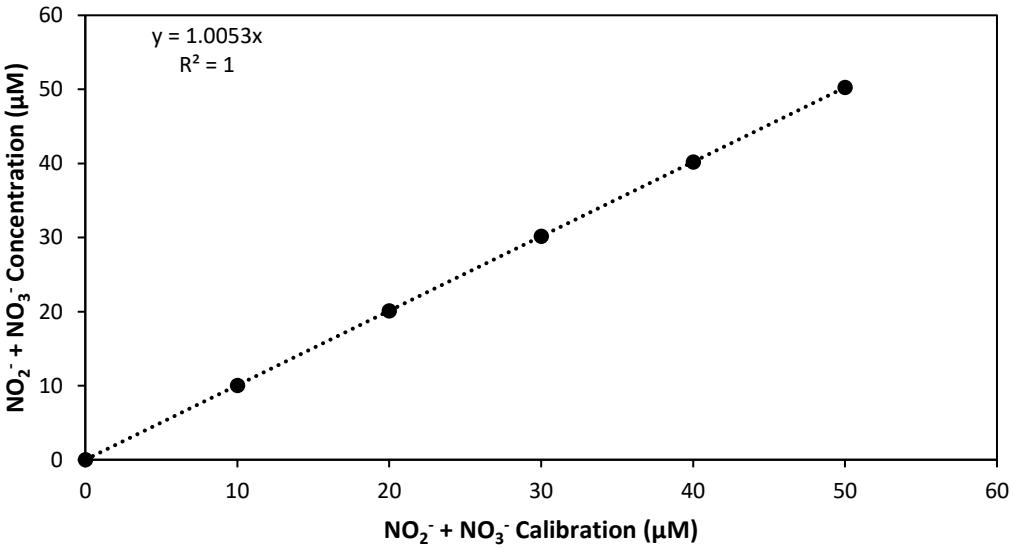


**Figure C8.** Nitrite plus nitrate calibration curve using Flow Injection Autoanalysis (Lachat 8500, Hach Lange, UK) and manually integrated as concentration (µM) using Omnion 3.0 software (Lachat Instruments, Hach Lange, UK).

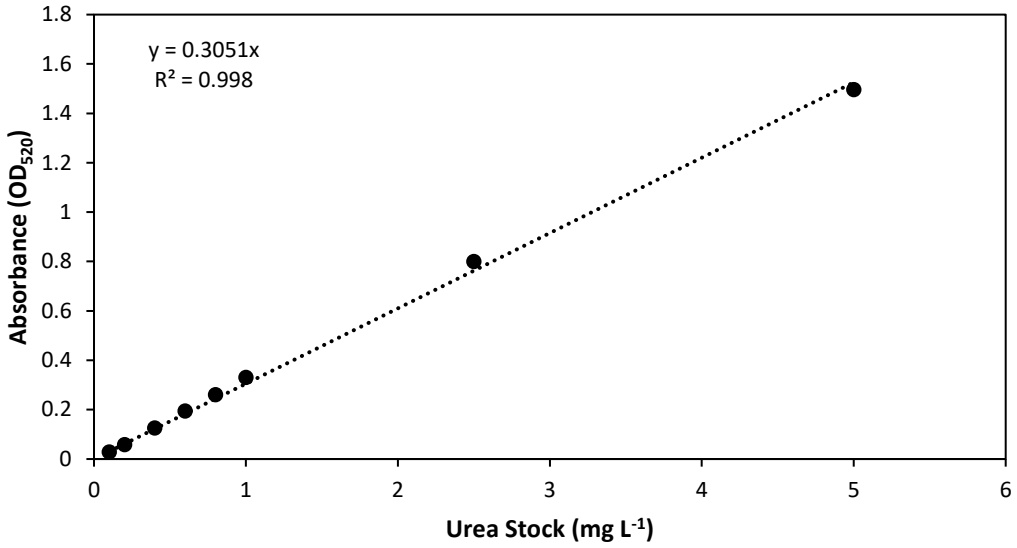


**Figure C9.** Urea calibration curve using a colorimetric method derived from that of Mulvenna and Savidge [514] (*n* = 2, *error bars* = 1 SD).

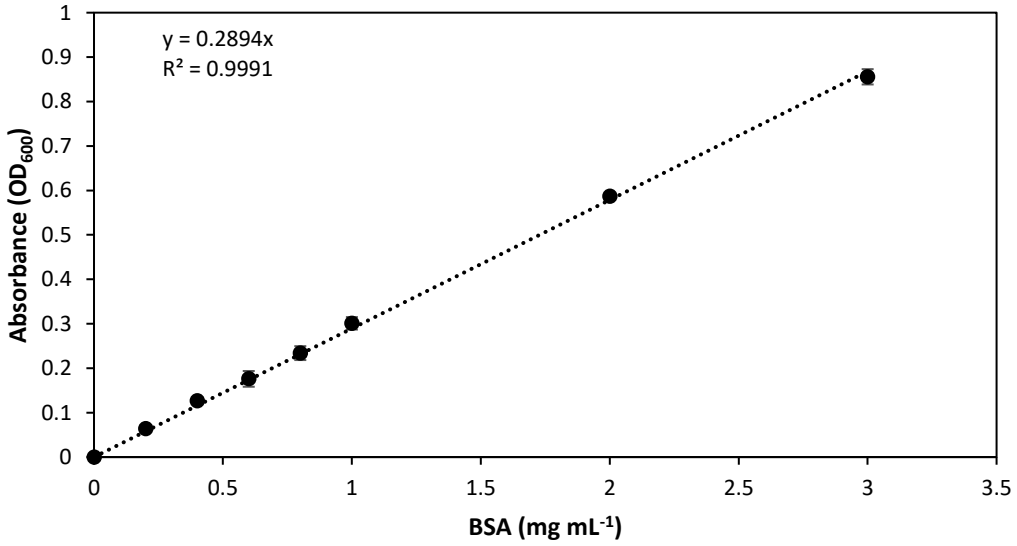


**Figure C10.** BSA calibration curve used for protein quantification (*n* = 3, *error bars* = 1 SD).

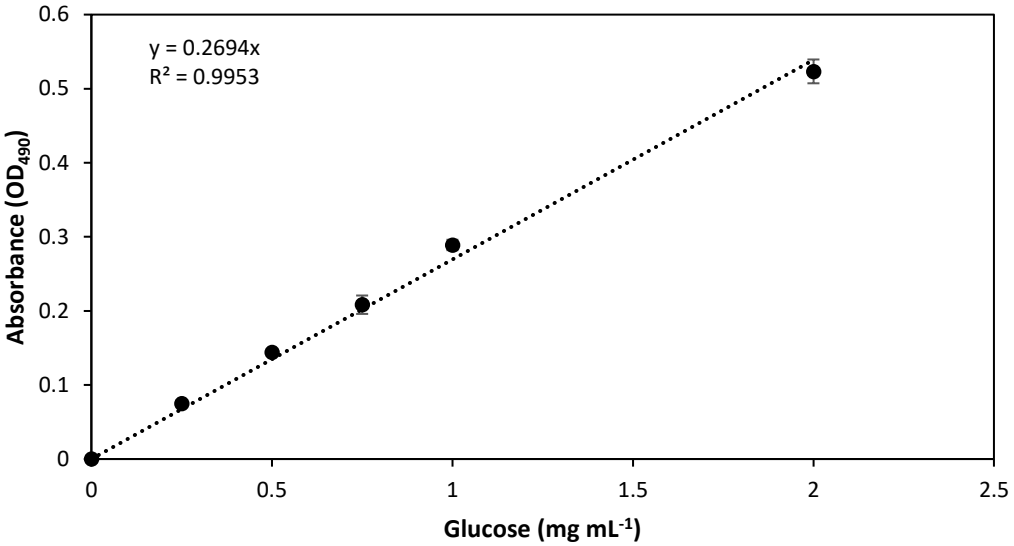


**Figure C11.** Glucose calibration curve used for carbohydrate quantification (*n* = 3, *error bars* = 1 SD).

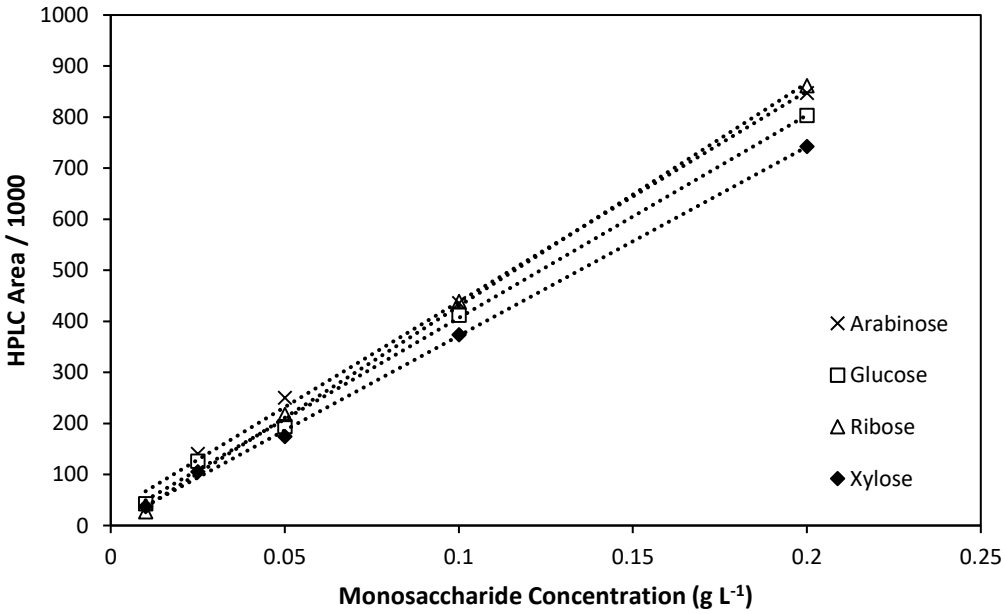


**Figure C12.** Calibration curve of HPLC peak area of monosaccharides arabinose, glucose, ribose, and xylose.

**Table – C1.** Equations and $R^2$ values of the monosaccharide calibration curves of from Appendix C, Fig. C12.

| Monosaccharide | Equation | $R^2$ |
|---|---|---|
| **Arabinose** | $y = 4123.9x + 25.764$ | 0.9974 |
| **Glucose** | $y = 3970.4x + 9.5232$ | 0.9984 |
| **Ribose** | $y = 4370.9x - 7.44$ | 0.9994 |
| **Xylose** | $y = 3702.2x + 1.2952$ | 0.9991 |

# Appendix D – List of Reagents

**Urea Determination**

- **Urea Reagent A**:

  1.7 g of diacetylmonoxime was dissolved in 46 mL $dH_2O$, plus 4 mL of thiosemicarbazide solution (0.475 g in 100 mL $dH_2O$).

- **Urea Reagent B**:

  31.26 mL of dH2O has 40 mL conc. sulphuric acid added to it, then 66 µL of iron (III) chloride solution (0.15 g in 10 mL $dH_2O$) is added.

**Protein Determination**

- **Lowry Reagent A** – 2% (w/v) sodium carbonate (anhydrous) in 0.1N sodium hydroxide solution

  4 g of NaOH was dissolved in 1 L of deionised water. Then 20 g of $Na_2CO_3$ was dissolved in the sodium hydroxide solution.

- **Lowry Reagent B** – 1% (w/v) sodium potassium tartrate

  1 g of $C_4H_4KNaO_6 \cdot 4H_2O$ was dissolved in 100 mL of deionised water.

- **Lowry Reagent C** – 0.5% (w/v) copper sulphate solution

  500 mg of $CuSO_4 \cdot 5H_2O$ was dissolved in 100 mL deionised water.

- **Lowry Reagent D** – a 48/1/1 volumetric ratio of A/B/C.

- **Lowry Reagent E** – Folin Ciocalteu-Phenol solution

  Equal parts of 2N Folin Ciocalteu-Phenol was mixed with deionised water.

# Appendix E – Carbohydrate Method Development

The purpose of this study was to optimise the methodology for total soluble carbohydrate extraction and quantification of the three algal species used in this body of work (section 2.2.1). Several steps of the protocol were highlighted as critical in influencing the saccharification yield obtained, as such, these were targeted for optimisation.

## Materials and Method

The main operational factors investigated were pre-treatment of the biomass, molarity of the acid, hydrolysate volume used for quantification, the ratio of biomass to acid volume (B/A) during extraction, and the amount of biomass required to determine the sensitivity of extraction. A detailed overview of experimental parameters is described below (Table E1).

## Results and Discussion

Method development for dilute acid hydrolysis for the extraction of soluble carbohydrates was performed on *C. coelothrix*, *C. parriaudii*, and *S. varians*. Five aspects of the protocol were highlighted for optimisation and were: the biomass pre-treatment, the volume and molarity of the acid, the amount of biomass required, and the volume of the hydrolysate for quantification.

Biomass had been grown for the sole purpose of method development, preliminary trials *et.c.* Samples were not grown under a strict cultivation regime. As such, they will likely be of different ages, growth stages, and therefore biochemical content. This will explain the variability between trials and the values in comparison to what was obtained in the experimental chapters, where cultivation regime was more rigorously controlled.

**Table E1.** Experimental conditions used for the optimisation of the method for total soluble carbohydrate determination.

| Tested Parameter | Species | Treatment | Biomass (mg) | Acid (mL) | M | Hydrolysate (µL) |
|---|---|---|---|---|---|---|
| **Treatment** | *C. coelothrix*<br>*C. parriaudii* | FD/OD | 5 | 0.5 | 1 | 10 |
| **Molarity** | *C. coelothrix*<br>*S. varians* | FD | 5 | 0.5 | 0.1/0.5/<br>1/2 | 10 |
| **Hydrolysate** | Glucose | | | | | 10/20/30 |
| **Acid Vol.** | *C. coelothrix*<br>*C. parriaudii*<br>*S. varians* | FD | 5 | 0.1-<br>10 | 1 | 10/30* |
| **Biomass** | *C. coelothrix*<br>*C. parriaudii*<br>*S. varians* | FD | 2-5 | 2-5 /<br>1-2.5 | 1 | 30 |

*applies only to *S. varians*. FD = Freeze-dried, OD = Oven-dried.

The pre-treatment of the biomass was identified as a possible factor which may influence yield. Different drying techniques may be more stringent and may facilitate acid hydrolysis. It was observed however, that there was negligible difference between the two pre-treatment techniques (Fig. E1). For instance, yields of 23.9% and 24.3% were obtained by either oven-drying or lyophilisation of *C. coelothrix* biomass, respectively. As freeze-drying resulted in a marginally greater yield, it was selected as the drying protocol of choice for the majority of experiments.

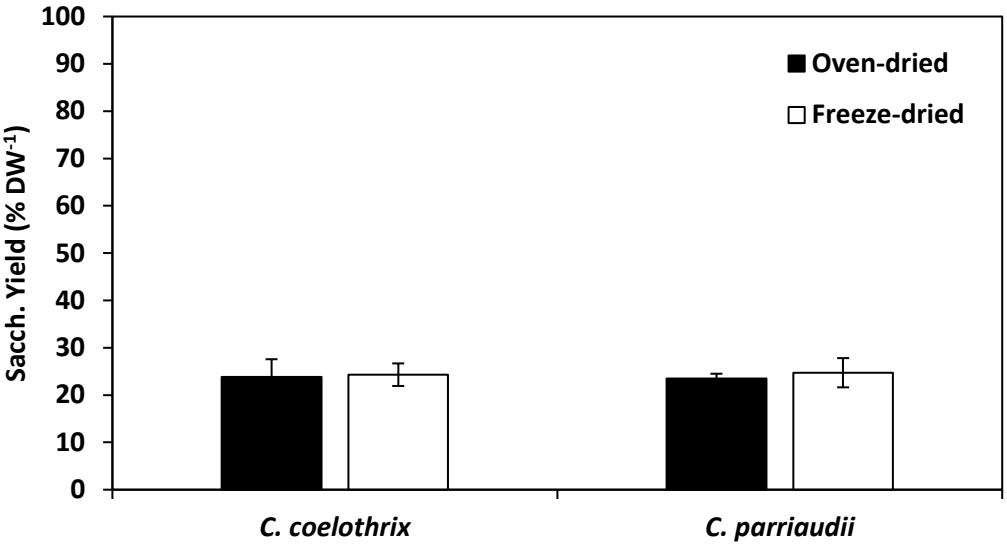


**Figure E1.** The effect of drying technique on the saccharification yield of *Cladophora coelothrix* and *Cladophora parriaudii*. Biomass was either oven-dried (black) or freeze-dried (white) and was reacted according to the method outlined in section 2.5.3.2. The remaining experimental conditions are outlined in Table E1 (*n* =3, *error bars* = 1 SD).

*Cladophora* have a recalcitrant cell wall, owing to the very crystalline nature of the cellulose that it is primarily composed of [186, 341]. Therefore, the strength of the acid used will likely have a strong influence in the success of extraction. As such, four different molarities were tested on freeze-dried *C. coelothrix* and *S. varians* (Fig. E2). *C. parriaudii* was not tested due to a potential shortfall of material for future optimisation steps. There was not a huge differentiation in saccharification yield with molarity, with values ranging from 28.2-34.9% $DW^{-1}$ for *C. coelothrix* and 68.6-75.4% $DW^{-1}$ for *S. varians*. The lowest yields were obtained with the strongest acid (2 M), this suggests that there may have been some form of sugar degradation. An acid concertation of 1 M was selected as optimal. It was believed to be strong enough to liberate sugars (i.e. glucose) from the recalcitrant cells (cellulose polymers), without resulting in the degradation of monosaccharides. In addition, a 1 M $H_2SO_4$ solution was found to be optimal elsewhere [103].

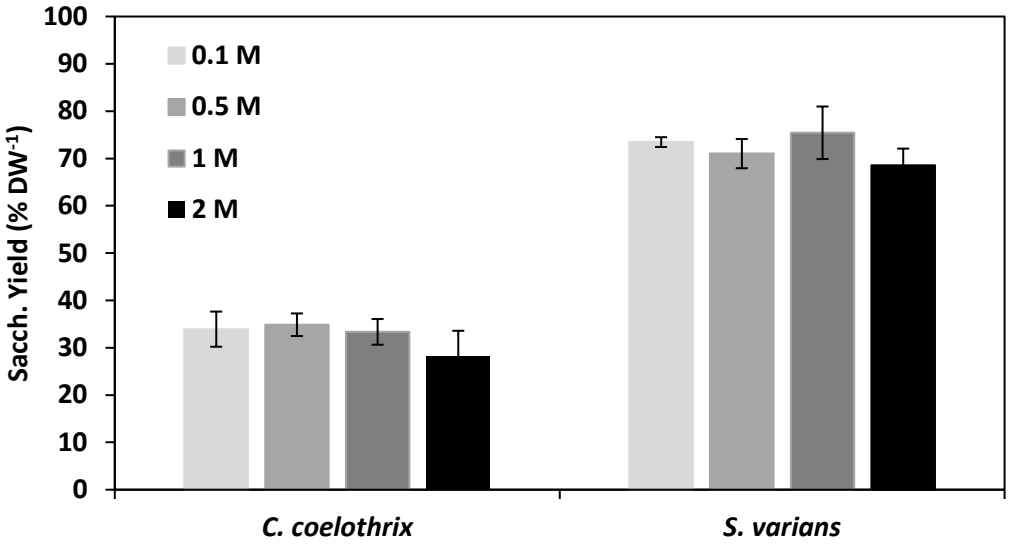


**Figure E2.** The effect of acid strength on the saccharification yield of *Cladophora coelothrix* and *Spirogyra varians*. Four different molarities of $H_2SO_4$ were tested, including 0.1, 0.5, 1 and 2M, and were reacted according to the method outlined in section 2.5.3.2. The remaining experimental conditions are outlined in Table E1 (*n* =3, *error bars* = 1 SD).

The volume of hydrolysate, therefore the mass of sugar present, for each sample will directly influence the signal strength of the reaction; more sugar, a stronger colour change. Three separate glucose calibration curves, in the range of 0.5-4 g $L^{-1}$ were generated, using three different sample volumes: 10, 20, and 30 µL (Fig. E3). All three volumes resulted in a very linear trends, with $R^2$ values ranging from 0.9903-0.9954. The 30 µL volume was selected as optimal as it gave the strongest signal. This was viewed as advantageous, as it would reduce the possibility of a lack of signal from biomass that had a low carbohydrate content, which may occur with a 10 µL sample volume. Furthermore, the $R^2$ value was high (0.9954) and the signal did not over-saturated within this calibration range.

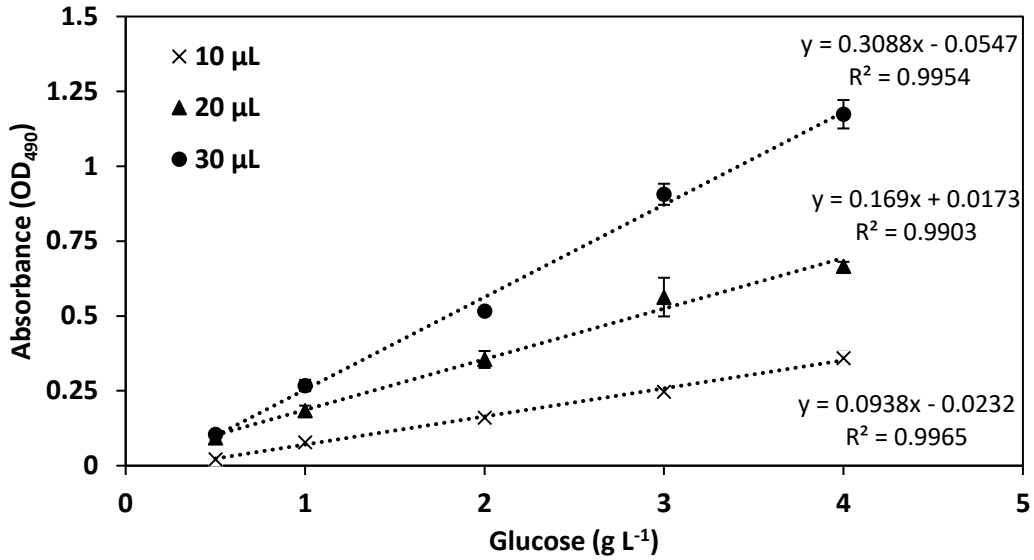


**Figure E3.** The effect of acid hydrolysate used for the colourimetric quantification. Either, 10, 20, or 30 µL of glucose stock solutions were reacted according to the method outlined in section 2.5.3.2 (*n* =3, *error bars* = 1 SD).

The volume of acid used for hydrolysis may influence its success. To investigate this aspect, six different volumes of 1 M $H_2SO_4$ were tested on 5 mg of freeze-dried biomass, for all species (Fig. E4). There was quite a high degree of variation in yield based upon acid volume. For example, saccharification yields ranged from 34.2-61.9%, 24.8-41.2%, and 60.5-67.1% $DW^{-1}$ from *C. coelothrix*, *C. parriaudii*, and *S. varians*, respectively (Fig. E4). Generally, yield increased with increasing volume up to 5 mL. However, further increasing the acid volume to 10 mL resulted in a reduction in yield. This may have been due to some dilution effect or a degradation of the sugars. This was most noticeable in *C. parriaudii*, which had the lowest carbohydrate content of the three species. Acid volumes of 0.1-1 mL typically resulted in lower saccharification yields, this may be due to an incomplete hydrolysis of the biomass, and was particularly evident for *C. coelothrix* (Fig. E4), which has a thick cell wall and is regarded as the most recalcitrant of the three species [319]. In each instance, the greatest yield was obtained with an acid volume of either 2.5 or 5 mL. In order to reduce chemical use, cost, and waste generation a volume of 2.5 mL was selected.

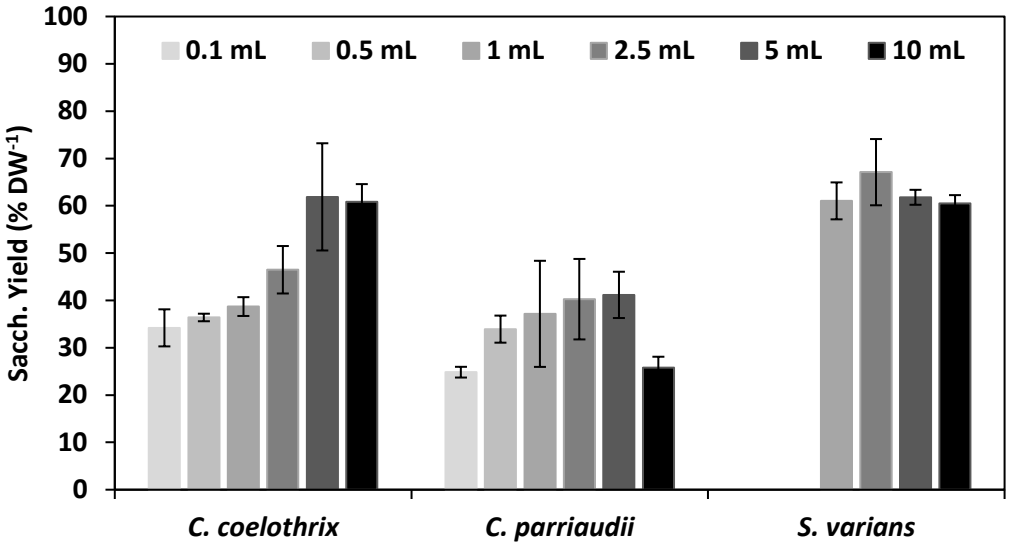


**Figure E4.** The influence of acid volume on carbohydrate yield for *Cladophora coelothrix*, *Cladophora parriaudii*, and *Spirogyra varians*. Volumes of 0.1, 0.5, 1, 2.5, 5, and 10 mL of 1 M $H_2SO_4$ were added to 5 mg of freeze-dried biomass and were reacted according to the method outlined in section 2.5.3.2. Greater detail on experimental parameters can be found in Table E1 (*n* =3, *error bars* = 1 SD).

Whilst maintaining the same biomass to acid volume ratio that was found to be optimal from Fig. E4, variable amounts of biomass were hydrolysed in order to investigate the sensitivity of the method (Fig. E5). It was observed there was a low degree of variation in yield when the initial mass was 3-5 mg. For instance, yields were 42.7-48.7%, 30.3-33.9%, and 47.6-54.4% $DW^{-1}$ for *C. coelothrix*, *C. parriaudii*, and *S. varians*, respectively. The hydrolysis of 2 mg of biomass, however, consistently resulted in a reduced yield. For instance, 31.9%, 23.7%, and 42.4% $DW^{-1}$, respective to the previous order of species (Fig. E5). This reduction may have been caused by a degradation of the liberated monosaccharides or by inaccuracies in weighing such small masses. As such, biomass in the range of 3-5 mg was deemed acceptable, provided that the volume of acid was adjusted accordingly, whereas lower biomass samples may result in an underestimation of the carbohydrate content and should be avoided.

The optimised protocol for the extraction of soluble carbohydrates from the three macro-algal species is described in section 2.5.3.

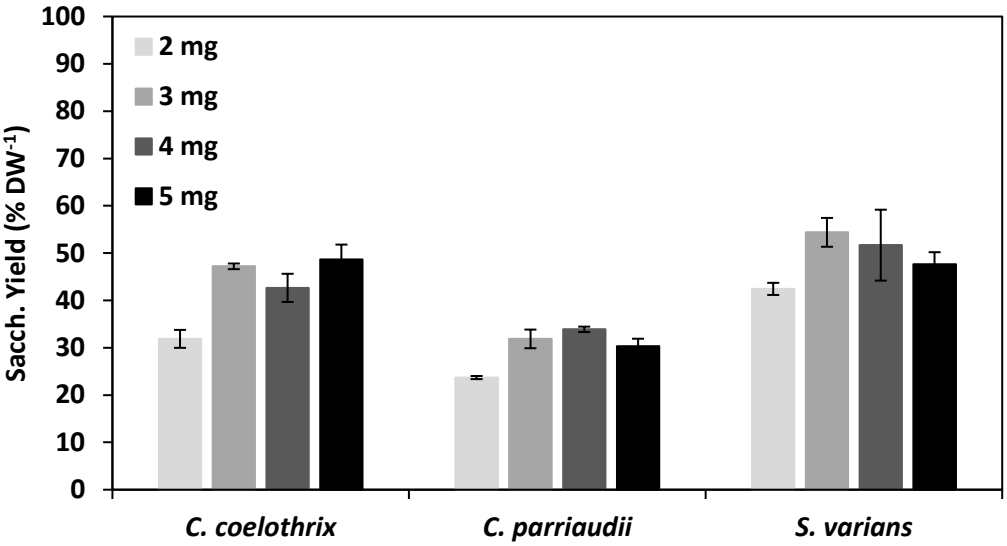


**Figure E5.** The influence of biomass amount on the saccharification yield of *Cladophora coelothrix*, *Cladophora parriaudii*, and *Spirogyra varians*. Samples of 2, 3, 4, and 5 mg of freeze-dried biomass were hydrolysed with 1, 1.5, 2, and 2.5 mL of 1 M $H_2SO_4$ and were reacted according to the method outlined in section 2.5.3.2. Greater detail on experimental parameters can be found in Table E1 (*n* =3, *error bars* = 1 SD).

# Appendix F – Urea Method Optimisation

The purpose of this study was to optimise a method for the determination of urea in brackish samples on a lab-scale.

## Materials and Method

The optimised method was based upon that originally described by [324]. In their original protocol, which was designed for urea determination in seawater, relatively large sample volumes were required (35 mL). Employing their method on a lab-scale was prohibitive, especially since several measurements were taken over a time-course. As such, all aspects of the protocol were proportionally reduced to suit a 2 mL sample size.

The method involves a direct condensation reaction between urea and diacetylmonoxime which elicits a colour change. The rate of the reaction is enhanced by temperature. Therefore, standardising the incubation period for this method is crucial. Three different incubation methods were employed, and included a heat block for 20 minutes (DB-2D Dri-Block®, Techne), or an incubator (Gallenkamp Plus II Incubator, Sanyo, UK) for either 20 or 30 minutes. In all instances, the temperature was maintained at 85°C, verified using a glass thermometer.

## Results and Discussion

The urea calibration curves generated using the three different incubation methods are shown in Fig. F1. The 20 minute maintenance in an incubator resulted in a consistently lower calibration curve, in comparison to the other two methods. As the reaction is dependent upon temperature and time, it is likely that the reaction using this technique is incomplete, given an extended incubation time, a more complete reaction may occur. On the other hand, the methods involving a heating block and an incubation time of 30 minutes result in an almost identical curve. Either of these methods would be sufficient for urea determination in seawater samples. The use of an incubator was preferred however, as the heating block is restricted to heating 12 samples at once. The calibration curve is linear until 4-6 mg $L^{-1}$, whereupon the absorbance begins to saturate. A calibration in the

range of 0-5 mg $L^{-1}$ was used throughout this work (Appendix C – Fig. C9), samples were diluted to fall within this range.

The optimised method for urea determination is given in section 2.4.5.

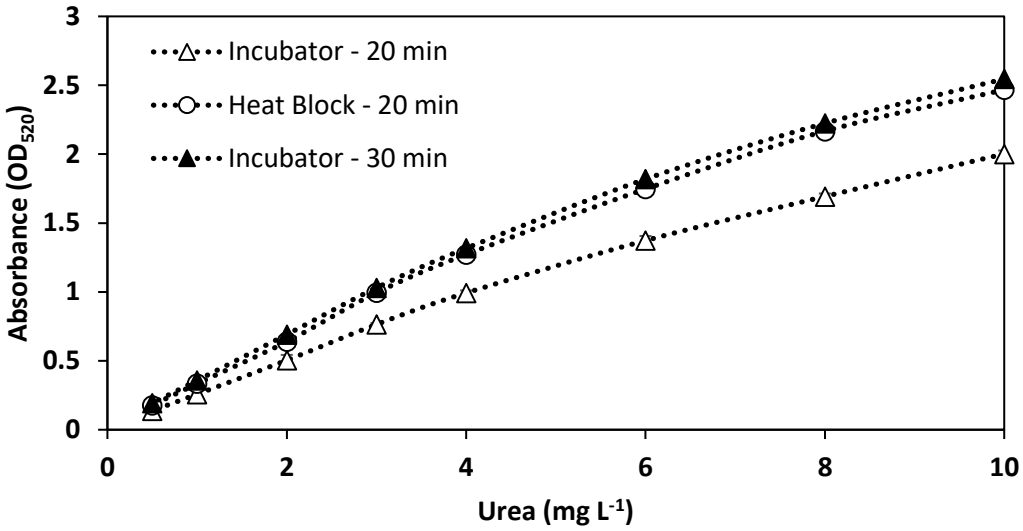


**Figure F1.** Urea standard curves generated using three different incubation methods; either heating in a block for 20 minutes (white circle), or kept in an incubator for 20 (white triangle) or 30 minutes (black triangle). The full protocol is described in section 2.4.5. Urea stocks solutions were formulated in the range of 0.5-10 mg $L^{-1}$ (*n* = 3, *error bars* = 1 SD).

# Appendix G – Protein Method Optimisation

The purpose of this study was to optimise the methodology for protein extraction and quantification from the two species of *Cladophora* used in this work (section 2.2.1).

## Materials and Method

The method employed was modified from that originally described by Slocombe *et al.* [327]. The original protocol was designed for general and high throughput use for micro-algae. The cell wall of *Cladophora* is highly crystalline and recalcitrant, therefore modification of the method for specific use is likely.

In order to achieve chemical lysis and liberate proteins, algal biomass is subjected to a sequential acid and alkaline extraction procedure. Followed by colourimetric quantification using the Lowry assay [326]. Both the acid and alkaline incubations were regarded as important steps in determining the final extraction efficiency, and were identified as areas for modification.

Firstly, either 15 or 30 minutes incubation time in hot TCA was examined. Secondly, the duration of the alkaline extraction in Lowry Reagent D (Appendix D) was investigated, with incubation times ranging from 1-24 h. The remaining extraction and quantification steps were performed as normal, as detailed in section 2.5.2.

## Results and Discussion

The effect of the hot TCA incubation time on protein yield is seen in Fig. G1. It can be seen that by lengthening the incubation time resulted in a greatly reduced protein yield. For instance, a reduction from 5.7 -5.3% and 5-3.2% $DW^{-1}$ for *C. coelothrix* and *C. parriaudii*, respectively. Therefore, an incubation time of 15 minutes was selected as optimal. The reduction in yield is most likely caused by a higher degree of protein degradation/deformation caused by longer exposure to heat and acid. The reduction in yield was not as pronounced in *C. coelothrix* in comparison to *C. parriaudii*, most likely

because *C. coelothrix* has a thicker cell wall, making it more robust and recalcitrant to acid hydrolysis [319].

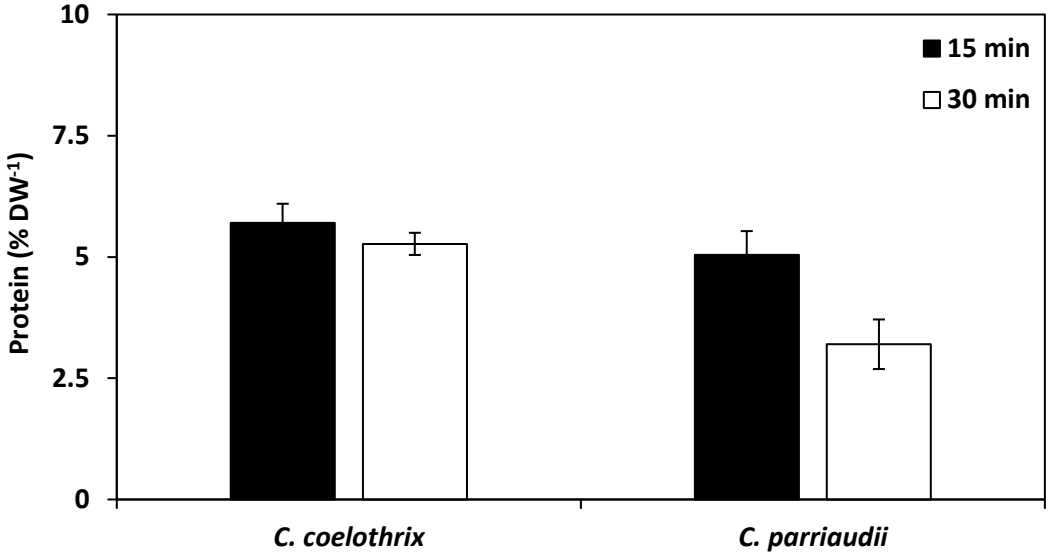


**Figure G1.** The effect of hot TCA incubation time on the protein extraction for *Cladophora coelothrix* and *Cladophora parriaudii*. Algal samples were exposed to either a 15 (black) or 30 (white) minute incubation, followed by a 6h alkaline incubation. All other extraction and quantification steps adhere to the protocol outlined in section 2.5.2 (*n* = 3, *error bars* = 1 SD).

The effect of varying the alkaline incubation step is shown in Figure G2. This optimisation step was only performed on *C. parriaudii*, due to a shortage of *C. coelothrix* biomass. Furthermore, protein degradation/deformation is more likely to occur in *C. parriaudii* as it is a less robust species (Fig. G1) [319]. It can be seen that by lengthening the incubation time from 1-6 hours resulted in an increase in yield from 3.76-4.76% $DW^{-1}$ (Fig. G2). Shorter incubation times may have led to an incomplete protein extraction. Whereas, an overnight incubation yielded 4.78% $DW^{-1}$ and hence did not result in any further extraction or degradation, in comparison to 6 h incubation. The protein extraction protocol, although simple, involves a number of steps. In order to improve time management, an overnight incubation step was preferred.

The optimised method is described in section 2.5.2.

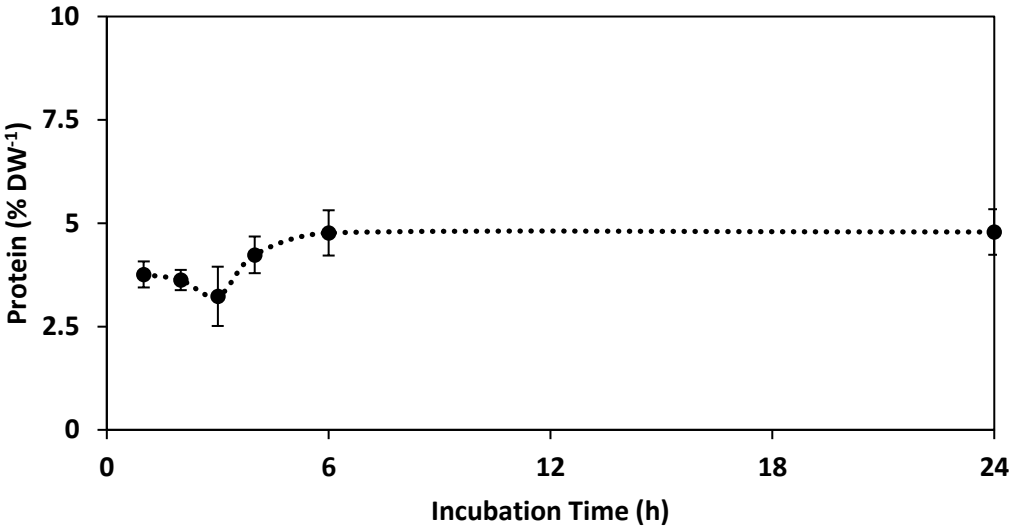


**Figure G2.** The effect of incubation time in Lowry Reagent D (Appendix D) on the extraction and protein yield of *Cladophora parriaudii*. After extraction in hot TCA for 15 minutes, algal samples were then incubated for varying times, ranging from 1 h to overnight, in Lowry Reagent D. All other extraction and quantification steps adhere to the protocol outlined in section 2.5.2 (*n* = 3, *error bars* = 1 SD).

# Appendix H – Pigment Extraction Optimisation

The purpose of this study was to optimise the methodology for extraction and quantification of pigments from all three macro-algal species used in this work (section 2.2.1).

## Materials and Method

There are a wealth of methods available for the extraction of pigments from algae. Most methods are centred upon solvent extraction and primarily use acetone, DMSO, and methanol, or combinations of these, with the nuances of each method are usually dependent upon the species being used [330, 515, 516].

In this optimisation procedure solvent type and incubation method were tested. Firstly, biomass of *C. parriaudii* was extracted using either 90% acetone or DMSO, followed by an 18 hour incubation in an oven or a water bath, set to 65°C. The second aspect was to determine the optimal incubation method by extracting pigments from all three species (section 2.2.1) using DMSO and an overnight incubation in either an oven (Gallenkamp Plus II Incubator, Sanyo, UK) or water bath, both set to 65°C.

## Results and Discussion

Figure H1. Shows the extraction of pigments from *C. parriaudii* using either 90% acetone or DMSO, coupled with an incubation in an oven or water bath. Greatest extraction pigment extraction was attained by acetone and oven incubation, with a total pigment yield of 0.84% $DW^{-1}$. This treatment resulted in cloudy pigment extracts, and would have overestimated the pigment concentration. As a precaution, acetone was ruled out for future use. The pigment yield from DMSO extracted biomass was 0.46 and 0.43%, using an oven and water bath, respectively (Fig. H1). Given the consistency in extraction, DMSO was selected as the solvent of choice.

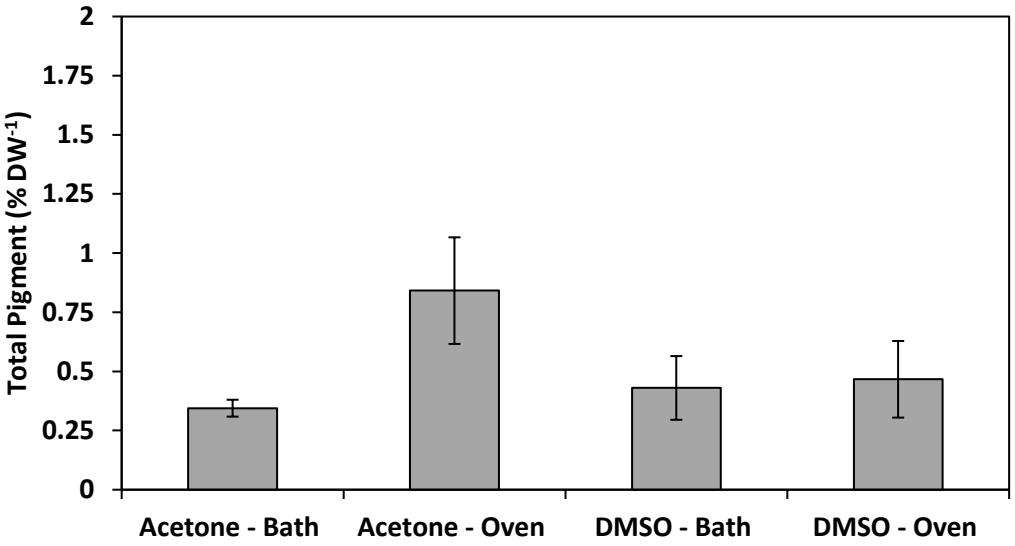


**Figure H1.** The effect of solvent and incubation type on the extraction of pigments from *Cladophora parriaudii*. Samples of 2 mg were extracted with 2 mL of either 90% acetone or DMSO. Mixtures were then incubated in either an oven or a water bath. Extracts were then read spectrophotometrically at three wavelengths (section 2.5.4) (*n* = 3, *error bars* = 1 SD).

The method of incubation was further studied for all three species (Fig. H2). The incubation method had little effect on the extraction of pigments from *Cladophora*. For instance, the yields were 1.17-1.19% $DW^{-1}$ for *C. coelothrix* and 0.43-0.47% $DW^{-1}$ for *C. parriaudii* (Fig. H2). There was, however, a greater difference in pigment extraction from *S. varians* depending upon heating method. The yield increased from 1.17% to 1.79% $DW^{-1}$ when incubated in an oven rather than a water bath. Regardless of this, a water bath was the preferred incubation method as it gave consistent yields with low error. In addition to the concerns that were raised from Fig H1, where it is uncertain whether acetone or oven incubation (or both) was the causative factor for the cloudy extracts.

The full method for pigment extraction is given in section 2.5.4.

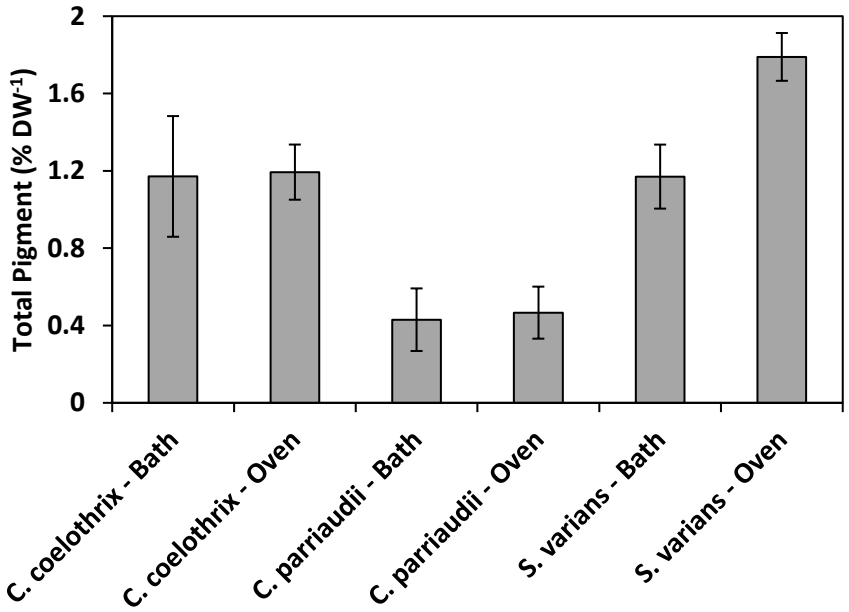


**Figure H2.** The effect of incubation method on the extraction of pigments of *Cladophora coelothrix*, *Cladophora parriaudii*, and *Spirogyra varians*. Samples of 2 mg were extracted with 2 mL of DMSO and incubated overnight in an oven or water bath. Extracts were then read spectrophotometrically at three wavelengths (section 2.5.4) (*n* = 3, *error bars* = 1 SD).

# Appendix I – Metal Equilibrium Isotherms

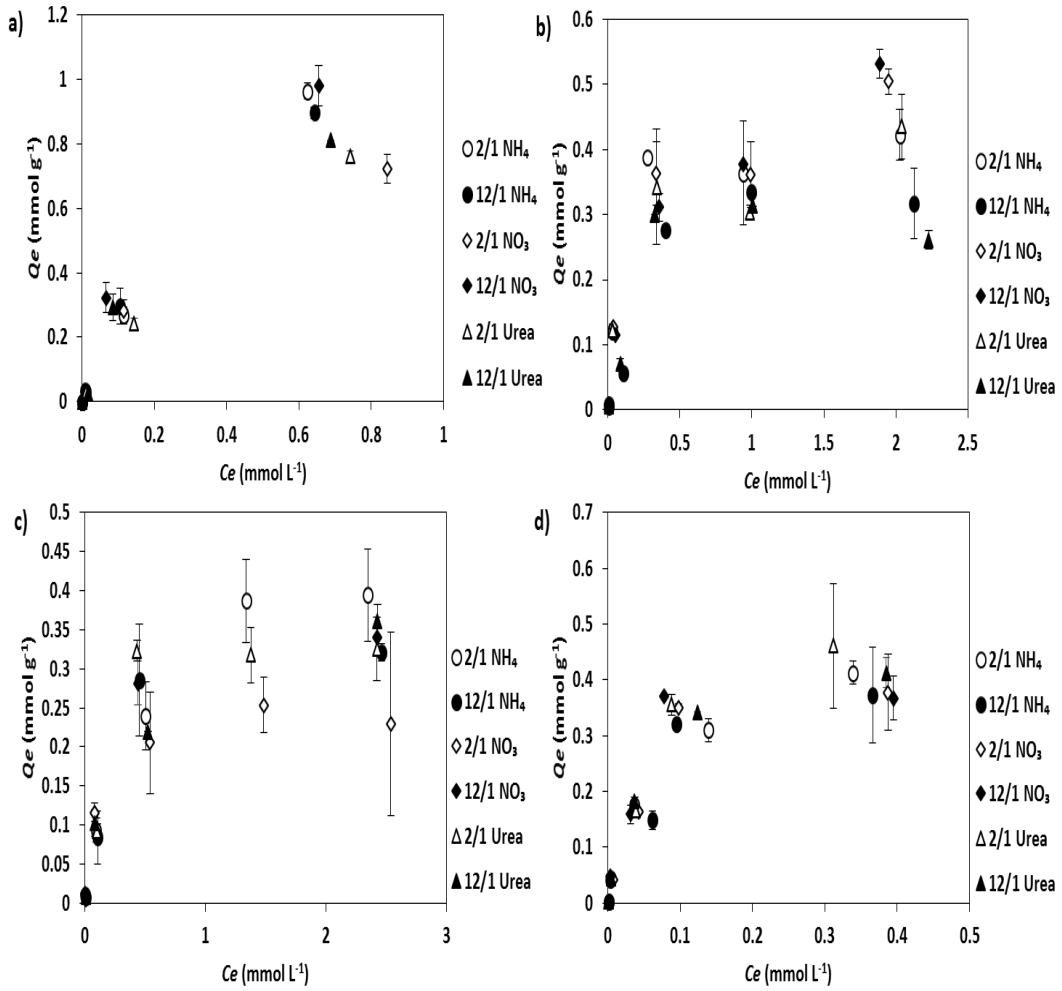


**Figure I1.** Sorption isotherms of $Al^{2+}$ (A), $Cu^{2+}$ (B), $Mn^{2+}$ (C), and $Pb^{2+}$ (D) by *Cladophora parriaudii* cultivated under different N/P ratios and nitrogen sources; 2/1 $NH_4^+$ (white circle), 12/1 $NH_4^+$ (black circle), 2/1 $NO_3^-$ (white diamond), 12/1 $NO_3^-$ (black diamond), 2/1 Urea (white triangle), 12/1 Urea (black triangle). The adsorption conditions were; pH = 4.5, contact time = 24 h, biosorbent dose = 1 g $L^{-1}$, agitation = 100 rpm, metal concentration = 1-150 mg $L^{-1}$ (except $Al^{2+}$ = 1-40 mg $L^{-1}$), temperature = 24°C, light = 24/0 L/D h with 30-40 µmol photons $m^{-2}$ $s^{-1}$ (*n* = 1-3, *error bars* = 1 SD.).

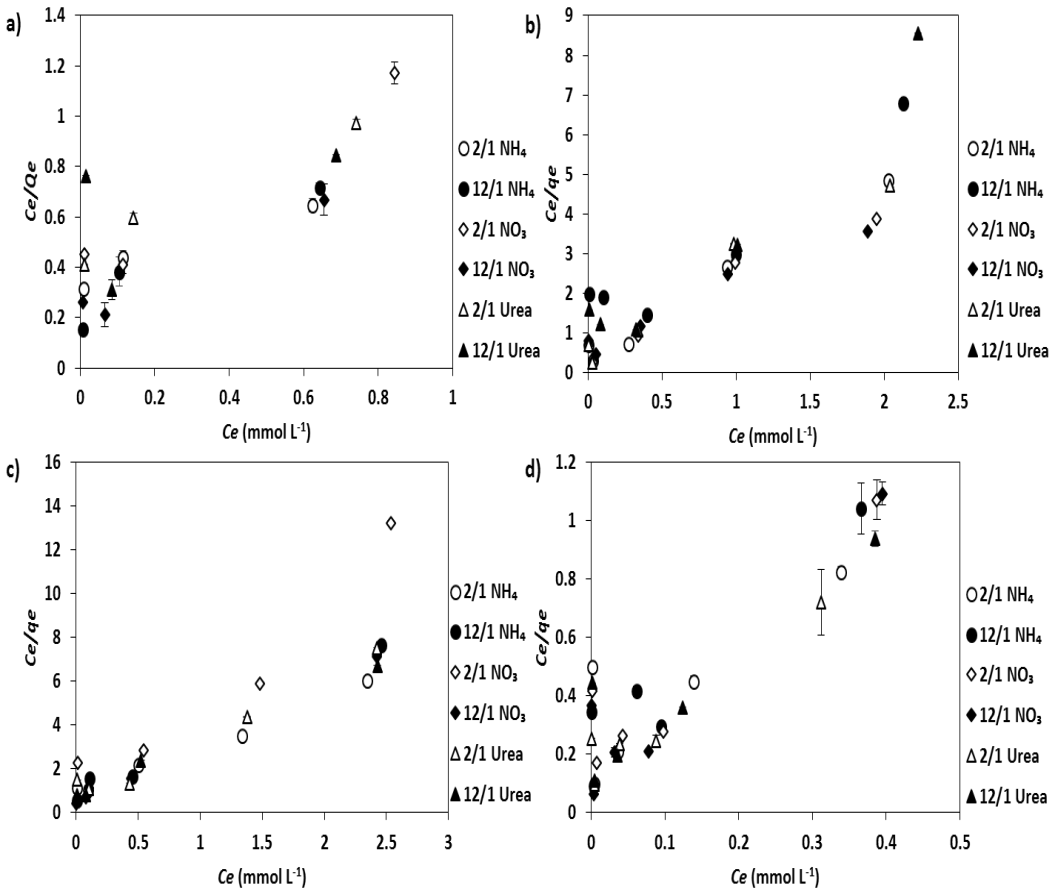


**Figure I2.** The Langmuir adsorption isotherms of $Al^{2+}$ (A), $Cu^{2+}$ (B), $Mn^{2+}$ (C), and $Pb^{2+}$ (D) obtained by *Cladophora parriaudii* cultivated under different N/P ratios and nitrogen sources; 2/1 $NH_4^+$ (white circle), 12/1 $NH_4^+$ (black circle), 2/1 $NO_3^-$ (white diamond), 12/1 $NO_3^-$ (black diamond), 2/1 Urea (white triangle), 12/1 Urea (black triangle). The adsorption conditions were; pH = 4.5, contact time = 24 h, biosorbent dose = 1 g $L^{-1}$, agitation = 100 rpm, metal concentration = 1-150 mg $L^{-1}$, temperature = 24°C, light = 24/0 L/D h with 30-40 µmol photons $m^{-2}$ $s^{-1}$ (*n* = 1-3, *error bars* = 1 SD.).

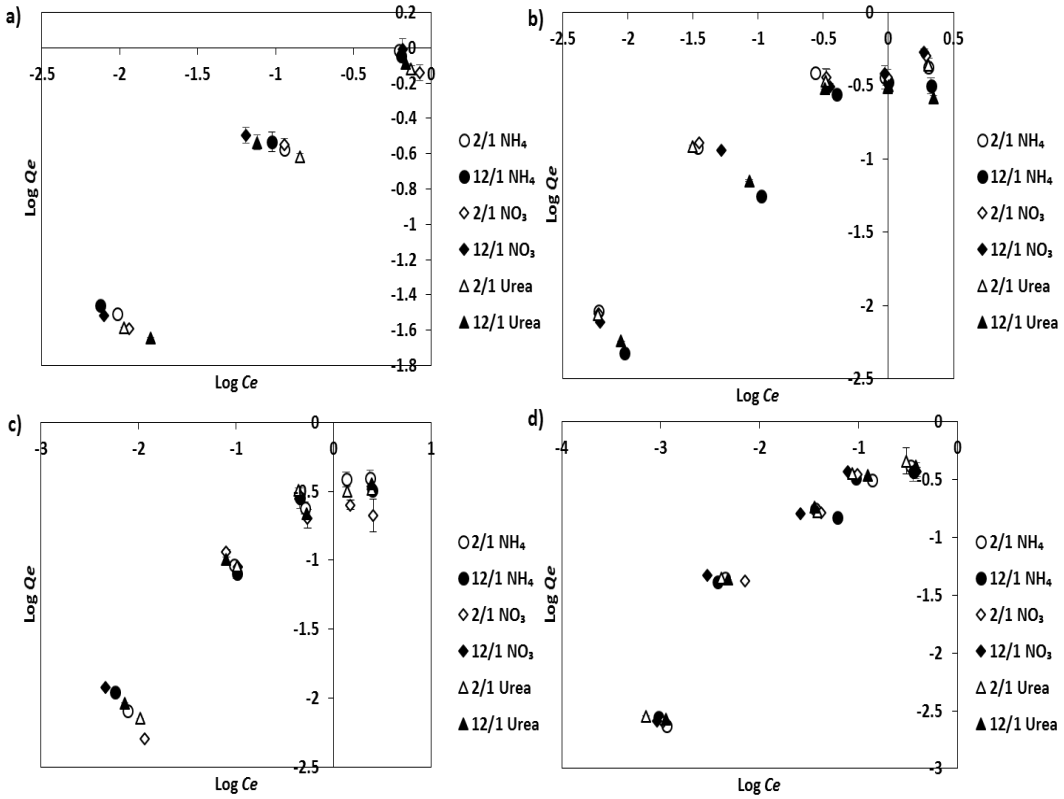


**Figure I3.** The Freundlich adsorption isotherms of $Al^{2+}$ (A), $Cu^{2+}$ (B), $Mn^{2+}$ (C), and $Pb^{2+}$ (D) obtained by *Cladophora parriaudii* cultivated under different N/P ratios and nitrogen sources; 2/1 $NH_4^+$ (white circle), 12/1 $NH_4^+$ (black circle), 2/1 $NO_3^-$ (white diamond), 12/1 $NO_3^-$ (black diamond), 2/1 Urea (white triangle), 12/1 Urea (black triangle). The adsorption conditions were; pH = 4.5, contact time = 24 h, biosorbent dose = 1 g $L^{-1}$, agitation = 100 rpm, metal concentration = 1-150 mg $L^{-1}$, temperature = 24°C, light = 24/0 L/D h with 30-40 µmol photons $m^{-2}$ $s^{-1}$ (*n* = 1-3, *error bars* = 1 SD.).

# Appendix J – IR band assignments

**Table J1.** Main IR absorption bands of *Cladophora parriaudii* obtained using FTIR-ATR.

| Wavenumber ($cm^{-1}$) | Band Assignment | Functional Groups | Refs |
|---|---|---|---|
| 3400 - 3100 | $_{V}$C-H of CH=CH | Hydroxyl group and water | [455, 462, 464, 517] |
| | $_{V}$N-H / $_{V}NH_2$ | Protein (Amide Group A) | |
| | $_{V}$O-H | Double bond in fatty acids | |
| 3000 - 2800 | $_{V}$C-H / $_{V}CH_2$ / $_{V}CH_3$ | Aliphatics of cell walls, aldehydes, methylene groups | [455, 459, 462, 464] |
| | $_{VAS}CH_2$ / $_{VAS}CH_3$ | | |
| 2900 | $_{V}CH_2$ / $_{V}CH_3$ | Cellulose | [518] |
| 1650 - 1630 | $_{V}$C=N / $_{V}$C=O / $_{\delta}NH_2$ | Protein (Amide I) | [455, 462, 464, 517] |
| 1550-1530 | $_{\delta}$C-N / $_{V}$C-N / $_{\delta}$N-H | Protein (Amide II) | [455, 459, 462, 464] |
| 1460 - 1450 | $_{\delta}$C-H of $CH_2$ or $CH_3$ | Aliphatics of cell wall. | [455, 459, 462, 464] |
| | $_{\delta AS}CH_2$ / $_{\delta AS}CH_3$ | Methyl and methylene, proteins and lipids | |
| 1430-1425 | $_{\delta AS}CH_2$ | Cellulose | [519] |
| 1405 | $_{\delta}$N-H | Amine Group | [520] |
| 1375 - 1360 | $_{\delta}$C-H / $_{V}$S=O | Cellulose, sulphur components | [519, 521, 522] |
| 1335 | $_{\delta}$O-H / $_{V}$S=O | Cellulose, Phenols, Sulfone | [519, 522] |
| 1320 - 1310 | $_{\rho}CH_2$ | Cellulose | [519, 521] |
| 1250 - 1210 | $_{V}$C-N / $_{VAS}$P=O | Phosphodiester of nucleic acids and phospholipids, xylan, Amide III | [455, 459, 461, 462, 464, 521, 523] |

| | | | |
|---|---|---|---|
| 1200 - 900 | $\nu_{AS}$C=O / $\nu$C-O-C / $\nu$C-N / $\nu$C-O / $\nu_{AS}$P=O / $\nu_{AS}$P-O-P / $\nu$S=O | Glycopeptides, ribose, aliphatic esters, polysaccharides, cellulose, sulphur components, amine | [455, 462, 464, 519, 521, 522] |
| 900 - 820 | $\delta$C-H / C-O-C | Monosaccharides | [523, 524] |
| 745 | $\delta_{AS}$C-C-C / $\nu$C-H | Benzene ring, monosaccharides | [524-526] |

$\nu$ = symmetrical stretching, $\nu_{AS}$ = asymmetrical stretching, $\delta$ = symmetrical deformation (bend), $\delta_{AS}$ = asymmetrical deformation (bend), $\rho$ = in-plane bending (rocking).

# Appendix K – SEM BSE Images

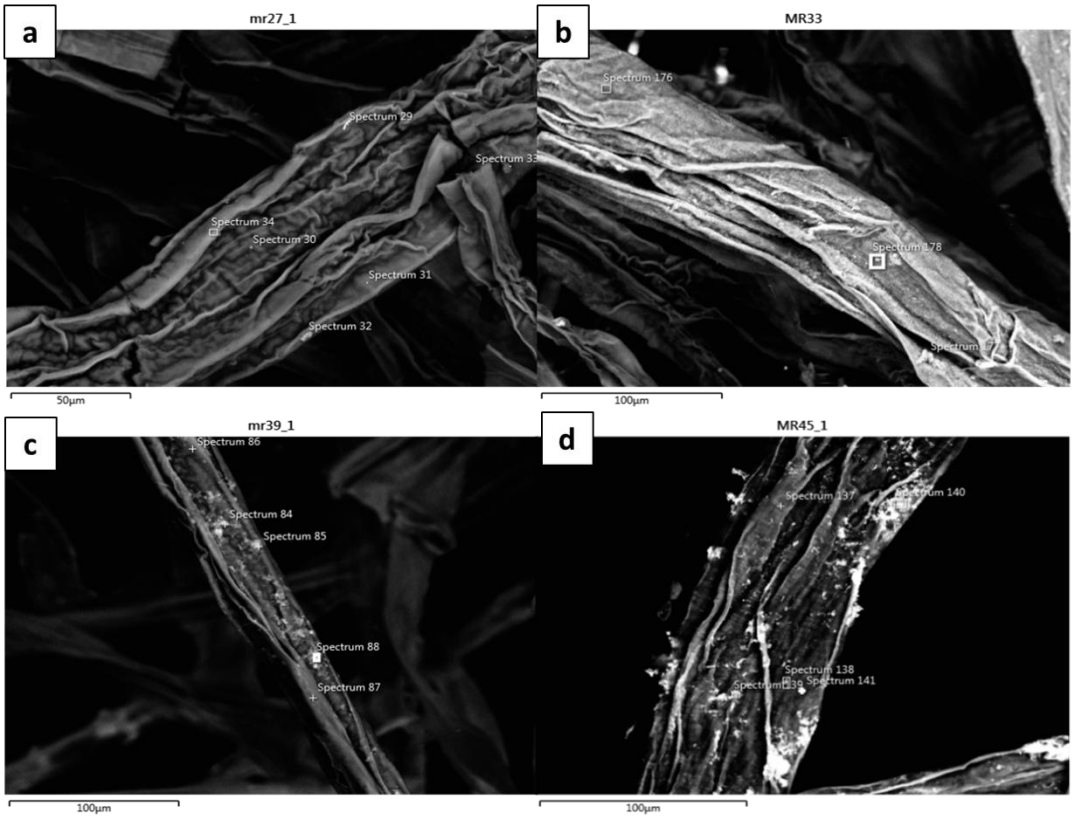


**Figure K1.** The cell surface of *Cladophora parriaudii*, previously cultivated under a 2/1 $NH_4^+$ nutrient regime, after exposure to a) $Al^{2+}$, b) $Cu^{2+}$, c) $Mn^{2+}$, d) $Pb^{2+}$. Images were attained with an SEM using the back-scattered electrons (BSE) technique, at 20 kV and ~1.0-1.5 K X.

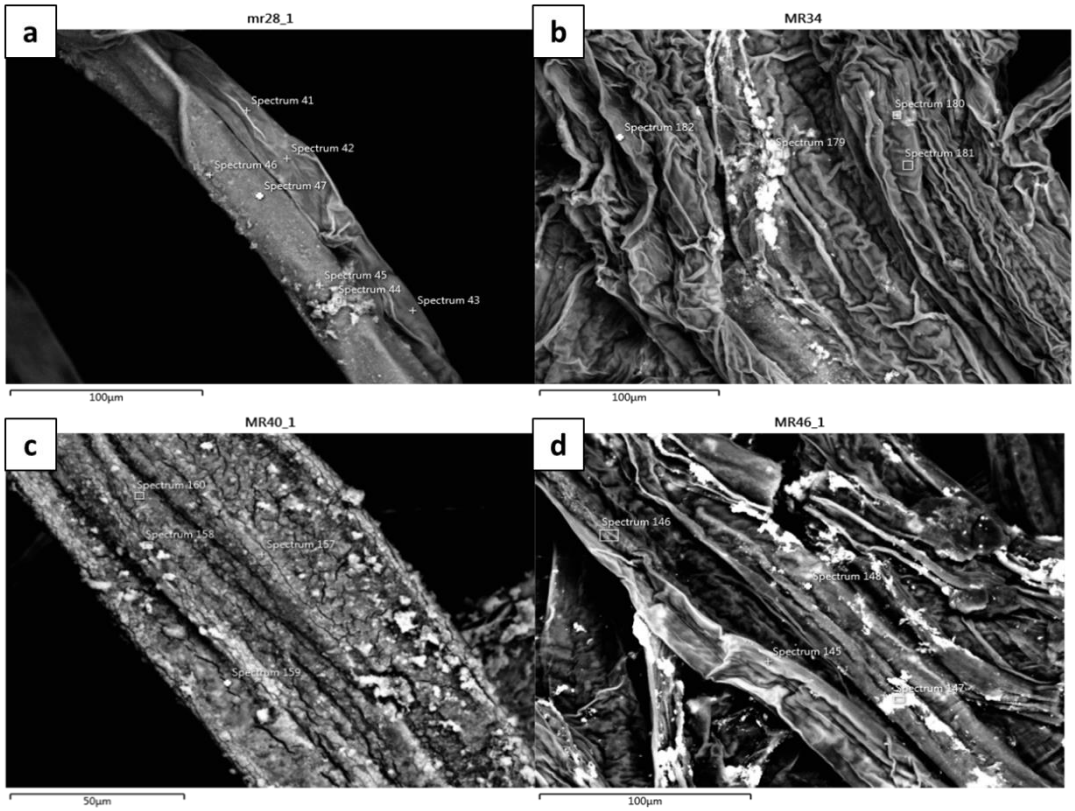


**Figure K2.** The cell surface of *Cladophora parriaudii*, previously cultivated under a 12/1 $NH_4^+$ nutrient regime, after exposure to a) $Al^{2+}$, b) $Cu^{2+}$, c) $Mn^{2+}$, d) $Pb^{2+}$. Images were attained with an SEM using the back-scattered electrons (BSE) technique, at 20 kV and ~1.1-2.2 K X.

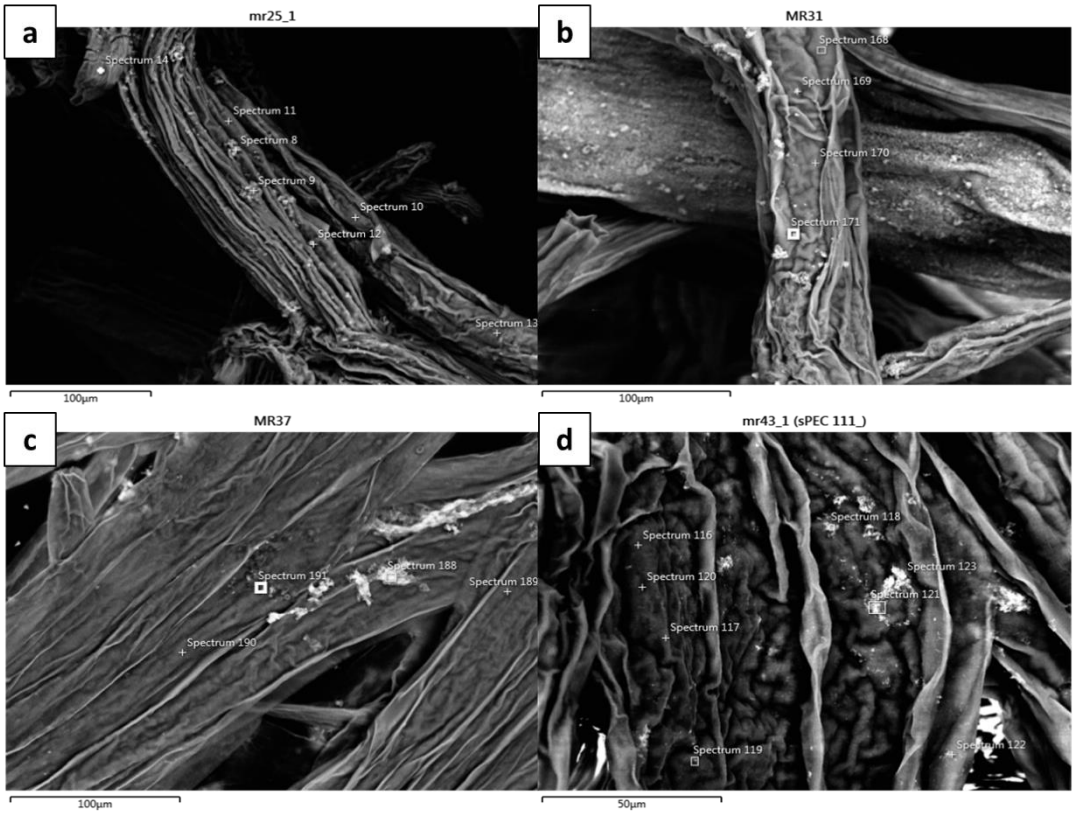


**Figure K3.** The cell surface of *Cladophora parriaudii*, previously cultivated under a 2/1 $NO_3^-$ nutrient regime, after exposure to a) $Al^{2+}$, b) $Cu^{2+}$, c) $Mn^{2+}$, d) $Pb^{2+}$. Images were attained with an SEM using the back-scattered electrons (BSE) technique, at 20 kV and ~860-1.2 K X.

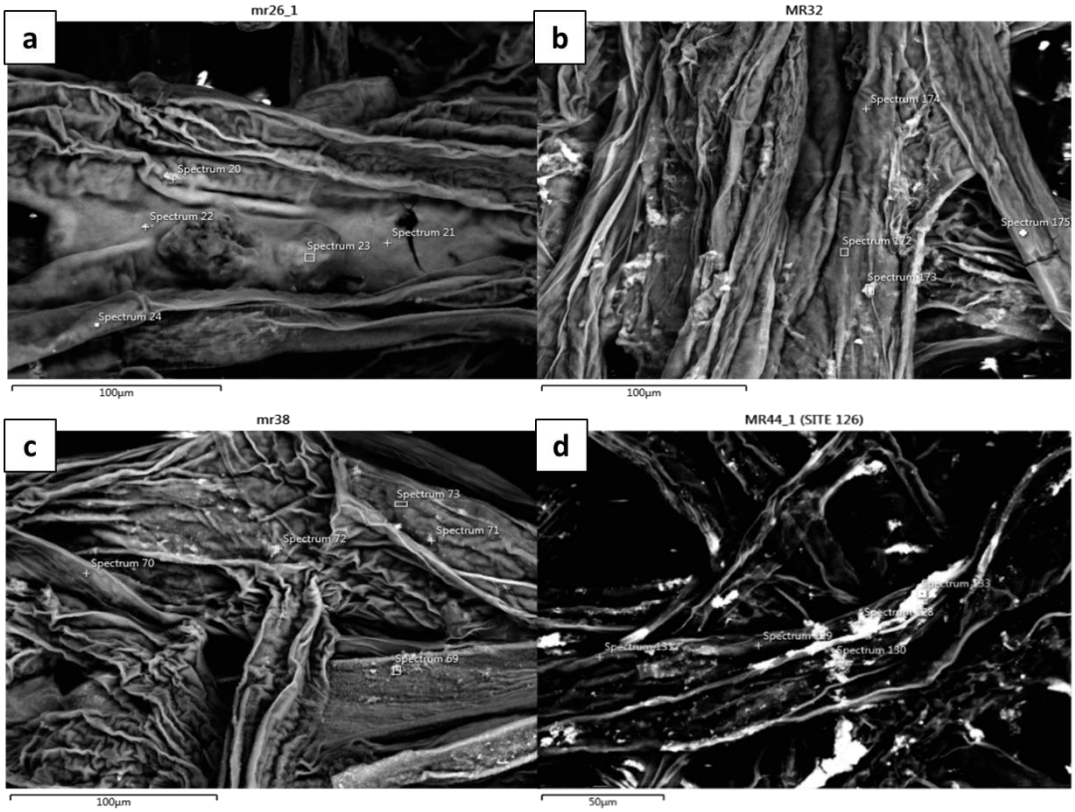


**Figure K4.** The cell surface of *Cladophora parriaudii*, previously cultivated under a 12/1 $NO_3^-$ nutrient regime, after exposure to a) $Al^{2+}$, b) $Cu^{2+}$, c) $Mn^{2+}$, d) $Pb^{2+}$. Images were attained with an SEM using the back-scattered electrons (BSE) technique, at 20 kV and ~1.2-1.5 K X.

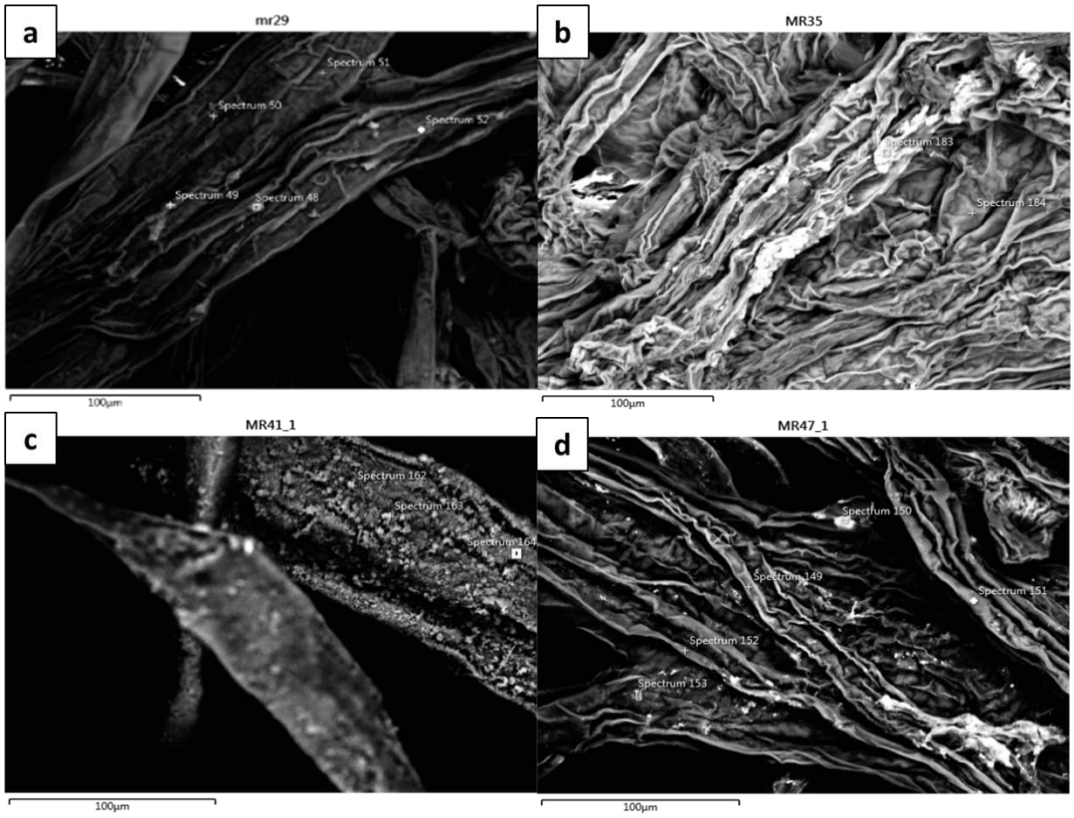


**Figure K5.** The cell surface of *Cladophora parriaudii*, previously cultivated under a 2/1 Urea nutrient regime, after exposure to a) $Al^{2+}$, b) $Cu^{2+}$, c) $Mn^{2+}$, d) $Pb^{2+}$. Images were attained with an SEM using the back-scattered electrons (BSE) technique, at 20 kV and ~1.0-1.3 K X.

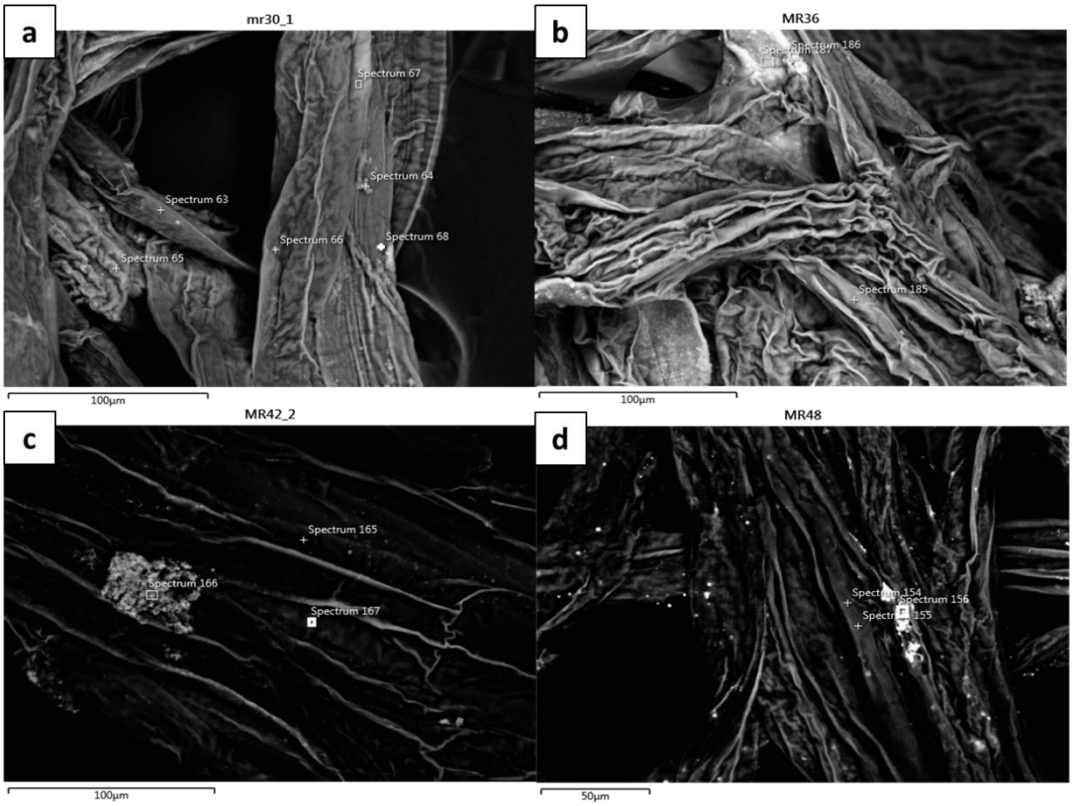


**Figure K6.** The cell surface of *Cladophora parriaudii*, previously cultivated under a 12/1 Urea nutrient regime, after exposure to a) $Al^{2+}$, b) $Cu^{2+}$, c) $Mn^{2+}$, d) $Pb^{2+}$. Images were attained with an SEM using the back-scattered electrons (BSE) technique, at 20 kV and ~1.2-1.3 K X.

# Appendix L – SEM BSE Elemental Spectra

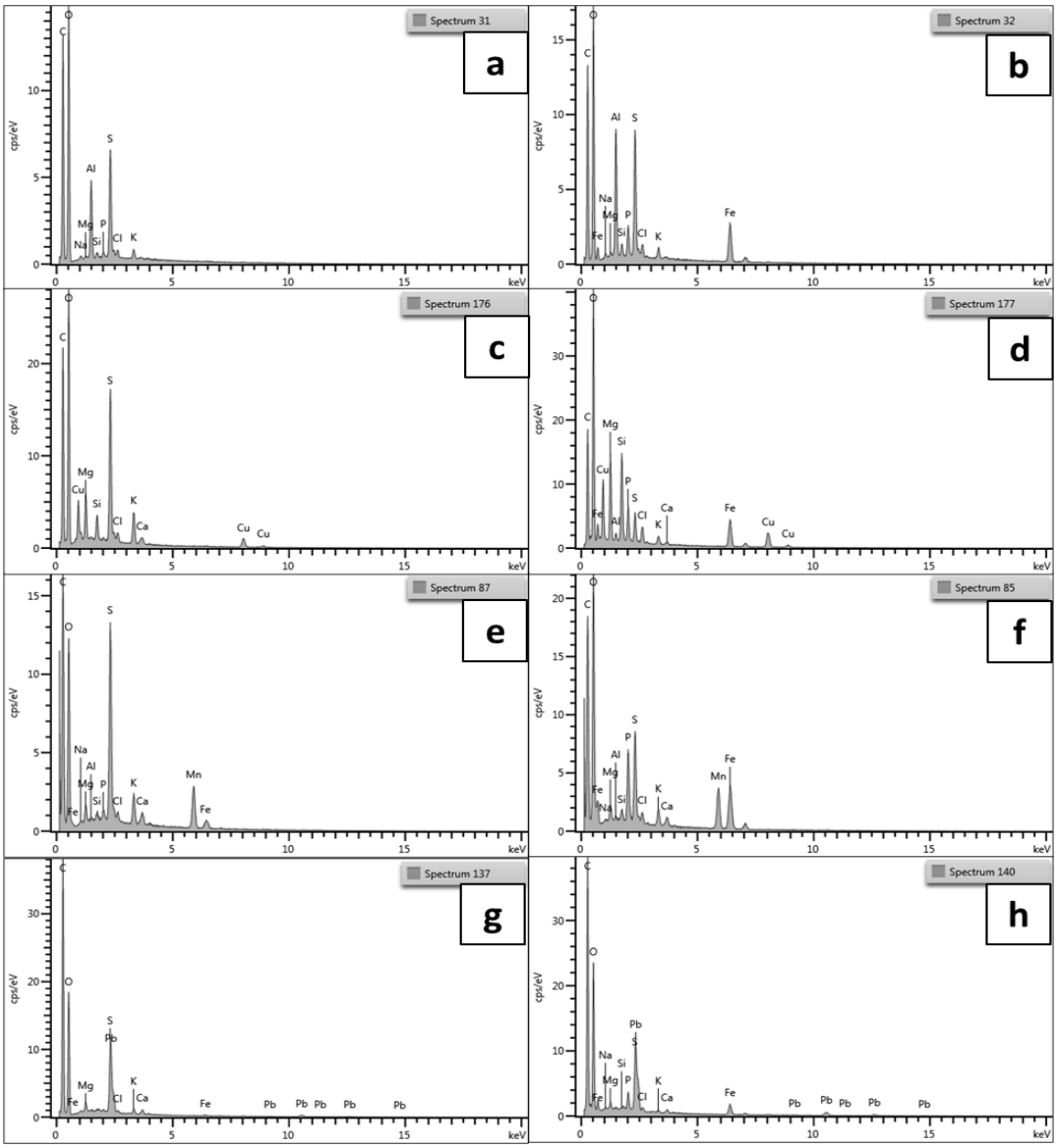


**Figure L1.** The SEM elemental spectra of *Cladophora parriaudii*, previously cultivated under a 2/1 $NH_4^+$ nutrient regime and after exposure to metals: $Al^{2+}$ (a and b), $Cu^{2+}$ (c and d), $Mn^{2+}$ (e and f), $Pb^{2+}$ (g and h). The spectra on the left hand side (a, c, e, and g) were obtained from areas on the cell surface which were deemed "pristine", or as having no visual evidence of metal/contaminant bonding. Whereas, spectra on the right hand side (b, d, f, and h) were obtained from areas on the cell surface in which metal was present, typically as a bright "cluster". The specific locations of each spectrum are denoted in the corresponding images in Figure K1.

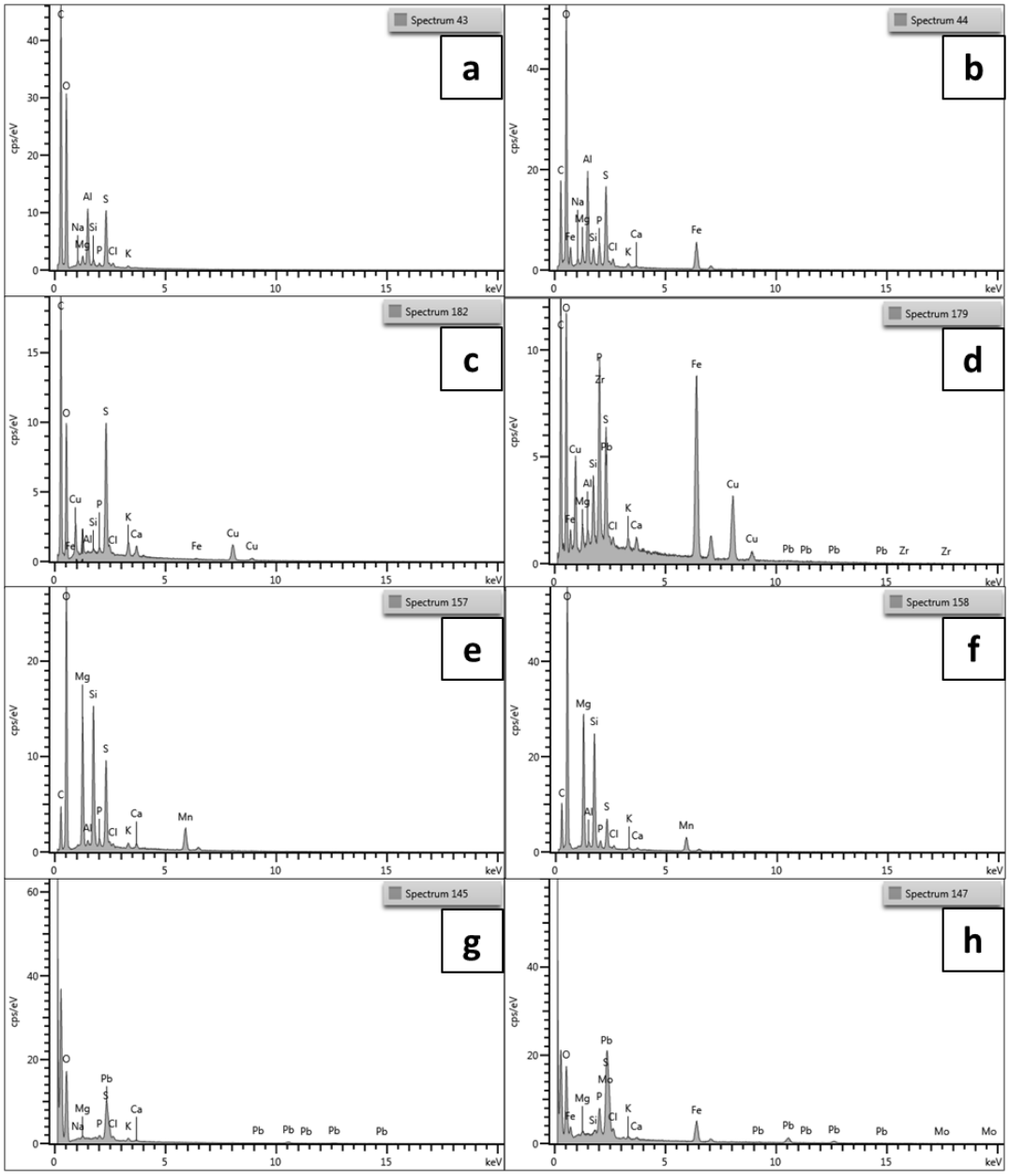


**Figure L2.** The SEM elemental spectra of *Cladophora parriaudii*, previously cultivated under a 12/1 $NH_4^+$ nutrient regime and after exposure to metals: $Al^{2+}$ (a and b), $Cu^{2+}$ (c and d), $Mn^{2+}$ (e and f), $Pb^{2+}$ (g and h). The spectra on the left hand side (a, c, e, and g) were obtained from areas on the cell surface which were deemed "pristine", or as having no visual evidence of metal/contaminant bonding. Whereas, spectra on the right hand side (b, d, f, and h) were obtained from areas on the cell surface in which metal was present, typically as a bright "cluster". The specific locations of each spectrum are denoted in the corresponding images in Figure K2.

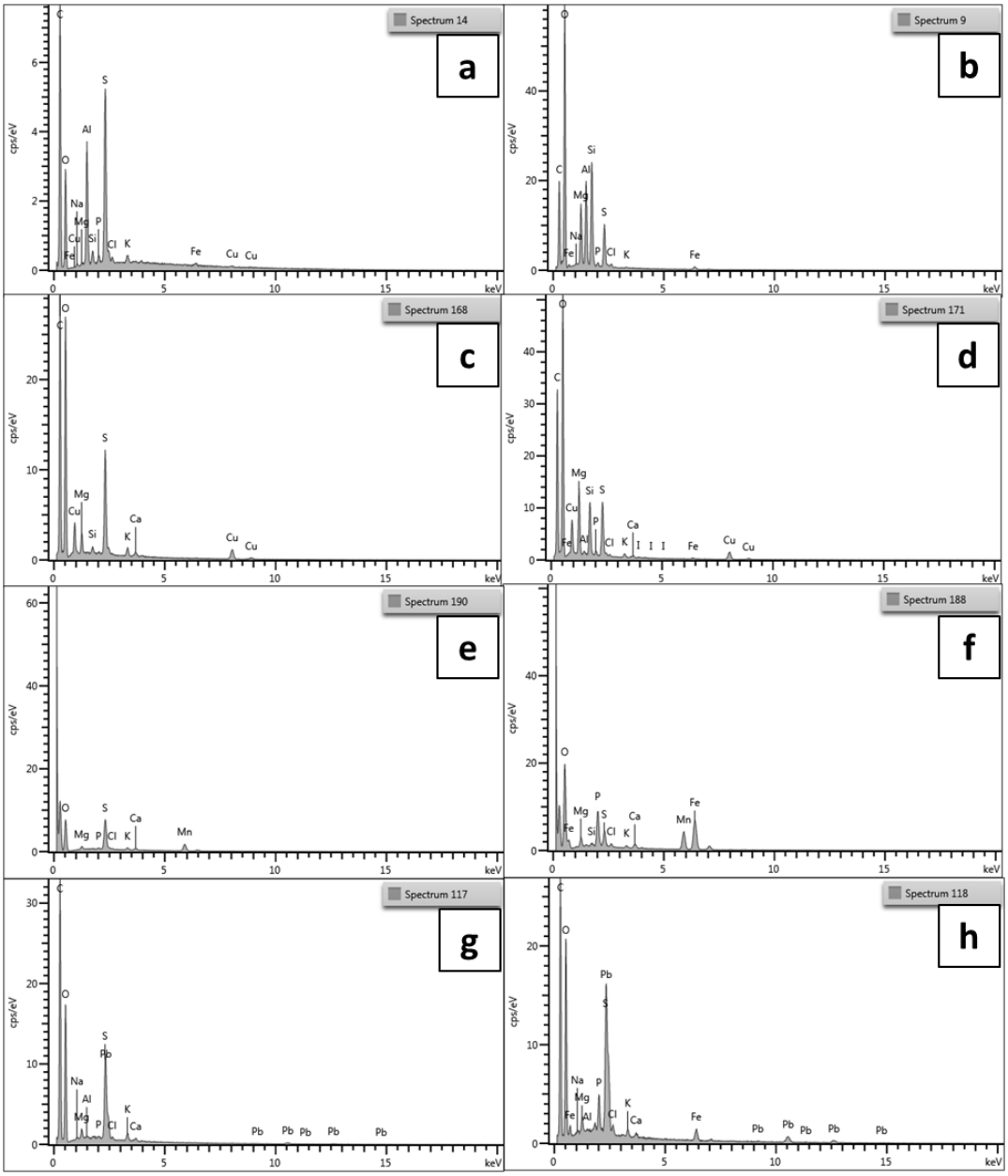


**Figure L3.** The SEM elemental spectra of *Cladophora parriaudii*, previously cultivated under a 2/1 $NO_3^-$ nutrient regime and after exposure to metals: $Al^{2+}$ (a and b), $Cu^{2+}$ (c and d), $Mn^{2+}$ (e and f), $Pb^{2+}$ (g and h). The spectra on the left hand side (a, c, e, and g) were obtained from areas on the cell surface which were deemed "pristine", or as having no visual evidence of metal/contaminant bonding. Whereas, spectra on the right hand side (b, d, f, and h) were obtained from areas on the cell surface in which metal was present, typically as a bright "cluster". The specific locations of each spectrum are denoted in the corresponding images in Figure K3.

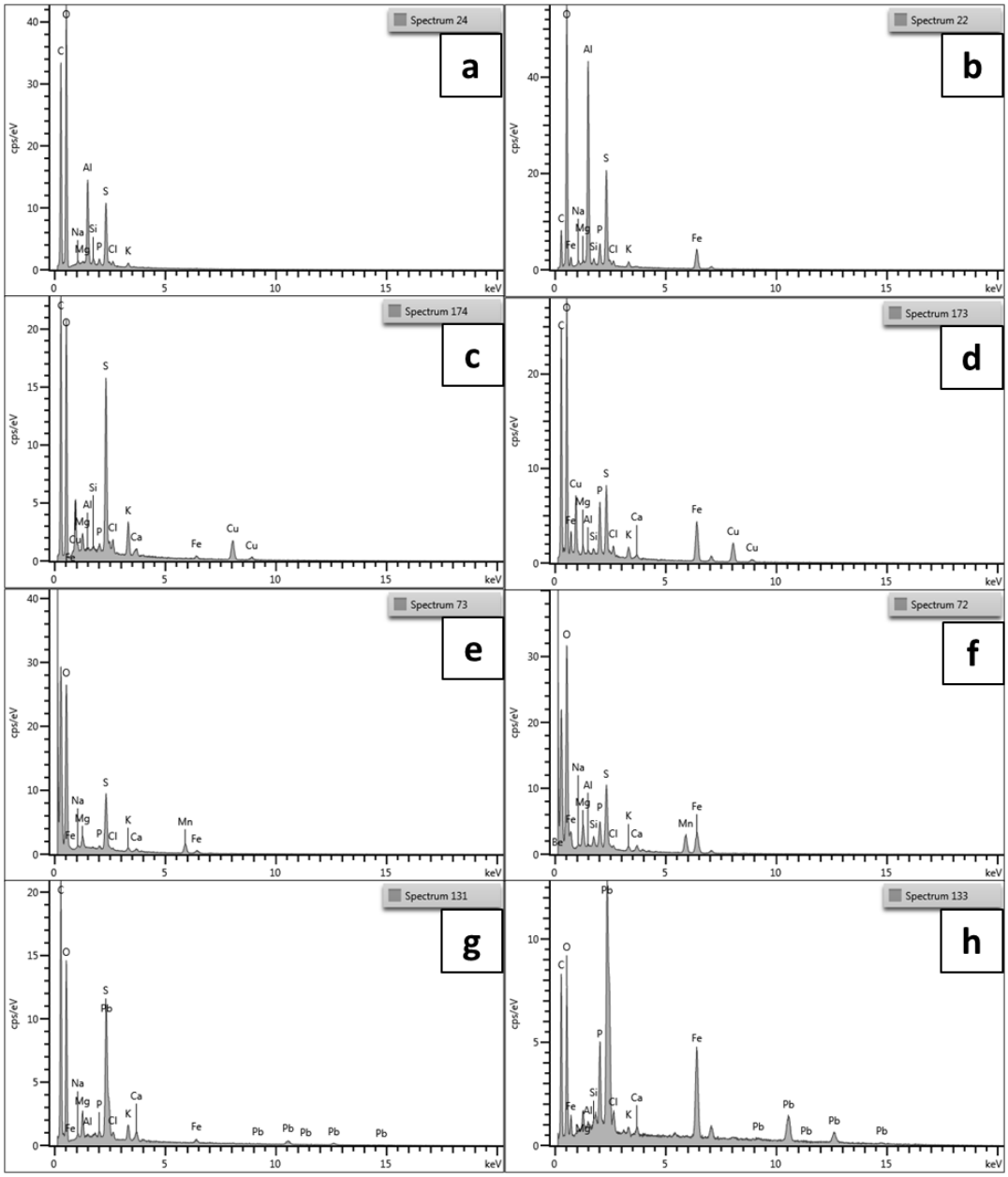


**Figure L4.** The SEM elemental spectra of *Cladophora parriaudii*, previously cultivated under a 12/1 $NO_3^-$ nutrient regime and after exposure to metals: $Al^{2+}$ (a and b), $Cu^{2+}$ (c and d), $Mn^{2+}$ (e and f), $Pb^{2+}$ (g and h). The spectra on the left hand side (a, c, e, and g) were obtained from areas on the cell surface which were deemed "pristine", or as having no visual evidence of metal/contaminant bonding. Whereas, spectra on the right hand side (b, d, f, and h) were obtained from areas on the cell surface in which metal was present, typically as a bright "cluster". The specific locations of each spectrum are denoted in the corresponding images in Figure K4.

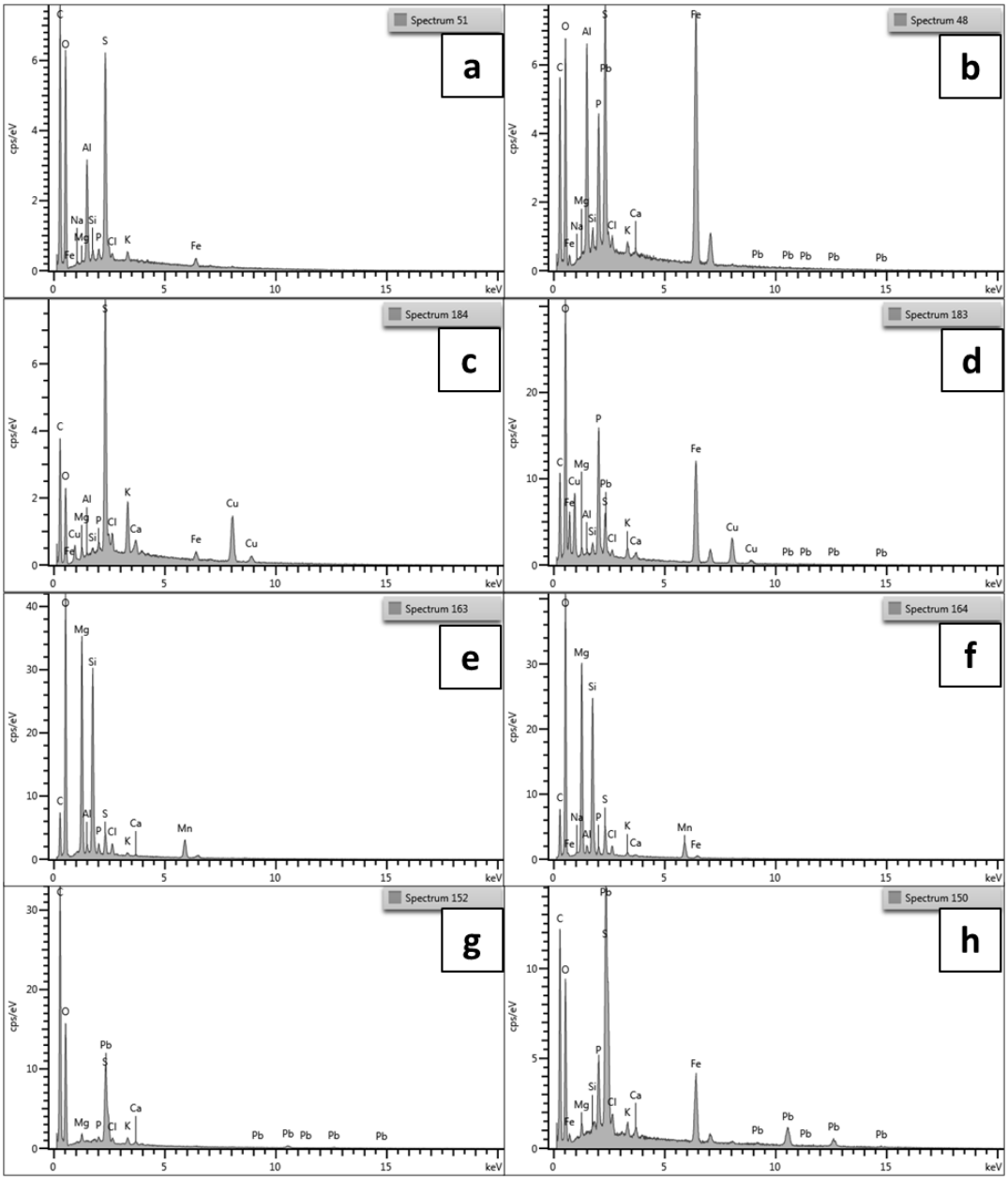


**Figure L5.** The SEM elemental spectra of *Cladophora parriaudii*, previously cultivated under a 2/1 urea nutrient regime and after exposure to metals: $Al^{2+}$ (a and b), $Cu^{2+}$ (c and d), $Mn^{2+}$ (e and f), $Pb^{2+}$ (g and h). The spectra on the left hand side (a, c, e, and g) were obtained from areas on the cell surface which were deemed "pristine", or as having no visual evidence of metal/contaminant bonding. Whereas, spectra on the right hand side (b, d, f, and h) were obtained from areas on the cell surface in which metal was present, typically as a bright "cluster". The specific locations of each spectrum are denoted in the corresponding images in Figure K5.

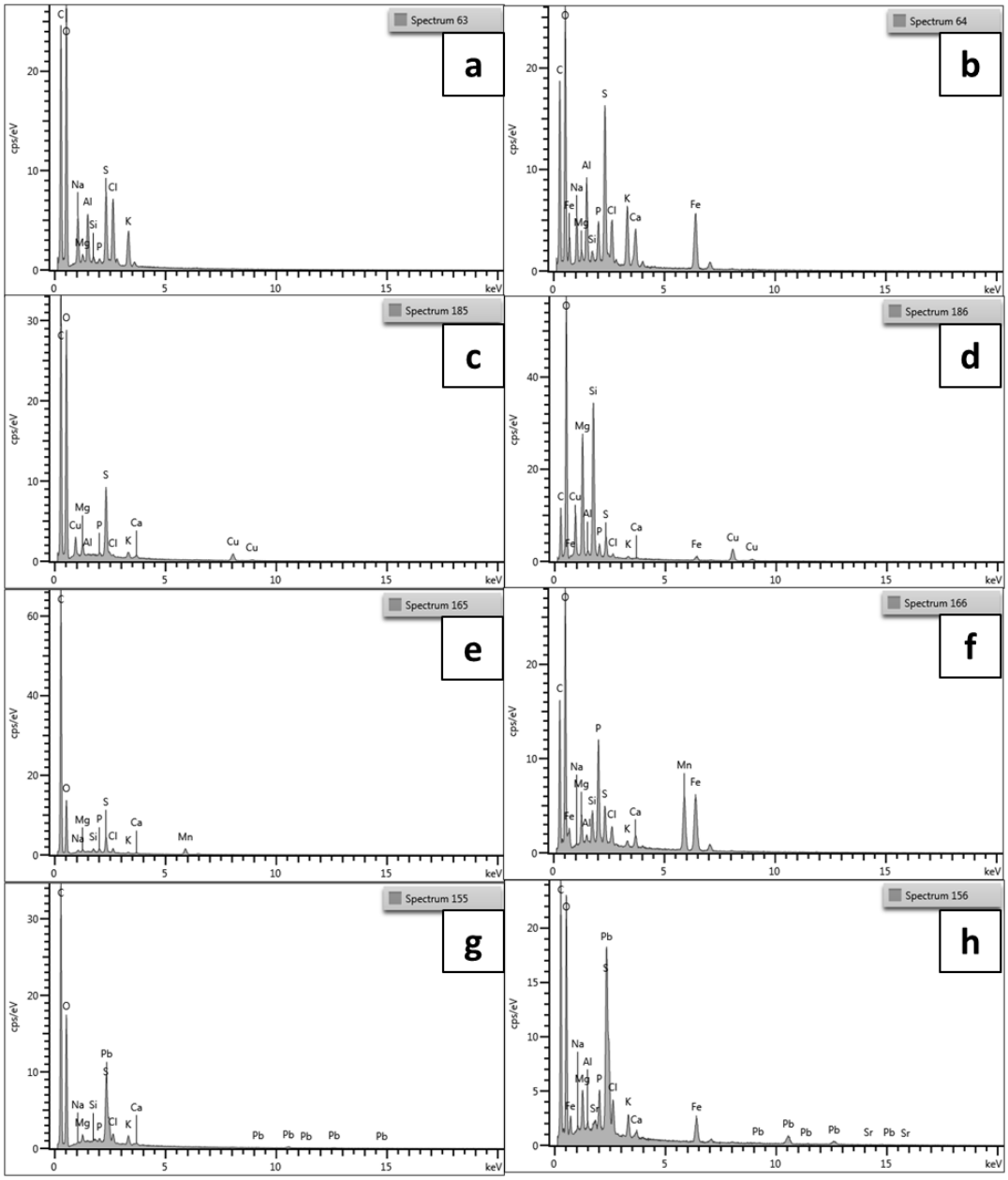


**Figure L6.** The SEM elemental spectra of *Cladophora parriaudii*, previously cultivated under a 12/1 urea nutrient regime and after exposure to metals: $Al^{2+}$ (a and b), $Cu^{2+}$ (c and d), $Mn^{2+}$ (e and f), $Pb^{2+}$ (g and h). The spectra on the left hand side (a, c, e, and g) were obtained from areas on the cell surface which were deemed "pristine", or as having no visual evidence of metal/contaminant bonding. Whereas, spectra on the right hand side (b, d, f, and h) were obtained from areas on the cell surface in which metal was present, typically as a bright "cluster". The specific locations of each spectrum are denoted in the corresponding images in Figure K6.

# Appendix M – Conference Participation

**Conferences Attended:**

- 2nd IIE Postgraduate Conference – Edinburgh, September 2014 – Poster
- School of Engineering, PGR Conference – Edinburgh, April 2015 – Poster & Presentation
- CIWEM, Scottish Branch, Annual Dinner – Edinburgh, April 2015 – Poster
- IIE Lunchtime Seminar Series – Edinburgh, May 2015 – Presentation
- XV World Water Congress – Edinburgh, May 2015 – e-Poster
- 5th UK Algal Conference – Glasgow, July 2015 – Presentation
- MBRE Conference – Glasgow, March 2016 – Presentation
- School of Engineering, PGR Conference – Edinburgh, April 2016 – Demonstration
- 6th UK Algal Conference – Sheffield, July 2016 – Poster & Presentation
- STEM for Britain – London, March 2017 – Poster
- 4th IIE Postgraduate Conference – Edinburgh, May 2017 – Poster
- 6th ISAP Congress – Nantes, June 2017 – Poster

# INSTITUTE FOR INFRASTRUCTURE AND ENVIRONMENT (IIE)

## Wastewater Bioremediation and Bioenergy from Filamentous Algae

Michael Ross[a,b], Andrea J C Semião[a], Michele S Stanley[b], and John G Day[b]
[a]University of Edinburgh, Edinburgh, UK. [b]SAMS, Scottish Marine Institute, Oban, UK

SAMS EPSRC NERC SCIENCE OF THE ENVIRONMENT THE UNIVERSITY of EDINBURGH School of Engineering

**Aim:** Exploring the potential of the **filamentous macro-alga** *Cladophora* to **remediate wastewaters** and **produce bioenergy**

### Background

#### 1 Decreased Clean Water Availability

Water is invaluable to life on Earth. However, we are currently facing a global water crisis:

(1) From 1995-2010 human population has risen from 5.7 to 6.8 billion[1];
(2) Global water withdrawal consequentially increased from 3600 to 3900 km$^3$/year[2,3];
(3) Increased urbanization and poor freshwater management;
(4) Increasing poverty: lack of clean drinking water and sanitation (3 billion people)[4];
(5) Climate change and hydrological variability.

Figure 1. Examples of impacted water bodies. (a) a heavily polluted river[4] (b) an extreme drought in China[5]

#### 2 Wastewater (WW) Pollution

Wastewaters can be high in contaminants **(Table 1&2)** and current treatment practices **(Fig. 2a-d)** often have high capital and operational costs and incomplete removal of pollutants.

Table 1. EU maximum permissible discharges from WWTPs with a catchment of >100,000 people equivalent[6] vs. nutrient concentrations found in agricultural effluents[7,8].

| Parameter | Permissible Discharge (mg/l) | % Reduction | Agricultural WW (mg/l) |
|---|---|---|---|
| Nitrogen | 10 | 70-80 | 22-2960 |
| Phosphorous | 1 | 70-80 | 1-115 |

Table 2. WHO drinking water guidelines[9] vs. heavy metal concentrations found in industrial effluent[8].

| Parameter | Drinking Water Guidelines (mg/l) | Industrial WW (mg/l) |
|---|---|---|
| Cadmium | 0.003 | 0.003-1.25 |
| Lead | 0.01 | <0.05-13.4 |
| Nickel | 0.07 | <0.01-7.3 |

This has obvious negative consequences for the environment, notably eutrophication, and associated animal and human health risks.

#### 3 Energy Crisis

Energy prices are becoming heightened:

- anthropogenic climate change;
- growing population;
- diminishing fossil fuel reserves.

Figure 2. Technologies typically employed in wastewater treatment plants (WWTPs). (a) activated sludge[10] (b) membrane filtration[11] (c) activated carbon[12] (d) reed beds

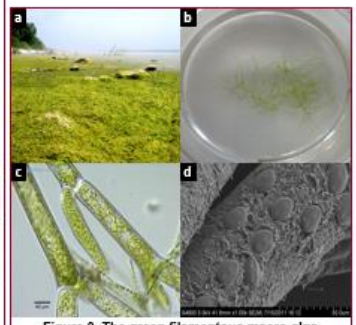

Figure 3. The green filamentous macro-alga *Cladophora* (a) a dense population on the shore of Lake Erie, US[13] (b) small-scale *Cladophora parriaudii* (c) light microscopy displaying filamentous nature[14] (d) SEM image showing epibacteria and diatom colonization[15].

### Solution: Wastewater Treatment with Macroalgae using *Cladophora*

*Cladophora* **(Fig. 3a-d)** is a cosmopolitan, filamentous, green macro-alga with species found in both temperate and tropical regions, from fresh to marine waters: very adaptable and robust.

- Capable of nutrient uptake: thrives in high nutrient concentrations, often associated with eutrophic waters and having bioremediation potential.
- Complex cell wall structure: adsorbs heavy metals.
- Potential use in WWTP to treat wastewater for water recovery, reuse, and recycling.
- Highly persistent in nature, and resistant to grazing by herbivores.
- Improves biodiversity by increasing benthic habitat complexity e.g. spatial refugia
- Potential to act as a feedstock for renewable bioenergy production.

### Experimentation

(1) Nutrient uptake efficiencies of *Cladophora* in different wastewater media;
(2) Heavy metal adsorption and recovery of *Cladophora* and how that affects growth and remediation capacity;
(3) Determine upper and lower tolerance levels of different abiotic factors (e.g. nutrient concentrations, salinity, temperature);
(4) Macro-algal biochemical composition and bioenergy yields;
(5) Heavy metals influence in bioenergy yield and downstream processing.

### Acknowledgements

This Ph.D. project is funded by EPSRC and NERC.

### References

[1] United States Census Bureau, "[1] USCENSUS 2006 & 2010," [2] Wikisource, World Water Resources, 1998," Wikisource, 2014," [3] www.eea.europa.eu/soer, "www.eea.europa.eu/soer," [4] Urban Wastewater Directive (91/271/EEC)," [5] Edwards, A.C., Withers, P.J.A. (2008) Transport and delivery of suspended solids, nitrogen and phosphorus from various sources to freshwaters in the UK. Journal of Hydrology 350, 144-153, [6] Wahl, J.J., Novak, J., Edwards-Jones, G., Jones, D.L., Williams, A.P. (2012) Fungal and bacterial growth following the application of slurry and anaerobic digestate of livestock manure to temperate pasture soils. Biology and Fertility of Soils 48, 809-820, [7] WHO, 2014," [8] www.scotwis.com," [9] www.indiamart.com," [10] infraconnect.com," [11] Inclusive risk and "www.investigatorsite.edu," Zubelzu, S.B., Graham, J.W., Young, D.M., Meyer, R.L., Rutowski, M.J., Smith, I., Graham, J.E., (2010) The great [illegible] Edinburgh as a globally de[illegible] ecological engineer. Journal of Physiology 48, 1-17.

THE UNIVERSITY of EDINBURGH HERIOT WATT UNIVERSITY

**Figure M1.** Poster presented at the 2nd IIE Postgraduate Conference – Edinburgh, September 2014.

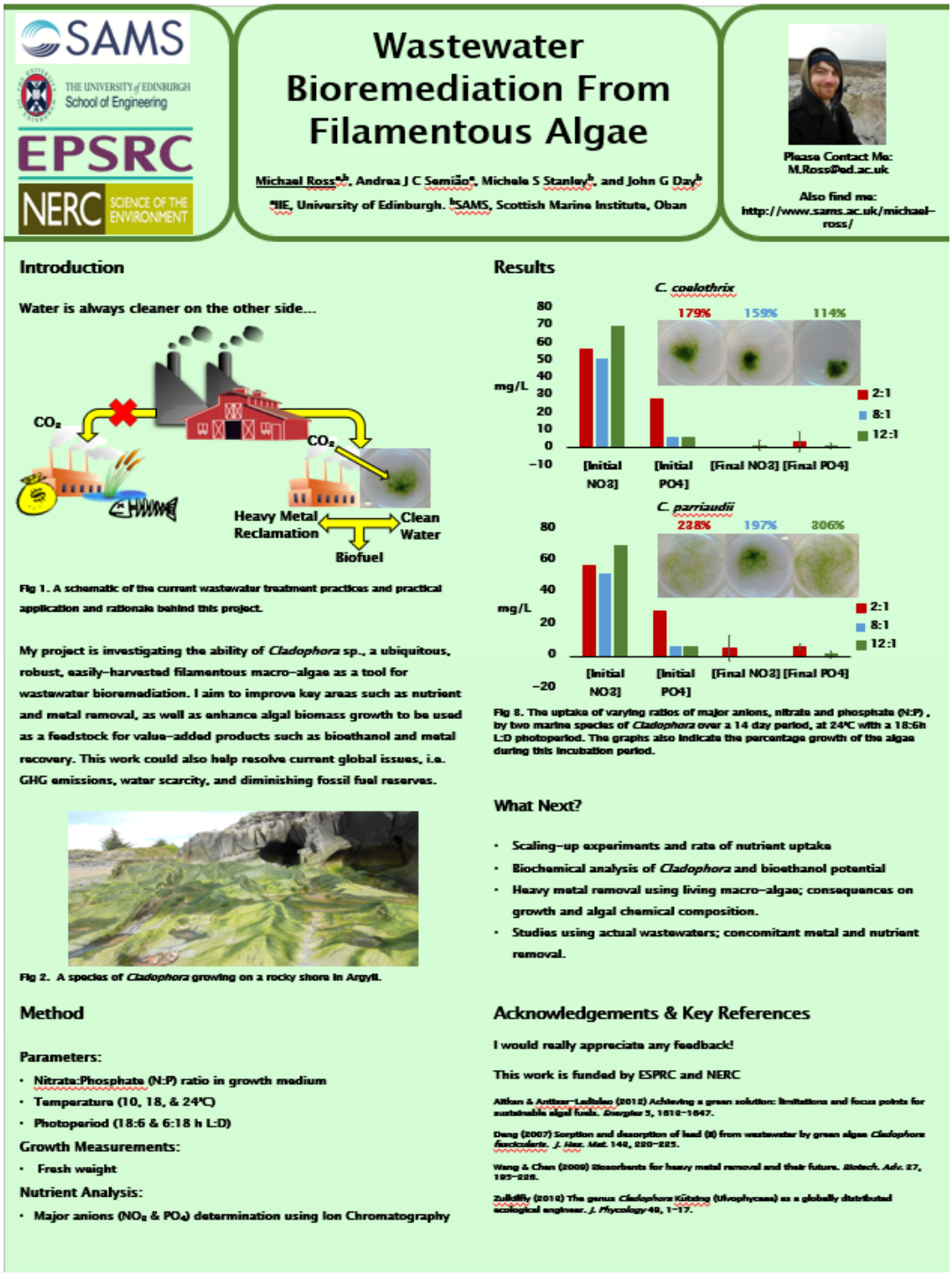


**Figure M2.** Poster presented at the School of Engineering, PGR Conference and at CIWEM, Scottish Branch, Annual Dinner; both in Edinburgh, April 2015.

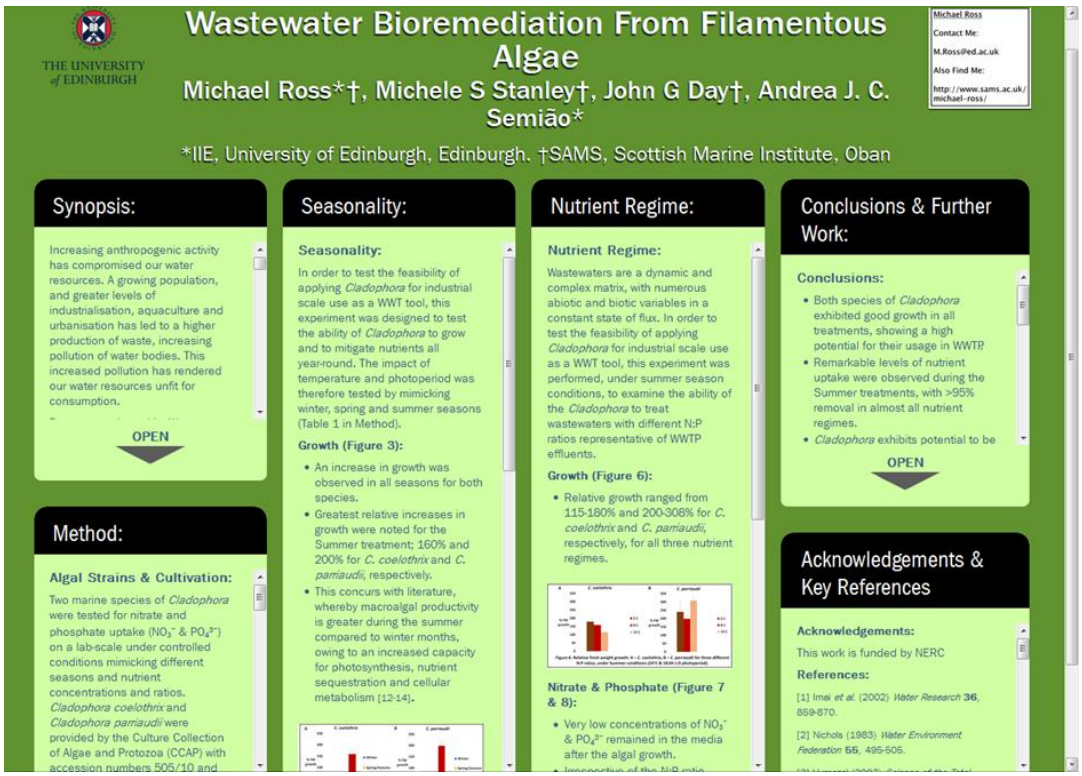


**Figure M3.** e-Poster presented at the XV world Water congress – Edinburgh, May 2015.

# Wastewater Treatment and Biofuel Potential of *Cladophora* sp.

Michael Ross[a,b], Michele S Stanley[b], John G Day[b], Katharine Davis[a], Rory McColl[a], Andrea J C Semião[a]

[a]School of Engineering, University of Edinburgh.
[b]SAMS, Scottish Marine Institute, Oban.
m.ross@ed.ac.uk

THE UNIVERSITY of EDINBURGH School of Engineering

SAMS

## INTRODUCTION

Increased anthropogenic activity has led to greater level of fossil fuel usage, heightening greenhouse gas emissions and diminishing fossil fuel reserves. In parallel, water as a resource is under threat due to high levels of pollution as a result of a growing population and industrialisation.

Current wastewater treatment (WWT) practices are inefficient:

- High energy usage;
- Large area requirement;
- Incomplete removal of nutrients: WWTP effluent concentrations ranged from 2-45 mg/L and 0.02-5 mg/L for N and P, respectively [1-3].

Macro-algae have been suggested as a possible tertiary treatment step in WWT owing to their high growth rates, nutrient sequestration capabilities and ease of harvest. A tertiary treatment pond in Sweden containing a mixture of species, including *Cladophora glomerata*, removed 62% and 86% of Total-N and total-P from the effluent, respectively, during the summer [4].

Moreover, there is considerable interest in utilizing algal biomass rich in carbohydrates for bioenergy production, such as bioethanol [5-6].

## AIMS & METHODS

*Cladophora* are characterised by their green filamentous morphology. Often associated with eutrophic conditions, they are renowned for their high rates of growth and persistence in nature.

This project aims at assessing the efficiency of *C. coelothrix* and *C. parriaudii* (**Figure 1**) in:

- Remediating different N species present in wastewater (**Table 1**);
- Remediating different N:P ratios (**Table 1**);
- Quantify biomass production (DW) and carbohydrate yield.

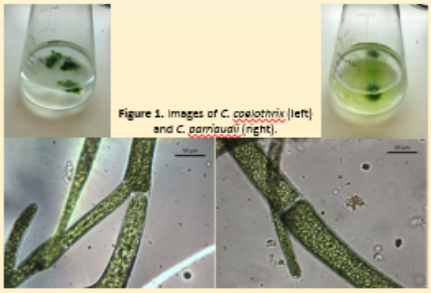

**Figure 1.** Images of *C. coelothrix* (left) and *C. parriaudii* (right).

**Table 1.** Experimental variables

| Variable | Setting |
|---|---|
| Temperature | 25°C |
| Initial pH | 8.0 |
| Photoperiod | 18/6 h, L/D |
| Agitation | 100 rpm |
| N-source | $NH_4^+$, $NO_2^-$, $NO_3^-$, Urea |
| N:P ratio | 2:1, 12:1, 22:1, 32:1 |
| Species | *C. coelothrix* & *C. parriaudii* |
| Carbohydrate (% DW) | DuBois assay |

## RESULTS

*C. coelothrix*

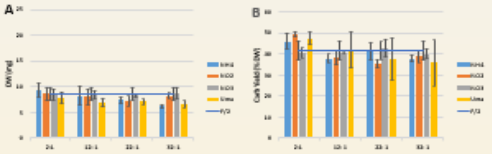


*C. parriaudii*

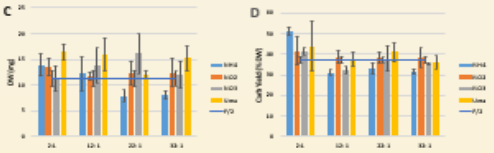


**Figure 2 A-D.** The mean dry weight (A & C) of *Cladophora coelothrix* and *Cladophora parriaudii*, respectively, and the carbohydrate yield (B & D) of *C. coelothrix* and *C. parriaudii*, respectively, as determined by the DuBois assay. Algae were grown under four different sources of nitrogen; $NH_4^+$, $NO_2^-$, $NO_3^-$, and Urea. The amount of nitrogen added to the media varied to give initial N:P ratios of 2:1, 12:1, 22:1 and 32:1. F/2 media was used as a control, it is $NO_3^-$ based with an N:P ratio of 11:1. (n=3, errors = 1 S.D.).

## CONCLUSIONS & FUTURE WORK

For both species:

- A reduction in growth in $NH_4^+$ with 22:1 and 32:1 ratios due to toxic effects of ammonia: $NH_3$ concentration> 1 mg/L;
- Highest carbohydrate yield at 2:1 ratios;
- Almost complete N removal at 2:1 ratio: removal> 75% for *C. coelothrix*; >85% *C. parriaudii*.

Differences between species:

- *C. parriaudii* has a higher biomass yield, particularly with urea;
- Great potential for use as a bioremediator for low N:P wastewaters;
- Potential to be used as a feedstock for biofuels (i.e. bioethanol).

What next?:

- Chemical profiling for determination of carbohydrate composition;
- Test with other contaminants present in wastewaters;
- Test with real wastewaters.

### References & Acknowledgments

[1] Imai *et al.* (2002) *Water Research* **36**, 859-870; [2] Nichols (1983) *J Water Pollut Control Fed* **55**, 495-505; [3] Vymazal (2007) *Sci Total Environ* **380**, 48-65; [4] Gumbricht (1993) *Ecol.Eng* **2**, 1-30; [5] Adams *et al.* (2011) *Bioresour Tech* **102**, 9976-9984; [6] Aitken & Antizar-Ladislao (2012) *Energies* **5**, 1613-1647

This Ph.D. project is funded by ESPRC and NERC.

EPSRC NERC SCIENCE OF THE ENVIRONMENT

**Figure M4.** Poster presented at the 6th UK Algal Conference – Sheffield, July 2016.

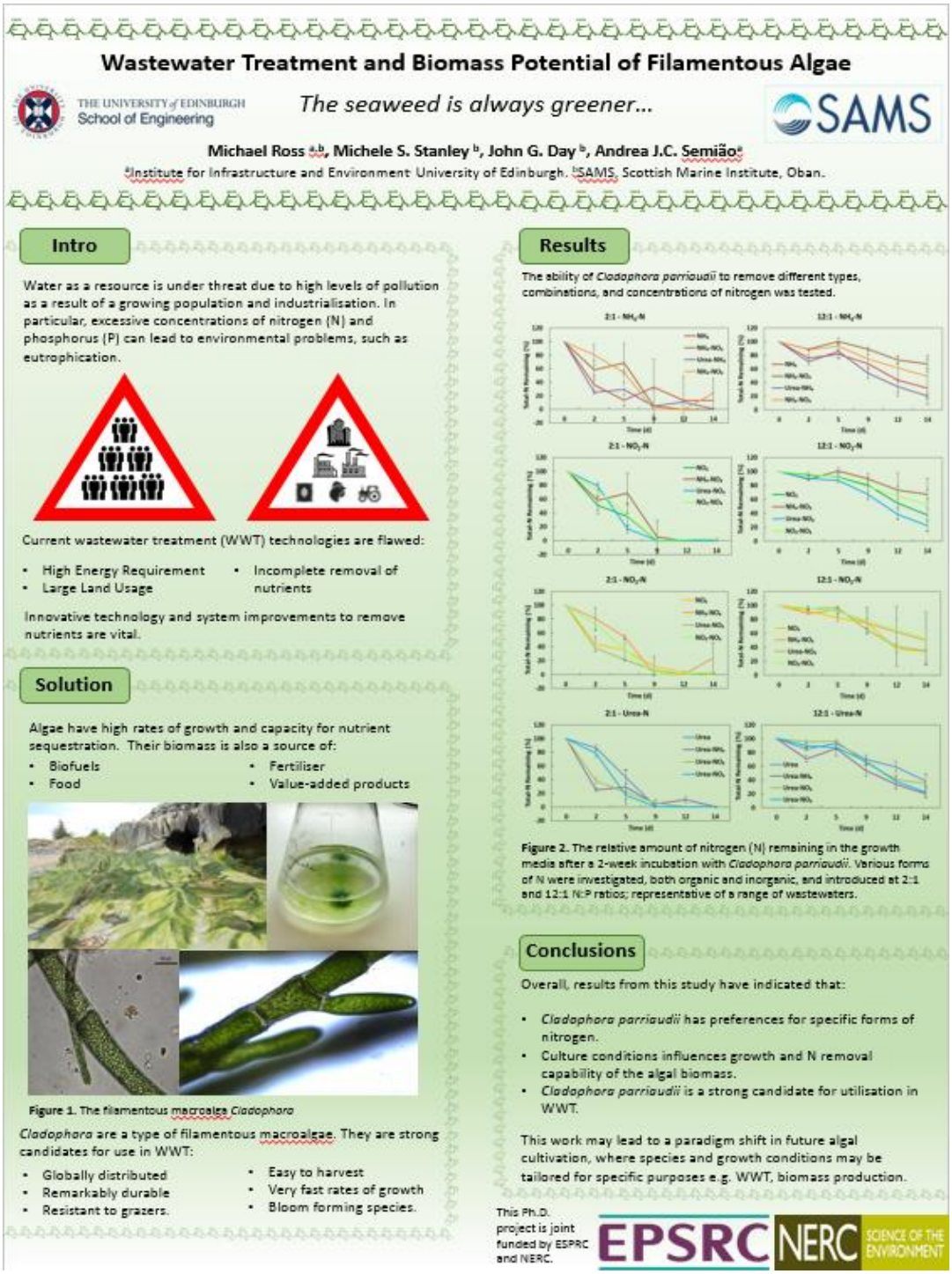


**Figure M5.** Poster presented at STEM for Britain – London, March 2017 and the 4th IIE Postgraduate Conference – Edinburgh, May 2017.

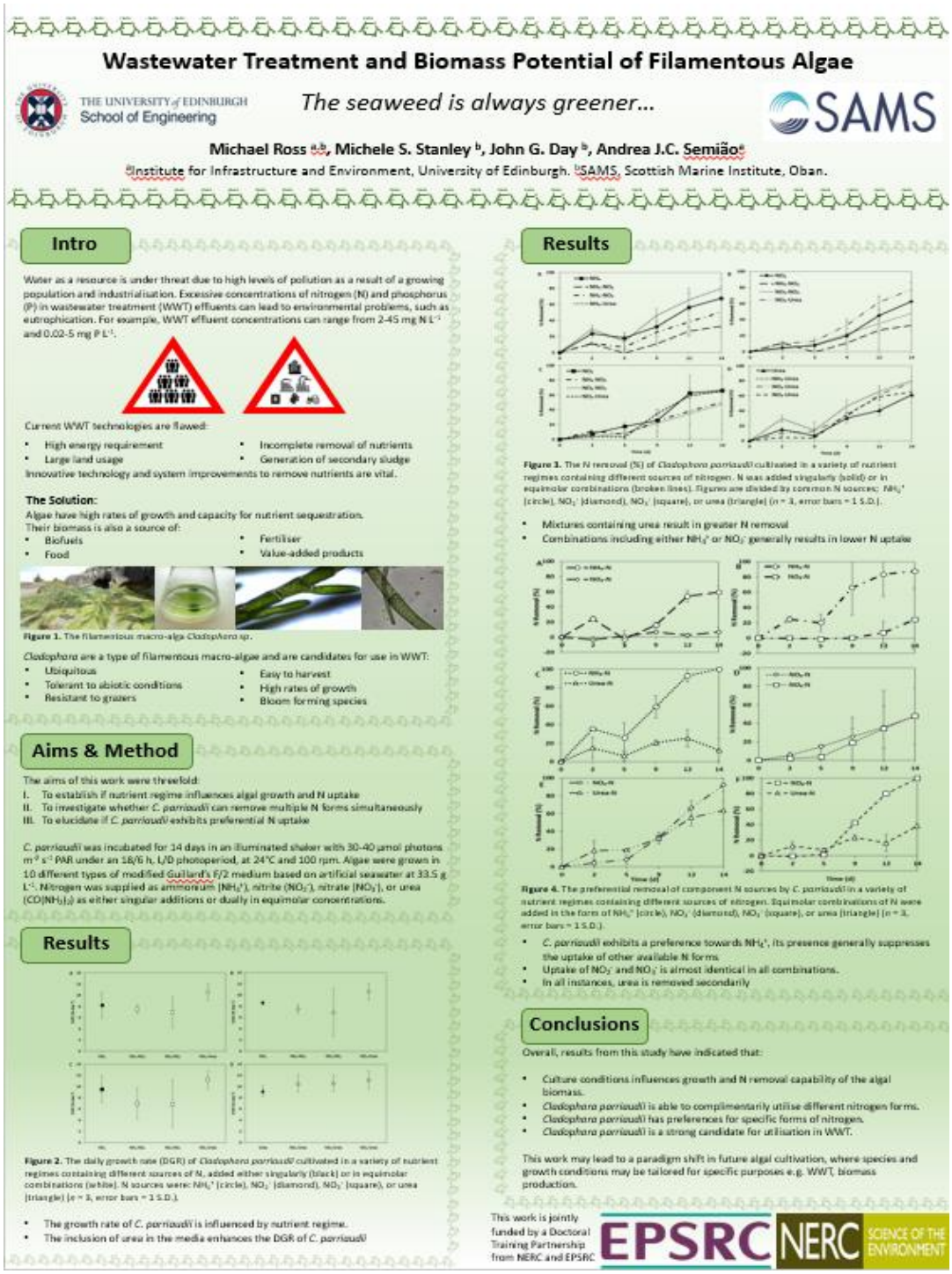


**Figure M6.** Poster presented at 6th ISAP Congress – Nantes, June 2017.